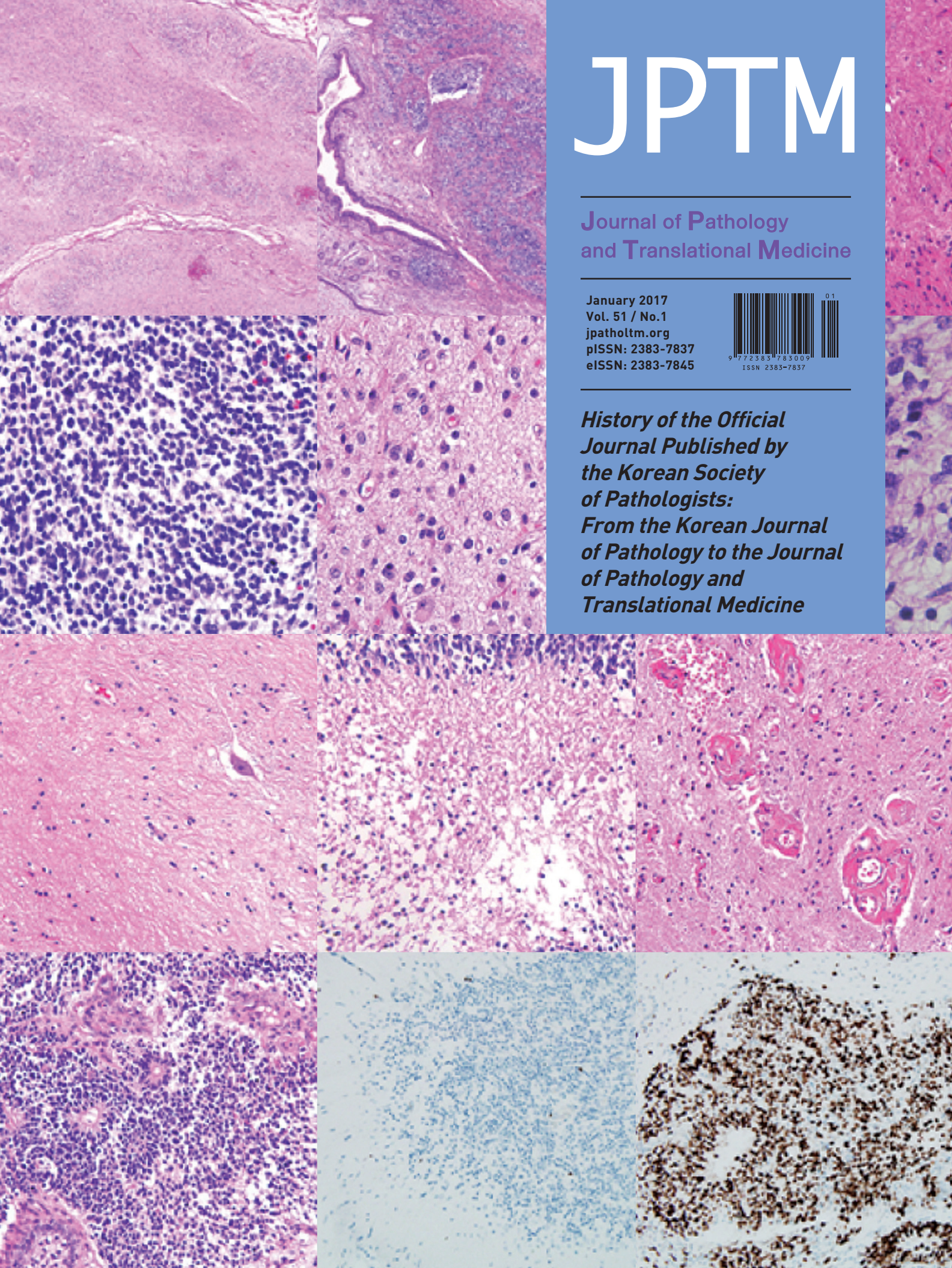

JPTM

Journal of Pathology and Translational Medicine

January 2017
Vol. 51 / No.1
jpatholtm.org
pISSN: 2383-7837
eISSN: 2383-7845

History of the Official Journal Published by the Korean Society of Pathologists: From the Korean Journal of Pathology to the Journal of Pathology and Translational Medicine

Journal of Pathology and Translational Medicine

Volume 51 • Number 1 • January 2017 (bimonthly)
Published since 1967
Printed on 11 January 2017 Published on 15 January 2017

J Pathol Transl Med
pISSN: 2383-7837
eISSN: 2383-7845

Aims & Scope

The Journal of Pathology and Translational Medicine is an open venue for the rapid publication of major achievements in various fields of pathology, cytopathology, and biomedical and translational research. The Journal aims to share new insights into the molecular and cellular mechanisms of human diseases and to report major advances in both experimental and clinical medicine, with a particular emphasis on translational research. The investigations of human cells and tissues using high-dimensional biology techniques such as genomics and proteomics will be given a high priority. Articles on stem cell biology are also welcome. The categories of manuscript include original articles, review and perspective articles, case studies, brief case reports, and letters to the editor.

Subscription Information

To subscribe to this journal, please contact the Korean Society of Pathologists/the Korean Society for Cytopathology. Full text PDF files are also available at the official website (http://jpatholtm.org). *Journal of Pathology and Translational Medicine* is indexed by PubMed, PubMed Central, Scopus, KoreaMed, KoMCI, WRPIM and CrossRef. Circulation number per issue is 700.

Contact the Korean Society of Pathologists/the Korean Society for Cytopathology

Publishers: Han Kyeom Kim, MD, Hye Kyoung Yoon, MD
Editors-in-Chief: Soon Won Hong, MD, Chong Jai Kim, MD
Published by the Korean Society of Pathologists/the Korean Society for Cytopathology

Editorial Office
Room 1209 Gwanghwamun Officia, 92 Saemunan-ro, Jongno-gu,
Seoul 03186, Korea/#406 Lilla Swami Bldg, 68 Dongsan-ro,
Seocho-gu, Seoul 06784, Korea
Tel: +82-2-795-3094/+82-2-593-6943
Fax: +82-2-790-6635/+82-2-593-6944
E-mail: office@jpatholtm.org

Printed by iMiS Company Co., Ltd.
Jungang Bldg. 18-8 Wonhyo-ro 89-gil, Yongsan-gu, Seoul 04314, Korea
Tel: +82-2-717-5511 Fax: +82-2-717-5515 E-mail: ml@smileml.com

Manuscript Editing by InfoLumi Co.
210-202, 421 Pangyo-ro, Bundang-gu, Seongnam 13522, Korea
Tel: +82-70-8839-8800 E-mail: infolumi.chang@gmail.com

Front cover image: Histopathologic features of mature teratoma and immature teratoma (Fig. 3). p51.

This journal was supported by the Korean Federation of Science and Technology Societies Grant funded by the Korean Government.

Journal of Pathology and Translational Medicine

J Pathol Transl Med
pISSN: 2383-7837
eISSN: 2383-7845

Volume 51, Number 1, January 2017

CONTENTS

EDITORIAL

LETTER TO THE EDITOR

ORIGINAL ARTICLES

CONTENTS CONTINUED

CASE REPORTS

Instructions for Authors for *Journal of Pathology and Translational Medicine* are available at http://jpatholtm.org/authors/authors.php

Journal of Pathology and Translational Medicine 2017; 51: 1-6
https://doi.org/10.4132/jptm.2017.01.07

■ EDITORIAL ■

History of the Official Journal Published by the Korean Society of Pathologists: From the *Korean Journal of Pathology* to the *Journal of Pathology and Translational Medicine*

Se Hoon Kim · Chong Jai Kim[1] · SoonWon Hong[1]

Department of Pathology and Medical History, Yonsei University College of Medicine, Seoul, Korea;
[1]Editors-in-Chief, Journal of Pathology and Translational Medicine

Historically, Western medicine as we know today was first introduced in Korea at the end of the 19th century by the missionaries, who periodically reported their medical experience in Korea in the newspapers and magazines of their mother countries and Korea.[1-4]

During the Japanese colonial period, the first medical journal published in Korea was 'Chosen igakkai zasshi (朝鮮醫學會雜誌),' although it was published in Japanese. 'Mansen No Ikai (滿鮮之醫界)' was also published in that period.[5,6] Afterwards, a journal named 'Mitteilungen aus der Medizischen Akademie zu Keizo (京城醫學專門學校紀要)' was published in German by the Keijo Medial College founded by the Japanese Governor-General of Korea. It was a general medical journal.

A few other journals were published by medical schools, and much of the pathology articles were published in such general medical journals. In 1929, the Korean Medical Association founded by Korean doctors started publication of the *Korean Medical Journal* (朝鮮醫報), which was the first medical journal published in Korean language then. Dr. Il Sun Yoon, professor in the Department of Pathology at Severance Union Medical College, was an editorial member of the journal, and he often published articles on his visiting experience in pathology departments at many of the European medical schools. Besides Dr. Yoon's articles, a few other pathology articles in that period were published in the *Korean Medical Journal* (朝鮮醫報). Its publication was continued until 1937.[5,6] As for an English journal, there was one named *The Journal of Severance Union Medical College*, the first English journal in Korea, published by Severance Union Medical College from 1933 to 1935. It consisted of five volumes.[4-6] In these early days, there were only three journals that could be classified as "Departmental Academic Journal": *Clinical Internal Medicine* (臨床內科學), *Clinical Surgery* (臨床外科), and *Keijo Imperial Univerisity Pediatric Journal* (城大小兒科雜誌). They were published by each department of Medical Faculty, Keijo Imperial University.[5]

The first medical journal published after the Liberation from Japan in 1945 was the *Journal of Korean Doctors* (朝鮮醫師新報) by United States Army Military Government in Korea, Education Bureau, Medical Education part (朝鮮軍政廳 學務局 醫學教育係). Various associations and academic societies of medical doctors were founded during this period, and as a result, diverse medical journals, i.e., the *Journal of the Korean Medical Association* (朝鮮醫學協會會報 → 大韓醫學協會誌) in 1948, were published. The *Korean Journal of Internal Medicine* published by the Korean Association of Internal Medicine was the first departmental academic journal and its publication is continued to date.[5]

After the Korean War, many military medical journals were published by the militaries, followed by a number of departmental academic journals, i.e., *Tuberculosis* in 1954, and other journals published by medical schools, research institutions, and general hospitals. General commercial medical journals such as the *Korean Medical Journal* (綜合醫學) (1956) and the *New Medical Journal* (最新醫學) (1958) were also published during the post-Korean War period.[5]

Corresponding Author
Se Hoon Kim, MD, PhD, FIAC
Department of Pathology, Yonsei University College of Medicine, 50-1 Yonsei-ro, Seodaemun-gu, Seoul 03722, Korea
Tel: +82-2-2228-1769, Fax: +82-2-362-0860, E-mail: paxco@yuhs.ac

Received: January 5, 2017 **Accepted:** January 7, 2017

pISSN 2383-7837
eISSN 2383-7845

HISTORY OF THE *KOREAN JOURNAL OF PATHOLOGY*

In September 1967, 20 years after the foundation of the Korean Society of Pathologists in 1947, the *Korean Journal of Pathology* was officially launched. Before then, pathology articles were submitted to the aforementioned university journals, the *Journal of the Korean Medical Association*, or other general medical journals. Publication of the society's official journal was first agreed upon in the Board Meeting of the society in December 1961, and after 6 years in 1967, the first issue of the *Korean Journal of Pathology* (Fig. 1) was published on September 30. Professors Chae Koo Lee, Ki Hong Kim, Suk Jae Hong, Jong Moo Lee, Sang Kook Lee, and Sang In Kim were members of the Editorial Board.[7,8] In the first issue, the Editorial Board published Chae Koo Lee's (president) first publication address, Il Sun Yoon's (honorary president) congratulatory message and memoirs of two late members, In Sup Hyun (1963, Ewha Womans University) and Sung Soo Lee (1964, Seoul National University). A short history of the Korean Society of Pathologists was also included in the first issue.[7]

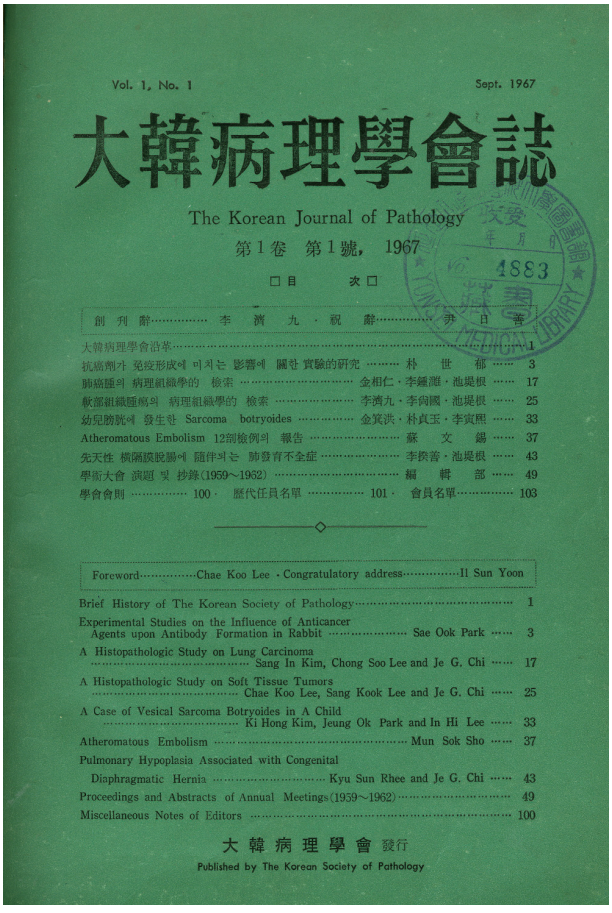
Vol. 1, No. 1 Sept. 1967

大韓病理學會誌

The Korean Journal of Pathology

第1卷 第1號, 1967

目 次

創刊辭 …… 李 濟 九 · 祝 辭 …… 尹 日 善

大韓病理學會沿革 …… 1

抗癌劑가 免疫形成에 미치는 影響에 關한 實驗的硏究 …… 朴 世 祁 …… 3

肺癌腫의 病理組織學的 檢索 …… 金相仁 · 李鍾謨 · 池堤根 …… 17

軟部組織腫瘍의 病理組織學的 檢索 …… 李濟九 · 李向國 · 池堤根 …… 25

幼兒膀胱에 發生한 Sarcoma botryoides …… 金箕洪 · 朴貞玉 · 李寅熙 …… 33

Atheromatous Embolism 12例檢例의 報告 …… 蘇 文 錫 …… 37

先天性 橫隔膜脫腸에 隨伴되는 肺發育不全症 …… 李換善 · 池堤根 …… 43

學術大會 演題 및 抄錄(1959~1962) …… 編 輯 部 …… 49

學會會則 …… 100 · 歷代任員名單 …… 101 · 會員名單 …… 103

Foreword …… Chae Koo Lee · Congratulatory address …… Il Sun Yoon

Brief History of The Korean Society of Pathology …… 1

Experimental Studies on the Influence of Anticancer Agents upon Antibody Formation in Rabbit …… Sae Ook Park …… 3

A Histopathologic Study on Lung Carcinoma …… Sang In Kim, Chong Soo Lee and Je G. Chi …… 17

A Histopathologic Study on Soft Tissue Tumors …… Chae Koo Lee, Sang Kook Lee and Je G. Chi …… 25

A Case of Vesical Sarcoma Botryoides in A Child …… Ki Hong Kim, Jeung Ok Park and In Hi Lee …… 33

Atheromatous Embolism …… Mun Sok Sho …… 37

Pulmonary Hypoplasia Associated with Congenital Diaphragmatic Hernia …… Kyu Sun Rhee and Je G. Chi …… 43

Proceedings and Abstracts of Annual Meetings(1959~1962) …… 49

Miscellaneous Notes of Editors …… 100

大韓病理學會 發行

Published by The Korean Society of Pathology

Fig. 1. The first issue of the *Korean Journal of Pathology* in 1967.

This historical first issue of the journal published six articles, along with programs and abstracts of the annual academic meetings of the society from 1959 to 1962, rules and regulations of the society, a list of the executives, and a list of the society members. The name of journal title was written in Chinese letters, and the first Editor-in-Chief was Professor Sang In Kim, who served for 3 years. The journal started as biannual, but it soon began to publish four times a year in 1977, and then it became bimonthly in 1991. In the early days of the publication, the journal contents were mainly composed of abstracts from the annual academic meetings of the society, but beginning in 1989, the abstracts were no longer published in the journal.[7,8]

In 1963, the Korean Society of Pathologists began to hold board examination for the residents, and 8 years later in 1975, the society decided to enforce a regulation that required at least one published article in the *Korean Journal of Pathology* as a prerequisite for application for the board examination. With the enactment of this regulation, the number of articles submitted to the *Korean Journal of Pathology* increased significantly; the number of published articles reached 123 per year in 1982. However, in 1981, the *Korean Journal of Clinical Pathology* was newly launched, and the number of published articles in the *Korean Journal of Pathology* subsequently decreased. There was one last article related to the clinical pathology in 1985, and no more clinical pathology articles were published in the *Korean Journal of Pathology*.[7,8]

In 1990, the *Korean Journal of Pathology* was officially registered in the Ministry of Culture and Media (Feb 26, Ma-1664) and it finally became a legitimate and official publication, 24 years after the journal was first started. A year later in 1991, the *Korean Journal of Pathology* received an ISSN (International Standardized Serial Number 0379-1149) through the Korean Academy of Medical Sciences and it was registered globally. In the same year, Professor Je Geun Chi wrote an article "The Korean Journal of Pathology: a review of the first 25 years" in the *Korean Journal of Pathology* (vol. 25, issue 6), in which he summarized the last 25 years of the journal and proposed Index Medicus or Science Citation Index (SCI) as the key aspiration of the journal in the upcoming years.[8]

Starting in the year 2000, articles published in the *Korean Journal of Pathology* became available for searching by authors, article names, and keywords. Soon after, the journal started providing abstracts and full texts. At present, PDF files of all articles can be downloaded in the journal homepage.[9]

In 2004, with the aim of being indexed in SCI, the *Korean*

 https://doi.org/10.4132/jptm.2017.01.07

Journal of Pathology started to print the name of the journal in English with "The Korean Society of Pathologists" listed as the publisher, starting with the publication of vol. 38. The journal received a new ISSN (ISSN 1738-1843).[9]

The first article written in English was about the pathogenesis of atherosclerosis by Sun Joo Ro in 1968.[8,10] Afterwards, one or two English articles per year were published consistently, but in 1991, the Editorial Board decided not to publish English articles anymore. Therefore, English articles had to be submitted to other journals. In 2001, however, the Editorial Board decided to accept English articles again, and the number of English articles subsequently started to increase; the ratio of articles written in Korean and those written in English was almost 1:1 (37 vs. 35) in 2005. In 2011, to take a step ahead as a global journal, the Editorial Board announced the *Korean Journal of Pathology* as an all-English journal.[11]

Meanwhile, an academic interest in cytopathology within the society had grown and the members started various researches in the field. The first lecture in cytopathology was "Cytopathological evaluation of malignant tumor cells in peritoneal fluid (Sung Soo Lee and Taek Koo Yoon)" and the first abstract was "The evaluation of cytopathological diagnosis (Sang In Kim *et al.*)" in the 11th Annual Meeting of the Korean Society of Pathologists in 1959.[12,13] As for the articles in cytopathology, Dong Wha Lee *et al*. published the first article in 1977; "The study on cytopathological diagnosis of carcinoma of the lung."[14] Afterwards, about one cytopathology article was published per year, and the number started to gradually increase as the fine needle aspiration had become popular. In 1986, the Korean Society for Cytopathology separated out from the Korean Society of Pathologists, and there was no official cytopathology journal until 1990. During that period, thirteen cytopathology articles were published in total. As the need for an official cytopathology journal had surfaced, an editorial board was put together with Jung Dal Lee as the first Editor-in-Chief in July 1990. The first issue (Fig. 2) was published on 30 June 1990, and the journal received an ISSN (ISSN 1017-0391) on 13 December 1990. In 2002, the articles published in the *Korean Journal of Cytopathology* since 1997 were indexed in KoreaMed, and soon afterwards, the entire archive was indexed. In 2006, it was registered as "Listed Candidate Journal" of the National Research Foundation of Korea, and it was indexed in various databases such as Google Scholar by the end of 2007.[13]

However, despite the active academic achievements in cytopathology, the gradual decrease in the number of pathology residents across the nation, subsequent increase in the workload of pathologists, and acknowledgment of publication in the SCI journals only as the prerequisite for promotion in universities all resulted in gradual decrease in the number of submitted articles. The number of original articles as opposed to the number of case reports became significantly low and the relative acceptance rate increased. The situation was the same for the *Korean Journal of Pathology* and many other medical journals in Korea. As the public evaluation criteria of academic journals became more and more strict, the Korean Academy of Medical Sciences and the National Research Foundation of Korea proposed a merger of journals in the same field and announced support for such merged journals. In accordance with their proposition, the society members of both the Korean Society of Pathologists and the Korean Society for Cytopathology decided to merge their journals and publish a unified journal with better quality.[11,13,15] After much discussion on the actual terms and conditions of the merger, both societies agreed upon the "grand principle" that the unification of the two journals would be a merger, not an acquisition of one by the other. Publication costs and the number of published articles per issue were agreed to be divided in a ratio

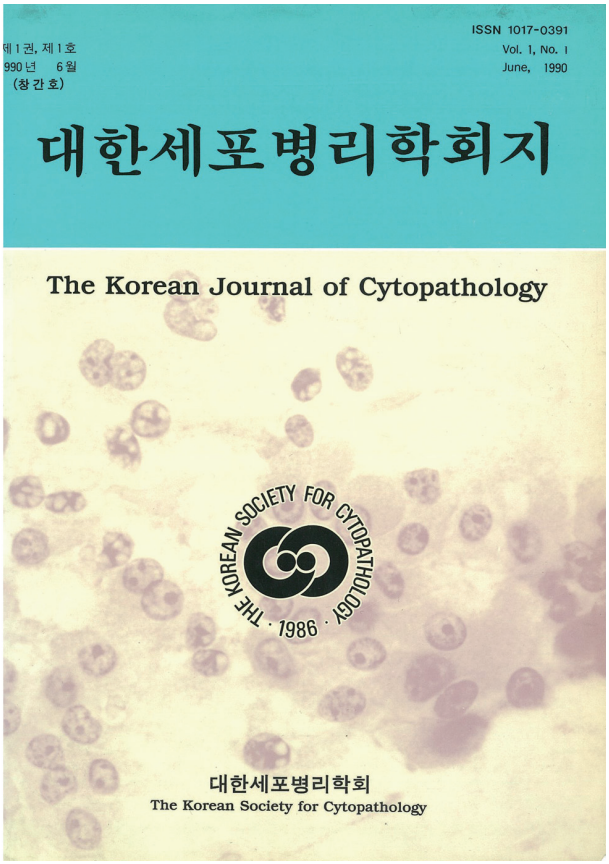

Fig. 2. The first issue of the *Korean Journal of Cytopathology* in 1990.

of 7:3. With confirmation of the board members of both societies (the Korean Society of Pathologists; May 15, 2008, the Korean Society for Cytopathology; May 30, 2008), the unified journal was to maintain the name "*The Korean Journal of Pathology*" along with its volume and issue (Fig. 3). The cover page, however, was newly designed with logos of both societies imprinted. Presidents of both societies were equally listed as the journal publisher, and the journal would have two editors-in-chief, one from each society. The *Korean Journal of Cytopathology*, after 19 years of its first launch, disappeared into the history and was finally reborn as "*The Korean Journal of Pathology*" in 2009.[13,15]

While the merge of the two journals was still in process, the *Korean Journal of Pathology* was listed in SCI-expanded (SCIE), and so the articles published afterwards in the unified journal were all indexed in SCIE.

As the *Korean Journal of Pathology* was an official journal of the Korean Society of Pathologists, the president of the society became the publisher ex officio. As previously said, the first Editor-in-Chief was Professor Sang In Kim. In 1970, the terms of office for both president and editor-in-chief changed to 1 year, and so the director of the general affairs undertook the role of editor-in-chief. In 1976 (vol. 10, issue 2), a new Editorial Board was organized, with Professor Eui Keun Ham as the Editor-in-Chief. Afterwards, a board of publication was newly formed within the society and the chief of the board of publication undertook the role of editor-in-chief.[8]

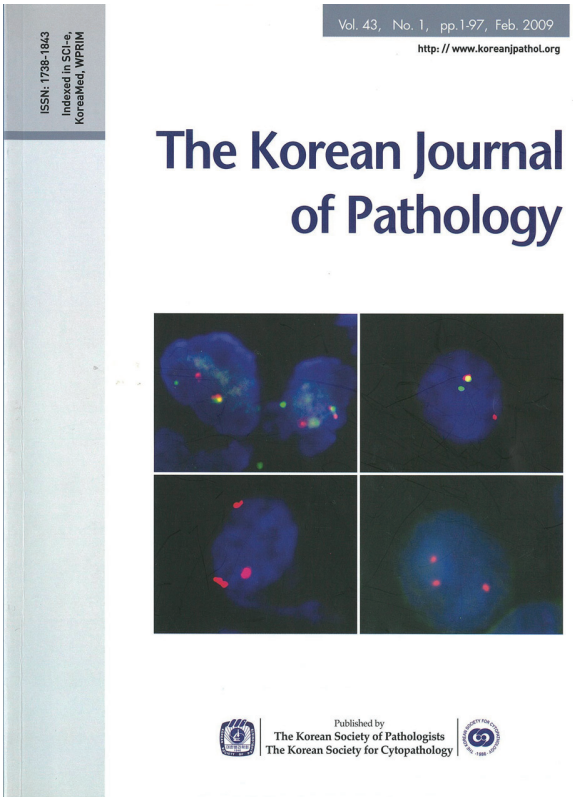

Fig. 3. The first unified issue of the *Korean Journal of Pathology* after the merger with the *Korean Journal of Cytopathology* in 2009.

In October 1992, the rules and regulations of the Korean Society of Pathologists were revised, and the Council of Directors became mainly responsible for the execution of duty. Accordingly, the publication of the society's official journal fell under the duty of the Editorial Board with the Director of Publication in charge.

The Editorial Board was initially composed of 9–11 executive editors and 40–66 contributing editors until 2004 (vol. 38). In 2005 (vol. 39), the editors were no longer classified into executive editors and contributing editors. In 2003 (vol. 37), four of foreign pathologists were added to the Editorial Board (three from the United States and one from Hong Kong). In 2004 (vol. 38, issue 6), five pathologists from the United States additionally joined the Editorial Board.[9]

Meanwhile, in accordance with the increasing demand for a globally recognized journal, the Korean Society for Cytopathology, the Korean Society of Legal Medicine, the Korean Association of Oral and Maxillofacial Pathology, the Korean Society of Toxicologic Pathology, and the Korean Society of Veterinary Clinics together launched a journal named *Basic and Applied Pathology* (BAAP) in 2008 through Wiley. However, with the *Korean Journal of Pathology* indexed in SCIE in 2009, the journal closed after 2 years. The articles that had been published in BAAP can still be searched in the internet.[11]

CRISIS AND JOURNEY OF *THE KOREAN JOURNAL OF PATHOLOGY*

Although indexed in SCIE, the *Korean Journal of Pathology* had to go through many difficulties of its own. The impact factor was low and in plateau, and its status as "Listed Candidate Journal" of the National Research Foundation of Korea was almost insignificant. The journal applied for SCOPUS and Medline in 2010. It was accepted by SCOPUS, but rejected by Medline.

The members of the society reached a consensus that the journal needs to be all-English; otherwise, the journal can not be indexed globally.

So, although some members still wanted the journal to be published in Korean, the society decided to go with printing an all-English journal (first issue, published in Feb 2012) (Fig. 4) in 2011, and as a result, the journal was soon indexed in PubMed

https://doi.org/10.4132/jptm.2017.01.07

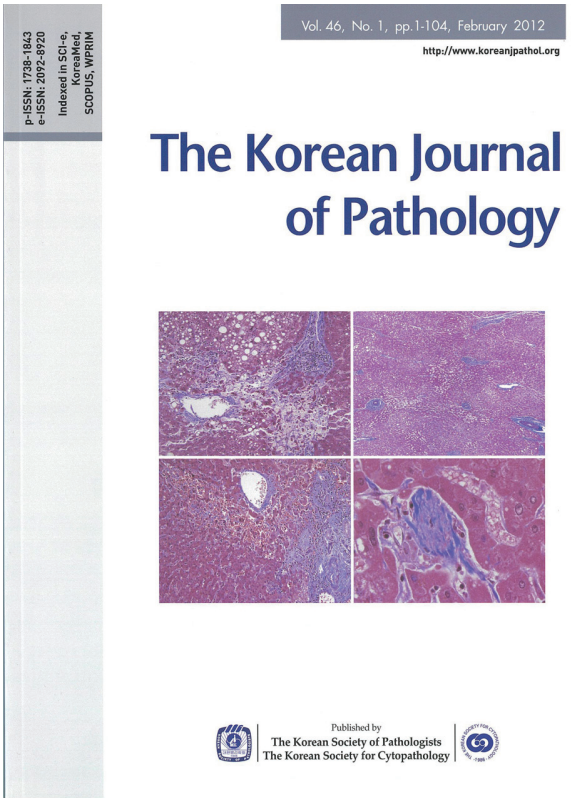

Fig. 4. The first all-English issue of the *Korean Journal of Pathology* in 2012.

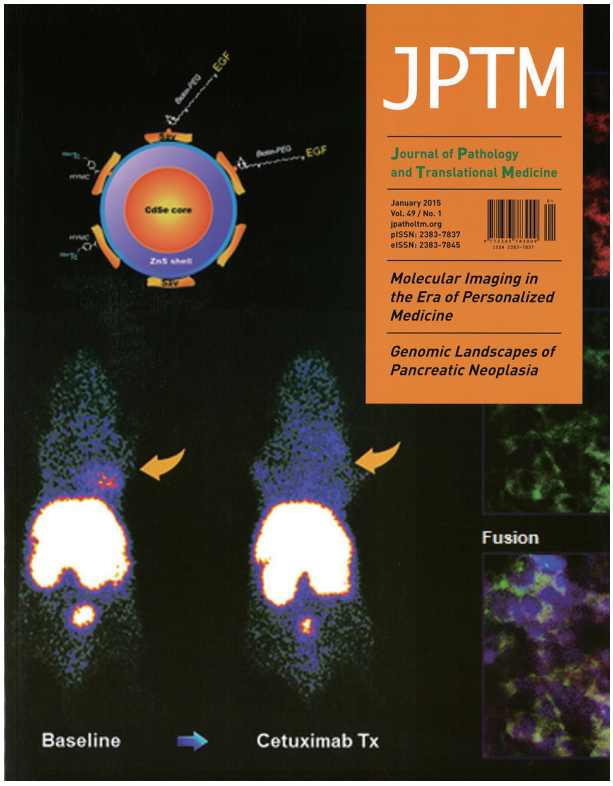

Fig. 5. The first issue of the *Journal of Pathology and Translational Medicine* after the change in name from the *Korean Journal of Pathology* in 2015.

and also in Google Scholar.

In an effort to publish an impactful journal, the society established an electronic submission system through a company named M2 Community and also created journal homepage. In order to upgrade the journal quality and encourage submission of quality articles, all accepted articles were sent for professional English editing. In addition, professional manuscript editors were hired. The journal also adopted CrossCheck and open access. In 2013, Thomson-Reuters dropped the *Korean Journal of Pathology* from SCIE on the grounds that the impact factor was low and in plateau from 2009 to 2012.[11]

With the dropout from SCIE, the society began to actively discuss reapplication for SCIE and sought effective measures. In 2014, Professor SoonWon Hong took charge of the Editorial Board as Editor-in-Chief and began innovative reformation of the journal in every possible way. Soon afterwards, Professor Chong Jai Kim was recruited as co-Editor-in-Chief. The Editorial Board was totally recomposed and internationally renowned foreign editors were additionally invited as contributing editors. In 2015, the journal name was changed to the *Journal of Pathology and Translational Medicine* (JPTM) (Fig. 5) in an effort to renew the journal image as a more globally recognized journal. As can be imagined, it was a very difficult decision for both societies, but the editors unanimously felt the need to discard "Korea" in order to refine the international image of the journal. Instead, "Translational Medicine" was chosen to be added to the journal name with an aim to encourage authors to submit articles in the field of molecular pathology. The volume and issue of the *Korean Journal of Pathology* were conserved in the *Journal of Pathology and Translational Medicine*. The electronic submission system was replaced by ScholarOne of Thomson-Reuters, a more internationally used system. ML Communication, the printing company, was newly selected in place of Academia. Moreover, the journal started e-pub ahead and open access in order to increase the citation rate. Mobile application was developed to enhance accessibility of the journal. The instructions for authors and reviewers were rewritten. Original articles were exempt from publication fee. Authors submitting invited reviews were given an honorarium. Besides these changes in the journal itself, three members of the Editorial Board had acquired membership in the BELS (Board of Editors in the Life Sciences) and became certified editors in the life sciences: SoonWon Hong, Eunah Shin, and Sun Och Yoon. They are expected to contribute to upgrading

the journal quality a step further. In November 2015, Professors SoonWon Hong and Eunah Shin visited Thomson-Reuters in Philadelphia to personally present the many improvements and accomplishments of the journal. In January the following year, Professor SoonWon Hong submitted reapplication for evaluation of the *Journal of Pathology and Translational Medicine* to be indexed in SCIE.[11]

FUTURE OF THE *JOURNAL OF PATHOLOGY AND TRANSLATIONAL MEDICINE*

Re-listing in SCIE is only a short-term goal of the *Journal of Pathology and Translational Medicine*. In the long term, however, we need to focus on the quality improvement of the journal itself. Demands on the development of more accurate evaluation criteria for journal quality have recently been growing, and the change in journal publication in every perspective has been accelerated. In adaptation to these changes, the *Journal of Pathology and Translational Medicine* has to be ready to take a leading role in Asia as a pathology journal with an impact. The Editorial Board will strive to take a step ahead every moment through relentless effort and effective education. The *Journal of Pathology and Translational Medicine* of the Korean Society of Pathologists and the Korean Society for Cytopathology will aspire to be a globally eminent journal leading the frontier in the field of pathology.

CHRONICLES IN BRIEF

1967 Official launch of the *Korean Journal of Pathology*

1981 Official launch of the *Korean Journal of Clinical Pathology*

1990 Official launch of the *Korean Journal of Cytopathology*

2004 Change in the journal title to English (the *Korean Journal of Pathology*) from Korean

2008 Official launch of the *Basic and Applied Pathology*

2009 The *Korean Journal of Pathology* indexed in SCIE

2009 Merger of the *Korean Journal of Cytopathology* with the *Korean Journal of Pathology*

2009 Establishment of electronic submission system

2010 Closure of the *Basic and Applied Pathology*

2011 Start of the *Korean Journal of Pathology* as an all-English journal

2013 The *Korean Journal of Pathology* dropped from SCIE

2015 Change in the name to the *Journal of Pathology and Translational Medicine*

2015 Replacement of the electronic submission system by ScholarOne of Thomson-Reuters

Conflicts of Interest

No potential conflict of interest relevant to this article was reported.

REFERENCES

1. Allen HN. Surgery in the Hermit Kingdom. Medical Record 1885; 27: 671.
2. Avison OR. Disease in Korea. The Korean Repository. Seoul: The Trilingual Press, 1897; 207-11.
3. Weir HH. Arterio-sclerosis, constipation, and animal food. Br Med J 1904; 2: 863.
4. Park HW. History of research in Yonsei University, College of Medicine. Seoul: Yonsei University Press, 2014.
5. Korean Academy of Medical Sciences. The history of the modern Korean medicine. Seoul: Korean Academy of Medical Sciences, 1988.
6. Yoo HS. History of modern medical research in Korea, 1910-1945. Seoul: Korea Institute of Medicine, 2011.
7. Korean Society of Pathologists. The history of the Korean Society of Pathologists: its first 50 years. Seoul: Korean Society of Pathologists, 1996.
8. Chi JG. The Korean Journal of Pathology: a review of the first 25 years. Korean J Pathol 1991; 25: 497-508.
9. Korean Society of Pathologists. The history of the Korean Society of Pathologists (1996-2005). Seoul: Korean Society of Pathologists, 2006.
10. Ro SJ. Theory on arteriosclerosis. Korean J Pathol 1968; 2: 33-7.
11. Korean Society of Pathologists. The history of Korean Society of Pathologists (2006-2015). Seoul: Korean Society of Pathologists, 2016.
12. Korean Society for Cytopathology. The history of the Korean Society for Cytopathology, 1986-2005. Seoul: Korean Society for Cytopathology, 2007.
13. Jin SY, Kang CS. The Korean Journal of Cytopathology: from foundation to unification with the Korean Journal of Pathology. Korean J Pathol 2009; 43: 1-3.
14. Lee DW, Choi IJ, Lee YB, Kim DS. The study on cytopathological diagnosis of carcinoma of the lung. Korean J Pathol 1977; 11: 87-95.
15. Korean Society for Cytopathology. The history of the Korean Society for Cytopathology, 2006-2015. Seoul: Korean Society of Cytopathology, 2016.

Journal of Pathology and Translational Medicine 2017; 51: 7-8
https://doi.org/10.4132/jptm.2016.10.26

Perivascular Epithelioid Cell Tumors (PEComas) of the Orbit

Panagiotis Paliogiannis · Giuseppe Palmieri[1] · Francesco Tanda · Antonio Cossu

Department of Surgical, Microsurgical and Medical Sciences, University of Sassari, Sassari;
[1]Institute of Biomolecular Chemistry, Cancer Genetics Unit, C.N.R., Sassari, Italy

Dear editor,

We read with great interest the case recently reported by Kim *et al*.[1] on a rare malignant perivascular epitheliod cell neoplasm (PEComa) involving the right lung. As mentioned by Kim *et al*.[1] and as we reported in a previous article, PEComas are very rare, with approximately 50 reported cases in several anatomical sites, including the bladder, uterus, vulva, vagina, prostate, lung, liver, pancreas, and other tissues.[2] In this letter, we briefly describe our experience with a PEComa in an unusual anatomical site, the orbit.

The lesion involved a 46-year-old male patient who was referred to surgery for a painful round lesion of the internal aspect of the right orbit. The surgeons removed the lesion, which measured 1.5 cm in maximum diameter and presented a brownish color and a soft-elastic consistency. The lesion was well circumscribed and characterized by an expansive growth pattern. It predominantly comprised epithelioid cells with clear to lightly eosinophilic cytoplasm and occasionally showed granular cell changes. The epithelioid elements were organized in aggregates, trabeculas, and cordons, often surrounding vascular structures (Fig. 1). The nuclei presented a round-shaped, vesicular aspect with frequent nucleoli. The mitotic rate was 2 mitoses per 10 high power fields. No signs of necrosis or vascular invasion were evidenced, and the margins of resection were free of tumor. The immunohistochemical results were as follows: strong positivity for human melanoma black 45 (HMB-45) (Fig. 2) and cathepsin K, weak positivity for actin, and negativity for Melan-A, vimentin, S-100, and cytokeratins. Despite the benign aspect of the lesion and the low mitotic rate, a careful follow-up was suggested,

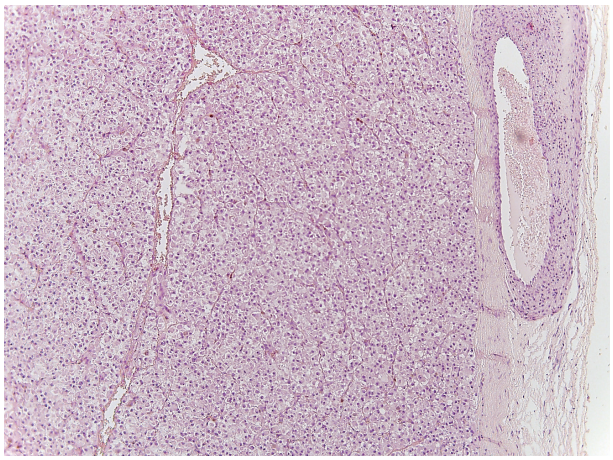

Fig. 1. A section of the lesion stained with hematoxylin and eosin, evidencing its microscopic features and perivascular origin.

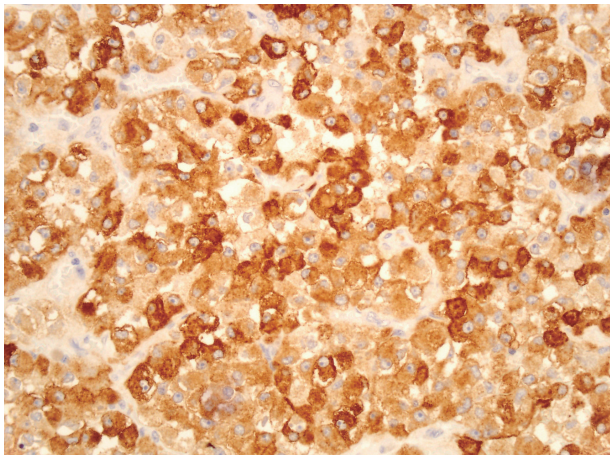

Fig. 2. Human melanoma black 45 immunostaining of the tumor.

Corresponding Author
Panagiotis Paliogiannis, MD, PhD
Department of Surgical, Microsurgical and Medical Sciences, University of Sassari,
Viale San Pietro 43, 07100, Sassari, Italy
Tel: +39079228596, Fax: +39-0079228596,
E-mail: panospaliogiannis@gmail.com

Received: September 29, 2016 **Revised:** October 21, 2016
Accepted: October 26, 2016

pISSN 2383-7837
eISSN 2383-7845

because of the lack of prognostic data due to the small number of cases described in the literature. No recurrence of the disease was observed in the final clinical evaluation 50 months after surgery.

Orbital PEComas are very rare. According to Goto *et al*.,[3] only four cases of PEComa with ocular involvement have been reported in the recent literature, and only two of them originated from the orbit. The first orbital case was described in 2005 by Iyengar *et al*.[4] in a 9-year-old female patient, and the authors demonstrated that characteristic histologic features and an immunohistochemical profile of negativity for epithelial markers and positivity for melanogenesis-related markers are useful to define such lesions. The second case was described in 2008 by Guthoff *et al*.[5] in a 54-year-old man. In that case, the lesion was surgically removed, and no recurrence has occurred after 17 months of follow-up. The tumor showed strong immunohistochemical positivity for both HMB-45 and Melan-A and a low proliferation index (Ki-67 < 1%). Interestingly, in our case, Melan-A was negative, as opposed to the findings of Iyenqar *et al*.[4] and Guthoff *et al*.[5] The low proliferative activity and low mitotic index found in our case suggest that orbital PEComas are generally benign, as those of other anatomical districts. Nevertheless, aggressive PEComas have been described, and this should be considered in cases of orbital PEComas, especially when features of aggressiveness (necrosis, high mitotic rate, great size, infiltrative growth pattern, hypercellularity) are present.

Conflicts of Interest

No potential conflict of interest relevant to this article was reported.

REFERENCES

1. Kim HY, Choi JH, Lee HS, Choi YJ, Kim A, Kim HK. Sclerosing perivascular epithelioid cell tumor of the lung: a case report with cytologic findings. J Pathol Transl Med 2016; 50: 238-42.
2. Cossu A, Paliogiannis P, Tanda F, Dessole S, Palmieri G, Capobianco G. Uterine perivascular epithelioid cell neoplasms (PEComas): report of two cases and literature review. Eur J Gynaecol Oncol 2014; 35: 309-12.
3. Goto H, Usui Y, Nagao T. Perivascular epithelioid cell tumor arising from ciliary body treated by local resection. Ocul Oncol Pathol 2015; 1: 88-92.
4. Iyengar P, Deangelis DD, Greenberg M, Taylor G. Perivascular epithelioid cell tumor of the orbit: a case report and review of the literature. Pediatr Dev Pathol 2005; 8: 98-104.
5. Guthoff R, Guthoff T, Mueller-Hermelink HK, Sold-Darseff J, Geissinger E. Perivascular epithelioid cell tumor of the orbit. Arch Ophthalmol 2008; 126: 1009-11.

 https://doi.org/10.4132/jptm.2016.10.26

Journal of Pathology and Translational Medicine 2017; 51: 9-16
https://doi.org/10.4132/jptm.2016.08.23

■ ORIGINAL ARTICLE ■

Increased Expression of Thymosin β_4 Is Independently Correlated with Hypoxia Inducible Factor-1α (HIF-1α) and Worse Clinical Outcome in Human Colorectal Cancer

Seung Yun Lee · Mee Ja Park
Hye Kyung Lee · Hyun Jin Son
Chang Nam Kim[1] · Joo Heon Kim
Dong Wook Kang

Departments of Pathology and [1]Surgery, Eulji University Hospital, Daejeon, Korea

Received: May 6, 2016
Revised: August 9, 2016
Accepted: August 23, 2016

Corresponding Author
Joo Heon Kim, MD, PhD
Department of Pathology, Eulji University Hospital, 95 Dunsanseo-ro, Seo-gu, Daejeon 35233, Korea
Tel: +82-42-611-3454
Fax: +82-42-611-3459
E-mail: kjh2000@eulji.ac.kr

Dong Wook Kang, MD, PhD
Department of Pathology, Eulji University Hospital, 95 Dunsanseo-ro, Seo-gu, Daejeon 35233, Korea
Tel: +82-42-611-3454
Fax: +82-42-611-3459
E-mail: astrias@eulji.ac.kr

Background: Thymosin β_4 is a multi-functional hormone-like polypeptide, being involved in cell migration, angiogenesis, and tumor metastasis. This study was undertaken to clarify the clinicopathologic implications of thymosin β_4 expression in human colorectal cancers (CRCs). **Methods:** We investigated tissue sections from 143 patients with CRC by immunohistochemistry. In addition, we evaluated the expression patterns and the clinico-pathological significance of thymosin β_4 expression in association with hypoxia inducible factor-1α (HIF-1α) expression in the CRC series. **Results:** High expression of thymosin β_4 was significantly correlated with lymphovascular invasion, invasion depth, regional lymph node metastasis, distant metastasis, and TNM stage. Patients with high expression of thymosin β_4 showed poor recurrence-free survival ($p = .001$) and poor overall survival ($p = .005$) on multivariate analysis. We also found that thymosin β_4 and HIF-1α were overexpressed and that thymosin β_4 expression increased in parallel with HIF-1α expression in CRC. **Conclusions:** A high expression level of thymosin β_4 indicates poor clinical outcomes and may be a useful prognostic factor in CRC. Thymosin β_4 is functionally related with HIF-1α and may be a potentially valuable biomarker and possible therapeutic target for CRC.

Key Words: Thymosin β_4; Hypoxia inducible factor-1α; Hypoxia; Immunohistochemistry; Colorectal cancer

The incidence of colorectal cancer (CRC) has been rapidly increasing and CRC is one of the leading causes of cancer mortality worldwide. Despite earlier detection and advances in molecular pathology-based treatments, we continue to encounter CRC patients with early-stage cancer who present with recurrence. Human CRC is a heterogeneous and complex disease with various genetic and/or epigenetic alterations that result in a biologically aggressive tumor phenotype.[1-3] Various genetic alterations accompanied with genetic instability can be induced in the hypoxic tumor state.[1-7] Interactions between neoplastic cells and the hypoxic microenvironment modify CRC tumor cell phenotype.[8-11]

The β thymosins are a family of hormone-like polypeptides that consist of 40–44 amino acids and are further divided into 15 subfamilies.[12] Of these β thymosins, thymosin β_4 is the most common subtype and the differential expression of thymosin β_4 has been reported in fibrosarcoma,[13] malignant melanoma,[14] breast cancer,[15] gastric cancer,[16] and colon cancer.[17-23] We previously reported that thymosin β_4 expression was increased in breast cancer tissue and correlated this expression with tumor progression and lymph node metastasis via hypoxia inducible factor-1α (HIF-1α) modulation.[24]

In this study, we examined the expression patterns of thymosin β_4 and HIF-1α in 143 CRC patients using immunohistochemical staining. We also evaluated the clinico-pathological significance of thymosin β_4 and HIF-1α expression levels and their correlation with various prognostic factors of CRC.

pISSN 2383-7837
eISSN 2383-7845

MATERIALS AND METHODS

Case selection and immunohistochemistry

CRC cases were selected from patients who underwent surgical treatment at Eulji University Hospital from January 2000 to June 2005. We excluded those specimens obtained from patients who underwent preoperative neoadjuvant chemoradiation. Pertinent clinical and pathological information was obtained from electronic operation records and pathology reports. All cases were histologically confirmed to be primary colorectal adenocarcinoma and hematoxylin and eosin slides were re-evaluated by two independent pathologists. The tumor grade of the adenocarcinoma was classified into low grade (≥50% of tumor glands) and high grade (<50% of tumor glands).[25] For signet ring cell carcinoma and mucinous adenocarcinoma, less than 50% glands were defined as high grade. Tumor budding was defined as a single or group of less than five detached tumor cells and classified into two grades.[26,27] Tumor recurrence was designated as tumor occurring at the anastomosing site, in the regional lymph nodes, and the pelvic cavity diagnosed by radiology, colonoscopy, exploratory surgical, and/or histological examination. In addition, metastasis was defined as the presence of tumor cells outside the area of resection, including the liver, pancreas, lung, and other organs.

All cases of CRC tissue with accompanying normal mucosal tissue were fixed in 10% buffered formalin for 24 hours and embedded in paraffin. Tissue sections of 3–4 μm thickness were cut and mounted on ProbeOn slides (Fisher Scientific, Pittsburgh, PA, USA). Sections that contained both tumor and adjacent uninvolved colonic mucosa were selected for immunohistochemistry (IHC) in most cases. In a few cases, sections were trimmed in order to decrease the surface area for an even distribution of antibodies, so that only the tumor portion was included in the IHC evaluation. IHC conditions for thymosin β_4 and HIF-1α were optimized according to the manufacturers' instructions. Paraffin embedded tissue sections were deparaffinized and rehydrated through a series of xylene and alcohol. Slides were then treated with 10 mM/L sodium citrate buffer (pH 6.1) for 15 minutes and autoclaved at 120°C for antigen retrieval. All slide sections for IHC were incubated in 3% H_2O_2 for 10 minutes to inactivate endogenous peroxidase, washed with 10 mM/L phosphate buffered saline buffer (pH 7.4), and then incubated with normal bovine serum to reduce false-positive staining. Mouse monoclonal antibodies against thymosin β_4 (1:100, Biodesign Int., Saco, ME, USA) and HIF-1α (1:50, Novus Biologicals, Littleton, CO, USA) were used as primary antibodies. Slide sections were incubated with primary antibodies overnight at 4°C in a wet chamber and stained with diaminobenzidine as the substrate using an EnVision-HRP kit (Dako, Glostrup, Denmark). An irrelevant mouse IgG of the same isotype served as a negative control. Sections were counterstained with Mayer's hematoxylin solution and then mounted.

Assessment of IHC staining

To evaluate the expression of thymosin β_4 and HIF-1α in association with various clinico-pathological factors, the immunoreactivity of both thymosin β_4 and HIF-1α were analyzed in a semi-quantitative manner by two independent pathologists who were blinded to outcomes. Immunoreactivity for thymosin β_4 and HIF-1α was observed primarily in the cytoplasm and nuclei of normal mucosal epithelium and tumor cells, respectively. The intensity of immunohistochemical staining was scored as 0 to 2 (0, weaker staining than the normal mucosal epithelium; 1, staining similar to the normal mucosal epithelium; and 2, stronger staining than the normal mucosal epithelium). The percentage of positive cells was scored as 1 (<25% of tumor cells), 2 (25%–49% of tumor cells), 3 (50%–74% of tumor cells), and 4 (≥75% of tumor cells). To evaluate the statistical significance between thymosin β_4 and HIF-1α expression and clinico-pathological factors, the median value (25% of tumor cells showing a strong positive reaction than normal epithelium) of the series was used as the cutoff value to distinguish between tumor cells with low expression (<25% tumor cells) and high expression (≥25% of tumor cells). Cases with conflicting results were re-evaluated and a consensus was reached.

Statistical analysis of prognostic parameters

We performed statistical analysis using the SPSS ver. 18 (SPSS Inc., Chicago, IL, USA). The correlation between thymosin β_4 and the various clinico-pathological parameters were analyzed with the Pearson's chi-square test or Fisher exact test. To evaluate statistical analysis, recurrence-free survival was defined as the duration from the date of surgery to the first date of recurrence or the date of last follow-up. Similarly, overall survival was defined as the duration from the date of surgical therapy to the date of death or date of last follow-up. The mean follow-up duration for all patients was 53.3 months, ranging from 0.6 to 121.9 months. Using the Kaplan-Meier method, the recurrence-free survival curve and the overall survival curve were formulated. To examine the statistical significance of the differences in survival distribution, log-rank test was utilized. Multivariate analysis for overall survival and recurrence-free survival was performed using Cox proportional hazard regression analysis. In all statistical

 https://doi.org/10.4132/jptm.2016.08.23

analyses, p-values less than .05 were considered statistically significant.

Ethical permission

The Institutional Review Board of Eulji University Hospital approved the study protocol and provided all necessary ethical permission.

RESULTS

Association of clinico-pathological characteristics with thymosin β4 and HIF-1α expression status

The median age of the 143 CRC patients (75 men and 68 women) at surgery was 62.2 years (range, 28 to 86 years) and the median tumor size was 5.2 cm (range, 0.8 to 12.0 cm) in maximum diameter. The majority of CRCs were moderately differentiated adenocarcinoma and 111 cases (77.6%) were classified as low grade and 32 cases (22.4%) as high grade (poorly differentiated 19, signet ring cell carcinoma 3, and mucinous carcinoma 10). One hundred and four cases (72.7%) showed lymphovascular tumor invasion and 106 cases (74.1%) exhibited high-grade tumor budding. According to the seventh edition of the AJCC TNM system,[28] 26 patients (18.2%) were diagnosed with early-stage tumor invasion (five cases of pT1 and 21 cases of pT2) and 117 patients (81.8%) were diagnosed with advanced-stage tumor invasion (105 cases of pT3 and 12 cases of pT4). Seventy-six patients (53.1%) presented with regional lymph node metastasis and 22 patients (15.4%) with distant metastasis. Twenty-one patients (14.7%) were at pTNM stage I, 45 patients (31.5%) were at stage II, 55 patients (38.5%) were at stage III, and 22 patients (15.4%) were at stage IV. Twenty-seven patients (18.9%) were treated with chemoradiation after the first surgery (data not shown). Clinico-pathological characteristics of the 143 CRC patients are summarized in Table 1.

In the normal colonic epithelium, immunoreactivity for thymosin β4 and HIF-1α was mostly none or weak. While thymosin β4 expression was found primarily in the cytoplasm of cancer cells, HIF-1α was stained predominantly in the nuclei of tumor cells (Fig. 1A–H). A high level of thymosin β4 and HIF-1α expression was observed in 66 of the 143 patients (46.2%) and in 67 of the 143 patients (46.9%), respectively. We analyzed whether thymosin β4 expression level was associated with clinico-pathological factors. We found that predictive factors for prognosis, such as lymphovascular invasion, invasion depth (pT), regional lymph node metastasis (pN), distant metastasis, and TNM stage showed statistically significant correlations with thymosin β4 immunoreactivity (Table 1). Patients with high thymosin β4 expression levels showed a significantly greater presence of lymphovascular invasion, more frequent regional lymph node metastasis, deeper invasion depth, and more advanced tumor

Table 1. Clinico-pathological variables and thymosin β4 expression status

Characteristic	Total	Thymosin β4 expression level		p-value
		Negative/Low	High	
Age (yr)				
<50	26	10 (13.0)	16 (24.2)	<.082
≥50	117	67 (87.0)	50 (75.8)	
Gender				
Female	68	35 (45.5)	33 (50.0)	<.587
Male	75	42 (54.5)	33 (50.0)	
Site				
Right/Transverse colon	34	20 (26.0)	14 (21.2)	<.505
Left colon and rectum	109	57 (74.0)	52 (78.8)	
Size				<.814
<5 cm in diameter	60	33 (42.9)	27 (40.9)	
≥5 cm in diameter	83	44 (57.1)	39 (59.1)	
Grade				<.926
Low	111	60 (54.1)	51 (45.9)	
High	32	17 (53.1)	15 (46.9)	
LV invasion				<.001*
Not identified	39	31 (40.3)	8 (12.1)	
Present	104	46 (59.7)	58 (87.9)	
Tumor border				.560
Pushing	13	8 (10.4)	5 (7.6)	
Infiltrating	130	69 (90.6)	61 (92.4)	
Tumor budding				<.118
Low	37	24 (31.2)	13 (19.7)	
High	106	53 (68.6)	53 (80.3)	
Invasion depth				<.001*[a]
pT1	5	5 (6.5)	0	
pT2	21	18 (23.4)	3 (4.5)	
pT3	105	50 (64.9)	55 (83.3)	
pT4	12	4 (5.2)	8 (12.1)	
LN metastasis				<.001*
pN0	67	52 (67.5)	15 (22.7)	
pN1	23	8 (10.4)	15 (22.7)	
pN2	53	17 (22.1)	36 (54.5)	
Distant metastasis				<.001*[a]
M0	121	74 (96.1)	47 (71.2)	
M1	22	3 (3.9)	19 (28.8)	
TNM stage				<.001*[a]
I	21	20 (26.0)	1 (1.5)	
II	45	32 (41.6)	13 (19.7)	
III	55	22 (28.6)	33 (50.0)	
IV	22	3 (3.9)	19 (28.8)	

Values are presented as number (%).
LV, lympho-vascular invasion; LN, lymph node.
*p<.05.
[a]Fisher exact test.

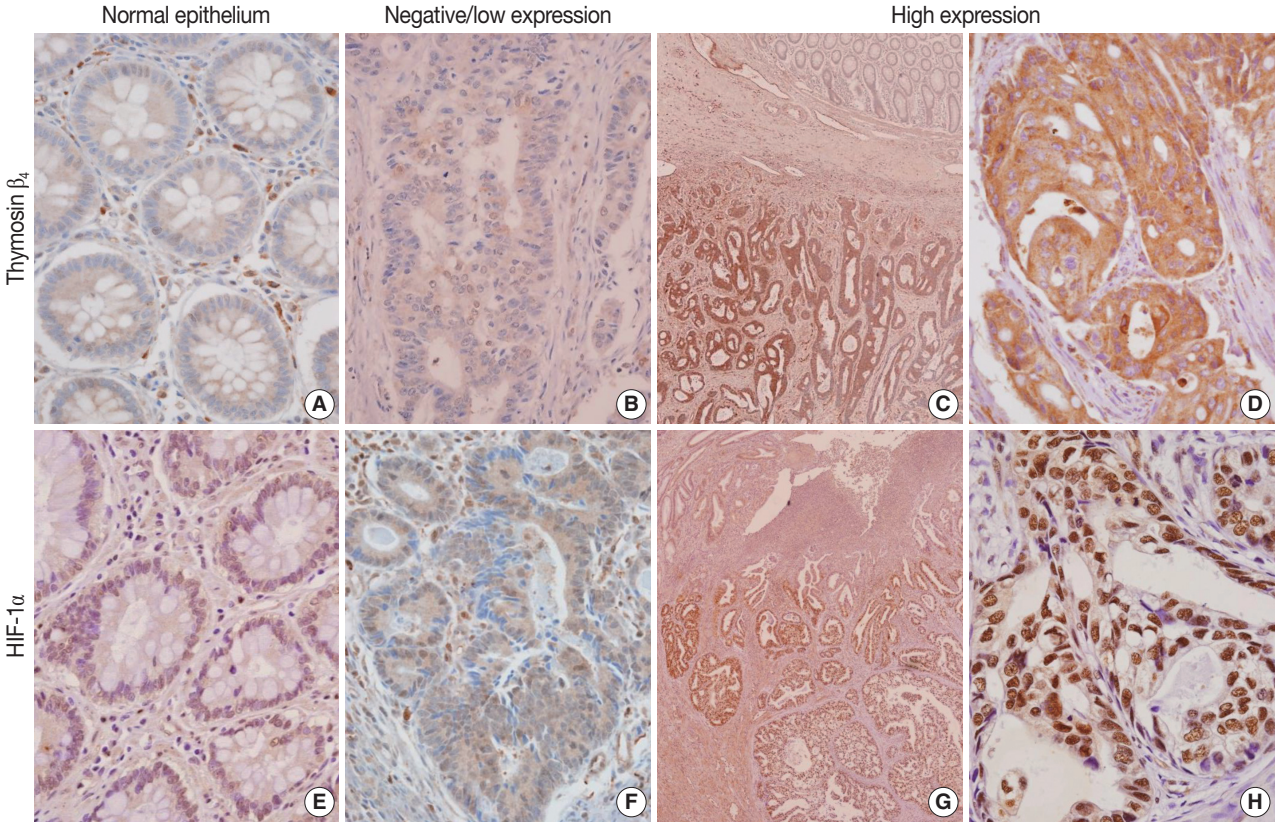

Fig. 1. Immunohistochemical expression of thymosin β_4 (A–D) and hypoxia inducible factor-1α (HIF-1α) (E–H) in human colorectal cancer. (A) No or weak expression of thymosin β_4 in normal colonic epithelium. (B) Low expression of thymosin β_4 in tumor glands. (C) Tumor cells show high thymosin β_4 expression, but no or weak thymosin β_4 expression in normal colonic epithelium. (D) Tumor cells reveal strong thymosin β_4 expression primarily in the cytoplasm of tumor cells. (E) No or weak immunoreactivity of HIF-1α in normal colonic epithelium. (F) Low expression of HIF-1α in tumor cells. (G) Tumor cells show strong HIF-1α expression. (H) HIF-1α is highly expressed predominantly in the nucleus of tumor cells.

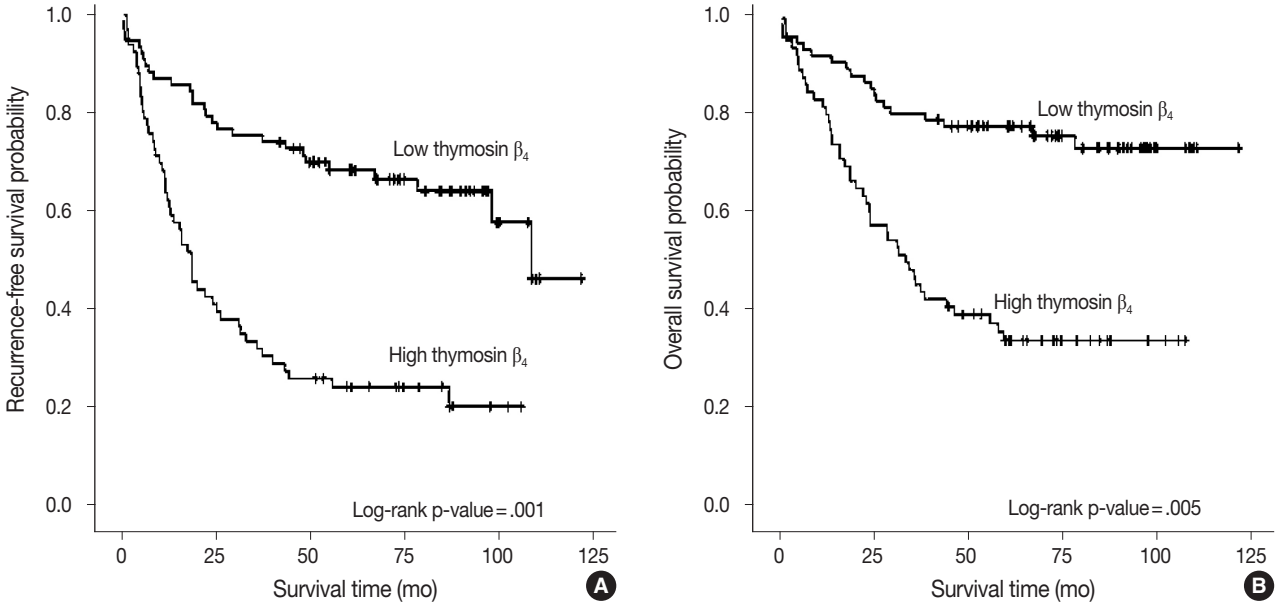

Fig. 2. Kaplan-Meier survival analysis by thymosin β_4 expression status. (A) Cumulative recurrence-free survival differences between patients with high and low thymosin β_4 expression. (B) Cumulative overall survival differences between patients with high and low thymosin β_4 expression. p-values were obtained using the log-rank test of differences.

https://doi.org/10.4132/jptm.2016.08.23

stage than in those with low thymosin β_4 expression levels ($p < .001$). We also evaluated the association between HIF-1α expression levels and clinico-pathological variables. We found a statistically significant correlation between high HIF-1α immunohistochemical expression and clinico-pathological factors such as lymphovascular invasion ($p = .006$), invasion depth ($p = .002$), regional lymph node metastasis ($p = .007$), distant metastasis ($p = .029$), and TNM stage ($p = .002$) (data not shown).

High thymosin β_4 expression level correlated with tumor recurrence and overall survival

We performed multivariate analysis to examine the correlation between thymosin β_4 expression levels with recurrence-free survival and overall survival. Forty patients (28.0%) presented with cancer recurrence during follow-up and 55 patients (38.5%) died of CRC with or without metastasis. Seven patients (4.9%) died of unknown causes, 17 patients (11.9%) were alive with local recurrence and/or distant metastasis, and 64 patients (44.8%) remained alive and recurrence-free. Kaplan-Meier analysis showed that high thymosin β_4 expression was significantly correlated with decreased recurrence-free survival ($p < .001$) (Fig. 2A).

Recurrence-free survival was shorter in patients with high expression levels of thymosin β_4, with a mean duration of 37.3 months (95% confidence interval [CI], 27.833 to 46.684), and was longer in patients with low levels of thymosin β_4 expression, with a mean duration of 84.6 months (95% CI, 73.538 to 95.571). We also found that high thymosin β_4 expression significantly correlated with worse overall survival ($p = .001$). Thymosin β_4 expression status also significantly split the cumulative overall survival curves (Fig. 2B). While the overall survival of CRC patients with high thymosin β_4 expression was mean duration of 51.7 months (95% CI, 41.381 to 61.939), the overall survival of CRC patients with low thymosin β_4 expression was longer with mean duration of 96.8 months (95% CI, 86.952 to 106.732). Multivariate analysis was also performed to assess the prognostic value of thymosin β_4 expression for recurrence-free survival and overall survival using various clinico-pathological parameters. Patients with high thymosin β_4 expression were found to have worse survival outcomes. Statistically significant clinico-pathological factors that were correlated with overall survival were high thymo-

Table 2. Multivariate Cox proportional hazard analysis for recurrence-free survival and overall survival

Characteristic	No.	Recurrence-free survival		Overall survival	
		Relative risk (95% CI)	p-value	Relative risk (95% CI)	p-value
Thymosin β_4			.001*		.005*
Low/negative	77	1.000		1.000	
High	66	2.540 (1.479–4.362)		2.457 (1.315–4.592)	
Size (diameter, cm)			.230		.094
<5	60	1.000		1.000	
≥5	83	1.349 (0.828–2.197)		1.636 (0.919–2.913)	
Grade			.048*		.013*
Low	111	1.000		1.000	
High	32	1.785 (1.005–3.171)		2.241 (1.186–4.236)	
LV invasion			.938		.974
Not identified	39	1.000		1.000	
Present	104	1.025 (0.547–1.922)		1.012 (0.485–2.111)	
Budding			.022*		.047*
Low	37	1.000		1.000	
High	106	2.094 (1.112–3.942)		2.068 (1.010–4.235)	
Invasion depth			.022*		.074
pT1+pT2	26	1.000		1.000	
pT3+pT4	117	3.491 (1.194–10.206)		3.849 (0.878–16.868)	
LN metastasis			.833		.437
Not identified	67	1.000		1.000	
Present	76	1.060 (0.617–1.821)		1.290 (0.678–2.455)	
Distant metastasis			.005*		.001*
M0	121	1.000		1.000	
M1	22	2.368 (1.301–4.311)		2.997 (1.586–5.664)	

p-values were obtained by Cox proportional hazards analysis modeled.
CI, confidence interval; LV, lympho-vascular invasion; LN, lymph node.
*$p < .05$.

sin β_4 expression (p = .005), high tumor grade (p = .013), high tumor budding (p = .047), and presence of distant metastasis (p = .001). The relative risk (RR) of death in patients with a high expression level of thymosin β_4 was more than two times greater (RR, 2.457; 95% CI, 1.315 to 4.592) than those with low thymosin β_4 expression levels. High thymosin β_4 expression was also an independent and relevant factor of decreased recurrence-free survival (p = .001). The RR of recurrence for patients with high thymosin β_4 expression level was 2.540 (95% CI, 1.479 to 4.362). Table 2 summarizes the results from the Cox proportional hazards analysis.

A statistically significant correlation between high HIF-1α expression and high thymosin β_4 expression was also found (p < .001). Specifically, of the 66 cases exhibiting high thymosin β_4 expression, 49 cases (74.2%) also showed high nuclear immunoreactivity of HIF-1α. Of the 77 cases expressing low thymosin β_4 expression, 59 cases (76.6%) revealed corresponding low HIF-1α expression (Table 3).

DISCUSSION

Growing tumors require oxygen and nutrient delivery through neovasculature. However, intratumoral hypoxia induced by imbalance between tumor growth and insufficient angiogenesis can lead to expression of HIF-1α, which is a transcriptional factor that activates tumor survival in an unstable hypoxic tumor microenvironment.[29-32] Recent reports have shown that thymosin β_4 stabilizes HIF-1α in human cancer cells[7] and that thymosin β_4 also induces migration and metastasis of colon cancer cells via the ILK/IQGAP1/Rac1 signal transduction pathway.[22,33]

Few studies have evaluated whether overexpression of thymosin β_4 influences clinical prognosis and whether thymosin β_4 is related to HIF-1α in CRCs. To better understand the relationship, we analyzed the clinical significance and expression status of thymosin β_4 and HIF-1α in CRC patients. Our study demonstrates that high thymosin β_4 expression has a significant association with lymphovascular invasion, nodal status, distant metastasis, and tumor progression in CRC patients (p < .001). This finding is consistent with our previous study showing hypoxia-induced high expression of thymosin β_4, which also significantly correlated with regional lymph node metastasis in breast cancer.[24] In a previous study, we found thymosin β_4 to be up-regulated under hypoxic conditions (5% O_2) using an *in vitro* hypoxia-induced model to generate transcription profiles in human CRC. Based on these findings, for this study we examined the association between thymosin β_4 expression and HIF-1α expression in CRC specimens. We then discovered that the overexpression of thymosin β_4 in CRC is closely related to the restricted overexpression of HIF-1α in the CRC cells (p < .001).

Recently, there have been reports regarding the association between thymosin β_4 expression with tumor development and epithelial mesenchymal transition (EMT).[18,34] In particular, Nemolato *et al.*[34] reported high expression of thymosin β_4 at the invasive front in colon cancer and discussed its associated with EMT as well as invasion and metastasis of tumor cells. However, from our study, since we were unable to find an association between thymosin β_4 expression and tumor budding (p = .118) and tumor border (p = .560), we found the direct association of thymosin β_4 expression with EMT to be weak.

The HIF complex, which involves various hypoxia-regulated genes, is a group of critical gene products in the tumor microenvironment of hypoxic adaptation and in angiogenesis.[35] The HIF complex is also an essential mediator in coordinating transcription of various factors in the tumor cells to survive in the hypoxic environment and its overexpression has been associated with increased mortality in various cancer types.[31,35-37] Among HIF complex proteins, HIF-1α is the best-characterized isoform. Whether HIF-2α, HIF-3α, and HIF-1β also play critical roles in the HIF pathway and regulate HIF target genes is not yet clearly known.[38-41] Hypoxic conditions induce HIF-1α expression in normal cells. HIF-1α is frequently upregulated in various cancer cells and the overexpression of HIF-1α correlates with advanced cancer progression or aggressiveness.[42] However, the clinical significance of HIF-1α in CRC has not been extensively studied. In this study, we observed a significant association between thymosin β_4 expression and HIF-1α expression (p < .001). This result coincides with previous studies that found overexpression of HIF-1α to be associated with poor prognosis.[36,37]

Table 3. Correlation between thymosin β_4 and HIF-1α expression status

	Frequency	Total	HIF-1α		p-value
			High	Low/negative	
Thymosin β_4	High	66	49 (74.2)	17 (25.8)	< .001
	Low/negative	77	18 (23.4)	59 (76.6)	

Values are presented as number (%).
HIF-1α, hypoxia inducible factor-1α.

https://doi.org/10.4132/jptm.2016.08.23

Thymosin β_4 has various functional roles in normal cell biology and its mechanism of action has recently been studied in various tumors. In this study, we found that high cytoplasmic expression of thymosin β_4 is clinically important and an independent prognostic factor for CRC patients. As our results demonstrate that high thymosin β_4 expression significantly correlates with tumor recurrence and worse overall survival, we suggest that high thymosin β_4 expression may be a useful prognostic factor in CRC.

Our results demonstrate that HIF-1α is correlated with overexpression of thymosin β_4 in human CRC. Although further studies are necessary to further validate our findings, we suggest that thymosin β_4, has potential as a prognostic biomarker and has potential as a HIF pathway target in human CRC.

Conflicts of Interest

No potential conflict of interest relevant to this article was reported.

REFERENCES

1. Cannito S, Novo E, Compagnone A, *et al.* Redox mechanisms switch on hypoxia-dependent epithelial-mesenchymal transition in cancer cells. Carcinogenesis 2008; 29: 2267-78.
2. Lluis JM, Buricchi F, Chiarugi P, Morales A, Fernandez-Checa JC. Dual role of mitochondrial reactive oxygen species in hypoxia signaling: activation of nuclear factor-κB via c-SRC and oxidant-dependent cell death. Cancer Res 2007; 67: 7368-77.
3. Sansone P, Piazzi G, Paterini P, *et al.* Cyclooxygenase-2/carbonic anhydrase-IX up-regulation promotes invasive potential and hypoxia survival in colorectal cancer cells. J Cell Mol Med 2009; 13: 3876-87.
4. To KK, Koshiji M, Hammer S, Huang LE. Genetic instability: the dark side of the hypoxic response. Cell Cycle 2005; 4: 881-2.
5. Huang LE, Bindra RS, Glazer PM, Harris AL. Hypoxia-induced genetic instability: a calculated mechanism underlying tumor progression. J Mol Med (Berl) 2007; 85: 139-48.
6. Bristow RG, Hill RP. Hypoxia and metabolism: hypoxia, DNA repair and genetic instability. Nat Rev Cancer 2008; 8: 180-92.
7. Oh JM, Ryoo IJ, Yang Y, Kim HS, Yang KH, Moon EY. Hypoxia-inducible transcription factor (HIF)-1 alpha stabilization by actin-sequestering protein, thymosin beta-4 (TB4) in Hela cervical tumor cells. Cancer Lett 2008; 264: 29-35.
8. Koukourakis MI, Giatromanolaki A, Simopoulos C, Polychronidis A, Sivridis E. Lactate dehydrogenase 5 (LDH5) relates to up-regulated hypoxia inducible factor pathway and metastasis in colorectal cancer. Clin Exp Metastasis 2005; 22: 25-30.
9. Sivridis E, Giatromanolaki A, Koukourakis MI. Proliferating fibroblasts at the invading tumour edge of colorectal adenocarcinomas are associated with endogenous markers of hypoxia, acidity, and oxidative stress. J Clin Pathol 2005; 58: 1033-8.
10. Giles RH, Lolkema MP, Snijckers CM, *et al.* Interplay between VHL/HIF1alpha and Wnt/beta-catenin pathways during colorectal tumorigenesis. Oncogene 2006; 25: 3065-70.
11. Koukourakis MI, Giatromanolaki A, Polychronidis A, *et al.* Endogenous markers of hypoxia/anaerobic metabolism and anemia in primary colorectal cancer. Cancer Sci 2006; 97: 582-8.
12. Huff T, Müller CS, Otto AM, Netzker R, Hannappel E. Beta-thymosins, small acidic peptides with multiple functions. Int J Biochem Cell Biol 2001; 33: 205-20.
13. Kobayashi T, Okada F, Fujii N, *et al.* Thymosin-beta4 regulates motility and metastasis of malignant mouse fibrosarcoma cells. Am J Pathol 2002; 160: 869-82.
14. Clark EA, Golub TR, Lander ES, Hynes RO. Genomic analysis of metastasis reveals an essential role for RhoC. Nature 2000; 406: 532-5.
15. Xie D, Jauch A, Miller CW, Bartram CR, Koeffler HP. Discovery of over-expressed genes and genetic alterations in breast cancer cells using a combination of suppression subtractive hybridization, multiplex FISH and comparative genomic hybridization. Int J Oncol 2002; 21: 499-507.
16. Kim L, Kim YJ, Choi SJ, *et al.* Prognostic significance of thymosin- 4 in gastric adenocarcinoma patients. Korean J Pathol 2007; 41: 176-82.
17. Hsiao HL, Wang WS, Chen PM, Su Y. Overexpression of thymosin beta-4 renders SW480 colon carcinoma cells more resistant to apoptosis triggered by FasL and two topoisomerase II inhibitors via downregulating Fas and upregulating Survivin expression, respectively. Carcinogenesis 2006; 27: 936-44.
18. Huang HC, Hu CH, Tang MC, Wang WS, Chen PM, Su Y. Thymosin beta4 triggers an epithelial-mesenchymal transition in colorectal carcinoma by upregulating integrin-linked kinase. Oncogene 2007; 26: 2781-90.
19. Wang WS, Chen PM, Hsiao HL, Ju SY, Su Y. Overexpression of the thymosin beta-4 gene is associated with malignant progression of SW480 colon cancer cells. Oncogene 2003; 22: 3297-306.
20. Wang WS, Chen PM, Hsiao HL, Wang HS, Liang WY, Su Y. Overexpression of the thymosin beta-4 gene is associated with increased invasion of SW480 colon carcinoma cells and the distant metastasis of human colorectal carcinoma. Oncogene 2004; 23: 6666-71.
21. Wang WS, Chen PM, Su Y. Colorectal carcinoma: from tumorigenesis to treatment. Cell Mol Life Sci 2006; 63: 663-71.
22. Piao Z, Hong CS, Jung MR, Choi C, Park YK. Thymosin beta4 induces invasion and migration of human colorectal cancer cells through the ILK/AKT/beta-catenin signaling pathway. Biochem

Biophys Res Commun 2014; 452: 858-64.
23. Kang YJ, Jo JO, Ock MS, *et al.* Thymosin beta4 was upregulated in recurred colorectal cancers. J Clin Pathol 2014; 67: 188-90.
24. Yoon SY, Lee HR, Park Y, *et al.* Thymosin beta4 expression correlates with lymph node metastasis through hypoxia inducible factor-alpha induction in breast cancer. Oncol Rep 2011; 25: 23-31.
25. Washington MK, Berlin J, Branton P, *et al.* Protocol for the examination of specimens from patients with primary carcinoma of the colon and rectum. Arch Pathol Lab Med 2009; 133: 1539-51.
26. Prall F. Tumour budding in colorectal carcinoma. Histopathology 2007; 50: 151-62.
27. Wang LM, Kevans D, Mulcahy H, *et al.* Tumor budding is a strong and reproducible prognostic marker in T3N0 colorectal cancer. Am J Surg Pathol 2009; 33: 134-41.
28. Puppa G. TNM staging system of colorectal carcinoma: surgical pathology of the seventh edition. Diagn Histopathol 2011; 17: 243-62.
29. Höckel M, Vaupel P. Biological consequences of tumor hypoxia. Semin Oncol 2001; 28(2 Suppl 8): 36-41.
30. Foo SS, Abbott DF, Lawrentschuk N, Scott AM. Functional imaging of intratumoral hypoxia. Mol Imaging Biol 2004; 6: 291-305.
31. Mabjeesh NJ, Amir S. Hypoxia-inducible factor (HIF) in human tumorigenesis. Histol Histopathol 2007; 22: 559-72.
32. Lee JW, Ryu YK, Ji YH, Kang JH, Moon EY. Hypoxia/reoxygenation-experienced cancer cell migration and metastasis are regulated by Rap1- and Rac1-GTPase activation via the expression of thymosin beta-4. Oncotarget 2015; 6: 9820-33.
33. Tang MC, Chan LC, Yeh YC, *et al.* Thymosin beta 4 induces colon cancer cell migration and clinical metastasis via enhancing ILK/IQGAP1/Rac1 signal transduction pathway. Cancer Lett 2011; 308: 162-71.
34. Nemolato S, Restivo A, Cabras T, *et al.* Thymosin beta 4 in colorectal cancer is localized predominantly at the invasion front in tumor cells undergoing epithelial mesenchymal transition. Cancer Biol Ther 2012; 13: 191-7.
35. Jo JO, Kim SR, Bae MK, *et al.* Thymosin beta4 induces the expression of vascular endothelial growth factor (VEGF) in a hypoxia-inducible factor (HIF)-1alpha-dependent manner. Biochim Biophys Acta 2010; 1803: 1244-51.
36. Brahimi-Horn MC, Pouysségur J. HIF at a glance. J Cell Sci 2009; 122(Pt 8): 1055-7.
37. Ryan HE, Poloni M, McNulty W, *et al.* Hypoxia-inducible factor-1alpha is a positive factor in solid tumor growth. Cancer Res 2000; 60: 4010-5.
38. Swami M. Hypoxia: the HIF2alpha puzzle. Nat Rev Cancer 2010; 10: 603.
39. Gu YZ, Moran SM, Hogenesch JB, Wartman L, Bradfield CA. Molecular characterization and chromosomal localization of a third alpha-class hypoxia inducible factor subunit, HIF3alpha. Gene Expr 1998; 7: 205-13.
40. Kietzmann T, Cornesse Y, Brechtel K, Modaressi S, Jungermann K. Perivenous expression of the mRNA of the three hypoxia-inducible factor alpha-subunits, HIF1alpha, HIF2alpha and HIF3alpha, in rat liver. Biochem J 2001; 354(Pt 3): 531-7.
41. Clottes E. Hypoxia-inducible factor 1: regulation, involvement in carcinogenesis and target for anticancer therapy. Bull Cancer 2005; 92: 119-27.
42. Zhong H, De Marzo AM, Laughner E, *et al.* Overexpression of hypoxia-inducible factor 1alpha in common human cancers and their metastases. Cancer Res 1999; 59: 5830-5.

 https://doi.org/10.4132/jptm.2016.08.23

Journal of Pathology and Translational Medicine 2017; 51: 17-23
https://doi.org/10.4132/jptm.2016.09.23

■ ORIGINAL ARTICLE ■

Clinicopathologic Significance of Survivin Expression in Relation to CD133 Expression in Surgically Resected Stage II or III Colorectal Cancer

Wanlu Li[1] · Mi-Ra Lee[1] · EunHee Choi[2] · Mee-Yon Cho[1,3]

[1]Department of Pathology, [2]Institute of Lifestyle Medicine, [3]Institute of Genomic Cohort, Yonsei University Wonju College of Medicine, Wonju, Korea

Received: July 18, 2016
Revised: September 20, 2016
Accepted: September 23, 2016

Corresponding Author
Mee-Yon Cho, MD, PhD
Department of Pathology, Yonsei University Wonju College of Medicine, 20 Ilsan-ro, Wonju 26426, Korea
Tel: +82-33-731-1553
Fax: +82-33-731-6590
E-mail: meeyon@yonsei.ac.kr

Background: Cancer stem cells have been investigated as new targets for colorectal cancer (CRC) treatment. We recently reported that CD133$^+$ colon cancer cells showed chemoresistance to 5-fluorouracil through increased survivin expression and proposed the survivin inhibitor YM155 as an effective therapy for colon cancer in an *in vitro* study. Here, we investigate the relationship between survivin and CD133 expression in surgically resected CRC to identify whether the results obtained in our *in vitro* study are applicable to clinical samples. **Methods:** We performed immunohistochemical staining for survivin and CD133 in surgically resected tissue from 187 stage II or III CRC patients. We also comparatively analyzed apoptosis according to survivin and CD133 expression using terminal deoxynucleotidyl transferase-mediated deoxyuridine triphosphate nick-end labeling. **Results:** The results of the Mantel-Haenszel test established a linear association between nuclear survivin and CD133 expression ($p = .018$), although neither had prognostic significance, according to immunohistochemical expression level. No correlation was found between survivin expression and the following pathological parameters: invasion depth, lymph node metastasis, or histologic differentiation ($p > .05$). The mean apoptotic index in survivin$^+$ and CD133$^+$ tumors was higher than that in negative tumors: 5.116 ± 4.894 in survivin$^+$ versus 4.103 ± 3.691 in survivin$^-$ ($p = .044$); 5.165 ± 4.961 in CD133$^+$ versus 4.231 ± 3.812 in CD133$^-$ ($p = .034$). **Conclusions:** As observed in our *in vitro* study, survivin expression is significantly related to CD133 expression. Survivin may be considered as a new therapeutic target for chemoresistant CRC.

Key Words: Colorectal neoplasms; Neoplastic stem cells; Survivin; CD133 protein; Apoptosis

Colorectal cancer (CRC) is the third most common cancer and the fourth most common cause of cancer-related death worldwide.[1] Despite the availability of preventive measures, early screening tests, and improved surgical treatments and chemotherapy, the mortality rate remains high. The complexity of mechanisms involved in tumor recurrence, metastasis, and chemoresistance[2] has spurred cancer stem cell studies to seek novel and more effective targets for CRC treatment. In our *in vitro* study, we found that CD133$^+$ cells showed high levels of survivin expression, which was related to chemoresistance to 5-fluorouracil (5-FU), and a survivin inhibitor was more effective than 5-FU in decreasing the viability of colon cancer cells.[3,4]

CD133, a transmembrane glycoprotein, is a cancer stem cell marker in several human tumors,[5] including CRC.[6] CD133 expression in CRC has been reported to be associated with Wnt,[7,8] Notch,[9] STAT3,[10] and transforming growth factor-beta signaling pathways,[11] which are essential for self-renewal,[2] tumorigenesis,[2] progression,[12] and chemoresistance in CRC.[3] However, the relationship of CD133 with survivin expression in clinical samples has not been evaluated.

Since tumor development and progression are based on the balance of cell apoptosis and proliferation, Alcaide *et al.*[13] described that a higher rate of apoptosis is associated with more aggressive behavior of tumors and poorer prognosis in CRC patients. Survivin, a member of the inhibitor of apoptosis family, plays a dual role in cell apoptosis and proliferation. As a subunit of the chromosomal passenger complex, nuclear survivin regulates the chromosomal central spindle in various cell division processes, whereas cytoplasmic survivin inhibits apoptosis. This suggests that survivin can be a good target for cancer therapy because it promotes cell survival.[14] In meta-analyses, survivin expression has shown a positive correlation with poorer prognosis in CRC patients.[15,16] However, a previous study has reported that survivin expression was associated with good prognosis.[17] Furthermore, most immunohistochemical studies of survivin did not clearly define the sublocation of survivin expression. Therefore, the clinical significance of survivin expression in CRC remains to be clarified.

The aim of the present study was to determine the clinico-

pISSN 2383-7837
eISSN 2383-7845

pathologic significance of survivin expression in relation to CD133 expression in CRC. In addition, we comparatively analyzed apoptosis according to survivin and CD133 expression in CRC.

MATERIALS AND METHODS

Patients and tissue samples

We used formalin-fixed and paraffin-embedded tissues from surgically resected stage II or III CRCs that were registered to the Department of Pathology at Wonju Severance Christian Hospital between January 2000 and December 2006. We analyzed the data from 187 patients with follow-up information. Patients who received preoperative chemotherapy or radiotherapy were excluded. Clinicopathological data of patient age, sex, tumor location, invasion depth, histologic differentiation, and lymph node metastasis were collected from pathology reports.

Ethics approval

This study was approved by the Institutional Ethics Committee of Yonsei University, Wonju College of Medicine (YWMR-14-4-102) and was carried out in compliance with the guidelines of the Declaration of Helsinki.

Immunohistochemical staining

Paraffin-embedded tissue sections from representative blocks were warmed to 75°C for 4 minutes. Slides were deparaffinized with EZPrep (Ventana Medical Systems, Tucson, AZ, USA), and an antigen-retrieval step was performed for 60 minutes with cell conditioning solution #1 for survivin staining and #2 for CD133 staining (Ventana Medical Systems). Then, endogenous peroxidase activity was blocked by applying an ultraviolet inhibitor for 4 minutes. After washing with the reaction buffer several times at room temperature (RT), an Ultra View Universal DAB Detection Kit (Ventana Medical Systems) was used for immunohistochemical (IHC) staining. The slides were incubated with monoclonal antibodies against survivin (Abcam, Cambridge, MA, USA) for 1 hour and against CD133/1 (MACS, Miltenyi Biotec, Bergisch Gladbach, Germany) for 2 hours at 37°C in an autostainer (Benchmark XT, Ventana Medical Systems). After incubating with the primary antibodies, the slides were rinsed with the reaction buffer. Drops of HRP UNIV MULT, DAB, and DAB H_2O_2 (Ventana Medical Systems) were applied sequentially on each slide (8 minutes per reagent), with intermittent rinsing with reaction buffer. The slides were then treated with a drop of COPPER for 4 minutes. Finally, a bluing agent was added and rinsed with reaction buffer. In addition, the sections were counterstained with hematoxylin for nuclei staining.

CD133 and survivin expression was manually counted in selected hot-spot fields.

IHC expression for CD133 was scored as 0 when there was no expression, 1+ when the expression for CD133 was detected in 1%–10% of the whole tumor area, and 2+ and 3+ when the expression was in 11%–50% and 51%–100% of the tumor area, respectively. We set a cut-off point at 10% between the positive and negative groups. Survivin expression was scored as 1+ (0%–25%), 2+ (26%–50%), 3+ (51%–75%), and 4+ (76%–100%) according to the level of nuclear reactivity among total tumor cells.[18] We set a cut-off point at 25% between the positive and negative groups. The IHC staining results were independently evaluated by two pathologists who were unaware of patient clinical and pathological information. Discrepancies between the pathologists were resolved by consensus.

Terminal deoxynucleotidyl transferase-mediated deoxyuridine triphosphate nick-end labeling assay

All patient samples were stained using an In situ Cell Death Detection Kit (Roche Diagnostics, Mannheim, Germany) in formalin-fixed and paraffin-embedded sections. The slides were deparaffinized and rehydrated. After washing, the slides were incubated for 30 minutes at RT with 0.1 M Tris-HCl (pH 7.5), 3% bovine serum albumin, and 20% normal bovine serum for blocking. Then, the slides were washed twice with phosphate-buffered saline (PBS). The terminal deoxynucleotidyl transferase-mediated deoxyuridine triphosphate nick-end labeling (TUNEL) reaction mixture (50 μL) was applied to each section for 1 hour at 37°C in a humidified chamber. After three washes with PBS, the slides were treated with 0.3% H_2O_2 in methanol for 10 minutes (RT). The blocking step was then repeated.

After washing with PBS, 50 mL Converter-POD was applied to each slide, and the slides were incubated for 30 minutes at 37°C in a humidified chamber. After three washes with PBS, 100 μL DAB substrate solution was added, and the slides were incubated for 1–3 minutes at RT. The slides were then washed thoroughly with tap water and counterstained with hematoxylin before mounting. Under light microscopy, we calculated the apoptotic index (AI) by counting the number of apoptotic nuclei per 1,000 cells in a high-power field. Cells were considered positive if the entire nuclear area of the cell was stained brown. Cells in areas with necrosis and the margins of sections were excluded from the analysis.

https://doi.org/10.4132/jptm.2016.09.23

Statistical analysis

Data are displayed according to the properties of the variable. Continuous variables are presented as mean and standard deviation. Categorical variables are noted as frequency and percentage. The Mantel-Haenszel test was performed to evaluate the linear association between two variables on an ordinal scale. To compare the survivin IHC groups, we performed one-way analysis of variance or the chi-square test (Fisher exact test), as appropriate. The survival curve was estimated by the Kaplan-Meier method and was compared by the log-rank test. To estimate hazard ratio and 95% confidence interval, we used a Cox proportional hazard regression model. A p-value less than 0.05 was considered statistically significant, and all statistical analyses were performed with SAS ver. 9.2 (SAS Inc., Cary, NC, USA).

RESULTS

Relationships between survivin expression, clinicopathological parameters, and CD133 expression

The demography of cases examined in this study is presented in Table 1. Representative cases with high and low survivin expression are shown in Fig. 1A–D with matched CD133 expression. CD133 showed a luminal membranous expression pattern (Fig. 1A), whereas survivin showed distinct nuclear expression with weak and vague cytoplasmic expression in CRC cells (Fig. 1B). We analyzed only the nuclear survivin expression in this

Table 1. Patients demographics for the current study

	No. (%)
Sex	
Male	117 (62.5)
Female	70 (37.4)
Age (yr)	
≥50	156 (83.4)
<50	31 (16.6)
Tumor differentiation grade	
Well differentiated	10 (5.3)
Moderately differentiated	159 (85)
Poorly differentiated	18 (9.6)
Tumor stage	
II	72 (38.5)
III	115 (61.5)
Location	
Cecum, appendix, and ascending colon	44 (23.5)
Transverse, descending, and sigmoid colon	64 (34.2)
Rectum	79 (42.2)
Regional lymph node	
N0	73 (39)
N1	70 (37.4)
N2	44 (23.5)

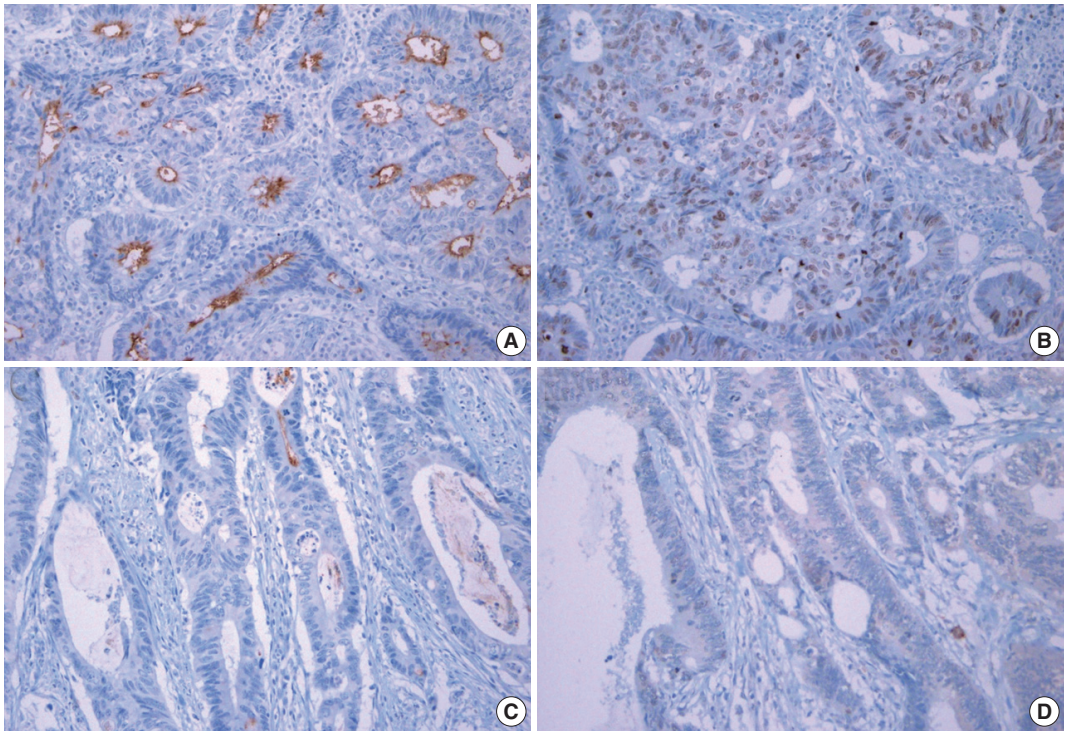

Fig. 1. Photomicrographs showing representative cases of high CD133 (A) and survivin (B) expression and low CD133 (C) and survivin (D) expression in colorectal cancer tumor cells. CD133 expression localized to the luminal surface of the cytoplasm, and survivin expression localized to the nucleus.

study because the cytoplasmic expression was too diffuse and weak to be scored.

Survivin expression showed a significant correlation with CD133 expression (p = .018) when analyzed by the Mantel-Haenszel test; however, survivin showed no significant relationship with other pathological parameters (Table 2).

Survival analysis according to survivin expression

The mean overall survival (OS) according to survivin expression was 113.1 ± 9.1 months for score 1+, 47.0 ± 1.7 months for score 2+, 41.8 ± 1.4 months for score 3+, and 7.4 ± 0.1 months for score 4+. However, survivin expression had no prognostic significance in the survival analysis (p = .480). Disease-free survival was also not related to survivin expression (p = .488).

Difference in apoptosis according to survivin and CD133 expression

Apoptosis detected by TUNEL analysis showed rare positive cells in normal mucosa (Fig. 2A), in contrast to occasionally scattered positive cells in CRC cells (Fig. 2B). AI was significantly higher in $CD133^+$ tumors (5.165 ± 4.961) than in $CD133^-$

Table 2. Survivin expression according to the pathologic parameters (n = 187)

Parameter	Survivin expression (number of cases)				Total	p-value
	1+	2+	3+	4+		
Histologic differentiation						.531
Well	2	4	4	0	10	
Moderate	32	52	59	16	159	
Poor	5	3	7	3	18	
Invasion depth						.267
T2	1	3	3	1	8	
T3	36	52	60	16	164	
T4	2	4	7	2	15	
Lymph node metastasis						.815
N0	17	20	26	10	73	
N1	13	25	27	5	70	
N2	9	14	17	4	44	
Adjuvant therapy						.297
Yes	32	54	65	18	169	
No	7	5	5	1	18	
CD133 IHC expression						.018
Negative	18	14	18	3	53	
1+	11	12	15	6	44	
2+	3	16	12	5	36	
3+	7	17	25	5	54	

IHC, immunohistochemistry.

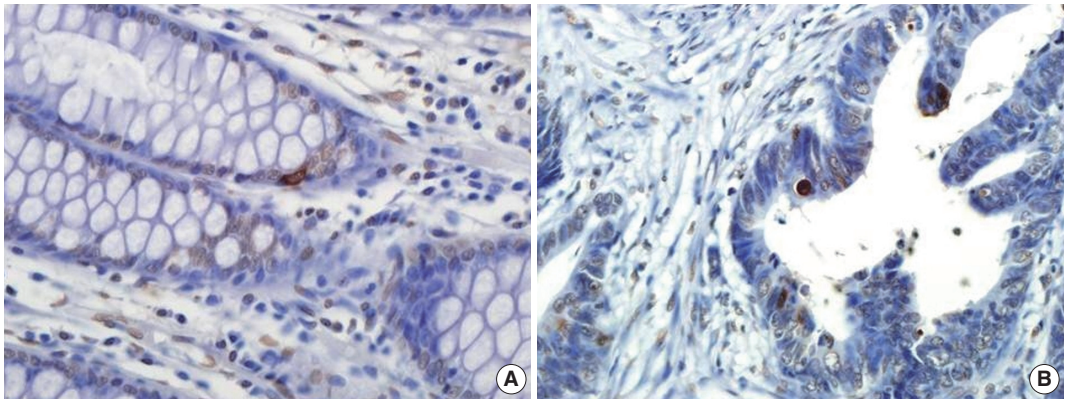

Fig. 2. There was rare apoptosis in normal mucosa (A), but scattered positively-stained apoptotic cells in colorectal cancer (B) were observed by the terminal deoxynucleotidyl transferase-mediated deoxyuridine triphosphate nick-end labeling assay.

https://doi.org/10.4132/jptm.2016.09.23

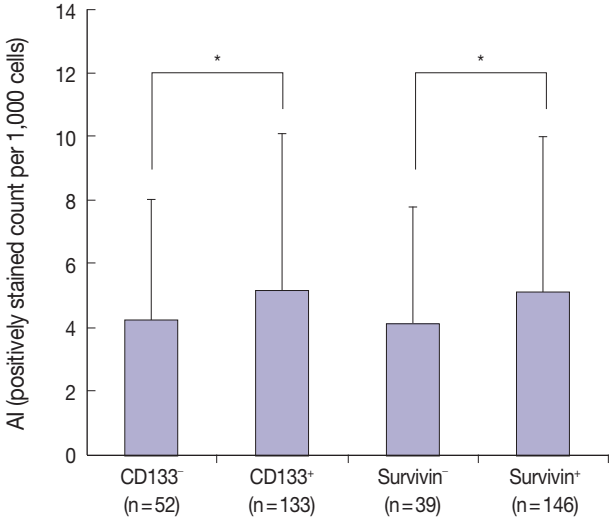

Fig. 3. Compared with that in CD133⁻ and survivin⁻ tumors, the mean apoptotic index (AI) obtained by the transferase-mediated deoxyuridine triphosphate nick-end labeling assay was significantly higher in CD133⁺ and survivin⁺ tumors (*p<.05).

tumors (4.231 ± 3.812, p = .034). Further, compared with survivin⁻ tumors, survivin⁺ tumors had a higher AI (5.116 ± 4.894 vs 4.103 ± 3.691, p = .044) (Fig. 3).

DISCUSSION

In our previous *in vitro* study, we described that CD133⁺ colon cancer cells showed chemoresistance to 5-FU through high survivin expression. In addition, we demonstrated that the survivin inhibitor YM155 was more effective than 5-FU in inducing cell death of colon cancer cells.[4] YM155 is a novel small-molecule survivin inhibitor that acts by inhibiting survivin promoter activity.[19] Inhibitors of apoptosis have been used as new targeted therapies in CRC.[20] Recently, Gyuraszova *et al*.[21] also reported that the combined use of YM155 with hypericin is effective in the treatment of CRC and lung adenocarcinoma through induction of apoptosis. To determine whether the results of our *in vitro* study are applicable to clinical samples, we examined the significance of survivin expression in relation to clinicopathological parameters and CD133 expression of CRC in the present study. We found a correlation between CD133 expression and nuclear survivin expression in CRC in a sample size of 187. It agrees with our previous *in vitro* study, which indicates that both the mRNA and protein expression levels of survivin in CD133⁺ cells are remarkably higher than those in small interfering RNA (siRNA)-induced CD133⁻ cells,[3] These findings are also concordant with those of the transcriptome analysis reported by Kim *et al*.[22]

In two recently published meta-analyses, the authors concluded that survivin expression is closely associated with high mortality.[16,23] However, these studies did not specify whether the positive correlation was observed with nuclear or cytoplasmic survivin expression. In most data used in these meta-analyses, the subcellular localization of survivin expression was unstated or cytoplasmic. As previously mentioned, nuclear survivin expression can improve cell proliferation by regulating chromosome alignment and segregation in mitosis, whereas cytoplasmic survivin expression inhibits the apoptosis pathway. Another recent report suggested that nuclear survivin expression is related to better patient prognosis.[17] However, this finding is contrasted with results reported by Kim *et al*.,[22] who showed that nuclear survivin expression can be an independent poor prognostic factor for disease-free survival and OS. It remains controversial whether nuclear survivin expression is related to patient prognosis. Nuclear survivin expression has been reported to be significantly higher than cytoplasmic expression in CRC.[24] Therefore, further large-scale studies are required to confirm the prognostic significance of subcellular survivin expression in CRC.

In a previous study, we found that CD133 expression was related to survivin expression in CRC cell lines.[3,4] However, we found that survivin expression increased in Caco-2 cells after transfection with Ctrl-siRNA and CD133-siRNA. This may indicate that transfection affects survivin expression as a cell-damaging force. To avoid the bias induced by transfection, we analyzed survivin and CD133 expression together with apoptosis in clinical samples of CRC.

The balance between proliferation and apoptosis maintains the homeostasis of the colonic epithelium, but uncontrolled cell proliferation and apoptosis contribute to tumor development.[18] Alcaide *et al*.[13] reported that AI in CRC is higher than that in adenomas and normal tissue. We also found that AI in tumor tissue was higher than that in the surrounding normal mucosa. In addition, CD133⁺ and survivin⁺ tumors showed a higher mean AI than CD133⁻ and survivin⁻ tumors. However, AI was not significantly related with either survivin or CD133 expression in this study. Bedi *et al*.[25] reported that apoptosis is inhibited during CRC development, owing to abnormal expression of the *BCL2* gene. Zhao *et al*.[26] reported that a low dose of bcl-2 inhibitor could up-regulate survivin expression in hepatocellular carcinoma. These results indicate that apoptosis is regulated by not only survivin, but also bcl-2. In addition, the effects of apoptotic proteins on CD133⁺ colon cancer cells have been rarely reported. In a study by Kemper *et al*.,[27] activated caspase-9 was found to induce a high level of apoptosis in CD133⁺ CRC stem cells.

Sam *et al*.[28] demonstrated that inhibiting survivin and caspase 3 triggers apoptosis in colon cancer stem-like cells.

In this study, we found that nuclear survivin expression was correlated with CD133 expression in CRC, although it was not significantly related to pathological parameters or patient prognosis. Further *in vivo* investigations of the effect of survivin inhibitors and the mechanism of survivin expression in relation to cancer stem cell markers are required for verifying whether survivin is a new target for more effective treatment of CRC.

Conflicts of Interest

No potential conflict of interest relevant to this article was reported.

Acknowledgments

This study was supported by a research grant from the Korea Science and Engineering Foundation funded by the Korean government (Ministry of Education, Science, and Technology, grant code: 2015-51-0329).

REFERENCES

1. Ferlay J, Soerjomataram I, Dikshit R, *et al*. Cancer incidence and mortality worldwide: sources, methods and major patterns in GLOBOCAN 2012. Int J Cancer 2015; 136: E359-86.
2. Ren F, Sheng WQ, Du X. CD133: a cancer stem cells marker, is used in colorectal cancers. World J Gastroenterol 2013; 19: 2603-11.
3. Lee MR, Ji SY, Mia-Jan K, Cho MY. Chemoresistance of CD133(+) colon cancer may be related with increased survivin expression. Biochem Biophys Res Commun 2015; 463: 229-34.
4. Li WL, Lee MR, Cho MY. The small molecule survivin inhibitor YM155 may be an effective treatment modality for colon cancer through increasing apoptosis. Biochem Biophys Res Commun 2016; 471: 309-14.
5. Sung JJ, Noh SJ, Bae JS, *et al*. Immunohistochemical expression and clinical significance of suggested stem cell markers in hepatocellular carcinoma. J Pathol Transl Med 2016; 50: 52-7.
6. Dalerba P, Dylla SJ, Park IK, *et al*. Phenotypic characterization of human colorectal cancer stem cells. Proc Natl Acad Sci U S A 2007; 104: 10158-63.
7. Deng YH, Pu XX, Huang MJ, *et al*. 5-Fluorouracil upregulates the activity of Wnt signaling pathway in CD133-positive colon cancer stem-like cells. Chin J Cancer 2010; 29: 810-5.
8. Corbo C, Orrù S, Gemei M, *et al*. Protein cross-talk in CD133+ colon cancer cells indicates activation of the Wnt pathway and up-regulation of SRp20 that is potentially involved in tumorigenicity. Proteomics 2012; 12: 2045-59.
9. Sikandar SS, Pate KT, Anderson S, *et al*. NOTCH signaling is required for formation and self-renewal of tumor-initiating cells and for repression of secretory cell differentiation in colon cancer. Cancer Res 2010; 70: 1469-78.
10. Lin L, Fuchs J, Li C, Olson V, Bekaii-Saab T, Lin J. STAT3 signaling pathway is necessary for cell survival and tumorsphere forming capacity in ALDH(+)/CD133(+) stem cell-like human colon cancer cells. Biochem Biophys Res Commun 2011; 416: 246-51.
11. Roy S, Majumdar AP. Signaling in colon cancer stem cells. J Mol Signal 2012; 7: 11.
12. Dick JE. Looking ahead in cancer stem cell research. Nat Biotechnol 2009; 27: 44-6.
13. Alcaide J, Funez R, Rueda A, *et al*. The role and prognostic value of apoptosis in colorectal carcinoma. BMC Clin Pathol 2013; 13: 24.
14. Mobahat M, Narendran A, Riabowol K. Survivin as a preferential target for cancer therapy. Int J Mol Sci 2014; 15: 2494-516.
15. Huang YJ, Qi WX, He AN, Sun YJ, Shen Z, Yao Y. The prognostic value of survivin expression in patients with colorectal carcinoma: a meta-analysis. Jpn J Clin Oncol 2013; 43: 988-95.
16. Krieg A, Werner TA, Verde PE, Stoecklein NH, Knoefel WT. Prognostic and clinicopathological significance of survivin in colorectal cancer: a meta-analysis. PLoS One 2013; 8: e65338.
17. Qi G, Tuncel H, Aoki E, *et al*. Intracellular localization of survivin determines biological behavior in colorectal cancer. Oncol Rep 2009; 22: 557-62.
18. De Oliveira Lima F, De Oliveira Costa H, Barrezueta LF, *et al*. Immunoexpression of inhibitors of apoptosis proteins and their antagonist SMAC/DIABLO in colorectal carcinoma: correlation with apoptotic index, cellular proliferation and prognosis. Oncol Rep 2009; 22: 295-303.
19. Rauch A, Hennig D, Schäfer C, *et al*. Survivin and YM155: how faithful is the liaison? Biochim Biophys Acta 2014; 1845: 202-20.
20. Miura K, Fujibuchi W, Ishida K, *et al*. Inhibitor of apoptosis protein family as diagnostic markers and therapeutic targets of colorectal cancer. Surg Today 2011; 41: 175-82.
21. Gyurászová K, Mikeš J, Halaburková A, Jendželovský R, Fedoročko P. YM155, a small molecule inhibitor of survivin expression, sensitizes cancer cells to hypericin-mediated photodynamic therapy. Photochem Photobiol Sci 2016; 15: 812-21.
22. Kim ST, Sohn I, Do IG, *et al*. Transcriptome analysis of CD133-positive stem cells and prognostic value of survivin in colorectal cancer. Cancer Genomics Proteomics 2014; 11: 259-66.
23. Li Y, Ma X, Wu X, Liu X, Liu L. Prognostic significance of survivin in breast cancer: meta-analysis. Breast J 2014; 20: 514-24.

24. Shintani M, Sangawa A, Yamao N, Kamoshida S. Immunohistochemical expression of nuclear and cytoplasmic survivin in gastrointestinal carcinoma. Int J Clin Exp Pathol 2013; 6: 2919-27.
25. Bedi A, Pasricha PJ, Akhtar AJ, *et al*. Inhibition of apoptosis during development of colorectal cancer. Cancer Res 1995; 55: 1811-6.
26. Zhao X, Ogunwobi OO, Liu C. Survivin inhibition is critical for Bcl-2 inhibitor-induced apoptosis in hepatocellular carcinoma cells. PLoS One 2011; 6: e21980.
27. Kemper K, Rodermond H, Colak S, Grandela C, Medema JP. Targeting colorectal cancer stem cells with inducible caspase-9. Apoptosis 2012; 17: 528-37.
28. Sam S, Sam MR, Esmaeillou M, Safaralizadeh R. Effective targeting survivin, caspase-3 and microRNA-16-1 expression by methyl-3-pentyl-6-methoxyprodigiosene triggers apoptosis in colorectal cancer stem-like cells. Pathol Oncol Res 2016; 22: 715-23.

Journal of Pathology and Translational Medicine 2017; 51: 24-31
https://doi.org/10.4132/jptm.2016.10.03

ORIGINAL ARTICLE

KRAS Mutation Test in Korean Patients with Colorectal Carcinomas: A Methodological Comparison between Sanger Sequencing and a Real-Time PCR-Based Assay

Sung Hak Lee*
Arthur Minwoo Chung*
Ahwon Lee · Woo Jin Oh
Yeong Jin Choi · Youn-Soo Lee
Eun Sun Jung

Department of Hospital Pathology, College of Medicine, The Catholic University of Korea, Seoul, Korea

Received: August 3, 2016
Revised: September 23, 2016
Accepted: October 2, 2016

Corresponding Author
Eun Sun Jung, MD
Department of Hospital Pathology, College of Medicine, The Catholic University of Korea, 222 Banpo-daero, Seocho-gu, Seoul 06591, Korea
Tel: +82-2-2258-1619
Fax: +82-2-2258-1628
E-mail: esjung@catholic.ac.kr

*Sung Hak Lee and Arthur Minwoo Chung contributed equally to this work.

Background: Mutations in the *KRAS* gene have been identified in approximately 50% of colorectal cancers (CRCs). *KRAS* mutations are well established biomarkers in anti–epidermal growth factor receptor therapy. Therefore, assessment of *KRAS* mutations is needed in CRC patients to ensure appropriate treatment. **Methods:** We compared the analytical performance of the cobas test to Sanger sequencing in 264 CRC cases. In addition, discordant specimens were evaluated by 454 pyrosequencing. **Results:** *KRAS* mutations for codons 12/13 were detected in 43.2% of cases (114/264) by Sanger sequencing. Of 257 evaluable specimens for comparison, *KRAS* mutations were detected in 112 cases (43.6%) by Sanger sequencing and 118 cases (45.9%) by the cobas test. Concordance between the cobas test and Sanger sequencing for each lot was 93.8% positive percent agreement (PPA) and 91.0% negative percent agreement (NPA) for codons 12/13. Results from the cobas test and Sanger sequencing were discordant for 20 cases (7.8%). Twenty discrepant cases were subsequently subjected to 454 pyrosequencing. After comprehensive analysis of the results from combined Sanger sequencing–454 pyrosequencing and the cobas test, PPA was 97.5% and NPA was 100%. **Conclusions:** The cobas test is an accurate and sensitive test for detecting *KRAS*-activating mutations and has analytical power equivalent to Sanger sequencing. Prescreening using the cobas test with subsequent application of Sanger sequencing is the best strategy for routine detection of *KRAS* mutations in CRC.

Key Words: KRAS mutation test; Sanger sequencing; Cobas test; 454 pyrosequencing

The *KRAS* gene was recognized more than 30 years ago as the component of Kirsten sarcoma virus responsible for oncogenesis.[1] Mutations in the *KRAS* gene that lead to its constitutive activation have been identified in approximately 50% of colorectal cancer (CRC) tumors and are common in other tumor types such as pancreas (90%), lung (30%), thyroid (50%), and myeloid leukemia tumors (30%).[2] Most activating mutations in CRCs occur in codons 12 (~82%) and 13 (~17%) of exon 2 of the *KRAS* gene. However, mutations in codon 61 of exon 3 have also been described.[3]

Monoclonal antibodies against epidermal growth factor receptor (EGFR), including cetuximab (Erbitux, ImClone Systems, Branchburg, NJ, USA) and panitumumab (Vectibix, Amgen, Thousand Oaks, CA, USA), have been approved for the treatment of CRC tumors.[4] However, a number of studies have demonstrated that CRC patients with *KRAS* mutations in codons 12 and 13 do not benefit from treatment with anti-EGFR monoclonal antibodies. KRAS is downstream from EGFR in the KRAS-BRAF-MEK-ERK pathway, and blocking EGFR has little effect due to downstream activation of KRAS.[5] Therefore, assessment of the mutational status of KRAS is mandatory in CRC patients to ensure appropriate treatment choice.

A number of methods for detecting *KRAS* mutations are currently in clinical use. However, it is not clear which technique offers the best performance. Sanger sequencing, which theoretically can identify all possible mutations in an exon, is a common reference method used to detect somatic mutations in tumor specimens. However, Sanger sequencing suffers from limited sensitivity for low level mutant alleles, particularly in formalin-fixed paraffin-embedded tissue specimens, and has slow turnaround time.[6] The cobas KRAS mutation test (Roche Molecular Systems, Pleasanton, CA, USA) is a real-time polymerase chain

pISSN 2383-7837
eISSN 2383-7845

reaction (PCR)–based assay designed to identify *KRAS* mutations in codons 12, 13, and 61. This platform reveals whether a mutation is present in a specific hot spot.

The aim of this study was to compare the analytical performance and workflow characteristics of the cobas KRAS mutation test to Sanger sequencing in order to provide optimal care to metastatic colorectal cancer (mCRC) patients through optimal selection of anti-EGFR therapy. In addition, discordant specimens were subjected to next-generation 454 pyrosequencing.

MATERIALS AND METHODS

Selection of patients and tumor samples

A total of 264 patients with CRC who had undergone radical surgery at Seoul St. Mary's Hospital, The Catholic University of Korea between 2008 and 2010 were enrolled in this study. All cases were sporadic without any family history of CRC and were examined by a pathologist who specializes in gastrointestinal tract pathology. The formalin-fixed, paraffin-embedded (FFPE) tissue samples from CRC patients were tested in accordance with protocols approved by the Institutional Review Board of The Catholic University of Korea (KC12SISI0705). Estimated tumor content ranged from 50% to 90%. The study scheme is summarized in Fig. 1.

Direct sequencing technique for *KRAS* mutation

For DNA isolation, 10-μm-thick sections from FFPE tissue samples were used for each case. The hematoxylin and eosin sections used as references were marked with a pen to indicate the tumor-rich area, and the tumor area was scraped off with a scalpel under a dissecting microscope. For genomic DNA extraction, we used the DNeasy Blood and Tissue Kit (Qiagen, Hilden, Germany) according to manufacturer's recommendations. DNA yields were quantified using a Nanodrop spectrophotometer ND-1000 (Thermo Fisher Scientific Inc., Waltham, MA, USA). Sanger sequencing was performed using an ABI 3730 automated sequencer (Applied Biosystems Inc., Foster City, CA, USA) to detect the presence of KRAS exon 2 mutations with previously reported primers.[7] The resulting PCR products were purified using the QIAquick PCR Purification Kit (Qiagen) and the appropriate protocol on the QIAcube robotic workstation. Each chromatogram was visually inspected for abnormalities (Fig. 2).

The cobas KRAS mutation test

The TaqMelt PCR assay cobas KRAS Mutation Test (Roche Diagnostics) was used according to manufacturer's protocol. First, manual specimen preparation was conducted to obtain genomic DNA from FFPE CRC tissue samples (50 ng of DNA), and PCR amplification and detection of target DNA were performed on the cobas 4800 system. Data were automatically processed by the COBAS software.

454 Quantitative massively parallel pyrosequencing

Specimens showing discordant cobas test and Sanger sequencing results were retested using a quantitative massively parallel pyrosequencing method (454 GS Titanium, 454 Life Sciences,

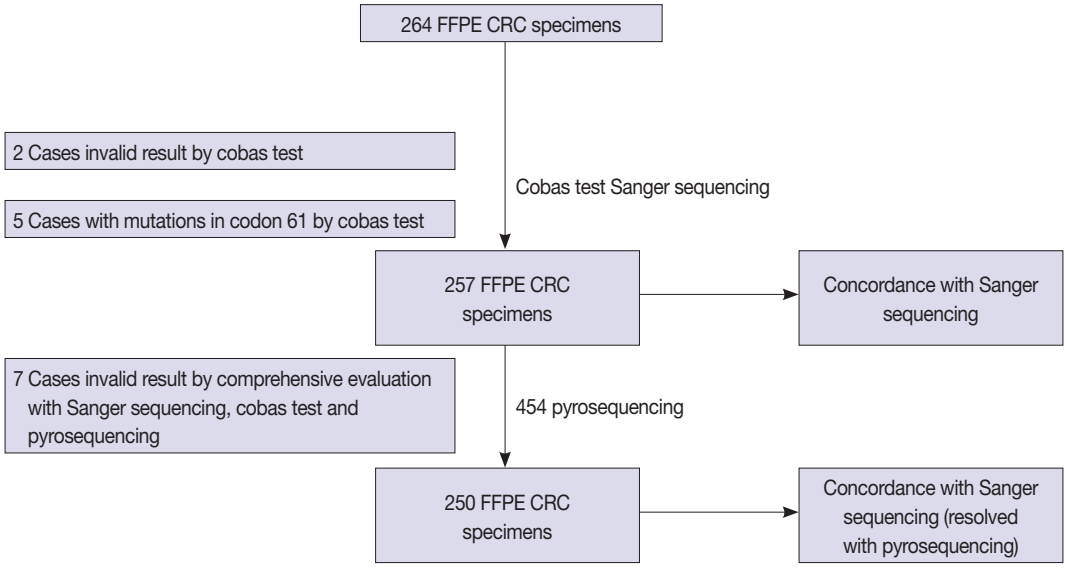

Fig. 1. Study design and specimen selection. Two hundred sixty-four formalin-fixed, paraffin-embedded (FFPE) colorectal cancer (CRC) specimens were selected and processed using Sanger sequencing and cobas test.

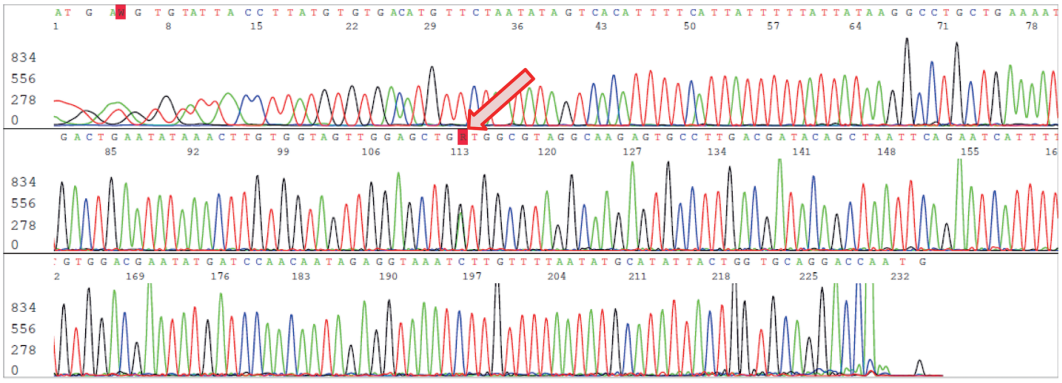

Fig. 2. Electropherogram from Sanger sequencing. Representative sample shows mutant codon 12 with GGT>GAT (arrow).

Branford, CT, USA) by Roche R&D Center China (RRDCC, Shanghai, China) using a validated protocol.

Statistical analysis

Data were analyzed using the SPSS statistical software ver. 21.0 (IBM Corp., Armonk, NY, USA) for Windows. The analytical performance of the cobas test compared with Sanger sequencing for the detection of *KRAS* mutations was evaluated by positive percent agreement (PPA), negative percent agreement (NPA), positive predictive value, and negative predictive value with two-sided 95% confidence intervals.

RESULTS

Patients and samples characteristics

The characteristics of the patients and samples are summarized in Table 1. Patients included 161 men (61.0%) and 103 women (39.0%) with a median age of 62 years (range, 32 to 93 years). Most tissue samples were from primary tumors, while the remaining 1.5% of samples (4 of 264) were metastatic. A total of 262 patients were diagnosed with adenocarcinoma and two patients were diagnosed with neuroendocrine tumor, grade 1 (carcinoid tumor) and gastrointestinal stromal tumor. The median DNA concentration was 199.59 (range, 8.35 to 1,180.87).

Frequency of mutations in *KRAS* exon 2 by Sanger sequencing and the cobas test

The detailed mutation status of 264 cases using Sanger sequencing and the cobas test is summarized in Table 2 and Supplementary Table S1. *KRAS* mutations in codons 12 and 13 were detected in 114 cases (43.2%) by Sanger sequencing. *KRAS* mutations in codons 12, 13, and 61 were revealed in 123 cases (46.6%) by the cobas test. Among the 123 mutation cases on the cobas test, five cases were revealed to have mutations in codon 61 that were not detected by Sanger sequencing, but instead only by the cobas test. Therefore, we excluded five cases of codon 61 mutation from comparison. Two cases had invalid results on the cobas test due to inadequate specimen and were excluded from comparison. In total, we evaluated 257 cases for comparison.

Table 1. Patients and samples characteristics

Characteristic	No. (%)
Total patients	264
Age, median (range, yr)	62 (32–93)
Gender	
Male	161 (61.0)
Female	103 (39.0)
Sites	
Primary	260 (98.5)
Metastasis	4 (1.5)
DNA concentration (ng/μL)	199.59 (8.35–1,180.87)
DNA purity (260/280)	1.99 (1.59–3.01)

Table 2. Frequency of mutations in *KRAS* exon 2 by Sanger sequencing and the cobas test

	Sanger sequencing	The cobas test
Mutation		
Codon 12	90 (34.1)	118 (44.7)
Codon 13	24 (9.1)	
Codon 61	-	5 (1.9)
No mutation	150 (56.8)	139 (52.7)
N/A specimen	0	2 (0.8)
Total	264 (100)	264 (100)

Values are presented as number (%).
N/A, not available.

Overall concordance for detecting *KRAS* mutation of codons 12/13 by Sanger sequencing and the cobas test

KRAS mutations for 257 evaluable cases were detected in 112 cases (43.6%) by Sanger sequencing and 118 cases (45.9%) by

https://doi.org/10.4132/jptm.2016.10.03

the cobas test. Concordance between the cobas test and Sanger sequencing for each lot was 93.8% PPA and 91.0% NPA for codons 12/13. Discordant ratio of Sanger sequencing and cobas test was 7.7% (20 out of 257 cases) (Table 3).

Analysis for 20 discrepant cases with 454 pyrosequencing

For further analysis of 20 discordant cases, we performed 454 pyrosequencing. Among 20 cases, seven cases showed inconclusive results due to low allele frequency on 454 pyrosequencing (Nos. 32 and 82), different mutation types among test modalities (Nos. 26, 100, and 104), and inadequate specimen for 454 pyrosequencing (Nos. 34 and 116).

In one case (No. 54), the result of Sanger sequencing coincides with that of 454 pyrosequencing. In the remaining cases, 10 cases (Nos. 49, 80, 85, 86, 88, 103, 125, 149, 159, and 221) had no mutation with Sanger sequencing, whereas a single nucleotide variant (SNV) was identified by the cobas test and 454 pyrosequencing. In those cases, mutations with high allele frequency by 454 sequencing were regarded as the final results. In two cases (Nos. 97 and 223), no mutation was identified by the cobas test while different mutation types were shown between Sanger sequencing and 454 sequencing. Considering repetitive failure for PCR amplification or inconsistent results on the cobas test, this discrepancy might be due to extensive DNA fragmentation and/or FFPE-related artifacts. Thus, mutations with a high allele frequency by 454 sequencing were considered as the final results in these cases (Table 4, Supplementary Tables S2, S3).

Overall concordance for detecting *KRAS* mutation of codons 12/13 (the cobas test and combined Sanger and 454 sequencing resolution)

After discordant resolution with 454 pyrosequencing, we ana-

Table 3. Summary of overall concordance for detecting *KRAS* mutation of codon 12/13

The cobas test	Sanger sequencing		
	Mutation detected	Mutation not detected	Total
Mutation detected	105 (40.9)	13 (5.1)	118 (45.9)
Mutation not detected	7 (2.7)	132 (51.3)	139 (54.1)
Total	112 (43.6)	145 (56.4)	257[a] (100)

Values are presented as number (%). Positive percent agreement (sensitivity): 93.8% (95% confidence interval [CI], 87.6 to 97.5). Negative percent agreement (specificity): 91.0% (95% CI, 85.2 to 95.1). Positive predictive value: 89.0% (95% CI, 81.9 to 94.0). Negative predictive value: 95.0% (95% CI, 89.9 to 98.0). Positive likelihood ratio: 10.5 (95% CI, 6.2 to 17.6). Negative likelihood ratio: 0.1 (95% CI, 0.0 to 0.1).
[a]Of 264 cases, two cases showed invalid result and five cases revealed *KRAS* mutations in codon 61 by the cobas test.

Table 4. Analysis for 20 discrepant cases with 454 pyrosequencing

Sample ID	Sanger sequencing	The cobas test	454 Pyrosequencing		Combined result
			Variant	Frequency	
026	G12D	Not detected	G13D	0.65	N/A
054	G12D	Not detected	G12D	0.69	G12D
082	G12D	Not detected	G12D/G12V	0.68/1.78	N/A
097	G12D	Not detected	G12V	10.92	G12V
100	G12D	Not detected	G12A/G12S/G12V	3.13/0.45/13.2	N/A
104	G13D	Not detected	G12D/G12S/G12V/G13D	1.06/0.79/3.62/0.36	N/A
223	G12D	Not detected	G12V	17.58	G12V
032	Negative	Codon 12/13	G12C/G13D	2.43/0.38	N/A
034	Netative	Codon 12/14	N/A	N/A	N/A
049	Negative	Codon 12/13	G12V/G13S	23.56/0.34	G12V
080	Negative	Codon 12/13	G12C/G12V/G13D/G13S	15.25/6.5/1.62/1.29	G12C
085	Negative	Codon 12/13	G12D/G12V	4.2/13.53	G12V
086	Negative	Codon 12/13	G12V/G13D	9.72/1.09	G12V
088	Negative	Codon 12/13	G12V	17.5	G12V
103	Negative	Codon 12/13	G12D/G12V/G13D	1.86/4.47/0.81	G12V
116	Negative	Codon 12/13	N/A	N/A	N/A
125	Negative	Codon 12/13	G12V/G13D	15.66/3.88	G12V
149	Negative	Codon 12/13	G12V	24.9	G12V
159	Negative	Codon 12/13	G12D/G12S/G12V	0.4/1.41/6.7	G12V
221	Negative	Codon 12/13	G12V/G13S	8.92/1.64	G12V

N/A, not available.

Table 5. Summary of overall concordance for detecting *KRAS* mutation (the cobas test and combined Sanger and 454 sequencing resolution)

The Cobas test	Sanger sequencing and 454 pyrosequencing		
	Mutation detected	Mutation not detected	Total
Mutation detected	115 (46.0)	0	115 (46.0)
Mutation not detected	3 (1.2)	132 (52.8)	135 (54.0)
Total	118 (47.2)	132 (52.8)	250[a] (100)

Values are presented as number (%). Positive percent agreement (sensitivity): 97.5% (95% confidence interval [CI], 92.8 to 99.5). Negative percent agreement (specificity): 100% (95% CI, 97.2 to 100). Positive predictive value: 100% (95% CI, 96.9 to 100). Negative predictive value: 97.8% (95% CI, 93.7 to 99.5). Negative likelihood ratio: 0.03 (95% CI, 0.0 to 0.1).
[a]Of 257 cases, seven cases showed invalid result by comprehensive evaluation with Sanger sequencing, the cobas test and 454 pyrosequencing.

lyzed 250 cases for concordance between the cobas test and combined Sanger sequencing–454 pyrosequencing. *KRAS* mutations for 250 evaluable cases were detected in 118 cases (46.0%) by combined Sanger sequencing–454 pyrosequencing and 115 cases (46.0%) by the cobas test. Concordance between the cobas test and combined Sanger sequencing–454 pyrosequencing was 97.5% PPA and 100% NPA. The discordant ratio of the Sanger sequencing and the cobas test was 1.2% (3 out of 250 cases) (Table 5).

DISCUSSION

There are various testing assays available for *KRAS* mutations, and several comparative studies on the analytical power of these methods in the clinical context have been conducted.[3,8-10] In this study, we compared the performance of two platforms for detecting *KRAS*-activating mutations in Korean CRC cohorts. Determination of the *KRAS* mutation status is now obligatory for treatment with anti-EGFR monoclonal antibodies such as cetuximab and panitumumab in patients with metastatic CRC, as only patients with wild-type *KRAS* may respond to treatment.[11,12] Furthermore, in patients with metastatic CRC and *KRAS*-activating mutations, treatment with anti-EGFR monoclonal antibodies may result in deleterious effects on progression-free survival, which highlights the necessity of maximizing the detection of *KRAS* mutations.[13,14] However, validated and standardized procedures for *KRAS* somatic mutation testing were lacking until recently. Sanger sequencing remains the gold standard assay for detecting all possible mutations, but is generally considered to be less sensitive than other methods.[15]

The cobas (*KRAS* mutation) test is a CE-IVD validated method based on real-time PCR and TaqMelt technology.[16] The accuracy of this method is similar to that of massively parallel pyrosequencing. In this study, the cobas test showed a ≥95% correct mutation call rate for the recommended DNA input of ≥50 ng. It has been designed to detect 19 common *KRAS* mutations in codons 12, 13, and 61 in FFPE-derived DNA from CRC samples.[17] Moreover, the cobas test has been reported to detect mutations in tissue samples containing a minimal amount of 5% of tumor DNA and showed comparable and greater sensitivity for low-level mutant allele burden than Sanger sequencing.[17] The results indicate the presence or absence of *KRAS* mutations without detailed information regarding the exact mutated site. While 454 pyrosequencing also shows a sensitivity of 5%, this method did not confirm the results obtained from other test assays. We used 454 pyrosequencing as a reference method to evaluate discrepant results between the cobas test and Sanger sequencing.

In this study, there were 20 discordant results (7.8%) between the cobas test and the Sanger sequencing, excluding two cases with invalid results and five cases with *KRAS* mutations in codon 61 by the cobas test. For further evaluation of samples with discrepant mutation results, each sample was run three times on Sanger sequencing and the cobas test. If invalid results are obtained, a new sample from a different tissue block was used if possible, which might result in different mutation types from intratumoral heterogeneity. In those cases, we made a great effort to choose the tissue section with the higher tumor portions (> 70%), and no necrotic or mucinous areas.

In five cases (Nos. 26, 97, 100, 104, and 223), different mutation types were identified between Sanger sequencing and 454 sequencing. In addition, two cases (Nos. 32 and 82) showed low allele frequency on 454 pyrosequencing. Considering repetitive failure for PCR amplification in Sanger sequencing and/or invalid results in the cobas test, this discrepancy among test modalities might come from extensive DNA fragmentation from old formalin-fixed tissues. FFPE-related artifacts, i.e., spontaneous deamination of cytosine bases, might have a great effect on this inconsistency. Recently, uracil lesions in which hydrolytic deamination of cytosine bases to uracil takes place have been identified as major sources of sequence artifacts in FFPE DNA, leading to artifactual C:G>T:A variants.[18] These sequence artifacts are known to be detected more frequently when low copy numbers of FFPE DNA are provided.[19]

 https://doi.org/10.4132/jptm.2016.10.03

In ten cases (Nos. 49, 80, 85, 86, 88, 103, 125, 149, 159, and 221), no mutation was detected by Sanger sequencing, whereas SNVs were identified by the cobas test and 454 sequencing. These discrepancies might result from low analytical sensitivity of Sanger sequencing. Although Sanger sequencing is considered to be the gold standard in mutation testing, it has a modest limit of detection that can be highly variable depending on the specific mutation sequence. A recent study has shown that Sanger sequencing yielded 11.1% false-positives and 6.1% false-negatives for *KRAS* mutation detection using an automated interpretation algorithm with a 10% threshold, highlighting the need for manual review of all Sanger sequencing data (Table 4, Supplementary Tables S2, S3).[20]

In addition to the above mentioned factors, artifactual mutations from FFPE tissues can be caused by various sources, including over-fixation in 10% non-buffered formalin, oxidative DNA damage during sample preparation, DNA polymerase error, pseudogene amplification, sequencing chemistry, and errors of alignment and/or annotation.[19,21-24] Several studies have shown that the numbers of SNV identified in formalin-fixed tissues were higher than those in matched frozen tissues, which suggests the possibilities of artifactual sequence changes, thus increasing the risk of false-positive mutation calls.[25,26] Additionally, the discrepant results may have also come from uncommon *KRAS* mutations that cannot be detected using the cobas design. Understanding these issues is important for accurate interpretation of various mutations detected.

Although a "mutated in codon 12/13 or 61" result in the cobas KRAS mutation test is a sufficient basis for the application of anti-EGFR monoclonal antibodies in mCRC, several studies suggest that different mutation sites have different clinical impacts on cetuximab and/or panitumumab efficacy. The potential differential sensitivity of *KRAS* G13D mutation to anti-EGFR monoclonal antibodies has been reported in a small number of studies, suggesting that the addition of cetuximab may be beneficial to CRC patients with a *KRAS* G13D mutation.[27,28] However, no significant difference between *KRAS* G13D and other *KRAS* mutated CRCs was detected in terms of treatment benefit from anti-EGFR monoclonal antibodies for mCRC.[29]

Detection of *KRAS*-activating mutations in CRC has largely only focused on mutations in codons 12 and 13. However, recent data has shown that clinicopathological features and gene expression profiles of CRCs harboring non-traditional *KRAS* mutations appear to be similar to those of tumors with *KRAS* mutations in codons 12 and 13.[30] *KRAS* mutations in codon 61 and/or 146 are additional hotspots in CRC, and the available data from a small number of studies suggest that resistance to anti-EGFR therapy is associated with *KRAS* mutation at these sites.[31,32] Pre-screening using the cobas KRAS mutation test, which accurately detects all main *KRAS* mutations in codons 12, 13, and 61, with further evaluation by Sanger sequencing enables the identification of codon 12 and 13 mutations. This may be an easy and reliable approach for routine diagnostic purposes regarding *KRAS* mutations in mCRC. In addition, combining both mutation assays greatly reduces the probability of obtaining false-negative or false-positive results.

This study also emphasized that the preanalytical step must be strictly controlled because DNA degradation was the main cause of "not available" results, which leads to non-conclusive results, and samples cannot be evaluated using other genetic tests.

Several techniques for detecting *KRAS* mutations are currently available, but there is limited data supporting the analytical performance of individual methods compared with other methods.[33-35] In addition, recent studies demonstrated the variability of mutation tests resulting from different clinical laboratories.[36] In contrast to other *KRAS* mutation detecting kits, such as the Therascreen KRAS mutation test, the cobas test can detect 12 additional mutation sites, representing approximately 1% of all *KRAS* mutation cases of CRC based on data from the Catalogue of Somatic Mutations in Cancer (COSMIC) database.[3] However, several studies revealed that *KRAS* mutations in codon 61 are more prevalent than reflected by the COSMIC data in CRC.[3,37,38] Thus, more comprehensive *KRAS* mutation coverage may be helpful for selecting patients for anti-EGFR target therapies.

A limitation of this study is that the study design was retrospective and the sample size was unsatisfactory to evaluate the significance of infrequent *KRAS* mutation subtypes. Subsequent translational prospective studies from different cohorts are needed to confirm our data. In addition, some invalid and discrepant results were not sufficiently resolved. Nevertheless, we demonstrated that the cobas KRAS mutation test is a reproducible companion diagnostic test in patients with CRCs under consideration for anti-EGFR target therapies when used with Sanger sequencing.

In conclusion, we confirmed that the cobas KRAS mutation test is an accurate and sensitive test for detecting *KRAS*-activating mutations and has equivalent analytical power to the Sanger direct sequencing method. Therefore, pre-screening using the cobas KRAS mutation assay with subsequent application of Sanger sequencing is the best strategy for routine diagnostic purposes regarding *KRAS* mutations in mCRC.

Electronic Supplementary Material

Supplementary materials are available at Journal of Pathology and Translational Medicine (http://jpatholtm.org).

Conflicts of Interest

No potential conflict of interest relevant to this article was reported.

REFERENCES

1. Malumbres M, Barbacid M. RAS oncogenes: the first 30 years. Nat Rev Cancer 2003; 3: 459-65.
2. Bos JL. Ras oncogenes in human cancer: a review. Cancer Res 1989; 49: 4682-9.
3. Lee S, Brophy VH, Cao J, *et al*. Analytical performance of a PCR assay for the detection of *KRAS* mutations (codons 12/13 and 61) in formalin-fixed paraffin-embedded tissue samples of colorectal carcinoma. Virchows Arch 2012; 460: 141-9.
4. Venook AP. Epidermal growth factor receptor-targeted treatment for advanced colorectal carcinoma. Cancer 2005; 103: 2435-46.
5. Dahabreh IJ, Terasawa T, Castaldi PJ, Trikalinos TA. Systematic review: anti-epidermal growth factor receptor treatment effect modification by *KRAS* mutations in advanced colorectal cancer. Ann Intern Med 2011; 154: 37-49.
6. Querings S, Altmüller J, Ansén S, *et al*. Benchmarking of mutation diagnostics in clinical lung cancer specimens. PLoS One 2011; 6: e19601.
7. Kim SY, Choi EJ, Yun JA, *et al*. Syndecan-1 expression is associated with tumor size and EGFR expression in colorectal carcinoma: a clinicopathological study of 230 cases. Int J Med Sci 2015; 12: 92-9.
8. Harlé A, Busser B, Rouyer M, *et al*. Comparison of COBAS 4800 *KRAS*, TaqMan PCR and high resolution melting PCR assays for the detection of *KRAS* somatic mutations in formalin-fixed paraffin embedded colorectal carcinomas. Virchows Arch 2013; 462: 329-35.
9. Sharma A, Zhang G, Aslam S, Yu K, Chee M, Palma JF. Novel approach for clinical validation of the cobas *KRAS* mutation test in advanced colorectal cancer. Mol Diagn Ther 2016; 20: 231-40.
10. Gonzalez de Castro D, Angulo B, Gomez B, *et al*. A comparison of three methods for detecting *KRAS* mutations in formalin-fixed colorectal cancer specimens. Br J Cancer 2012; 107: 345-51.
11. Amado RG, Wolf M, Peeters M, *et al*. Wild-type *KRAS* is required for panitumumab efficacy in patients with metastatic colorectal cancer. J Clin Oncol 2008; 26: 1626-34.
12. Van Cutsem E, Köhne CH, Hitre E, *et al*. Cetuximab and chemotherapy as initial treatment for metastatic colorectal cancer. N Engl J Med 2009; 360: 1408-17.
13. Bokemeyer C, Bondarenko I, Makhson A, *et al*. Fluorouracil, leucovorin, and oxaliplatin with and without cetuximab in the first-line treatment of metastatic colorectal cancer. J Clin Oncol 2009; 27: 663-71.
14. Douillard JY, Siena S, Cassidy J, *et al*. Randomized, phase III trial of panitumumab with infusional fluorouracil, leucovorin, and oxaliplatin (FOLFOX4) versus FOLFOX4 alone as first-line treatment in patients with previously untreated metastatic colorectal cancer: the PRIME study. J Clin Oncol 2010; 28: 4697-705.
15. Malapelle U, Carlomagno C, Salatiello M, *et al*. *KRAS* mutation detection by high-resolution melting analysis significantly predicts clinical benefit of cetuximab in metastatic colorectal cancer. Br J Cancer 2012; 107: 626-31.
16. Malapelle U, Carlomagno C, de Luca C, Bellevicine C, Troncone G. *KRAS* testing in metastatic colorectal carcinoma: challenges, controversies, breakthroughs and beyond. J Clin Pathol 2014; 67: 1-9.
17. Angulo B, Lopez-Rios F, Gonzalez D. A new generation of companion diagnostics: cobas *BRAF, KRAS* and *EGFR* mutation detection tests. Expert Rev Mol Diagn 2014; 14: 517-24.
18. Do H, Dobrovic A. Sequence artifacts in DNA from formalin-fixed tissues: causes and strategies for minimization. Clin Chem 2015; 61: 64-71.
19. Sah S, Chen L, Houghton J, *et al*. Functional DNA quantification guides accurate next-generation sequencing mutation detection in formalin-fixed, paraffin-embedded tumor biopsies. Genome Med 2013; 5: 77.
20. Tsiatis AC, Norris-Kirby A, Rich RG, *et al*. Comparison of Sanger sequencing, pyrosequencing, and melting curve analysis for the detection of *KRAS* mutations: diagnostic and clinical implications. J Mol Diagn 2010; 12: 425-32.
21. Costello M, Pugh TJ, Fennell TJ, *et al*. Discovery and characterization of artifactual mutations in deep coverage targeted capture sequencing data due to oxidative DNA damage during sample preparation. Nucleic Acids Res 2013; 41: e67.
22. Kinde I, Wu J, Papadopoulos N, Kinzler KW, Vogelstein B. Detection and quantification of rare mutations with massively parallel sequencing. Proc Natl Acad Sci U S A 2011; 108: 9530-5.
23. Xuan J, Yu Y, Qing T, Guo L, Shi L. Next-generation sequencing in the clinic: promises and challenges. Cancer Lett 2013; 340: 284-95.
24. Li H, Ruan J, Durbin R. Mapping short DNA sequencing reads and calling variants using mapping quality scores. Genome Res 2008; 18: 1851-8.
25. Quach N, Goodman MF, Shibata D. *In vitro* mutation artifacts after formalin fixation and error prone translesion synthesis during PCR. BMC Clin Pathol 2004; 4: 1.

26. Wong SQ, Li J, Tan AY, *et al*. Sequence artefacts in a prospective series of formalin-fixed tumours tested for mutations in hotspot regions by massively parallel sequencing. BMC Med Genomics 2014; 7: 23.
27. De Roock W, Jonker DJ, Di Nicolantonio F, *et al*. Association of *KRAS* p.G13D mutation with outcome in patients with chemotherapy-refractory metastatic colorectal cancer treated with cetuximab. JAMA 2010; 304: 1812-20.
28. Benvenuti S, Sartore-Bianchi A, Di Nicolantonio F, *et al*. Oncogenic activation of the RAS/RAF signaling pathway impairs the response of metastatic colorectal cancers to anti-epidermal growth factor receptor antibody therapies. Cancer Res 2007; 67: 2643-8.
29. Misale S, Yaeger R, Hobor S, *et al*. Emergence of *KRAS* mutations and acquired resistance to anti-EGFR therapy in colorectal cancer. Nature 2012; 486: 532-6.
30. Morris VK, Lucas FA, Overman MJ, *et al*. Clinicopathologic characteristics and gene expression analyses of non-KRAS 12/13, *RAS*-mutated metastatic colorectal cancer. Ann Oncol 2014; 25: 2008-14.
31. Loupakis F, Ruzzo A, Cremolini C, *et al*. *KRAS* codon 61, 146 and *BRAF* mutations predict resistance to cetuximab plus irinotecan in *KRAS* codon 12 and 13 wild-type metastatic colorectal cancer. Br J Cancer 2009; 101: 715-21.
32. De Roock W, Claes B, Bernasconi D, *et al*. Effects of *KRAS, BRAF, NRAS*, and *PIK3CA* mutations on the efficacy of cetuximab plus chemotherapy in chemotherapy-refractory metastatic colorectal cancer: a retrospective consortium analysis. Lancet Oncol 2010; 11: 753-62.
33. Gao J, Li YY, Sun PN, Shen L. Comparative analysis of dideoxy sequencing, the KRAS StripAssay and pyrosequencing for detection of *KRAS* mutation. World J Gastroenterol 2010; 16: 4858-64.
34. Angulo B, García-García E, Martínez R, *et al*. A commercial real-time PCR kit provides greater sensitivity than direct sequencing to detect *KRAS* mutations: a morphology-based approach in colorectal carcinoma. J Mol Diagn 2010; 12: 292-9.
35. Whitehall V, Tran K, Umapathy A, *et al*. A multicenter blinded study to evaluate *KRAS* mutation testing methodologies in the clinical setting. J Mol Diagn 2009; 11: 543-52.
36. Beau-Faller M, Degeorges A, Rolland E, *et al*. Cross-validation study for epidermal growth factor receptor and *KRAS* mutation detection in 74 blinded non-small cell lung carcinoma samples: a total of 5550 exons sequenced by 15 molecular French laboratories (evaluation of the *EGFR* mutation status for the administration of EGFR-TKIs in non-small cell lung carcinoma [ERMETIC] project--part 1). J Thorac Oncol 2011; 6: 1006-15.
37. Richman SD, Seymour MT, Chambers P, *et al*. *KRAS* and *BRAF* mutations in advanced colorectal cancer are associated with poor prognosis but do not preclude benefit from oxaliplatin or irinotecan: results from the MRC FOCUS trial. J Clin Oncol 2009; 27: 5931-7.
38. Gaedcke J, Grade M, Jung K, *et al*. *KRAS* and *BRAF* mutations in patients with rectal cancer treated with preoperative chemoradiotherapy. Radiother Oncol 2010; 94: 76-81.

Journal of Pathology and Translational Medicine 2017; 51: 32-39
https://doi.org/10.4132/jptm.2016.10.17

■ ORIGINAL ARTICLE ■

Aurora Kinase A Is a Prognostic Marker in Colorectal Adenocarcinoma

Hyun Min Koh · Bo Geun Jang
Chang Lim Hyun · Young Sill Kim
Jin Won Hyun[1] · Weon Young
Chang[2] · Young Hee Maeng

Departments of Pathology, [1]Biochemistry, and [2]Surgery, Jeju National University School of Medicine, Jeju, Korea

Received: September 9, 2016
Revised: October 15, 2016
Accepted: October 17, 2016

Corresponding Author
Young Hee Maeng, MD, PhD
Department of Pathology, Jeju National University School of Medicine, 15 Aran 13-gil, Jeju 63241, Korea
Tel: +82-64-717-1410
Fax: +82-64-717-1131
E-mail: yhmaeng@jejunu.ac.kr

Background: Aurora kinase A (AURKA), or STK15/BTAK, is a member of the serine/threonine kinase family and plays important roles in mitosis and chromosome stability. This study investigated the clinical significance of AURKA expression in colorectal cancer patients in Korea. **Methods:** AURKA protein expression was evaluated by immunohistochemistry in 151 patients with colorectal adenocarcinoma using tissue microarray blocks. We analyzed the relationship between clinicopathological characteristics and AURKA expression. In addition, the prognostic significance of various clinicopathological data for progression-free survival (PFS) was assessed. Also we evaluated copy number variations by array comparative genomic hybridization and *AURKA* gene amplification using fluorescence *in situ* hybridization in colorectal carcinoma tissues. **Results:** *AURKA* gene amplification was found more frequently in the 20q13.2–13.33 gain-positive group than the group with no significant gain on the *AURKA*-containing locus. AURKA protein expression was detected in 45% of the cases (68/151). Positive staining for AURKA was observed more often in male patients ($p=.035$) and distally located tumors ($p=.021$). PFS was shorter in patients with AURKA expression compared to those with low-level AURKA expression ($p<.001$). Univariate analysis revealed that AURKA expression ($p=.001$), age ($p=.034$), lymphatic invasion ($p=.001$), perineural invasion ($p=.002$), and TNM stage ($p=.013$) significantly affected PFS. In a multivariate analysis of PFS, a Cox proportional hazard model confirmed that AURKA expression was an independent and significant prognostic factor in colorectal adenocarcinoma (hazard ratio, 3.944; $p<.001$). **Conclusions:** AURKA could serve as an independent factor to predict a poor prognosis in Korean colorectal adenocarcinoma patients.

Key Words: Aurora kinase A; Colorectal adenocarcinoma; Prognosis

Aurora kinases are key mitotic regulators required for the maintenance of chromosome stability.[1] In mammalian cells, Aurora kinases consist of three members (Aurora kinase A, B, and C), which are expressed in a cell cycle-dependent fashion.[1,2]

AURKA (STK15/BTAK) is a serine/threonine kinase family member involved in mitotic entry, bipolar spindle formation, centrosome maturation control, and segregation during mitosis. AURKA maps to chromosome 20q13.2, a region that is frequently amplified in several human malignant tumors,[2-4] including leukemia and breast, bladder, ovarian, gastric, esophageal, liver, colorectal, and pancreatic cancers.[2]

Recent studies have shown that AURKA overexpression is associated with tumorigenesis, clinical aggressiveness, and tumor progression in several cancers.[1,3,5,6] A few studies have implicated AURKA activity in oncogenic transformation through the development of chromosome instability and tumor cell heterogeneity and in tumor progression through the activation of epithelial-mesenchymal transition reprograming, which results in tumor-initiating cell generation.[1,7] Therefore, AURKA represents a valuable target for cancer therapy, and the development of small-molecule AURKA inhibitors currently undergoing advanced clinical trials may improve the clinical outcomes of cancer patients.[1,5,8]

Various studies have been performed to investigate the relationship between AURKA protein expression or amplification and prognosis in solid tumor patients, including colorectal cancer (CRC) patients.[4,5,9-18]

AURKA protein overexpression and amplification have been frequently observed in CRC.[12] Studies have shown that AURKA expression is associated with clinicopathological parameters and overall survival in CRC.[4,5,9,12,13,15,19] Lam *et al*.[13] found that Aurora kinase expression correlated with tumor location, histology, and grade; p16 expression; and telomerase activity in colorectal adenocarcinomas. Belt *et al*.[4] reported that high-level AURKA expression was significantly associated with recurrence in stage II or III colon cancer. In addition, Goos *et al*.[9] revealed that high-level AURKA expression was associated with poor overall survival in CRC liver metastasis. In contrast, Goktas *et al*.[15]

pISSN 2383-7837
eISSN 2383-7845

reported that AURKA overexpression had a positive effect on survival in metastatic CRC patients.

Despite these studies, the relationship between AURKA expression and CRC progression and clinical outcomes has not been reported in Korean patients. We aimed to investigate *AURKA*-related genetic changes and protein expression in Korean CRC patients. The study included array comparative genomic hybridization (aCGH) for copy number variations (CNV), fluorescence *in situ* hybridization (FISH) for *AURKA* gene amplification, and immunohistochemistry for protein expression. The relationship between AURKA expression, clinicopathological characteristics, and progression-free survival (PFS) was also assessed.

MATERIALS AND METHODS

Patients and clinicopathological data

Samples from 151 patients who underwent curative surgical resection for colorectal adenocarcinomas between January 2008 and July 2012 at Jeju National University Hospital (Jeju, Korea) were examined. Patients who did not undergo curative surgical resection and those who had any forms of preoperative chemotherapy and/or radiotherapy at the time of surgical resection were excluded. Staging was performed according to the American Joint Committee on Cancer TNM Classification of Malignant Tumors, seventh edition, while the histologic type and differentiation grade of the tumor were determined using the classification system of the World Health Organization, fourth edition.[14] PFS was measured from the date of CRC surgery until the time of recurrence or last follow-up. Clinical data from the patients were collected through medical record examination. The median age of the patients was 66 years (range, 35 to 88 years). Other clinicopathological information is shown in Table 1. This study was approved by the Institutional Review Board of Jeju National University Hospital (2016-06-004).

Array comparative genomic hybridization

DNA from 24 fresh tissue specimens of colorectal adenocarcinomas was analyzed versus reference DNA. Test and reference gDNAs were independently labeled with fluorescent dyes, co-hybridized to a NimbleGen Human CGH 135K Whole-Genome Tiling array (Roche NimbleGen Inc, Madison, WI, USA), and scanned using a 2 μm scanner. Log2-ratio values of the probe signal intensities (Cy3/Cy5) were calculated and plotted versus genomic position using Roche NimbleGen NimbleScan software. Data are displayed in Roche NimbleGen SignalMap software.

Table 1. Clinicopathological characteristics of the patients

Characteristic	No. (%) (n=151)
Age (yr)	
<65	60 (39.7)
≥65	91 (60.3)
Sex	
Male	104 (68.9)
Female	47 (31.1)
Tumor location	
Proximal	46 (30.5)
Distal	105 (69.5)
Tumor differentiation	
Well	18 (11.9)
Moderate	122 (80.8)
Poor	9 (6.0)
Mucinous	2 (1.3)
Vascular invasion	
Absent	140 (92.7)
Present	11 (7.3)
Lymphatic invasion	
Absent	82 (54.3)
Present	69 (45.7)
Perineural invasion	
Absent	105 (69.5)
Present	46 (30.5)
TNM stage	
I	22 (14.6)
II	61 (40.4)
III	68 (45)

TNM, tumor-node-metastasis.

Fluorescent *in situ* hybridization

FISH analysis targeting *AURKA* on 20q13.2 was done on the same cases used in aCGH. Fifteen cases of formalin-fixed, paraffin-embedded tissue were tested in total; 10 cases with copy number gain on 20q13.2–13.33 and five cases with no copy number gain. The examination was performed according to the manufacturer's instructions (Empire Genomics, Buffalo, NY, USA). Fluorescence was scored on a minimum of 20 non-overlapping nuclei in the representative tumor areas. The *AURKA*/CEP20 ratio was calculated by dividing the total number of *AURKA* signals by the total number of CEP20 signals and the cases with *AURKA*/CEP20 ratio≥2.0 were interpreted as positive.

Tissue microarray construction

In total, eight tissue microarrays (TMAs) were constructed as described previously.[4,9] Briefly, hematoxylin and eosin (H&E)–stained slides were reviewed and the most representative tumor area was marked. The area was carefully marked on H&E-stained slides as well as formalin-fixed, paraffin-embedded tissue blocks. A core (4 mm in diameter) of the tumor area was obtained from

each specimen. One section from each block was stained with H&E for tissue confirmation.

Immunohistochemistry

Immunohistochemistry was performed on 4-μm-thick sections from TMA blocks. Tissues were stained with polyclonal anti-AURKA antibodies at a dilution of 1:200 (HPA002636, ATLAS Sigma Life Science, St. Louis, MO, USA) using an automated immunostainer (Benchmark XT, Ventana Medical Systems Inc., Tucson, AZ, USA). The primary antibody was omitted for the negative control, and the adjacent ganglion cells in the nerve bundles within each slide served as an internal reference.

AURKA protein expression

Immunoreactivity was evaluated in each TMA sample by visual counting of the tumor cells. The extent of positively stained nuclei was scored as follows: 0, positive staining in 0%; 1, <10%; 2, ≥10% and <25%; 3, ≥25% and <50%; and 4, ≥50%. Scores of 2–4 were considered positive, and scores ≤1 were considered negative.[4,12,13] To confirm reproducibility, all samples were scored by two independent observers in a blinded manner. If discrepancies occurred, a consensus score was reached.

Statistical analysis

Pearson's chi-square test was used for categorical variables. PFS was analyzed using the Kaplan-Meier method with the log-rank test assessing differences in survival probability between groups. The prognostic significance of various clinicopathological characteristics for PFS was assessed by the Cox proportional hazard regression method. All values were based on two-sided statistical analyses; significance was set at $p < .05$. All statistical tests were performed with IBM SPSS ver. 21.0 (IBM Corp., Armonk, NY, USA).

RESULTS

CNVs in chromosome 20

In twenty-four cases of colorectal carcinomas, total 1,297 CNVs were detected (Fig. 1A). The locus of 20q13.2–13.33 containing *AURKA* gene were recurrently gained in 13 cases (54%), while only one case showed loss of the area (Fig. 1B) .

AURKA gene amplification status

AURKA amplification was assessed in 15 patients (group with 20q13.2–13.33 copy number gain, n = 10; gain-negative group, n = 5). One case of 20q13.2–13.33 gain-positive group was failed to express fluorescences. Three out of the remaining nine cases with 20q13.2–13.33 gain showed amplification of *AURKA* gene but none revealed gene amplification among the gain-negative group (Table 2, Fig. 2).

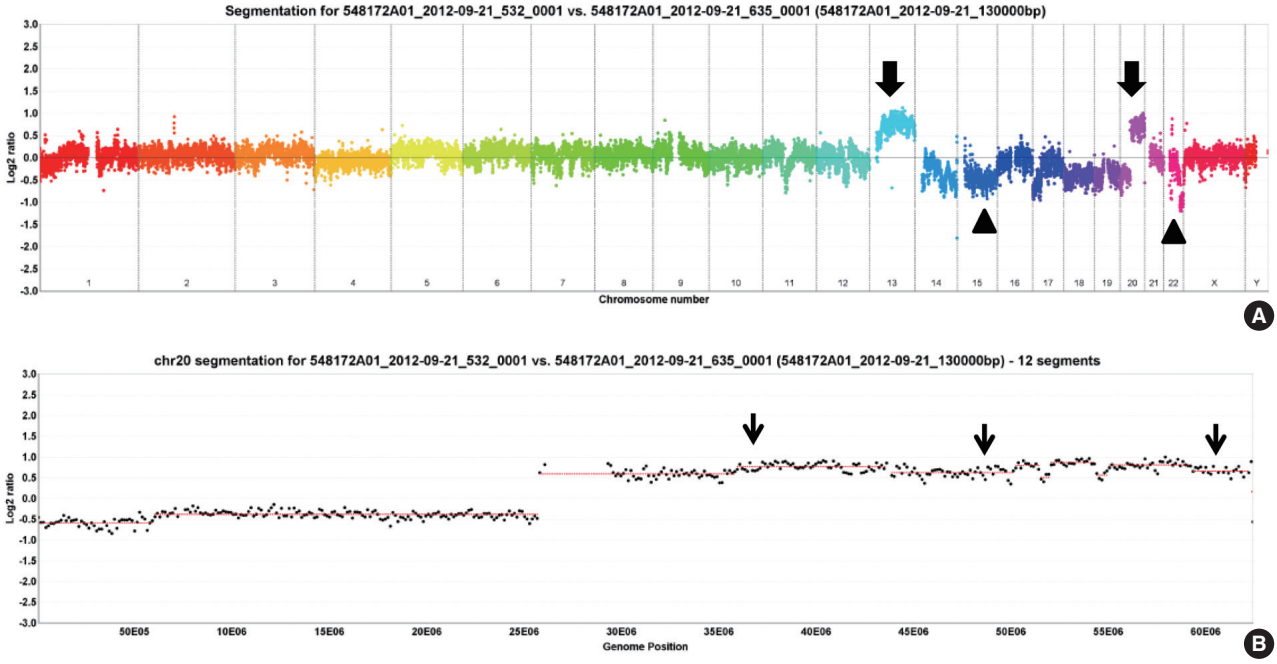

Fig. 1. (A) Genome wide array comparative genomic hybridization using DNA from colorectal carcinoma tissue showing copy number gains (block arrows) and losses (arrowheads) on multiple sites. (B) Copy number plots of chromosome 20 showing frequent gains in certain areas (line arrows).

https://doi.org/10.4132/jptm.2016.10.17

Table 2. Relationship between 20q13.2–13.33 copy number gain and *AURKA* gene amplification

20q13.2–13.33 copy number gain	*AURKA* gene amplification		
	Positive	Negative	Total cases
Positive	3	6	9
Negative	0	5	5
Total cases	3	11	14

AURKA, Aurora kinase A.

Relationship between AURKA expression and clinicopathological characteristics

AURKA protein was expressed in 45% of colorectal adenocarcinoma cases (68/151), while negative to faintly reactive staining was found in normal colorectal epithelial cells. The staining pattern was predominantly nuclear or nuclear and cytoplasmic (Fig. 3). Table 3 shows the relationship between AURKA expres-

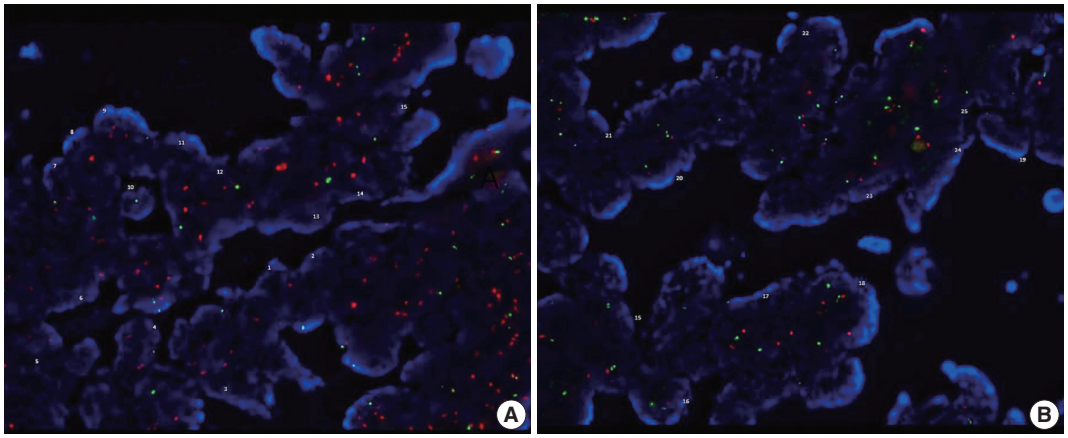

Fig. 2. Fluorescence *in situ* hybridization for Aurora kinase A (*AURKA*) in colorectal carcinomas showing significant amplification in the 20q13.2–13.33 gain-positive case (A) and no amplification in the case with no copy number gain on 20q13.2 (B).

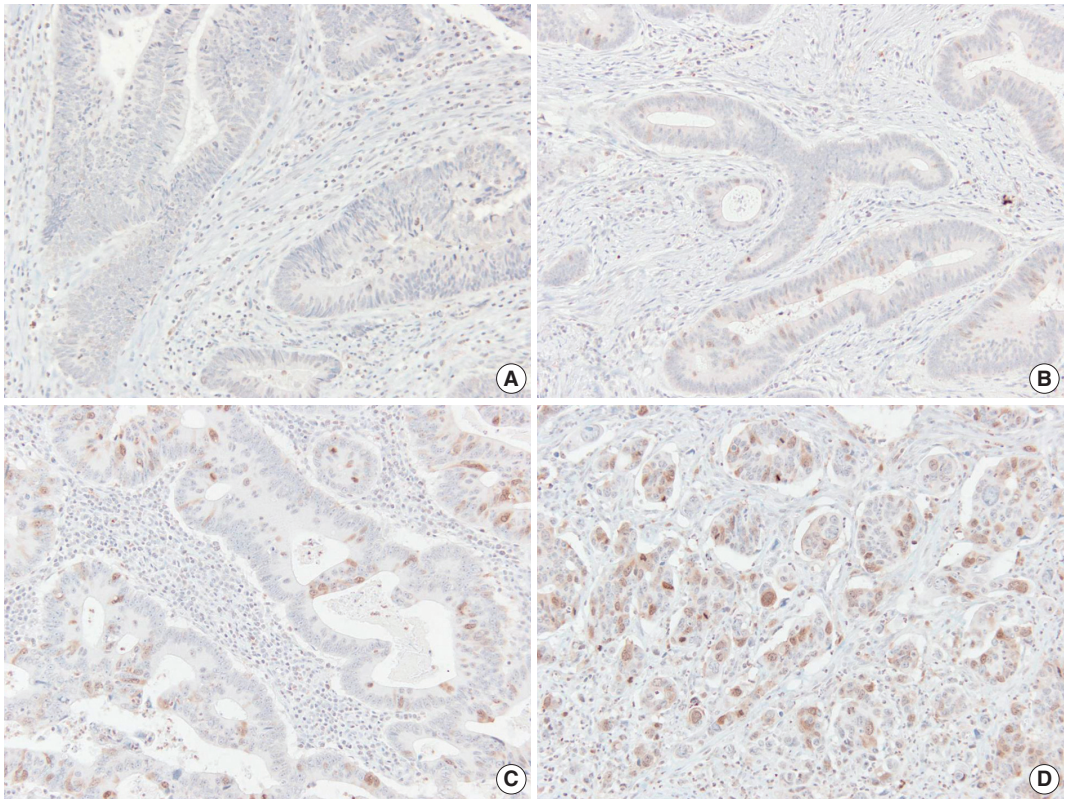

Fig. 3. Immunohistochemical staining with Aurora kinase A (*AURKA*). (A) Score 1, positive staining in <10%. (B) Score 2, positive staining in ≥10% and <25%. (C) Score 3, positive staining in ≥25% and <50%. (D) Score 4, positive staining in ≥50%.

Table 3. The relationship between Aurora kinase A expression and the clinicopathological characteristics of colorectal cancer patients

Characteristic	Aurora kinase A expression		p-value
	Positive	Negative	
Age (yr)			.616
<65	29 (48.3)	31 (51.7)	
≥65	39 (42.9)	52 (57.1)	
Sex			.035
Male	53 (51.0)	51 (49.0)	
Female	15 (31.9)	32 (68.1)	
Tumor location			.021
Proximal	14 (30.4)	32 (69.6)	
Distal	54 (51.4)	51 (48.6)	
Tumor differentiation			.517
Well	8 (44.4)	10 (55.6)	
Moderate	57 (46.7)	65 (53.3)	
Poor	3 (33.3)	6 (66.7)	
Mucinous	0	2 (100)	
Vascular invasion			.755
Absent	64 (45.7)	76 (54.3)	
Present	4 (36.4)	7 (63.6)	
Lymphatic invasion			.139
Absent	32 (39.0)	50 (61.0)	
Present	36 (52.2)	33 (47.8)	
Perineural invasion			.288
Absent	44 (41.9)	61 (58.1)	
Present	24 (52.2)	22 (47.8)	
TNM stage			.692
I	11 (50.0)	11 (50.0)	
II	25 (41.0)	36 (59.0)	
III	32 (47.1)	36 (52.9)	

Values are presented as numbers (%).
TNM, tumor-node-metastasis.

sion and clinicopathological characteristics. AURKA protein expression was significantly related to patient sex, and positive AURKA staining was detected more often in male patients than in female (51.0% vs 31.9%, p = .035). In addition, AURKA expression was closely associated with tumor location, and it was more frequently found in carcinomas of the rectum, sigmoid colon, and descending colon than in carcinomas of proximal colon (51.4% vs 30.4%, p = .021). AURKA protein expression was not significantly correlated with age; tumor differentiation; vascular, lymphatic, and perineural invasion; or TNM stage.

AURKA expression and survival analysis

The mean follow-up time of the patients in this study was 1,269 days (range, 8 to 2,892 days). In total, 23.8% of the patients (n = 36) had recurred (AURKA-positive group, n = 27; AURKA-negative group, n = 9). The recurrence rate was significantly higher in the AURKA-positive group compared to the negative group (39.1% vs 11%, p < .001).

The mean overall PFS time was 74.6 months (range, 68.6 to 80.7 months). The AURKA-positive patients had a significantly poorer PFS than the AURKA-negative patients (p < .001). A univariate analysis demonstrated that AURKA expression (p = .001) (Fig. 4A), age (p = .034), lymphatic invasion (p = .001) (Fig. 4B), perineural invasion (p = .002) (Fig. 4C), and TNM stage (p = .013) (Fig. 4D) significantly affected PFS. In a multivariate analysis of PFS, a Cox proportional hazard model confirmed that AURKA expression was an independent and significant prognostic factor in colorectal adenocarcinoma (hazard ratio, 3.944; 95% confidence interval [CI], 1.821 to 8.542; p < .001) (Table 4). Perineural invasion was also identified as a significant prognostic factor (hazard ratio, 2.037; 95% CI, 1.017 to 4.079; p = .045) (Table 3).

DISCUSSION

CRC is among the most common malignancies[13] and is the leading cause of cancer mortality in the world.[20] The identification of genes correlated with carcinogenesis and the research to silence these genes can improve the patient care by more accurately predicting the prognosis and selecting the most appropriate adjuvant therapy.[13,15]

The role of Aurora kinases in mitosis and tumorigenesis is well documented.[12,20,21] AURKA is required for mitotic entry, chromosome alignment, and cytokinesis, and its abnormal function can result in aberrant cell division and aneuploidy, which in turn increase genomic instability and contribute to carcinogenesis.[15,22] Further, AURKA is an oncogene that contributes to colorectal adenoma to carcinoma progression and is associated with the malignant transformation of colorectal adenomas but not with serrated neoplasia progression.[21,22]

Chromosomal abnormalities in CRC have been studied by multiple groups using either CGH or aCGH. This has led to the discovery of many chromosomal aberrations, including gains and losses. Particularly common findings are gains in 20q, 13q, 7p, and 8q and losses in 17p, 18q, 8p, 4q, and 5q.[23] Orsetti *et al.*[24] reported that most commonly altered regions (gains or losses in ≥35% of the samples) are gains at chromosomes 7p, 7q, 8q, 13q, 20 and losses at 8p, 17p, and 18 in the CRC. In this study, 20q13.2–13.33 copy number gain is recurrently observed in 13 cases (54%), which is consistent with the previous results.

We also assessed *AURKA* amplification using FISH in two subgroups. The gene amplification is observed more frequently in the copy number gain group (three cases out of nine), than the group with no significant gain on the *AURKA*-containing

https://doi.org/10.4132/jptm.2016.10.17

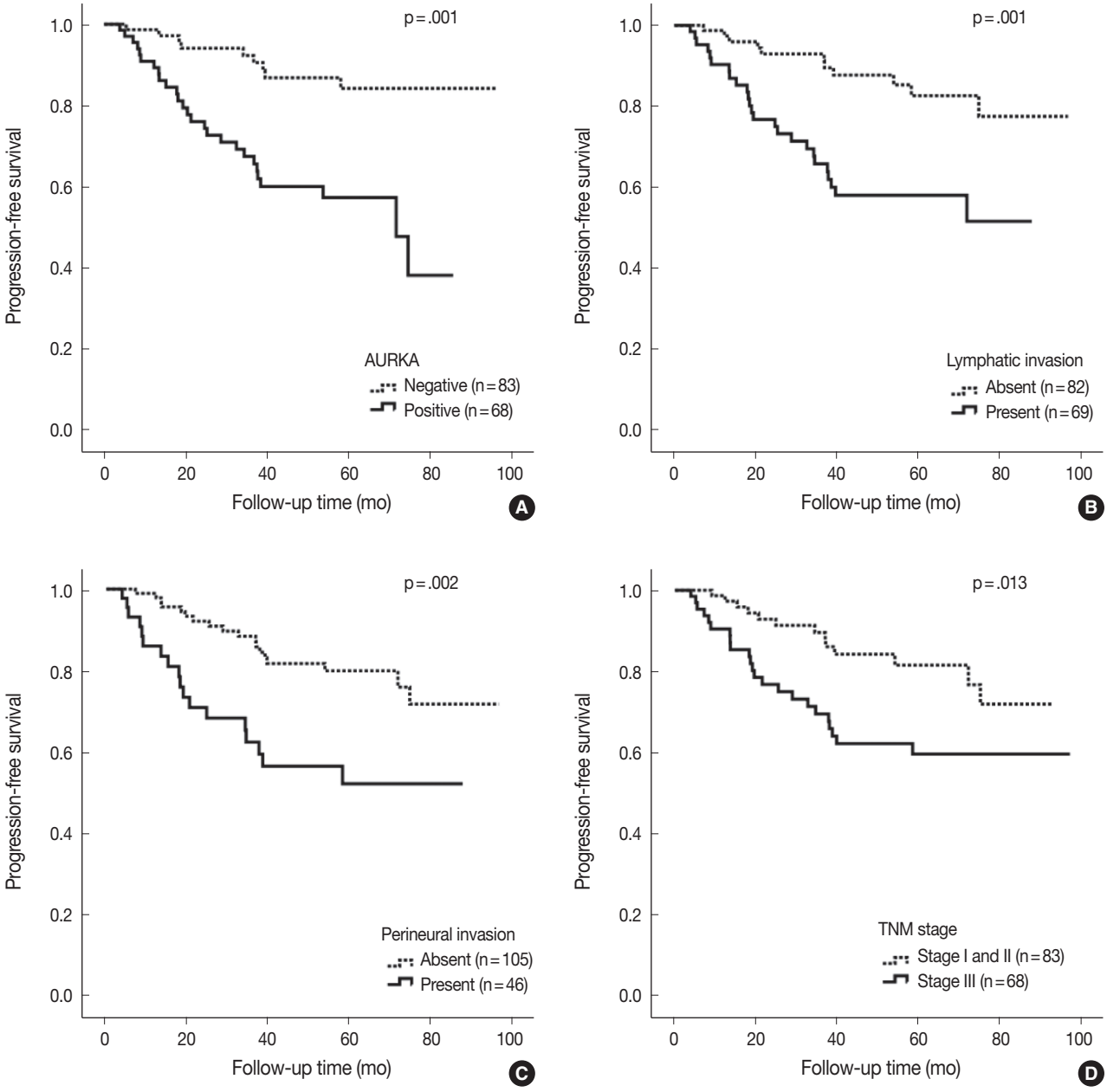

Fig. 4. The relationships between Aurora kinase A (AURKA) expression (A), lymphatic invasion (B), perineural invasion (C), TNM stage (D) and progression-free survival were analyzed using the Kaplan-Meier method with the log-rank test to assess the differences in survival probability between the groups.

locus. However, the data could not be analyzed statistically, due to a small number of cases. Further large-scale studies are required to assess the differences between the two groups.

A small number of reseachers have reported FISH result for *AURKA* gene amplification in various malignancies, such as melanomas and cancers of breast and prostate.[25-28] No reports on FISH for *AURKA* gene amplification in colorectal carcinoma tissue were found in the English literature in spite of a thorough searching.

Zhang *et al*.[29] demonstrated an increased AURKA gene copy number in 32.1% of advanced CRCs (43/134), and Casorzo *et al*.[22] reported AURKA gene overexpression in 85% of adenomas (17/20) containing invasive carcinoma of the colorectum, corresponding to early invasive carcinoma. In a previous study, 69% of metastatic CRC samples (41/59) showed an increased gene copy number.[12]

Table 4. Results of the multivariate Cox regression analysis of progression-free survival

Factors	Hazard ratio (95% CI)	p-value
AURKA expression (positive vs negative)	3.944 (1.821–8.542)	<.001
Age (<65 yr vs ≥65 yr)	1.453 (0.726–2.907)	.291
Lymphatic invasion (present vs absent)	1.654 (0.707–3.867)	.246
Perineural invasion (present vs absent)	2.037 (1.017–4.079)	.045
TNM stage (III vs I or II)	1.489 (0.688–3.224)	.312

CI, confidence interval; AURKA, Aurora kinase A; TNM, tumor-node-metastasis.

AURKA protein overexpression and gene amplification are common in CRCs.[4,9,12,13,15,19-22,29,30] In this study, we detected AURKA overexpression in 45% of colorectal adenocarcinoma samples (71/151) using immunohistochemistry. Similarly, Lam *et al*.[13] reported AURKA protein expression in 48.5% (97/200) of CRC samples. In other studies, 33% (9/20)[12] and 82.5% (33/40)[15] of metastatic CRC samples showed AURKA overexpression.

In our study, AURKA expression was related to patient sex and tumor location, along with several other clinicopathological parameters. Tumor location, histology, and grade were correlated with AURKA protein expression in the report by Lam *et al*.[13] Baba *et al*.[19] reported that AURKA expression was inversely associated with a family history of CRC and not correlated with tumor location, grade, histologic component, or stage. Goktas *et al*.[15] found a significant relationship between AURKA expression and the histologic grade of the tumor tissue.

These discrepancies in AURKA expression may not only be caused by the heterogeneity of the study groups (e.g., patient number, patient characteristics, and disease stage), but also by differences in various technical conditions.

Some authors reported that AURKA expression is correlated with clinicopathological factors in other malignancies. For example, positive AURKA expression was closely correlated with TNM stage in gastric cancer[10] and with initial clinical stage, Ki-67 labeling index, and the recurrence rate in triple-negative breast cancer.[14] Ogawa *et al*.[11] reported that perimembrane AURKA staining was significantly related to a higher pathologic stage and higher proliferative activity.

A few previous studies have investigated the prognostic impact of AURKA expression in CRC patients.[4,9,15] Belt *et al*.[4] suggested that high-level AURKA expression was significantly associated with recurrence in stage II or III colon cancer. Goos *et al*.[9] revealed that high-level AURKA expression was associated with poor overall survival in CRC patients with liver metastasis. In contrast, Goktas *et al*.[15] reported that AURKA overexpression may have a positive effect on survival in metastatic CRC. We analyzed the correlation between AURKA expression and survival in patients with CRC. Our data demonstrate that AURKA expression in CRC patients is associated with poor PFS. Moreover, our Cox model analysis indicated that AURKA expression is a prognostic factor for poor PFS in CRC patients. However, overall survival analysis could not be performed due to a short follow-up period.

Recent studies have shown that AURKA inhibitors have anticancer activity in various preclinical cancer models, and some inhibitors have entered clinical trials.[1,8] Such studies have underlined the incremental therapeutic efficacy of combining AURKA inhibitors with conventional anti-cancer drugs to inhibit tumor progression and restore chemosensitivity.[1] Our results suggest that targeted treatment with AURKA inhibitors can improve PFS and assist in planning the treatment of CRC patients.

In summary, AURKA expression was significantly associated with patient sex and CRC location, and it was an independent molecular prognostic factor for poor outcome in CRC patients. Thus, AURKA expression may serve as a valuable prognostic marker for CRC.

Conflicts of Interest

No potential conflict of interest relevant to this article was reported.

Acknowledgments

The fresh tissue specimens and data of colorectal adenocarcinomas were provided by the Biobank of Jeju National University Hospital (A-03).

REFERENCES

1. D'Assoro AB, Haddad T, Galanis E. Aurora-A kinase as a promising therapeutic target in cancer. Front Oncol 2015; 5: 295.
2. Katsha A, Belkhiri A, Goff L, El-Rifai W. Aurora kinase A in gastrointestinal cancers: time to target. Mol Cancer 2015; 14: 106.
3. Cammareri P, Scopelliti A, Todaro M, *et al*. Aurora-a is essential for the tumorigenic capacity and chemoresistance of colorectal cancer stem cells. Cancer Res 2010; 70: 4655-65.
4. Belt EJ, Brosens RP, Delis-van Diemen PM, *et al*. Cell cycle proteins predict recurrence in stage II and III colon cancer. Ann Surg Oncol 2012; 19 Suppl 3: S682-92.
5. Zhang J, Li B, Yang Q, Zhang P, Wang H. Prognostic value of Aurora kinase A (AURKA) expression among solid tumor patients: a sys-

tematic review and meta-analysis. Jpn J Clin Oncol 2015; 45: 629-36.
6. Fu J, Bian M, Jiang Q, Zhang C. Roles of Aurora kinases in mitosis and tumorigenesis. Mol Cancer Res 2007; 5: 1-10.
7. D'Assoro AB, Liu T, Quatraro C, *et al*. The mitotic kinase Aurora-A promotes distant metastases by inducing epithelial-to-mesenchymal transition in ERα(+) breast cancer cells. Oncogene 2014; 33: 599-610.
8. Cervantes A, Elez E, Roda D, *et al*. Phase I pharmacokinetic/pharmacodynamic study of MLN8237, an investigational, oral, selective aurora a kinase inhibitor, in patients with advanced solid tumors. Clin Cancer Res 2012; 18: 4764-74.
9. Goos JA, Coupe VM, Diosdado B, *et al*. Aurora kinase A (AURKA) expression in colorectal cancer liver metastasis is associated with poor prognosis. Br J Cancer 2013; 109: 2445-52.
10. Wang J, Yang S, Zhang H, *et al*. Aurora-A as an independent molecular prognostic marker in gastric cancer. Oncol Rep 2011; 26: 23-32.
11. Ogawa E, Takenaka K, Katakura H, *et al*. Perimembrane Aurora-A expression is a significant prognostic factor in correlation with proliferative activity in non-small-cell lung cancer (NSCLC). Ann Surg Oncol 2008; 15: 547-54.
12. Dotan E, Meropol NJ, Zhu F, *et al*. Relationship of increased aurora kinase A gene copy number, prognosis and response to chemotherapy in patients with metastatic colorectal cancer. Br J Cancer 2012; 106: 748-55.
13. Lam AK, Ong K, Ho YH. Aurora kinase expression in colorectal adenocarcinoma: correlations with clinicopathological features, p16 expression, and telomerase activity. Hum Pathol 2008; 39: 599-604.
14. Xu J, Wu X, Zhou WH, *et al*. Aurora-A identifies early recurrence and poor prognosis and promises a potential therapeutic target in triple negative breast cancer. PLoS One 2013; 8: e56919.
15. Goktas S, Yildirim M, Suren D, *et al*. Prognostic role of Aurora-A expression in metastatic colorectal cancer patients. J BUON 2014; 19: 686-91.
16. Li D, Zhu J, Firozi PF, *et al*. Overexpression of oncogenic STK15/BTAK/Aurora A kinase in human pancreatic cancer. Clin Cancer Res 2003; 9: 991-7.
17. Park HS, Park WS, Bondaruk J, *et al*. Quantitation of Aurora kinase A gene copy number in urine sediments and bladder cancer detection. J Natl Cancer Inst 2008; 100: 1401-11.
18. Jeng YM, Peng SY, Lin CY, Hsu HC. Overexpression and amplification of Aurora-A in hepatocellular carcinoma. Clin Cancer Res 2004; 10: 2065-71.
19. Baba Y, Nosho K, Shima K, *et al*. Aurora-A expression is independently associated with chromosomal instability in colorectal cancer. Neoplasia 2009; 11: 418-25.
20. Sillars-Hardebol AH, Carvalho B, de Wit M, *et al*. Identification of key genes for carcinogenic pathways associated with colorectal adenoma-to-carcinoma progression. Tumour Biol 2010; 31: 89-96.
21. Carvalho B, Postma C, Mongera S, *et al*. Multiple putative oncogenes at the chromosome 20q amplicon contribute to colorectal adenoma to carcinoma progression. Gut 2009; 58: 79-89.
22. Casorzo L, Dell'Aglio C, Sarotto I, Risio M. Aurora kinase A gene copy number is associated with the malignant transformation of colorectal adenomas but not with the serrated neoplasia progression. Hum Pathol 2015; 46: 411-8.
23. Jasmine F, Rahaman R, Dodsworth C, *et al*. A genome-wide study of cytogenetic changes in colorectal cancer using SNP microarrays: opportunities for future personalized treatment. PLoS One 2012; 7: e31968.
24. Orsetti B, Selves J, Bascoul-Mollevi C, *et al*. Impact of chromosomal instability on colorectal cancer progression and outcome. BMC Cancer 2014; 14: 121.
25. Park K, Chen Z, MacDonald TY, *et al*. Prostate cancer with Paneth cell-like neuroendocrine differentiation has recognizable histomorphology and harbors AURKA gene amplification. Hum Pathol 2014; 45: 2136-43.
26. Mosquera JM, Beltran H, Park K, *et al*. Concurrent AURKA and MYCN gene amplifications are harbingers of lethal treatment-related neuroendocrine prostate cancer. Neoplasia 2013; 15: 1-10.
27. Letessier A, Sircoulomb F, Ginestier C, *et al*. Frequency, prognostic impact, and subtype association of 8p12, 8q24, 11q13, 12p13, 17q12, and 20q13 amplifications in breast cancers. BMC Cancer 2006; 6: 245.
28. Diaz A, Puig-Butillé JA, Valera A, *et al*. TERT and AURKA gene copy number gains enhance the detection of acral lentiginous melanomas by fluorescence *in situ* hybridization. J Mol Diagn 2014; 16: 198-206.
29. Zhang C, Fang Z, Xiong Y, *et al*. Copy number increase of aurora kinase A in colorectal cancers: a correlation with tumor progression. Acta Biochim Biophys Sin (Shanghai) 2010; 42: 834-8.
30. Lassmann S, Danciu M, Müller M, *et al*. Aurora A is differentially expressed and regulated in chromosomal and microsatellite instable sporadic colorectal cancers. Mod Pathol 2009; 22: 1385-97.

Journal of Pathology and Translational Medicine 2017; 51: 40-48
https://doi.org/10.4132/jptm.2016.08.31

■ ORIGINAL ARTICLE ■

PD-L1 Expression and Combined Status of PD-L1/PD-1–Positive Tumor Infiltrating Mononuclear Cell Density Predict Prognosis in Glioblastoma Patients

Jiheun Han · Yongkil Hong[1]
Youn Soo Lee

Departments of Hospital Pathology and [1]Neurosurgery, Seoul St. Mary's Hospital, College of Medicine, The Catholic University of Korea, Seoul, Korea

Received: June 23, 2016
Revised: August 7, 2016
Accepted: August 31, 2016

Corresponding Author
Youn Soo Lee, MD, PhD
Department of Hospital Pathology, Seoul St. Mary's Hospital, College of Medicine, The Catholic University of Korea, 222 Banpo-daero, Seocho-gu, Seoul 06591, Korea
Tel: +82-2-2258-1613
Fax: +82-2-2258-1628
E-mail: lys9908@catholic.ac.kr

Background: Programmed death ligand 1 (PD-L1) in tumor cells is known to promote immune escape of cancer by interacting with programmed cell death 1 (PD-1) in tumor infiltrating immune cells. Immunotherapy targeting these molecules is emerging as a new strategy for the treatment of glioblastoma (GBM). Understanding the relationship between the PD-L1/PD-1 axis and prognosis in GBM patients may be helpful to predict the effects of immunotherapy. **Methods:** PD-L1 expression and PD-1–positive tumor infiltrating mononuclear cell (PD-1+tumor infiltrating mononuclear cell [TIMC]) density were evaluated using tissue microarray containing 54 GBM cases by immunohistochemical analysis; the associations with patient clinical outcomes were evaluated. **Results:** PD-L1 expression and high PD-1+TIMC density were observed in 31.5% and 50% of GBM cases, respectively. High expression of PD-L1 in tumor cells was an independent and significant predictive factor for worse overall survival (OS; hazard ratio, 4.958; p = .007) but was not a significant factor in disease-free survival (DFS). PD-1+TIMC density was not correlated with OS or DFS. When patients were classified based on PD-1 expression and PD-1+TIMC density, patients with PD-L1+/PD-1+TIMC low status had the shortest OS (13 months, p = .009) and DFS (7 months, p = .053). **Conclusions:** PD-L1 expression in GBM was an independent prognostic factor for poor OS. In addition, combined status of PD-L1 expression and PD-1+TIMC density also predicted patient outcomes, suggesting that the therapeutic role of the PD-1/PD-L1 axis should be considered in the context of GBM immunity.

Key Words: Glioblastoma; Programmed cell death 1; Programmed death ligand 1

Glioblastoma (GBM) is the most common and most aggressive adult brain tumor, with a median survival of only 12 to 15 months, even with optimal treatment.[1] The current management options for newly diagnosed GBM are surgical resection or biopsy, followed by radiotherapy and chemotherapy.[2] Unfortunately, GBM ultimately relapses in most patients due to infiltrative growth and frequent presence of multiple lesions at the time of diagnosis.[3] The limitations of conventional treatments for the improvement of GBM patient outcomes have prompted investigators to look for new therapeutic approaches and useful predictive biomarkers of treatment response. Immunotherapy, the idea of recruiting the immune system to fight against cancer, is one of these approaches.

A major determinant of cancer pathogenesis is the interaction of tumor cells with the immune system. An anticancer immune response occurs through a series of stepwise events, beginning with tumor antigen presentation by antigen-presenting cells (APCs) and progressing through priming and activation of T cells, trafficking of cytotoxic T cells (CD8+ cells) to tumors, and ultimately the killing of tumor cells.[4] This interaction is regulated by checkpoint molecules, which can be either co-stimulatory or co-inhibitory. Programmed death ligand 1 (PD-L1) and programmed cell death 1 (PD-1) are inhibitory immune checkpoint molecules. The association between PD-1 expression on a large proportion of tumor-infiltrating lymphocytes (TILs)[5] and PD-L1 upregulation in a number of cancer cells with poor clinical outcomes makes these checkpoint molecules an attractive target for an immunotherapeutic approach.[6]

Recent studies found that PD-L1 was overexpressed by GBM.[7,8] PD-L1 on the surface of tumor cells suppresses proliferation and cytotoxic activity of T cells and promotes regulatory T-cell activity.[9] The expression of PD-L1 in GBM is known to be regulated by both extrinsic and intrinsic mechanisms,[9] and interferon γ (IFN-γ)–mediated superinduction of PD-L1 in GBM with phosphatase and tensin homology (PTEN) deficiency has been reported.[10]

PD-1 is a member of the CD28 family that is expressed in

pISSN 2383-7837
eISSN 2383-7845

tumor infiltrating mononuclear cells (TIMCs), including activated T cells, B cells, dendritic cells, and macrophages.[11] PD-1 expression by tumor infiltrating lymphocytes (TILs) is known to be related to patient outcomes for other solid tumors.[12-14]

There is a current effort to develop more accurate predictive biomarkers of patient response to checkpoint blockade, particularly anti–PD-1/PD-L1, in conjunction with the tumor-host immune relationship based on PD-L1 expression and TILs.[15,16] TILs, a component of the adaptive antitumor host response, are known to be related to outcomes, and adoptive transfer of TILs can mediate regression of metastatic melanoma.[17]

However, data on the prognostic value of PD-L1 tumor expression and PD-1 expression in tumor infiltrating immune cells in GBM are limited, and the results of previous studies have been inconsistent. In the present study, we examined PD-L1 expression and PD-1 expression in TIMCs and evaluated their prognostic value in GBM patients.

MATERIALS AND METHODS

Patients

We retrospectively identified GBM patients who were diagnosed and treated in Seoul St. Mary's Hospital, College of Medicine, The Catholic University of Korea (Seoul, Korea), between 2004 and 2012. Patient clinicopathologic and clinical follow-up data were collected from the medical records. Histologic diagnosis of glioblastoma was performed according to the current World Health Organization (WHO) classification, fourth edition.[18] The ethics committee of Catholic University granted approval for this study (IRB No. KC16RISI0370).

Construction of tissue microarray

All tumor tissues were obtained at the time of the first surgery after diagnosis of GBM. A representative tumor area from each case was selected and marked on hematoxylin and eosin (H&E)-stained slides. Formalin-fixed and paraffin-embedded tissue blocks and the corresponding H&E-stained slides were overlaid for tissue microarray (TMA) sampling. A cylindrical core (2 mm in diameter) was obtained for each case. Sectioning of microarray blocks produced 4-μm thick sections.

Immunohistochemistry

Microslide tissue sections were deparaffinized with xylene, hydrated using a diluted alcohol series, and immersed in 0.3% H_2O_2 in methanol to extinguish endogenous peroxidase activity. Sections were then microwaved for 15 minutes in 10 mM citrate buffer (pH 6.0) for antigen retrieval. Each section was blocked with 4% bovine serum albumin in phosphate buffered saline with 0.1% Tween 20 (PBST) for 30 minutes to reduce non-specific staining. Sections were incubated with anti–PD-L1 (1:100, Cell Marque, Rocklin, CA, USA) or anti–PD-1 (1:100, Ventana, Tucson, AZ, USA) antibodies in PBST containing 3 mg/mL goat globulin (Sigma-Aldrich, St. Louis, MO, USA) for 60 minutes at room temperature, followed by three successive washes with a buffer. The sections were then incubated with an anti-mouse/rabbit antibody (Envision plus, Dako, Carpinteria, CA, USA) for 30 minutes at room temperature. The chromogen used was 3,3'-diaminobenzidine (Dako). The sections were counterstained with Meyer's hematoxylin. For positive controls, sections of human placenta and tonsil tissue were included in each staining run. Omission of the primary antibody for placenta and tonsil tissue sections was used as a negative control.

Immunohistochemical analysis

Two experienced pathologists (Y.S.L. and J.H) performed immunohistochemical analysis for PD-L1 and PD-1 by microscopic observation of the stained TMA slides. Cases were considered PD-L1+ if membranous staining of tumor cells was detected in at least 5% of the cells, irrespective of staining intensity. The cut-off threshold of PD-L1 expression was determined by receiver operating characteristic analysis of the survival rate.

PD-1 staining in TIMCs was assessed by identification of lymphocytes and macrophages on the basis of morphologic features. All TIMCs with membranous PD-1 expression of moderate to high intensity were manually counted in an entire area for each TMA core. The number of PD-1+TIMCs was divided by the total area of the TMA core (3.14 mm^2) to obtain the number of PD-1+TIMCs per unit area (/mm^2), the median value of which was used as a cut-off to define low versus high density.

Statistical analysis

Data were analyzed using the SPSS 21.0 statistical software package (IBM Corp., Armonk, NY, USA). Differences in patient characteristics between positive and negative PD-L1 expression or high and low density of PD-1+TIMCs were analyzed using chi-square tests, Fisher exact tests, and Student's t-tests. Comparative analysis of PD-L1 expression and the number of PD-1+ TIMCs was performed using Mann-Whitney tests. Survival time curves were drawn using the Kaplan-Meier method and a log-rank test was used to assess the significance of differences in survival. Survival time included overall survival (OS; the length of time from the date of surgery or biopsy to the date of death

from any cause, or to the last follow-up date if the patient is alive) and disease-free survival (DFS; the length of time from the date of surgery or biopsy to recurrence, progress or death from any cause). Univariate and multivariate analyses using the Cox proportional hazard model were performed to identify factors influencing OS and DFS. A step-down procedure was selected for multivariate analysis. In all statistical analyses, a two-tailed p-value less than .05 was considered to indicate a statistically significant difference.

RESULTS

Patient characteristics

The clinical characteristics of the 54 patients are summarized in Table 1. The mean patient age at diagnosis was 57.2 years, with a range of 31 to 85 years. The study group consisted of 26 males (48.1%) and 28 females (51.9%). Eleven patients (20.4%) had secondary GBM that developed from anaplastic astrocytoma and oligodendroglioma. Forty patients (74.1%) underwent total resection, 43 (79.6%) were treated with adjuvant radiotherapy plus concurrent temozolomide, and nine (16.7%) were treated with radiotherapy or temozolomide alone, based on performance status. Thirty-two patients (59.3%) had a single lesion and 22 (40.7%) had multifocal or multicentric lesions. Thirty-six patients (66.7%) were alive at the last follow-up and 40 patients (74.1%) experienced a progression or recurrence. Mean OS and DFS were 17.57 and 12.13 months, respectively.

PD-L1 expression and PD-1+TIMC density in GBM

PD-L1 staining in tumor cells was mostly of weak to moderate intensity with a membranous and cytoplasmic pattern (Fig. 1B, C). In most of the cases, PD-L1 stained only tumor cells. However,

Table 1. Summary of patient characteristics

Characteristic	No. (%)
Gender	
Male	26 (48.1)
Female	28 (51.9)
Primary/Secondary	
Primary	43 (79.6)
Secondary	11 (20.4)
Surgical treatment	
Total resection	40 (74.1)
Subtotal resection	11 (20.4)
Biopsy and others	3 (5.6)
Adjuvant treatment	
CCRT	43 (79.6)
CTx or RTx alone	9 (16.7)
No treatment	2 (3.7)
No. of lesions	
Single	32 (59.3)
Multiple (multifocal, multicentric)	22 (40.7)
Alive at last follow-up	
Yes	36 (66.7)
No	18 (33.3)
Progress/Recurrence	
Yes	40 (74.1)
No	14 (25.9)
Overall survival time, mean (range, mo)	17.57 (1.0–51.0)
Disease free survival, mean (range, mo)	12.13 (1.0–43.0)

CCRT, concurrent chemoradiotherapy; CTx, chemotherapy; RTx, radiotherapy.

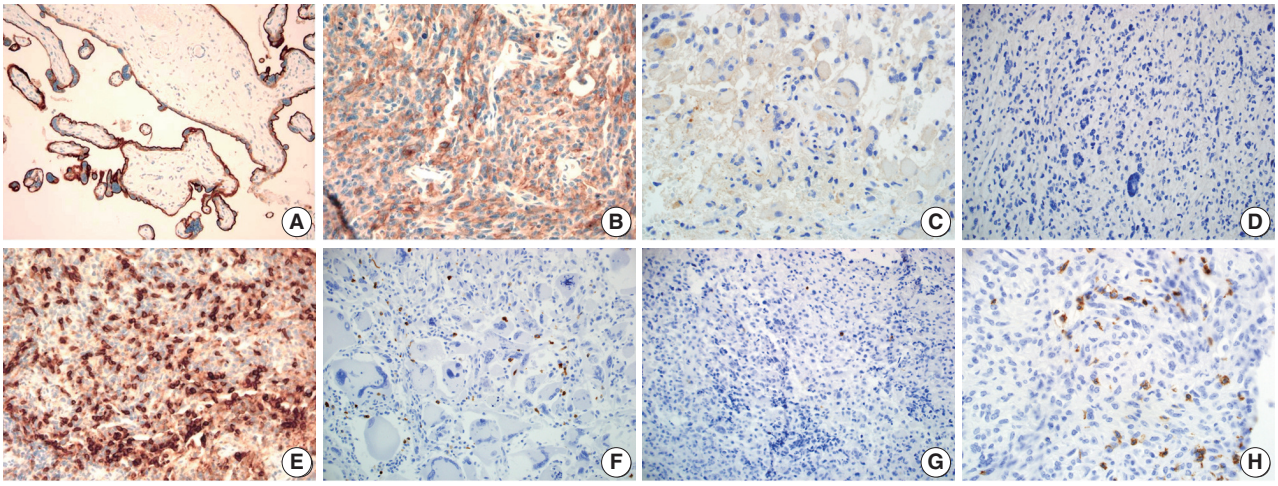

Fig. 1. Immunohistochemical staining pattern for programmed death ligand 1 (PD-L1) and programmed cell death 1 (PD-1). (A) Human placenta tissue as a positive control for endogenous PD-L1. PD-L1 positive tumor cells showing membranous and cytoplasmic staining with moderate (B) and weak (C) intensity. (D) PD-L1 negative tumor cells. (E) Tonsil tissue as a positive control for endogenous PD-1. Glioblastoma with high density (F) and low density (G) of PD-1 positive tumor infiltrating mononuclear cells (PD-1+tumor infiltrating mononuclear cell [TIMC]). (H) PD-1+TIMC consists of lymphocytes (most) and macrophages (some).

https://doi.org/10.4132/jptm.2016.08.31

in two cases (one case was PD-L1 positive, the other was not) a few dispersed TIMCs were stained with PD-L1 in their cytoplasm or membrane. In total, 17 patients (31.5%) were positive for PD-L1 expression in tumor cells.

The median PD-1+TIMC density in GBM was 1.75/mm^2 (range, 0 to 36.6/mm^2), and 27 patients (50%) were classified as PD-1+TIMC high density (Fig. 1F, G). Most of the PD-1+TIMC were lymphocytes with small round condensed nuclei and rims of cytoplasm. Occasionally, the cells had elongated or kidney shaped nuclei with a scant to moderate amount of cytoplasm (which were considered to be macrophages) that were stained with PD-1 (Fig. 1H).

No significant relationship between PD-L1 expression and PD-1+TIMC density was detected.

Correlations between PD-L1 expression and PD-1+TIMC density and GBM patient characteristics

Patient characteristics and their associations with PD-L1 expression and PD-1+TIMC density are summarized in Table 2. PD-L1 expression was significantly more frequent in patients who had died by the last follow up than in survivors (p = .038). No significant correlations were observed between PD-1+TIMC density and patient characteristics.

Prognostic implication of PD-L1 expression and PD-1+TIMC density for GBM

Univariate analysis revealed that PD-L1 expression was significantly associated with poor OS (p = .024; hazard ratio [HR], 3.058; 95% confidence interval [CI], 1.16 to 8.06) (Table 3), whereas none of the other factors, including PD-1+TIMC density, were significantly associated with OS. Multivariate analyses demonstrated that PD-L1 expression was an independent and significant predictive factor for worse OS (p = .007; HR, 4.958; 95% CI, 1.557 to 15.79) (Table 3).

Kaplan-Meier survival analysis revealed that patients with PD-L1 expression exhibited significantly shorter OS (median OS, 15 months vs 41 months, p = .017) (Fig. 2A), but that there was no significant difference in DFS (median DFS, 10

Table 2. Relationship between PD-L1 expression and density of PD-1+TIMC and GBM patient characteristics

	All cases (n=54)	PD-L1			PD-1+TIMC		
		Negative	Positive	p-value	Low	High	p-value
All cases		37 (68.5)	17 (31.5)		27 (50)	27 (50)	
Gender				.914			.586
Male	26	18 (69.2)	8 (30.8)		14 (53.8)	12 (46.2)	
Female	28	19 (67.9)	9 (32.1)		13 (48.1)	15 (55.6)	
Age at diagnosis (yr) Mean (min-max)		57.62 (31–85)	56.18 (36–78)	.814	54.26 (32–77)	60.07 (31–85)	.115
Primary/Secondary				.47			.311
Primary	43	28 (65.1)	15 (34.9)		23 (53.5)	20 (46.5)	
Secondary	11	9 (81.8)	2 (18.2)		4 (36.4)	7 (63.6)	
Surgical treatment				.672			.804
Total resection	40	26 (65.0)	14 (35.0)		19 (47.5)	21 (52.5)	
Subtotal resection	11	9 (81.8)	2 (18.2)		6 (54.5)	5 (45.5)	
Biopsy and others	3	2 (66.7)	1 (33.3)		2 (66.7)	1 (33.3)	
Adjuvant treatment				.257			.082
CCRT	43	27 (62.8)	16 (37.2)		23 (53.5)	20 (46.5)	
CTx or RTx alone	9	8 (88.9)	1 (11.1)		2 (22.2)	7 (77.8)	
No treatment	2	2 (100)	0		2 (100)	0	
No. of lesions				.713			.78
Single	33	22 (66.7)	11 (33.3)		16 (48.5)	17 (51.5)	
Multiple	21	15 (71.4)	6 (28.6)		11 (52.4)	10 (47.6)	
Alive at last follow-up				.038			.248
Yes	36	28 (77.8)	8 (22.2)		16 (44.4)	20 (55.6)	
No	18	9 (50.0)	9 (50.0)		11 (61.1)	7 (38.9)	
Progress/Recurrence				1			.214
Yes	40	27 (67.5)	13 (32.5)		22 (55.0)	18 (45.0)	
No	14	10 (71.4)	4 (28.6)		5 (35.7)	9 (64.3)	

Values are presented as number (%) unless otherwise indicated.
PD-L1, programmed death ligand 1; PD-1, programmed cell death 1; TIMC, tumor infiltrating mononuclear cell; GBM, glioblastoma; CCRT, concurrent chemoradiotheraphy; CTx, chemotherapy; RTx, radiation therapy.

Table 3. Univariate and multivariate analyses of clinicopathologic factors for OS and DFS

Variable	OS				DFS			
	Univariate		Multivariate		Univariate		Multivariate	
	HR (95% CI)	p-value	HR (95% CI)	p-value	Hazard ratio (95% CI)	p-value	HR (95% CI)	p-value
PD-L1 expression								
Positive	3.058 (1.160–8.060)	.024	4.958 (1.557–15.79)	.007	1.651 (0.821–3.319)	.16		
Negative	Reference		Reference		Reference			
PD-1+TIMC								
High	0.726 (0.280–1.879)	.509			0.842 (0.445–1.593)	.597		
Low	Reference				Reference			
Age (continuous)	0.989 (0.953–1.026)	.541			0.997 (0.973–1.002)	.825		
Gender								
Male	2.000 (0.747–5.360)	.168	4.053 (1.230–13.35)	.021	1.806 (0.940–3.472)	.076	2.142 (1.077–4.260)	.03
Female	Reference		Reference		Reference		Reference	
Primary vs secondary								
Primary	1.830 (0.418–8.007)	.423			1.023 (0.447–2.340)	.957		
Secondary	Reference				Reference			
Numver of lesions								
Single	Reference	.133	Reference	.078	Reference	.278	Reference	.092
Multiple	2.103 (0.797–5.547)		2.715 (0.893–8.253)		1.438 (0.746–2.772)		1.814 (0.907–3.629)	
Surgical treatment								
Total resection	Reference				Reference			
Subtotal resection	1.134 (0.365–3.528)	.828			1.099 (0.497–2.433)	.815		
Biopsy and others	1.453 (0.186–11.34)	.721			2.807 (0.838–9.405)	.094		
Adjuvant treatment								
CCRT	Reference		Reference		Reference			
CTx or RTx alone	1.309 (0.369–4.640)	.677	2.369 (0.562–9.989)	.024	0.706 (0.245–2.030)	.518		
No treatment	7.717 (0.880–67.674)	.065	5.760 (2.089–317.6)	.011	1.346 (0.181–10.011)	.771		
Recurrence or progression	2.238 (0.511–9.795)	.285						

OS, overall survival; DFS, disease free survival; HR, hazard ratio; CI, confidence interval; PD-L1, programmed death ligand 1; PD-1, programmed cell death 1; TIMC, tumor infiltrating mononuclear cell; CCRT, concurrent chemoradiation therapy; CTx, chemotherapy; RTx, radiation therapy.

months vs 14 months; p = .14) (Fig. 2B). There were no significant differences in OS or DFS according to PD-1+TIMC density (Fig. 2C, D).

Classification of patients based on PD-L1 expression and PD-1+TIMC density

We divided patients into four groups according to their PD-L1 expression status and PD-1+TIMC density: PD-L1+/PD-1+TIMC high (group 1; 10 patients, 18.5%), PD-L1+/PD-1+TIMC low (group 2; 7 patients, 13%), PD-L1–/PD-1+TIMC high (group 3; 17 patients, 31.5%), and PD-L1–/PD-1+TIMC low (group 4; 20 patients, 37%). The median OS was 24 months in group 1, 13 months in group 2, 27 months in group 3, and 41 months in group 4 (p = .0092) (Fig. 3A). The median DFS was 11 months in group 1, 7 months in group 2, and 24 months in groups 3 and 4 (p = .053) (Fig. 3B). Patients in group 2 had significantly worse rates of OS (Fig. 3C, E) and DFS (Fig. 3D, F) than those in groups 3 and 4. They also tended to have shorter OS (p = .049) (Fig. 3G) and DFS (p = .068) (Fig. 3H) than those in group 1.

Histologically, the GBM of group 2 tended to show marked tumor cellularity, low density of TIMCs, and a high Ki-67 index (≥20%). Patients in group 2 were younger at the age of diagnosis than the other groups, although this difference was not statistically significant (Table 4).

DISCUSSION

The expression rate of PD-L1 in glioblastoma patients in our study was 31.5%, which is comparable to that of other solid tumors, such as ~30% for melanoma[19] and ~36% for non-small cell lung cancer.[20] In recent studies, 38.3% of GBM[8] and 37.6% for newly diagnosed GBM[7] had at least 5% PD-L1 expression.

PD-L1 expression has been observed, not only in tumor cells, but also in non-cancerous interstitial cells[21] and stromal lymphocytes.[22] Nduom *et al*.[8] also observed that lymphocytes consisted of nearly 30% PD-L1 positive cells in GBM. However, in our study, PD-L1–positive lymphocytes were found in only two

 https://doi.org/10.4132/jptm.2016.08.31

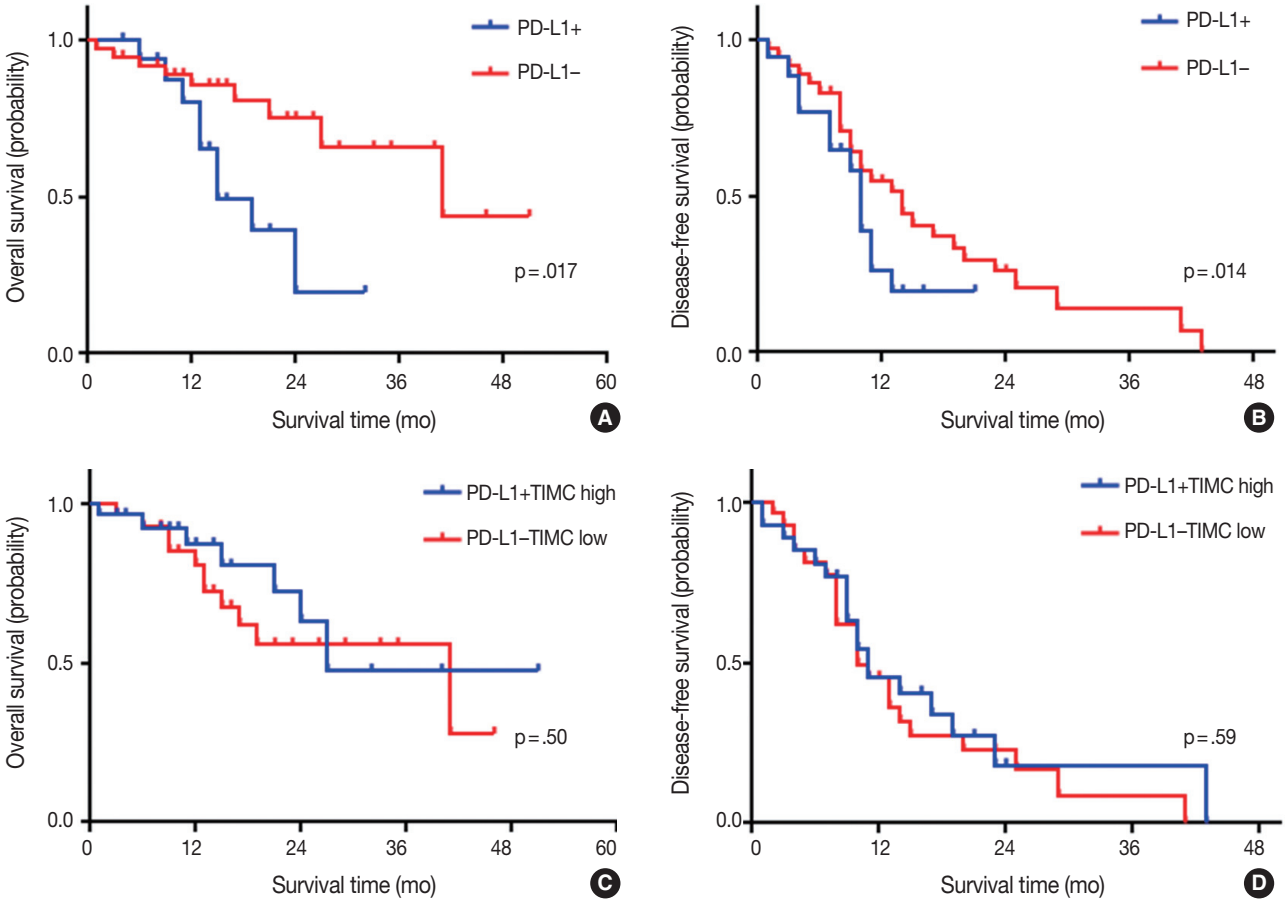

Fig. 2. Kaplan-Meier plots for overall survival and disease-free survival of glioblastoma patients according to the programmed death ligand 1 (PD-L1) expression status (A, B) and disease-free survival (C, D). TIMC, tumor infiltrating mononuclear cell.

out of 54 cases and their proportions were not significant. These differences may result from the use of different antibodies, differences in counting or detection methods, or different definitions for positivity. In addition, GBM is known to create an immunosuppressive microenvironment, resulting in sparse TILs in GBM relative to other solid tumors, which might affect the proportion of PD-L1 positive lymphocytes.

In the present study, patients with PD-L1 expression showed significantly poorer OS. However, the relationship between PD-L1 expression and prognosis in patients with GBM remains unclear. Recent studies have evaluated the prognostic implications of PD-L1 expression in GBM[7,8] and glioma[23] with inconsistent findings. Although the precise mechanism by which intratumoral PD-L1 negatively affects patient prognosis is yet to be determined, PD-L1 has been expressed in different cancer types, including kidney, liver, ovarian, pancreatic, lung, and gastric cancer, and PD-L1 expression by tumor cells has been reported to strongly correlate with a poor prognosis.[24-29]

Traditionally, the central nervous system has been presumed to be an immune privileged organ, primarily due to an intact blood-brain barrier (BBB). However, in GBM, the integrity of the BBB is compromised, enabling activated macrophages and lymphocytes to migrate across the BBB into the brain parenchyma.[30] Inflammatory infiltrates in GBM are relatively sparse; in the present study, the median density of PD-1+TIMCs was 1.75/mm^2, which is much lower than in other solid tumors, such as lung cancer (33.4 PD-1+TILs/mm^2).[31] Presurgical corticosteroid treatment may affect the number of TIMCs, although Berghoff *et al*.[32] found that corticosteroids did not affect the amount of TILs in melanoma brain metastases. It is known that GBM creates an immunosuppressive microenvironment by producing immunosuppressive cytokines, such as transforming growth factor β, prostaglandin-E, indoleamine 2,3-dioxygenase, interleukin 10, and STAT3.[33] In addition, ineffective presentation of tumor antigens by APCs or recruitment of immunosuppressive cells, such as regulatory T cells (Treg) or myeloid-derived suppressor cells, is known to contribute to an immunosuppressive condition.[33] The scarcity of PD-1+ infiltrating immune cells,

targets of anti–PD-1 therapy, might imply reduced efficacy of the treatment.

No relationship between PD-1 expression and clinical outcomes was observed in the present study, although previous studies have shown inconsistent results.[12,34] In a subgroup analysis dividing patients into four groups according to PD-L1 expression and PD-1+TIMC density, group 2 (PD-L1+/PD-1+TIMC low) had a significantly worse OS than the other three groups. This

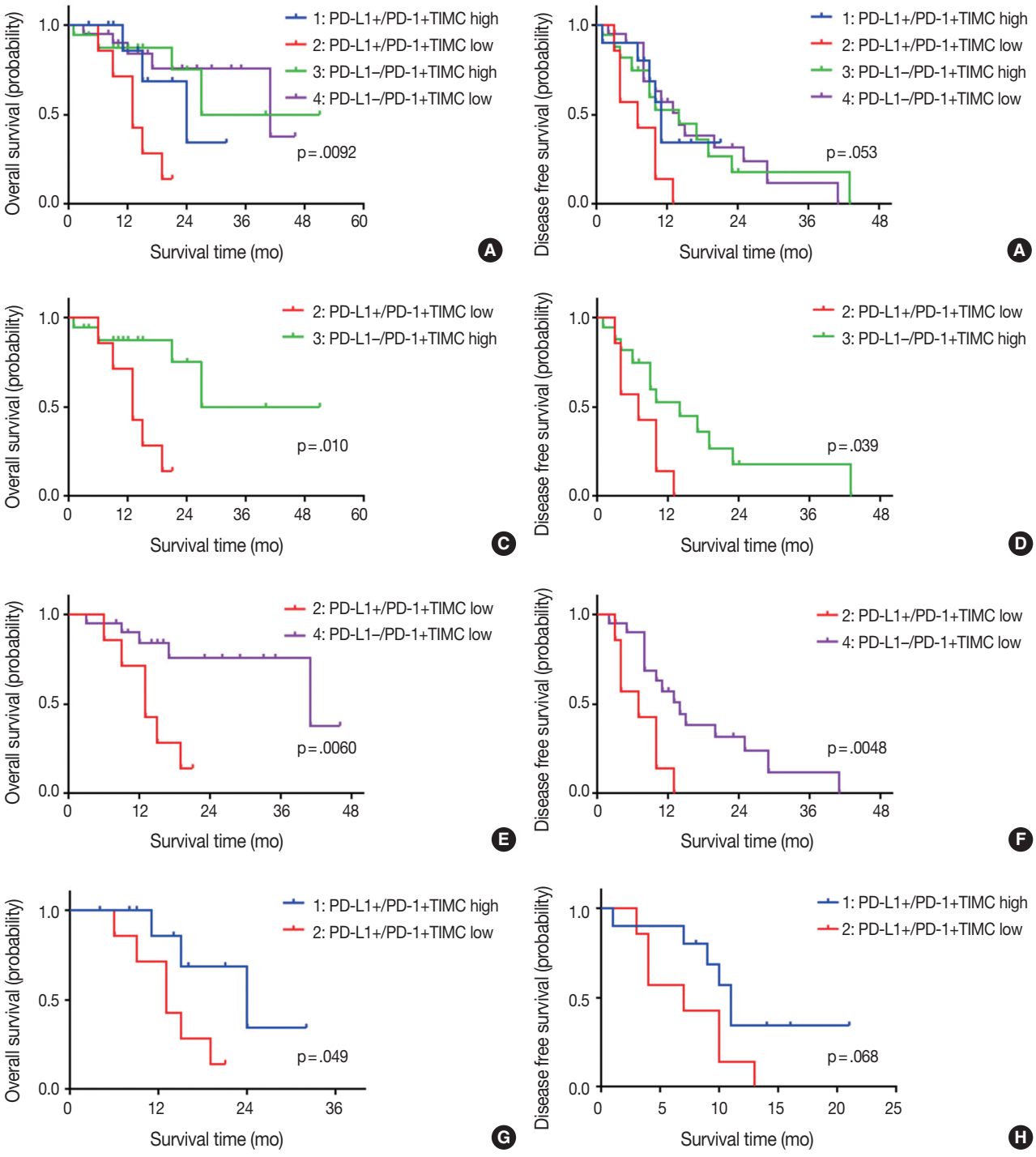

Fig. 3. Kaplan-Meier curves for overall survival (A, C, E, G), and disease free survival (B, D, F, H) of patients with positive or negative expression of programmed death ligand 1 (PD-L1) and high or low density of programmed cell death 1 (PD-1)+tumor infiltrating mononuclear cell (TIMC).

https://doi.org/10.4132/jptm.2016.08.31

Table 4. Clinicopathological features of groups classified on the basis of PD-L1 expression and PD-1+TIMC density

Variable	Group 1 (PD-L1+/high PD-1+TIMC)	Group 2 (PD-L1+/low PD-1+TIMC)	Group 3 (PD-L1-/high PD-1+TIMC)	Group 4 (PD-L1-/low PD-1+TIMC)
No. of patients (%)	10 (18.5)	7 (13)	17 (31.5)	20 (37)
Age, mean (range, yr)	59.6 (40–70)	51.3 (36–69)	60.3 (31–85)	55.3 (32–68)
Ki-67 index, mean (range, %)	28.3 (10–60)	41.4 (5–80)	29.9 (6–55)	32.3 (4–95)
Tumor cellularity	Moderate–marked	Marked	Mild–moderate	Mild–moderate
TIMC density	High	Low	High	Low~high

PD-L1, programmed death ligand 1; PD-1, programmed cell death 1; TIMC, tumor infiltrating mononuclear cell.

finding was in accordance with the poor prognostic effect of PD-L1 expression. In addition, the significant difference in OS between groups 1 and 2, both of which were PD-L1 positive, and the similar clinical outcomes of groups 1, 3, and 4, suggest that the prognostic impact of PD-L1 expression on GBM should be evaluated with PD-1+TIMC density. Thus, the combined status of PD-L1 expression with PD-1+TIMC density may more precisely predict clinical outcomes.

The PD-L1 expression in GBM is mediated by IFN-γ produced in an active immune response to the tumor or a constitutive oncogenic signaling pathway via the loss of PTEN.[10] Harter *et al*.[35] found a loco-regional overlap between TILs and PD-L1 expression in brain metastasis, suggesting induction of PD-L1 in brain metastasis by anti-tumor immune response. However, we observed that PD-L1–positive GBM tended to have equivocal (group 1) or even lower (group 2) TIMC density than PD-L1–negative groups, indicating that an intrinsic pathway might be associated with PD-L1 overexpression in GBM.

Our study has several limitations. First, the population enrolled in this study was relatively small, which could limit the statistical estimation. Second, TMA could not fully reflect the heterogeneity of GBM or the focal expression pattern of PD-L1, thus a false-negative evaluation could be possible. Lastly, as our study is retrospective, unknown factors that influence patient clinical outcomes might be present.

In summary, our study yielded two major findings: first, PD-L1 expression of GBM was an independent prognostic factor associated with poor OS; second, classification of patients based on PD-L1 expression and PD-1+TIMC density also predicts patient survival. Our results suggest that PD-L1 expression might be a useful prognostic factor and should be considered in the context of PD-1+TIMCs. The combination of PD-L1 expression status and PD-1+TIMC density appears to more effectively predict patient prognosis and might be helpful for selection of appropriate candidates for immunotherapy and for evaluating immunotherapeutic efficacy.

Conflicts of Interest

No potential conflict of interest relevant to this article was reported.

REFERENCES

1. Wen PY, Kesari S. Malignant gliomas in adults. N Engl J Med 2008; 359: 492-507.
2. Weller M, van den Bent M, Hopkins K, *et al*. EANO guideline for the diagnosis and treatment of anaplastic gliomas and glioblastoma. Lancet Oncol 2014; 15: e395-403.
3. Thomas RP, Xu LW, Lober RM, Li G, Nagpal S. The incidence and significance of multiple lesions in glioblastoma. J Neurooncol 2013; 112: 91-7.
4. Chen DS, Mellman I. Oncology meets immunology: the cancer-immunity cycle. Immunity 2013; 39: 1-10.
5. Ahmadzadeh M, Johnson LA, Heemskerk B, *et al*. Tumor antigen-specific CD8 T cells infiltrating the tumor express high levels of PD-1 and are functionally impaired. Blood 2009; 114: 1537-44.
6. Okazaki T, Honjo T. PD-1 and PD-1 ligands: from discovery to clinical application. Int Immunol 2007; 19: 813-24.
7. Berghoff AS, Kiesel B, Widhalm G, *et al*. Programmed death ligand 1 expression and tumor-infiltrating lymphocytes in glioblastoma. Neuro Oncol 2015; 17: 1064-75.
8. Nduom EK, Wei J, Yaghi NK, *et al*. PD-L1 expression and prognostic impact in glioblastoma. Neuro Oncol 2016; 18: 195-205.
9. Sanmamed MF, Chen L. Inducible expression of B7-H1 (PD-L1) and its selective role in tumor site immune modulation. Cancer J 2014; 20: 256-61.
10. Han SJ, Ahn BJ, Waldron JS, *et al*. Gamma interferon-mediated superinduction of B7-H1 in PTEN-deficient glioblastoma: a paradoxical mechanism of immune evasion. Neuroreport 2009; 20: 1597-602.
11. Keir ME, Butte MJ, Freeman GJ, Sharpe AH. PD-1 and its ligands in tolerance and immunity. Annu Rev Immunol 2008; 26: 677-704.
12. Thompson RH, Dong H, Lohse CM, *et al*. PD-1 is expressed by tu-

mor-infiltrating immune cells and is associated with poor outcome for patients with renal cell carcinoma. Clin Cancer Res 2007; 13: 1757-61.
13. Muenst S, Soysal SD, Gao F, Obermann EC, Oertli D, Gillanders WE. The presence of programmed death 1 (PD-1)-positive tumor-infiltrating lymphocytes is associated with poor prognosis in human breast cancer. Breast Cancer Res Treat 2013; 139: 667-76.
14. Webb JR, Milne K, Nelson BH. PD-1 and CD103 are widely coexpressed on prognostically favorable intraepithelial CD8 T cells in human ovarian cancer. Cancer Immunol Res 2015; 3: 926-35.
15. Taube JM, Anders RA, Young GD, *et al*. Colocalization of inflammatory response with B7-h1 expression in human melanocytic lesions supports an adaptive resistance mechanism of immune escape. Sci Transl Med 2012; 4: 127ra37.
16. Teng MW, Ngiow SF, Ribas A, Smyth MJ. Classifying cancers based on T-cell infiltration and PD-L1. Cancer Res 2015; 75: 2139-45.
17. Dudley ME, Wunderlich JR, Robbins PF, *et al*. Cancer regression and autoimmunity in patients after clonal repopulation with antitumor lymphocytes. Science 2002; 298: 850-4.
18. Louis DN, Ohgaki H, Wiestler OD, Cavanee WK. WHO classification of tumours of the central nervous system. 4th ed. Lyon: IARC Press, 2007.
19. Weber JS, Kudchadkar RR, Yu B, *et al*. Safety, efficacy, and biomarkers of nivolumab with vaccine in ipilimumab-refractory or -naive melanoma. J Clin Oncol 2013; 31: 4311-8.
20. Velcheti V, Schalper KA, Carvajal DE, *et al*. Programmed death ligand-1 expression in non-small cell lung cancer. Lab Invest 2014; 94: 107-16.
21. Droeser RA, Hirt C, Viehl CT, *et al*. Clinical impact of programmed cell death ligand 1 expression in colorectal cancer. Eur J Cancer 2013; 49: 2233-42.
22. Tokito T, Azuma K, Kawahara A, *et al*. Predictive relevance of PD-L1 expression combined with CD8+ TIL density in stage III non-small cell lung cancer patients receiving concurrent chemoradiotherapy. Eur J Cancer 2016; 55: 7-14.
23. Zeng J, Zhang XK, Chen HD, Zhong ZH, Wu QL, Lin SX. Expression of programmed cell death-ligand 1 and its correlation with clinical outcomes in gliomas. Oncotarget 2016; 7: 8944-55.
24. Hamanishi J, Mandai M, Iwasaki M, *et al*. Programmed cell death 1 ligand 1 and tumor-infiltrating CD8+ T lymphocytes are prognostic factors of human ovarian cancer. Proc Natl Acad Sci U S A 2007; 104: 3360-5.
25. Gao Q, Wang XY, Qiu SJ, *et al*. Overexpression of PD-L1 significantly associates with tumor aggressiveness and postoperative recurrence in human hepatocellular carcinoma. Clin Cancer Res 2009; 15: 971-9.
26. Wang L, Ma Q, Chen X, Guo K, Li J, Zhang M. Clinical significance of B7-H1 and B7-1 expressions in pancreatic carcinoma. World J Surg 2010; 34: 1059-65.
27. Thompson RH, Kuntz SM, Leibovich BC, *et al*. Tumor B7-H1 is associated with poor prognosis in renal cell carcinoma patients with long-term follow-up. Cancer Res 2006; 66: 3381-5.
28. Wang A, Wang HY, Liu Y, *et al*. The prognostic value of PD-L1 expression for non-small cell lung cancer patients: a meta-analysis. Eur J Surg Oncol 2015; 41: 450-6.
29. Liu YX, Wang XS, Wang YF, *et al*. Prognostic significance of PD-L1 expression in patients with gastric cancer in East Asia: a meta-analysis. Onco Targets Ther 2016; 9: 2649-54.
30. Razavi SM, Lee KE, Jin BE, Aujla PS, Gholamin S, Li G. Immune evasion strategies of glioblastoma. Front Surg 2016; 3: 11.
31. Kim MY, Koh J, Kim S, Go H, Jeon YK, Chung DH. Clinicopathological analysis of PD-L1 and PD-L2 expression in pulmonary squamous cell carcinoma: comparison with tumor-infiltrating T cells and the status of oncogenic drivers. Lung Cancer 2015; 88: 24-33.
32. Berghoff AS, Ricken G, Widhalm G, *et al*. Tumour-infiltrating lymphocytes and expression of programmed death ligand 1 (PD-L1) in melanoma brain metastases. Histopathology 2015; 66: 289-99.
33. Nduom EK, Weller M, Heimberger AB. Immunosuppressive mechanisms in glioblastoma. Neuro Oncol 2015; 17 Suppl 7: vii9-vii14.
34. Duchnowska R, Peksa R, Radecka B, *et al*. Immune response in breast cancer brain metastases and their microenvironment: the role of the PD-1/PD-L axis. Breast Cancer Res 2016; 18: 43.
35. Harter PN, Bernatz S, Scholz A, *et al*. Distribution and prognostic relevance of tumor-infiltrating lymphocytes (TILs) and PD-1/PD-L1 immune checkpoints in human brain metastases. Oncotarget 2015; 6: 40836-49.

Journal of Pathology and Translational Medicine 2017; 51: 49-55
https://doi.org/10.4132/jptm.2016.09.19

ORIGINAL ARTICLE

Diagnostic Significance of Cellular Neuroglial Tissue in Ovarian Immature Teratoma

Yun Chai · Chang Gok Woo[1]
Joo-Young Kim[2] · Chong Jai Kim
Shin Kwang Khang · Jiyoon Kim
In Ah Park · Eun Na Kim
Kyu-Rae Kim

Department of Pathology, Asan Medical Center, University of Ulsan College of Medicine, Seoul; [1]Department of Pathology, Soonchunhyang University Bucheon Hospital, Soonchunhyang University College of Medicine, Bucheon; [2]Department of Pathology, Korea University Anam Hospital, Korea University College of Medicine, Seoul, Korea

Received: July 4, 2016
Revised: August 30, 2016
Accepted: September 19, 2016

Corresponding Author
Kyu-Rae Kim, MD, PhD
Department of Pathology, Asan Medical Center, University of Ulsan College of Medicine, 88 Olympic-ro 43-gil, Songpa-gu, Seoul 05505, Korea
Tel: +82-2-3010-4514
Fax: +82-2-472-7898
E-mail: krkim@amc.seoul.kr

Background: Immature teratoma (IT) is a tumor containing immature neuroectodermal tissue, primarily in the form of neuroepithelial tubules. However, the diagnosis of tumors containing only cellular neuroglial tissue (CNT) without distinct neuroepithelial tubules is often difficult, since the histological characteristics of immature neuroectodermal tissues remain unclear. Here, we examined the significance of CNT and tried to define immature neuroectodermal tissues by comparing the histological features of neuroglial tissues between mature teratoma (MT) and IT. **Methods:** The histological features of neuroglial tissue, including the cellularity, border between the neuroglial and adjacent tissues, cellular composition, mitotic index, Ki-67 proliferation rate, presence or absence of tissue necrosis, vascularity, and endothelial hyperplasia, were compared between 91 MT and 35 IT cases. **Results:** CNTs with a cellularity grade of ≥ 2 were observed in 96% of IT cases and 4% of MT cases ($p < .001$); however, CNT with a cellularity grade of 3 in MT cases was confined to the histologically distinct granular layer of mature cerebellar tissue. Moreover, CNT in IT exhibited significantly higher rates of Ki-67 proliferation, mitoses, and necrosis than those in MT ($p < .001$). Furthermore, an infiltrative border of neuroglial tissue and glomeruloid endothelial hyperplasia were significantly more frequent in IT cases than in MT cases ($p < .001$). **Conclusions:** Our results suggest that if CNT with a cellularity grade of ≥ 2 is not a component of cerebellar tissue, such cases should be diagnosed as IT containing immature neuroectodermal tissue, particularly if they exhibit an infiltrative border, mitoses, necrosis, and increased Ki-67 proliferation.

Key Words: Immature teratoma; Neuroectodermal; Neuroglia; Neuroepithelium; Ki-67; Ovary

Immature teratoma (IT) is the second most common malignant germ-cell tumor of the ovary, and accounts for < 1% of all ovarian teratomas. Although the identification of the immature neuroectodermal component is important in the diagnosis and grading of IT, the histological definition of immature neuroectodermal tissue is ambiguous, regardless of whether it applies only to immature neuroepithelial tubules/rosettes or includes other types of immature neuroectodermal tissue, such as cellular neuroglial tissue (CNT). In some cases of CNT only, without any distinct immature neuroepithelial tubules/rosettes in the background of the mature teratomatous elements, the diagnosis is very difficult, particularly in cases where frozen sections are used (Fig. 1).

In the present study, we aimed to define the histological criteria of immature neuroectodermal tissue and examine the significance of CNT by comparing the histological features of neuroglial tissues between IT and mature teratoma (MT).

MATERIALS AND METHODS

Patient selection

Cases of IT and MT treated between January 1989 and December 2012, including neuroglial tissue of the ovary, were assessed from the database of the Department of Pathology, Asan Medical Center, Seoul, Korea. Of 70 cases of ovarian IT diagnosed during this period, 13 were excluded due to the presence of a mixed germ-cell tumor component and 22 were excluded due to unavailability of a specimen for slide review or because of the lack of distinct immature neuroepithelial tubules or rosettes. However, the histopathological review in the present study focused only on the areas of CNT. The diagnosis of IT in this study was

pISSN 2383-7837
eISSN 2383-7845

based on the presence of immature neuroepithelial tubules or rosettes within the tumor, regardless of the presence or absence of CNT; 35 IT cases and 91 mature cystic teratoma (MT) cases with a neuroglial component were finally included in this study. All of the tissue sections were formalin-fixed and paraffin-embedded. Hematoxylin and eosin–stained slides were available for review in all cases. The Institutional Review Board of the University of Ulsan College of Medicine, Asan Medical Center, Seoul, Korea, approved the collection and use of the samples in this study for research purposes (protocol number: S2016-1060-0001).

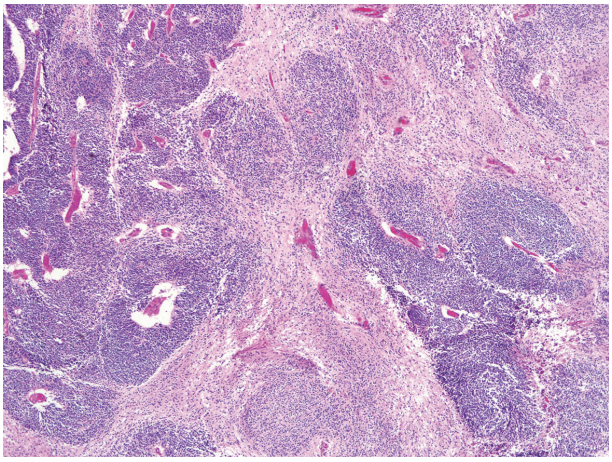

Fig. 1. Cellular neuroglial tissue. The diagnosis of immature teratoma containing only cellular neuroglial tissue without distinct neuroepithelial tubules is often difficult since the histological characteristics of immature neuroectodermal tissues have not been clearly defined.

Histological evaluation

Histopathological findings were reviewed by two pathologists blinded to the diagnosis (Y.C. and K-R.K.). We compared the histological features of the neuroglial components between the two groups (IT and MT). The histologic features examined included cellularity of the neuroglial tissue, border between the neuroglial and surrounding non-neuroglial tissues, cellular component within the CNT (either polymorphous or monomorphous), average number of mitoses per high-power (×400) field, presence or absence of necrosis, vascular proliferation, and glomeruloid endothelial hyperplasia.

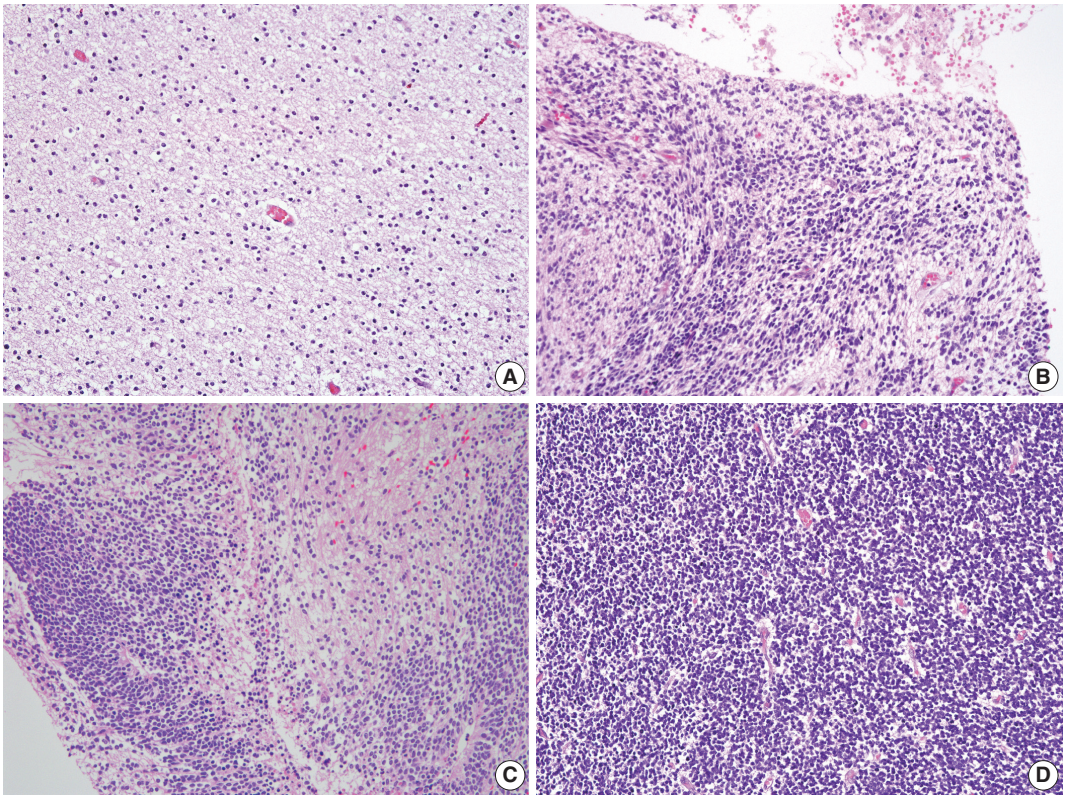

Fig. 2. Cellularity of neuroglial tissue in mature and immature teratomas. (A) Grade 1 referred to cellularity comparable to that of normal white matter or an inter-nuclear distance longer than 5 nuclear diameters. (B, C) Grade 2 applied to cases with either heterogeneous cellularity or with inter-nuclear distances similar to 2–4 nuclear diameters. (D) Grade 3 cellularity referred to cellularity comparable to that of the germinal matrix of the fetal brain or the granular layer of the normal adult cerebellum wherein nuclei touch each other, or an inter-nuclear distance shorter than 1 nuclear diameter.

https://doi.org/10.4132/jptm.2016.09.19

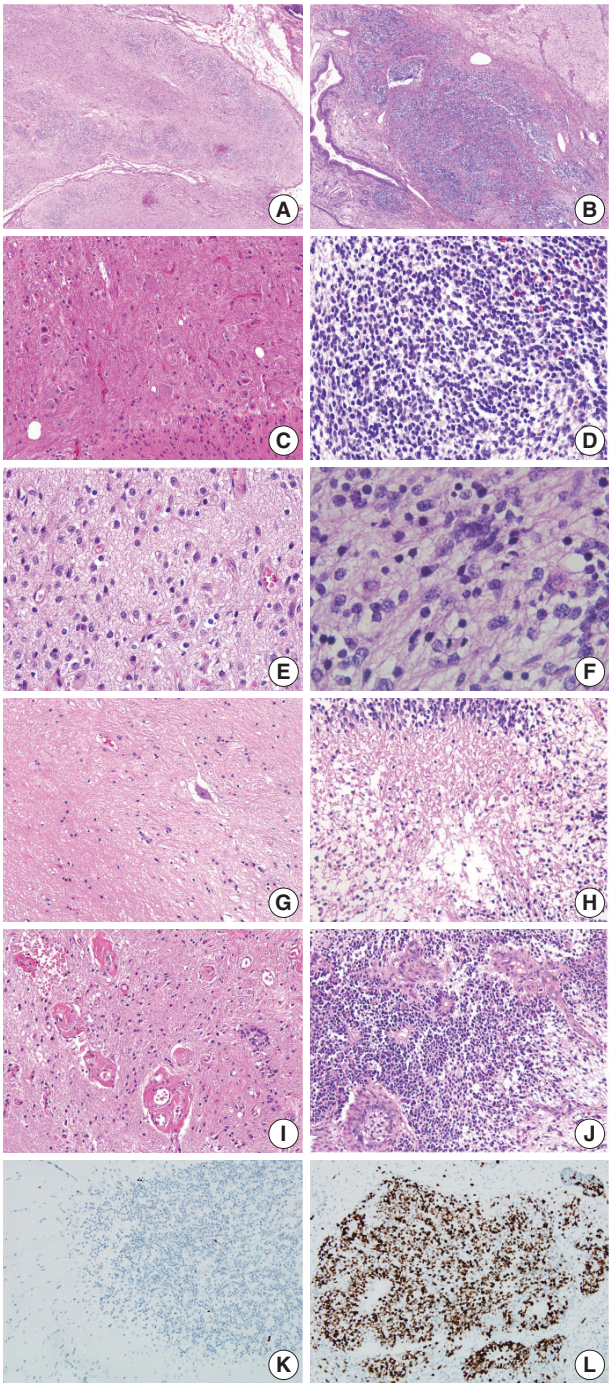

Fig. 3. Histopathologic features of mature teratoma and immature teratoma. Neuroglial cells in a mature teratoma show a smooth border (A), and comprise polymorphous cellular components (C). They show no mitotic activity (E) and no coagulative necrosis (G), but do exhibit focally glomeruloid endothelial proliferation (I) and rare Ki-67–positive proliferating cells (K). In contrast, cellular neuroglial cells in immature teratoma show an infiltrative border (B) more frequently, and comprise monomorphic germinal matrix-like cells (D). They also show frequent mitoses (F), coagulative necrosis (H), glomeruloid endothelial proliferation (J), and increased Ki-67–positive proliferating cells (L).

We selected the areas of highest cellularity within the tumor; cellularity was classified into three grades according to the density of the cellular component (Fig. 2). Grade 1 referred to cellularity comparable to that of normal white matter, or with an inter-nuclear distance longer than five nuclear diameters (Fig. 2A). Grade 2 applied to cases with either heterogeneous cellularity or with inter-nuclear distances corresponding to 2–4 nuclear diameters in the area with the highest cellularity (Fig. 2B, C). Grade 3 was assigned to cellularity similar to that of the germinal matrix of the fetal brain or granular layer of the normal adult cerebellum wherein the nuclei touch each other, or with an inter-nuclear distance shorter than 1 nuclear diameter (Fig. 2D).

The border status was divided into an infiltrative or pushing border (Fig. 3A, B). The infiltrative border (Fig. 3B) was assigned to cases with an irregular border, in contrast to the pushing border (Fig. 3A), which exhibited a smooth and well-circumscribed edge. The cellular component within the neuroglial tissue was categorized as polymorphous or monomorphous (Fig. 3C, D). When neuroglial tissue was composed of round, neuroblast-like cells and spindle or stellate-shaped glial cells, it was classified as polymorphous (Fig. 3C); when the tissue was uniformly composed of monotonous small and round to ovoid cells, it was categorized as monomorphous (Fig. 3D).

The mitotic score groups were established according to the average number of mitotic figures per high-power field, as score 1 (no mitotic activity), score 2 (1–4 mitoses per high-power field), score 3 (5–9 mitoses per high-power field), or score 4 (≥10 mitoses per high-power field) (Fig. 3E, F). The presence or absence of coagulative necrosis (Fig. 3G, H), vascular proliferation, and glomeruloid endothelial hyperplasia (Fig. 3I, J) was also recorded.

The presence of vascular proliferation in CNT was determined based on the number of small blood vessels in a high-power field, compared to that in the normal cerebral cortex. Glomeruloid endothelial hyperplasia was defined as compact stratification of proliferating endothelial and perithelial (smooth muscle) cells that resembles a renal glomerulus, similar to that observed in glioblastoma multiforme.

Statistical analysis

The differences between the two groups were analyzed using the chi-square test, Fisher exact test, and Mann-Whitney U test. A two-sided p-value <0.05 was considered statistically significant. All statistical calculations were performed using the SPSS ver. 18.0 (SPSS Inc., Chicago, IL, USA).

Table 1. Demographic data for the study patients with mature and immature teratomas of the ovary

Variable	MT	IT	p-value
Age (yr)	28.9 (3–67)	20.6 (5–36)	<.001
Tumor size (cm)	7.2 (1.2–16.5)	13.6 (2–26)[a]	<.001
Surgical procedure			<.001
Unilateral oophorectomy	9 (9.9)	21 (61.8)	
Bilateral oophorectomy	2 (2.2)	5 (14.7)	
Unilateral or bilateral cystectomy	76 (83.5)	4 (11.8)	
Unilateral oophorectomy+contralateral cystectomy	4 (4.4)	4 (11.8)	
Laterality			
Unilateral	74 (81.3)	33 (97.1)	.026
+Contralateral mature cystic teratoma		3 (8.8)	
+Contralateral mixed germ-cell tumor		1 (2.9)	
Bilateral	17 (18.7)	1 (2.9)[b]	

Values are presented as mean (range) or number (%).
MT, mature teratoma; IT, immature teratoma.
[a]Tumor size was evaluated only in 26 cases of IT; [b]This patient experienced recurrence in the opposite ovary 21 years after surgery.

Table 2. Demographic data for the study patients with immature teratoma of the ovary

Variable	Immature teratoma (%)
Tumor grade	
Grade 1	9 (25.7)
Grade 2	16 (45.7)
Grade 3	10 (28.6)
Increased serum levels of tumor markers	
AFP	14 (40.0)
β-hCG	1 (2.8)
CEA	1 (2.8)
CA125	17 (48.6)
CA19–9	6 (17.1)
FIGO stage	
IA	21 (60.0)
IC	5 (14.2)
IIB	1 (2.9)
IIIA	7 (20.0)
IIIC	1 (2.9)
Adjuvant chemotherapy	
Present	30 (85.7)
Absent	5 (15.3)
Overall survival	
Alive	34 (97.2)
dead	1 (2.8)

AFP, alpha-fetoprotein; β-hCG, beta-human chorionic gonadotropin; CEA, carcinoembryonic antigen; CA125, cancer antigen 125; CA19-9, carbohydrate antigen 19-9; FIGO, International Federation of Gynecology and Obstetrics.

RESULTS

Histopathological characteristics of MT and IT

The demographic data for 35 patients with ovarian IT (mean age, 20.6 years; range, 5 to 36 years) and MT (mean age, 28.9 years; range, 3 to 67 years) are summarized in Tables 1 and 2. Nine cases of IT were excluded in the analysis of demographic data due to insufficient information. Among the remaining 26 cases, those with IT showed a significantly larger tumor size (range, 2 to 26 cm; mean, 13.6 cm) as compared to those with MT (range, 1.2 to 16.5 cm; mean, 7.2 cm). The modalities of surgical treatment differed significantly between the two groups. In the IT group, unilateral oophorectomy was performed in 21 cases (61.8%), unilateral oophorectomy with contralateral cystectomy in four cases (11.8%), and bilateral oophorectomy in five cases (14.7%). Unilateral or bilateral cystectomy was used in only four cases (11.8%) in the IT group but was employed in a large proportion of MT cases (76 cases, 83.5%).

Bilaterality was observed in only one case of IT (2.9%) in contrast to 18.7% in mature cystic teratoma cases. In the case with bilateral IT, the patient had a recurrent tumor in the contralateral ovary 21 years after the first diagnosis. In three cases, IT was accompanied by mature cystic teratomas in the contralateral ovary. The serum tumor marker levels were within the normal range in almost half of the cases (15 cases, 42.9%).

Higher serum levels of cancer antigen 125 in 17 patients (48.6%), carbohydrate antigen 19-9 in six patients (17.1%), α-fetoprotein in 14 patients (40.0%), β-human chorionic gonadotropin in one patient (2.8%), and carcinoembryonic antigen in one patient (2.8%) with IT were observed. Moreover, 21 patients had International Federation of Gynecology and Obstetrics (FIGO) stage IA, five had FIGO stage IC, one had FIGO stage IIB, seven had FIGO stage IIIA, and one had FIGO stage IIIC. Thirty patients (85.7%) underwent postoperative adjuvant chemotherapy. All the patients with IT, except for one patient who died of sepsis during the chemotherapy, were alive without any tumor at the last follow-up. The patient with bilateral IT, who developed an IT in the opposite ovary, was also well without

 https://doi.org/10.4132/jptm.2016.09.19

any tumor at the last follow-up.

Histopathology of CNT

All patients with IT showed CNT with heterogeneous cellularity throughout the tumor; grade 2 cellularity was noted in 18 patients (51.4%) and grade 3 was noted in 17 patients (48.6%) in addition to the glial tissue with grade 1 cellularity. However, all of the patients with MT, except for four cases, demonstrated uniform grade 1 cellularity, which resembled normal white matter (95.6%). In the MT cases with CNT, the CNT was exclusively confined to the histologically distinct granular layer of mature cerebellar tissue, which could be recognized by the Purkinje cells. CNT, defined as neuroglial tissue with ≥ grade 2 cellularity, was significantly more frequent in IT than in MT cases ($p < .001$).

The infiltrative border was more frequent in IT than in MT cases, and the difference was statistically significant (74.3% and 36.3%, respectively; $p < .001$). The CNT in MT comprised a monomorphic cellular component, whereas the CNT in IT comprised polymorphous cells with varying morphology. Furthermore, vascular proliferation was more frequent in IT than in MT cases, although the difference was not statistically significant ($p = .512$). However, glomeruloid endothelial hyperplasia was significantly more frequent in IT than in MT cases (28.6% and 2.2%, respectively; $p < .001$).

The difference between the numbers of mitotic figures in the two groups was significant (Fig. 3E, F). High mitotic activity (≥ 5 mitotic figures per high-power field) was found only in the IT group. Coagulation necrosis was observed only in IT cases, and all these cases had mitotic score groups of 3 or 4 with > 5 mitoses per high-power field. The histopathological differences in the neuroglial tissue between the two groups are summarized in Table 3.

DISCUSSION

The diagnostic criteria of IT is somewhat ambiguous. At present, IT is defined either as a tumor containing immature or primitive immature neuroepithelial tubules or rosettes,[1-4] or a tumor containing immature embryonal or fetal-type tissue.[5] However, a more precise definition of IT is required for the differential diagnosis of pure IT from a pure yolk sac tumor or a mixed germ-cell tumor containing yolk sac tumor and IT components, as immature embryonal/fetal-type tissue other than the immature neuroectodermal tissue including immature enteric, hepatic, or endometrioid-like tissues is occasionally observed in yolk sac tumors.

The histopathological features of germ-cell tumors frequently

Table 3. Comparison of the histopathological features of the CNT between mature and immature teratoma

Variable	Mature teratoma (%)	Immature teratoma (%)	p-value
No. of cases	91	35	
Cellularity of CNT			< .001
Grade 1	87 (95.6)	0	
Grade 2	0	18 (51.4)	
Grade 3	4 (4.4)	17 (48.6)	
Border status			< .001
Pushing	58 (63.7)	9 (25.7)	
Infiltrative	33 (36.3)	26 (74.3)	
Cellular composition			< .001
Polymorphous	91 (100)	26 (74.3)	
Monomorphic	0	9 (25.7)	
Increased vascularity	2 (2.2)	0	.512
Glomeruloid endothelial hyperplasia	2 (2.2)	10 (28.6)	< .001
Mitoses			< .001
Score 1 (no mitosis)	90 (98.9)	13 (37.1)	
Score 2 (1–4/HPF)	1 (1.1)	14 (40.0)	
Score 3 (5–9/HPF)	0	2 (5.7)	
Score 4 (> 10/HPF)	0	6 (17.1)	
Necrosis			< .001
Present	0	29 (82.9)	
Absent	91 (100)	6 (17.1)	

Mitoses were expressed as a mean number of mitoses per one high power field.
CNT, cellular neuroglial tissue; HPF, high-power field.

recapitulate the normal developmental stages of the embryo/fetus. Dysgerminoma resembles undifferentiated germ cells, choriocarcinoma resembles the cells of a developing placenta, and IT resembles immature or developing brain tissue. Immature neuroepithelium is one of the few structures in the human body that disappears after the completion of fetal development, and only exists during the fetal period. Hence, it is reasonable to state that the diagnosis of IT should be limited to tumors containing immature neuroectodermal tissue rather than immature embryonal or fetal-type tissue.

It is important to accurately identify immature neuroectodermal tissue because the treatment and prognosis of patients with IT depend on the amount of immature neuroectodermal tissue, which also forms the basis of the histological grading systems of IT.[6,7] The immature neuroepithelial tubules of IT mimic the early neural tube during the normal developmental stage of the central nervous system. As the neural tube closes, the pseudostratified columnar epithelium in the neural tube develops into the ependymal zone in the innermost zone around the ventricular lumen, containing dividing neuroepithelial cells; the mantle zone around the neuroepithelial layer, containing neuroblasts derived from neuroepithelial cells; and the outermost marginal zone, containing nerve fibers emerging from neuroblasts. The neuroepithelial cells in the ependymal zone rapidly proliferate via symmetric and asymmetric cell divisions, and give rise to ependymoblasts, which remain in the ventricular zone, as well as glioblasts and post-mitotic neurons, which migrate to the marginal zone where they continue to differentiate.[8,9] The germinal matrix of the fetal brain is a highly cellular and vascularized area containing glioblasts and post-mitotic neurons,[10-12] from which all the neurons and supporting cells (glial cells) actively migrate during brain development. Our preliminary study has shown that small and round cells included in the CNT of IT showed immunoreactivity for nestin—a useful marker for precursor cells of neuroectodermal and mesenchymal lineages (data not shown). Moreover, the CNT is composed of polymorphous cellular components resembling glioblasts and neuroblasts, which suggests that the CNT may represent immature neuroectodermal tissue resembling the germinal matrix of the fetal brain.

In our present study, the neuroglial tissue in mature cystic teratoma cases exhibited grade 1 cellularity in all but four cases (96%). A review of the histopathological findings of the four cases indicated that the CNT in MT cases was exclusively confined to the well-developed and histologically distinct cerebellar tissue. The cellularity in the granular layer of the cerebellum in MT cases was almost indistinguishable from that of the CNT in IT cases; however, the number of mitotic figures differed significantly. Increased mitotic activity (≥ 5 mitotic figures per high-power field) was only observed in IT cases, whereas the granular layer of the cerebellum did not show any mitotic figures. Moreover, necrosis was observed only in the CNT of IT cases. The Ki-67 proliferation rate was also very low in the cerebellar granular layer, indicating that these are terminally differentiated cells. The gray matter of the cerebellar cortex is composed of three layers: the molecular layer, Purkinje cell layer, and granular layer. The cells in the granular layer are smallest cells in the body (4–5 μm in diameter), and have monomorphous, small and round nuclei with a coarse chromatin pattern. In contrast, the CNT of IT cases comprises polymorphous cells, which are similar to the glioblasts and neuroblasts in the germinal matrix of the fetal brain. Thus, the CNT in MT cases can be distinguished from the CNT in IT cases based on the monomorphic cellular component; presence of Purkinje cells; and absence of mitoses, necrosis, or proliferating activity. Moreover, the neuroglial tissue in IT cases showed heterogeneous cellularity throughout the tumor, whereas the neuroglial tissue in MT cases had a relatively uniform cellularity.

The diagnosis of IT in our current study was solely based on the presence of neuroepithelial tubules/rosettes in the tumor; however, all IT cases contained CNT with a cellularity grade of ≥ 2 in at least some areas within the tumors. Thus, CNT with a cellularity grade of ≥ 2 appears to be a characteristic feature of IT. However, additional tissue sampling would increase the likelihood of detecting immature neuroepithelial tubules in other areas, which would aid in the diagnosis.

As blood supply plays an important role in tumor growth,[13] we compared the presence or absence of coagulation necrosis, vascular proliferation, and glomeruloid endothelial hyperplasia between the two groups. Vascular proliferation and glomeruloid endothelial hyperplasia within neuroglial tissue are common features of malignant neuroglial tumors such as glioblastoma.[13,14] The number of blood vessels within the neuroglial tissue was not significantly different between the MT and IT cases in the present study; however, glomeruloid endothelial hyperplasia, reminiscent of glioblastoma, was significantly more frequent in IT cases than in MT cases.

Based on these results, we conclude that if CNT with a cellularity grade of ≥ 2 is not a component of mature cerebellar tissue, it may then represent an additional feature of ovarian IT. Higher rates of Ki-67 proliferation (Fig. 3K, L), mitoses, necrosis, infiltrative border of neuroglial tissue, polymorphous cellular compo-

 https://doi.org/10.4132/jptm.2016.09.19

nent, and the presence of glomeruloid endothelial hyperplasia within the CNT are the supporting features indicating IT.

Conflicts of Interest

No potential conflict of interest relevant to this article was reported.

REFERENCES

1. Koulos JP, Hoffman JS, Steinhoff MM. Immature teratoma of the ovary. Gynecol Oncol 1989; 34: 46-9.
2. Gershenson DM, del Junco G, Silva EG, Copeland LJ, Wharton JT, Rutledge FN. Immature teratoma of the ovary. Obstet Gynecol 1986; 68: 624-9.
3. Boor PJ, Schoene WC. Fetal cerebellar tissue associated with a primitive neuro-epithelial tumor in an ovarian teratoma. Can J Neurol Sci 1975; 2: 139-41.
4. Kleinman GM, Young RH, Scully RE. Primary neuroectodermal tumors of the ovary: a report of 25 cases. Am J Surg Pathol 1993; 17: 764-78.
5. Talerman A, Vang R. Germ cell tumors of the ovary. In: Kurman RJ, Ellenson LH, Ronnett BM, eds. Blaustein's pathology of female genital tract. 6th ed. New York: Springer, 2011; 847-907.
6. Smith HO, Berwick M, Verschraegen CF, *et al.* Incidence and survival rates for female malignant germ cell tumors. Obstet Gynecol 2006; 107: 1075-85.
7. Gallion H, van Nagell JR Jr, Donaldson ES, Hanson MB, Powell DF. Immature teratoma of the ovary. Am J Obstet Gynecol 1983; 146: 361-5.
8. Sanes DH, Reh TA, Harris WA. Development of the nervous system. 2nd ed. San Diego: Academic Press, 2006; 57-85.
9. Kierszenbaum AL. Histology and cell biology: an introduction to pathology. St. Louis: Mosby, 2002; 199-225.
10. Ballabh P, Braun A, Nedergaard M. Anatomic analysis of blood vessels in germinal matrix, cerebral cortex, and white matter in developing infants. Pediatr Res 2004; 56: 117-24.
11. Dummula K, Vinukonda G, Xu H, *et al.* Development of integrins in the vasculature of germinal matrix, cerebral cortex, and white matter of fetuses and premature infants. J Neurosci Res 2010; 88: 1193-204.
12. Sugiyama T, Osumi N, Katsuyama Y. The germinal matrices in the developing dentate gyrus are composed of neuronal progenitors at distinct differentiation stages. Dev Dyn 2013; 242: 1442-53.
13. Baker PM, Rosai J, Young RH. Ovarian teratomas with florid benign vascular proliferation: a distinctive finding associated with the neural component of teratomas that may be confused with a vascular neoplasm. Int J Gynecol Pathol 2002; 21: 16-21.
14. Gaudin PB, Rosai J. Florid vascular proliferation associated with neural and neuroendocrine neoplasms: a diagnostic clue and potential pitfall. Am J Surg Pathol 1995; 19: 642-52.

Journal of Pathology and Translational Medicine 2017; 51: 56-68
https://doi.org/10.4132/jptm.2016.09.17

■ ORIGINAL ARTICLE ■

Size of Non-lepidic Invasive Pattern Predicts Recurrence in Pulmonary Mucinous Adenocarcinoma: Morphologic Analysis of 188 Resected Cases with Reappraisal of Invasion Criteria

Soohyun Hwang · Joungho Han
Misun Choi · Myung-Ju Ahn[1]
Yong Soo Choi[2]

Department of Pathology and Translational Genomics, [1]Division of Hematology-Oncology, Department of Medicine, [2]Department of Thoracic Surgery, Samsung Medical Center, Sungkyunkwan University School of Medicine, Seoul, Korea

Received: August 16, 2016
Revised: September 8, 2016
Accepted: September 16, 2016

Corresponding Author
Joungho Han, MD
Department of Pathology and Translational Genomics, Samsung Medical Center, Sungkyunkwan University School of Medicine, 81 Irwon-ro, Gangnam-gu, Seoul 06351, Korea
Tel: +82-2-3410-2800
Fax: +82-2-3410-0025
E-mail: hanjho@skku.edu

Background: We reviewed a series of 188 resected pulmonary mucinous adenocarcinomas (MAs) to clarify the prognostic significance of lepidic and non-lepidic patterns. **Methods:** Non-lepidic patterns were divided into bland, non-distorted acini with uncertain invasiveness (pattern 1), unequivocal invasion into stroma (pattern 2), or invasion into alveolar spaces (pattern 3). **Results:** The mean proportion of invasive patterns (patterns 2 and 3) was lowest in small (≤ 3 cm) tumors, and gradually increased in intermediate (> 3 cm and ≤ 7 cm) and large (> 7 cm) tumors (8.4%, 34.3%, and 50.1%, respectively). Adjusted T (aT) stage, as determined by the size of invasive patterns, was positively correlated with adverse histologic and clinical features including older age, male sex, and ever smokers. aTis tumors, which were exclusively composed of lepidic pattern (n = 9), or a mixture of lepidic and pattern 1 (n = 40) without any invasive patterns, showed 100% disease-free survival (DFS). The aT1mi tumors, with minimal (≤ 5 mm) invasive patterns (n = 63), showed a 95.2% 5-year DFS, with recurrences (n = 2) limited to tumors greater than 3 cm in total size (n = 23). Both T and aT stage were significantly associated with DFS; however, survival within the separate T-stage subgroups was stratified according to the aT stage, most notably in the intermediate-stage subgroups. In multivariate analysis, the size of invasive patterns (p = .020), pleural invasion (p < .001), and vascular invasion (p = .048) were independent predictors of recurrence, whereas total size failed to achieve statistical significance (p = .121). **Conclusions:** This study provides a rationale for histologic risk stratification in pulmonary MA based on the extent of invasive growth patterns with refined criteria for invasion.

Key Words: Lung; Mucinous adenocarcinoma; Adenocarcinoma *in situ*; Lepidic; Disease-free survival

Invasive mucinous adenocarcinoma is a distinct histologic variant of lung adenocarcinoma that is characterized by tall columnar cells with basally oriented nuclei and intracytoplasmic mucin and was formerly referred to as mucinous bronchioloalveolar carcinoma.[1,2] In most cases, these tumors characteristically display lepidic growth. The clinical presentation of mucinous adenocarcinoma may vary from a small nodular lesion to lobar/multilobar consolidation, and it is not uncommon to encounter multicentric dissemination at presentation, probably reflecting aerogenous spread (AS).[3] In terms of genetics, the *KRAS* mutations are prevalent, and recent studies have discovered various new driver mutations such as *CD74-NRG1* fusion in *KRAS* wild-type cases.[4-6]

Although these advances further consolidate mucinous adenocarcinoma as a clinicopathologically distinct variant of lung adenocarcinoma, its prognostic factors are largely unknown. In conventional adenocarcinomas, multiple studies have validated the predictive role of histologic grading, primarily by the predominant architectural pattern, namely lepidic, acinar, papillary, micropapillary, and solid.[7-10] Among the histologic subclassification proposed by the International Association for the Study of Lung Cancer, American Thoracic Society and European Respiratory Society (IASLC/ATS/ERS), the lepidic pattern has attracted a great deal of attention because of its association with a favorable prognosis.[11-14] Based on an increasing number of studies showing excellent survival of lepidic predominant tumors, and in line with the IASLC/ATS/ERS classification, the new 2015 World Health Organization (WHO) classification introduced the concept of diagnostic categories of "minimally invasive adenocarcinoma" and "adenocarcinoma *in situ*" for completely resected, small (≤ 3 cm) solitary tumors with minimal (≤ 5 mm) or no invasion, respectively.[1,2] However, as most cases included in previous studies

pISSN 2383-7837
eISSN 2383-7845

were non-mucinous adenocarcinomas, the prognostic relevance and the prevalence of lepidic pattern have not been documented for mucinous adenocarcinomas. Furthermore, detailed histomorphologic analysis of the non-lepidic pattern in mucinous adenocarcinomas has not been performed.

To clarify the prognostic significance of lepidic and non-lepidic invasive patterns, we evaluated a series of resected pulmonary mucinous adenocarcinomas with refined criteria for invasion and correlated invasive patterns with clinical outcome.

MATERIALS AND METHODS

Patient identification

Between 1995 and 2013, we identified 4,119 cases of surgically resected lung adenocarcinoma at Samsung Medical Center, Korea. We initially collected 317 cases diagnosed as mucinous adenocarcinoma, as well as cases of mucinous bronchioloalveolar carcinoma, from our pathology reports. On pathologic review, the cytomorphologic features of these tumors were rigorously examined. Tall columnar or goblet cell morphology showing characteristic

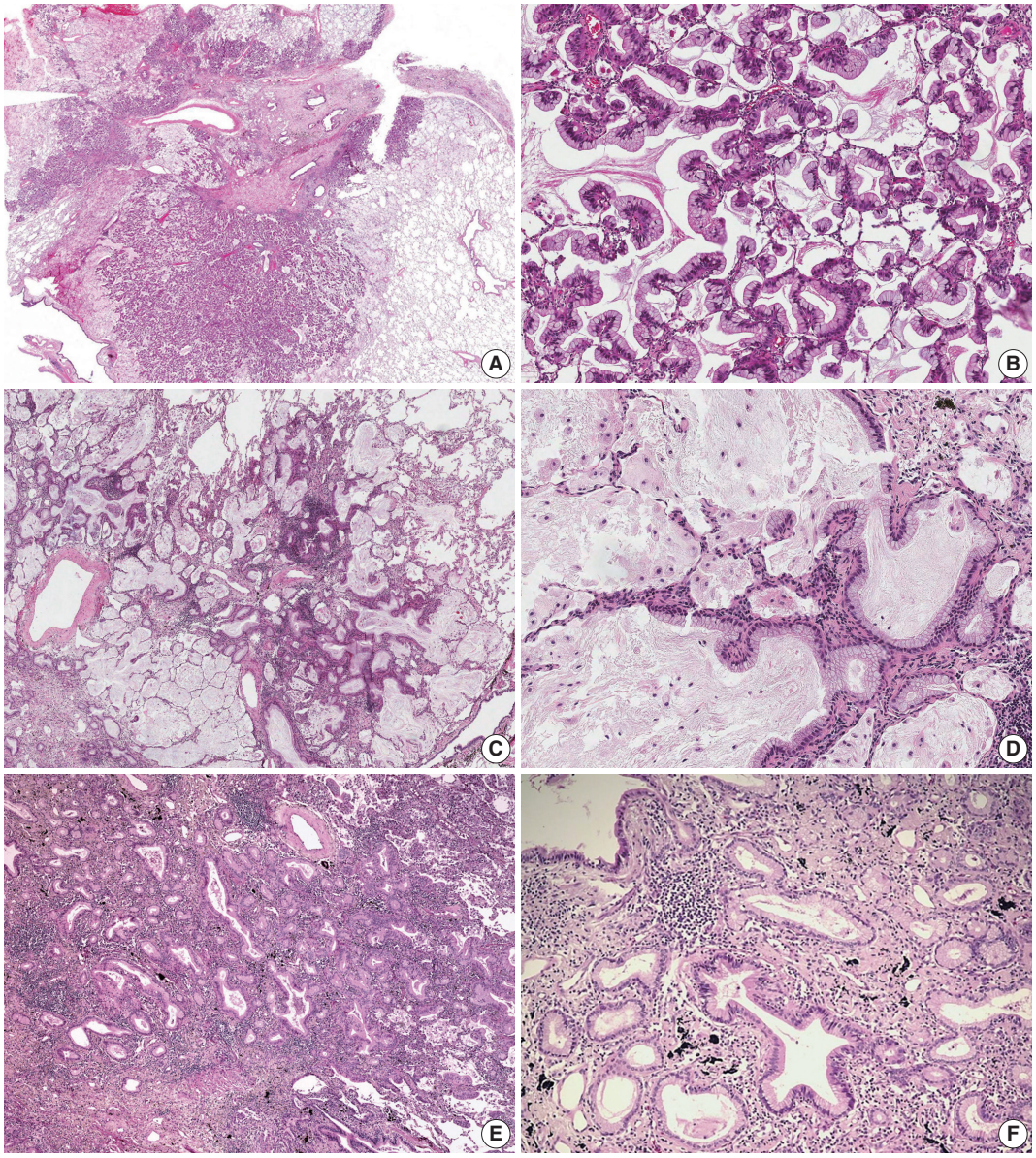

Fig. 1. Examples of lepidic pattern and non-distorted acini (pattern 1). (A–F) Low-powered (A, C, E) and high-powered (B, D, F) view. (A, B) Typical lepidic pattern showing strips of tumor cells clinging to alveolar walls. (C, D) In areas where the stroma is increased, acinar structures (pattern 1) are formed without alteration of cytomorphologic features. (E, F) Densely spaced, bland acinar structures (pattern 1). The stroma is elastotic, not desmoplastic.

(Continued to the next page)

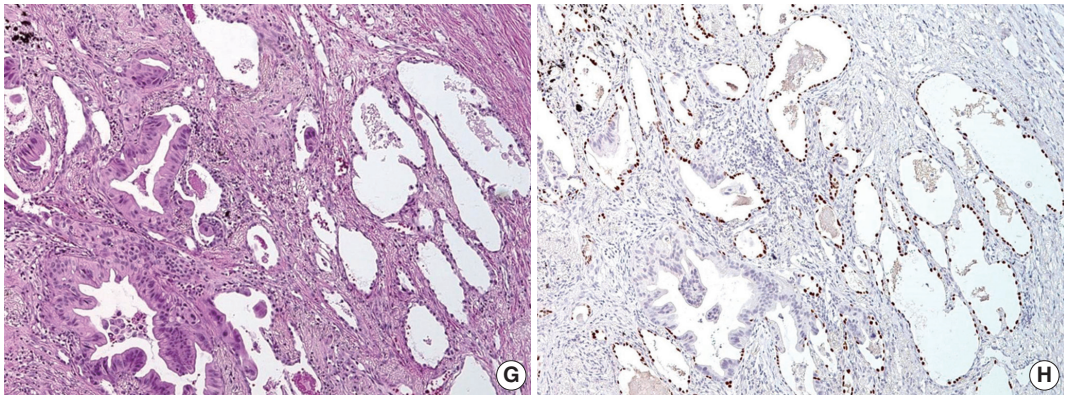

Fig. 1. *(Continued from the previous page)* (G, H) Immunohistochemical staining for thyroid transcription factor 1 reveals that round-to-oval spaces embedded in the central scar are alveolar spaces partially lined by tumor cells. Complete replacement of these spaces by tumor cells may form an acinar structure.

lepidic growth at the tumor periphery was set as the histologic inclusion criteria in this study. Mixed mucinous and non-mucinous tumors with extracellular rather than intracellular mucin, colloid adenocarcinomas predominantly composed of dissecting mucin pools, and enteric adenocarcinomas were excluded. Cases with a history of preoperative treatment and synchronous primary lung cancers were also excluded. Nine cases were excluded because they had multicentric disease at presentation and were resected for diagnostic purposes. Cases showing solid signet ring cells and a cribriform and tubulopapillary pattern were suspected to be anaplastic lymphoma kinase (ALK)–rearranged tumors, and 12 cases were excluded after subsequent ALK immunohistochemical staining for confirmation.[15,16] Finally, a total of 188 cases of surgically treated mucinous adenocarcinoma were evaluated. This study was approved by the Samsung Medical Center Institutional Review Board (file No. 2016-03-055).

Histologic review

All tumors were sectioned and stained in a routine manner and reviewed by two pathologists (S.H. and J.H.) who were blinded to patient outcome. The mean number of reviewed slides was 4.43 per case, corresponding to 1.25 per centimeter of tumor when the total number of reviewed slides was divided by the sum of the greatest dimensions. Lepidic pattern was defined as tumor growth along preexisting alveolar walls, as previously described (Fig. 1A, B).[1] For non-lepidic patterns, it was difficult to apply the conventional architectural patterns of non-mucinous adenocarcinomas to mucinous adenocarcinomas. Instead, we categorized non-lepidic patterns into three different patterns based on cytomorphologic, architectural and stromal characteristics compared to the lepidic pattern.

Pattern 1 was assigned to areas showing bland, non-distorted acinar structures with increased stroma compared to the lepidic pattern (Fig. 1C–F). Cytomorphologic alteration compared to the lepidic pattern was not apparent, with retention of tall columnar cells with preserved nuclear polarity. Architectural distortion was minimal to the extent that the pattern resembled uninvolved alveolar spaces. Increased stroma, which was the only feature distinguishing this pattern from the lepidic pattern, was almost always elastotic, not desmoplastic. Indeed, this pattern was often more reminiscent of lepidic pattern than a true invasive acinar pattern. Presence of the central scar itself did not permit exclusion of this pattern, unless accompanied by cytomorphologic or architectural changes or prominent desmoplasia.

Pattern 2 was assigned to areas showing invasion into the stroma, as evidenced by cytomorphologic alteration, architectural distortion and stromal desmoplasia (Fig. 2A–D). The tumor cells displayed an irregular, jagged, or anastomosing architecture that was clearly distinguishable from normal alveolar structure. Less columnar cytomorphology with loss of nuclear polarity was typically seen in this pattern. Infiltrating single cells with eosinophilic cytoplasm or fused glands with paler cytoplasm were often observed.

Pattern 3 was assigned to areas showing invasion into alveolar spaces. This pattern typically arose in the background of the lepidic pattern and showed proliferation toward alveolar spaces (Fig. 2E, F). A similar pattern in non-mucinous adenocarcinoma has been referred to as "low papillary structure" by Fukutomi *et al.*[17] Similar to papillary and micropapillary pattern in non-mucinous adenocarcinomas, this pattern did not require desmoplastic stroma. Excess proliferation into airspaces frequently caused tumor cells to float within airspaces. When these floating tumor cells were arranged as single cells, ring-like structures, or tight clusters, which were distinguishable from tumor branches at-

 https://doi.org/10.4132/jptm.2016.09.17

tached to the alveolar wall, they were further subcategorized as a micropapillary pattern (Fig. 2F).

Each pattern was recorded in terms of percentage, except for pattern 1. A clear distinction between pattern 1 and the lepidic pattern was not always feasible, since pattern 1 lacked cytomorphologic changes. Furthermore, since acinar structures in pattern 1 were devoid of any features of invasion such as desmoplasia or cytomorphologic atypia as seen in acinar pattern of invasion in non-mucinous adenocarcinoma, we postulated that pattern 1 might be a morphologic spectrum that still represents lepidic growth (Fig. 1G, H), or at least a growth pattern that is related to indolent biologic behavior as a lepidic pattern. We therefore regarded lepidic and pattern 1 as non-invasive patterns, whereas patterns 2 and 3 were considered unequivocally invasive patterns. To measure the size of invasive patterns, the proportions of patterns 2 and 3 were combined. Since the invasive patterns were frequently

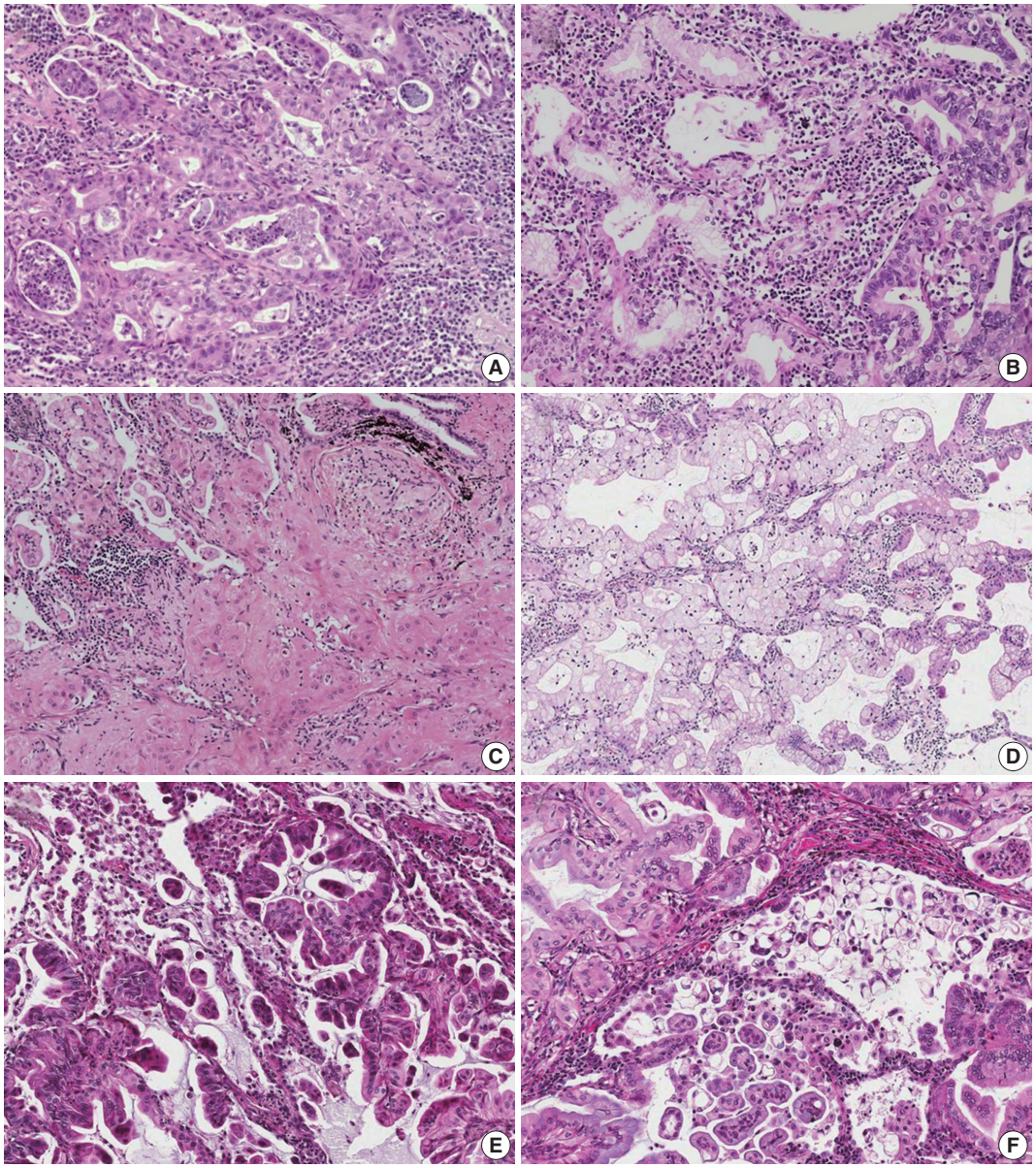

Fig. 2. Examples of invasive patterns: pattern 2, invasion into stroma (A–D) and pattern 3, invasion into alveolar spaces (E, F). (A) Jagged, fused glands with loss of nuclear polarity support invasiveness. (B) Anastomosing glands with increased nuclear atypia (pattern 2) seen on the right is distinguished from the bland, non-distorted acinar structure (pattern 1) noted on the left. The photomicrographs 2A and 2B were taken from the same case as in 1E and 1F. (C) Intracytoplasmic mucin is replaced by eosinophilic cytoplasm, resulting in squamoid appearance. (D) The area of glandular fusion shows loss of nuclear polarity and paler cytoplasm compared to the area of lepidic pattern on the right. (E) Proliferation towards alveolar spaces results in a serrated appearance. (F) A micropapillary pattern with ring-like structures is seen.

multifocal, the size of invasion was calculated by multiplying the percentage by the total size in the majority of cases. The size of confluent invasion measured in a single slide was adopted only when it exceeded the calculated value. According to the size of invasive pattern, conventional T staging was adjusted (aT) as follows: aTis, no invasion; aT1mi, minimal (≤5 mm) invasion; aT1a1, >5 mm, ≤1 cm invasion; aT1a2, >1 cm, ≤2 cm invasion; aT1b, >2 cm, ≤3 cm invasion; aT2a, >3 cm, ≤5 cm invasion or visceral pleural invasion (PL1-2); aT2b, >5 cm, ≤7 cm invasion; aT3, >7 cm invasion or satellite tumor nodule in the same lobe or parietal pleural invasion (PL3); and aT4, satellite tumor nodule in a different ipsilateral lobe. Conventional TNM staging and

Table 1. Correlation of clinicopathologic characteristics with adjusted T stage (aT[a])

Factor	All patients	aTis/1mi[a]	aT1a/1b[a]	aT2a/3/4[a]	p-value
Total	188 (100)	112 (59.6)	41 (21.8)	35 (18.6)	
Age (yr)					.004
<65	119 (63.3)	81 (72.3)	18 (43.9)	20 (57.1)	
≥65	69 (36.7)	31 (27.7)	23 (56.1)	15 (42.9)	
Sex					.003
Female	106 (56.4)	74 (66.1)	19 (46.3)	13 (37.1)	
Male	82 (43.6)	38 (33.9)	22 (53.7)	22 (62.9)	
Smoking					<.001
Never	117 (62.2)	82 (73.2)	21 (51.2)	14 (40.0)	
Ever	71 (37.8)	30 (26.8)	20 (48.8)	21 (60.0)	
Nuclear atypia					<.001
Mild	105 (55.9)	89 (79.5)	14 (34.1)	4 (11.4)	
Moderate	59 (31.4)	22 (19.6)	18 (43.9)	17 (48.6)	
Severe	24 (12.8)	1 (0.9)	9 (22.0)	14 (40.0)	
Micropapillary					<.001
0%	128 (68.1)	101 (90.2)	20 (48.8)	7 (20.0)	
1%–9%	25 (13.3)	10 (8.9)	8 (19.5)	7 (20.0)	
≥10%	35 (18.6)	1 (0.9)	13 (31.7)	21 (60.0)	
Aerogenous spread					<.001
Absent	136 (72.3)	99 (88.4)	25 (61.0)	12 (34.3)	
Present	52 (27.7)	13 (11.6)	16 (39.0)	23 (65.7)	
Vascular invasion					<.001
Absent	172 (91.5)	112 (100)	33 (80.5)	27 (77.1)	
Present	16 (8.5)	0	8 (19.5)	8 (22.9)	
Necrosis					<.001
Absent	170 (91.4)	111 (99.1)	37 (90.2)	22 (62.9)	
Present	18 (9.6)	1 (0.9)	4 (9.8)	13 (37.1)	
Neutrophils					<.001
Absent	118 (62.8)	97 (86.6)	10 (24.4)	11 (31.4)	
Present	70 (37.2)	15 (13.4)	31 (75.6)	24 (68.6)	
KRAS (n=59)					.014
Wild	34 (57.6)	23 (74.2)	2 (25.0)	9 (45.0)	
Mutated	25 (42.4)	8 (25.8)	6 (75.0)	11 (55.0)	
T stage					<.001
1a	61 (32.4)	57 (50.9)	4 (9.8)	0	
1b	42 (22.3)	29 (25.9)	13 (31.7)	0	
2a	49 (26.1)	21 (18.8)	18 (43.9)	10 (28.6)	
2b	18 (9.6)	3 (2.7)	5 (12.2)	10 (28.6)	
3/4[b]	18 (9.6)	2 (1.8)	1 (2.4)	15 (42.9)	
N stage					<.001
0	177 (94.1)	111 (99.1)	38 (92.7)	28 (80.0)	
1/2	11 (5.9)	1 (0.9)	3 (7.3)	7 (20.0)	

Values are presented as number (%).
[a]Adjusted T stage (aT): aTis, no invasion; aT1mi, minimal (≤5 mm) invasion; aT1a, >5 mm, ≤2 cm invasion; aT1b, >2 cm, ≤3 cm invasion; aT2a, >3 cm, ≤5 cm invasion or visceral pleural invasion (PL1-2); aT2b, >5 cm, ≤7 cm invasion; aT3, >7 cm invasion or satellite tumor nodule in same lobe or parietal pleural invasion (PL3); aT4, satellite tumor nodule in different ipsilateral lobe; [b]One T4 case was included.

 https://doi.org/10.4132/jptm.2016.09.17

Table 2. Correlation of clinicopathologic variables with DFS

Factor	No. (%)	5-year DFS (%)	p-value
Age (yr)			.097
<65	119 (63.3)	80.0	
≥65	69 (36.7)	65.7	
Sex			.159
Female	106 (56.4)	81.4	
Male	82 (43.6)	66.8	
Smoking			.012
Never	117 (62.2)	82.7	
Ever	71 (37.8)	61.0	
Nuclear atypia			<.001
Mild	105 (55.9)	90.2	
Moderate	59 (31.4)	60.5	
Severe	24 (12.8)	47.2	
Micropapillary			<.001
0%	128 (68.1)	88.0	
1%–9%	25 (13.3)	68.3	
≥10%	35 (18.6)	34.0	
Aerogenous spread			<.001
Absent	136 (72.3)	84.0	
Present	52 (27.7)	53.2	
Vascular invasion			<.001
Absent	172 (91.5)	79.5	
Present	16 (8.5)	24.9	
Necrosis			<.001
Absent	170 (90.4)	79.4	
Present	18 (9.6)	32.2	
Neutrophils			<.001
Absent	118 (62.8)	86.9	
Present	70 (37.2)	55.9	
Pleural status			<.001
PL0	175 (93.1)	79.6	
PL1–3	13 (6.9)	0.0[a]	
KRAS			.076
Wild	34 (57.6)	30.0	
Mutated	25 (42.4)	24.7	
N stage			<.001
0	177 (94.1)	78.3	
1/2	11 (5.9)	18.5[b]	
T stage			<.001
1a	61 (32.4)	100.0	
1b	42 (22.3)	89.6	
2a	49 (26.1)	62.7	
2b	18 (9.6)	51.0	
3/4	18 (9.6)	23.4	
aT stage			<.001
is	49 (26.1)	100.0	
1mi (≤5 mm)	63 (33.5)	95.2	
1a1 (≤1 cm)	17 (9.0)	75.3	
1a2 (>1 cm, ≤2 cm)	17 (9.0)	54.1	
1b	7 (3.7)	41.7	
2a	21 (11.2)	20.3	
2b/3/4	14 (7.4)	16.8[c]	

DFS, disease-free survival; aTis, no invasion; aT1mi, minimal (≤5 mm) invasion; aT1a1, >5 mm, ≤1 cm invasion; aT1a2, >1 cm, ≤2 cm invasion; aT1b, >2 cm, ≤3 cm invasion; aT2a, >3 cm, ≤5 cm invasion or visceral pleural invasion (PL1–2); aT2b, >5 cm, ≤7 cm invasion; aT3, >7 cm invasion or satellite tumor nodule in same lobe or parietal pleural invasion (PL3); aT4, satellite tumor nodule in different ipsilateral lobe.
[a,b,c]All patients were censored at 47-, 53-, and 32-month follow-up, respectively.

pleural invasion were assessed according to the seventh American Joint Committee on Cancer TNM staging manual.[18]

Nuclear atypia was measured in the area showing the highest degree of atypia, and graded as follows: "mild," small, slightly irregular nuclei with no nucleoli; "moderate," intermediate-sized, moderately irregular nuclei with small nucleoli; and "severe," large, markedly irregular nuclei with vesicular chromatin and prominent nucleoli. AS was considered present when tumor cells were present beyond 2 mm from the edge of the main mass. This included discontinuous tumor islands in lepidic pattern as well as single cells, micropapillary, or ring-like structures, termed tumor spread through air spaces in recent studies.[19,20] Vascular invasion, either lymphatic or venous, and tumor necrosis were examined. Intra-alveolar accumulation of neutrophils, which was previously reported to be related with adverse outcome in mucinous adenocarcinoma, was also evaluated.[21,22]

EGFR and *KRAS* mutation, and *ALK* rearrangement

EGFR gene mutation was detected by real-time polymerase chain reaction with PNA clamping using the PNA-Clamp EGFR Mutation Detection kit (PANAGENE, Inc., Daejeon, Korea) or by direct sequencing of exons 18, 19, 20, and 21, as previously described.[23] KRAS gene mutation was detected by direct sequencing of codons 12 and 13 in exon 2 and codon 61 in exon 3, as previously described.[23] Immunohistochemical staining for ALK protein (1:30, clone 5A4, Novocastra, Newcastle upon Tyne, UK) was used to detect *ALK* gene rearrangement, and diffuse moderate to strong cytoplasmic reactivity was regarded as positive, as previously described.[23]

Statistical analysis

The correlations between clinicopathologic variables and adjusted tumor (aT) stage were assessed by Fisher exact test and chi-square test. Disease-free survival (DFS) was evaluated using the Kaplan-Meier method, and the log-rank test was used for comparison. Multivariate survival analysis was performed using the Cox proportional hazards model. All statistical analyses were performed using SPSS Statistics ver. 19.0 (IBM Corp., Armonk, NY, USA).

RESULTS

Clinicopathologic characteristics

The clinicopathologic features are summarized in Table 1. The mean age was 59.9 years (range, 19 to 84 years), and 63.3% of patients were younger than 65 years. Female patients (56.4%) outnumbered male patients, and never smokers comprised 62.2% of all patients. Fifteen patients (8.0%) underwent wedge resection, one patient underwent segmentectomy, and 172 patients (91.5%) underwent at least lobectomy. Adjuvant chemotherapy was administered in 28 patients (14.9%), of which, eight were American Joint Committee on Cancer stage I, 16 were stage II, and four were stage III.

Mean tumor size was 3.6 cm (median, 2.8 cm; range, 0.5 to 20.0 cm). Nuclear atypia was mild in 105 (55.9%), moderate in 59 (31.4%), and severe in 24 (12.8%) cases. Micropapillary pattern was absent in 128 (68.1%), focally (1%–9%) present in 25 (13.3%), and substantially (≥10%) present in 35 (18.6%) cases. AS was present in 52 (27.7%) cases, which presented as lepidic, micropapillary, and both types in 34, 14, and four cases, respectively. Vascular invasion was present in 16 cases (8.5%). Necrosis and intra-alveolar neutrophil accumulation were present in 18 (9.6%) and 70 (37.2%) cases, respectively. Pleural invasion was present in 13 cases (6.9%). Nodal metastasis was present in 11 cases (5.9%).

Proportion of invasive patterns and distribution of aT stage

In all 188 patients, the mean proportion of invasive patterns was 21.4% (pattern 2, 13.0%; pattern 3, 8.4%), and the mean size of invasive patterns was 1.3 cm (median, 0.4 cm; range, 0.0 to 14.0 cm). In 49 cases (26.1%), the tumors were exclusively composed of non-invasive patterns (lepidic and pattern 1), and nine had a central scar. Among 49 non-invasive cases, nine showed a purely lepidic pattern, and 40 showed a mixture of lepidic and pattern 1. The proportion of invasive patterns increased in correlation with increased tumor size. The mean proportion of invasive pattern was 8.4% (pattern 2, 5.9%; pattern 3, 2.5%) in small (≤3 cm) tumors, 34.3% (pattern 2, 21.2%; pattern 3, 13.1%) in intermediate-sized (>3 cm and ≤7 cm) tumors, and 50.1% (pattern 2, 27.0%; pattern 3, 23.1%) in large (>7 cm) tumors. Accordingly, as shown in Table 1, 57 of 61 T1a cases (93.4%) and 29 of 42 T1b cases (69.0%) were adjusted to aTis/1mi, whereas only two of 18 T3/4 cases (11.1%) were adjusted to aTis/1mi. In other words, the 112 cases of aTis/1mi were generally small (≤3 cm, T1) tumors (86 cases, 76.8%), although intermediate-sized (>3 cm and ≤7 cm, T2) tumors (24 cases, 21.4%), and even large (>7 cm, T3) tumors (two cases, 1.8%) were also observed.

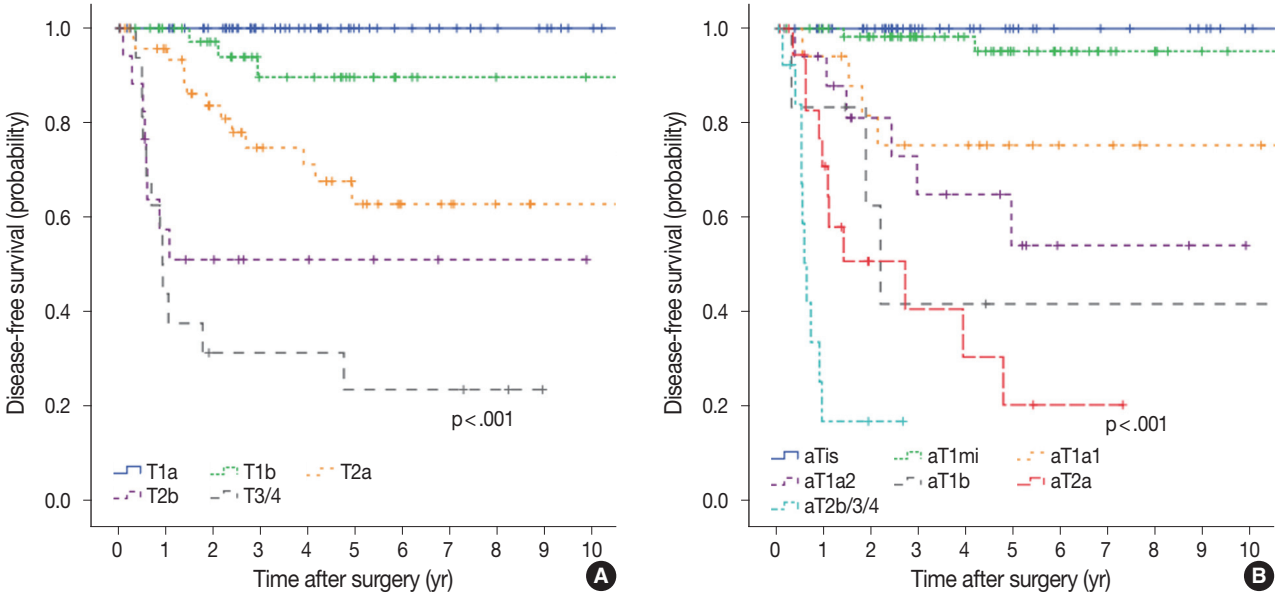

Fig. 3. Disease-free survival according to T stage (A) and adjusted T stage (B). aTis, no invasion; aT1mi, minimal (≤5 mm) invasion; aT1a1, >5 mm, ≤1 cm invasion; aT1a2, >1 cm, ≤2 cm invasion; aT1b, >2 cm, ≤3 cm invasion; aT2a, >3 cm, ≤5 cm invasion or visceral pleural invasion (PL1–2); aT2b, >5 cm, ≤7 cm invasion; aT3, >7 cm invasion or satellite tumor nodule in the same lobe or parietal pleural invasion (PL3); aT4, satellite tumor nodule in a different ipsilateral lobe.

https://doi.org/10.4132/jptm.2016.09.17

Correlation of clinicopathologic features with aT stage and predominant invasive pattern

Clinicopathologic features according to aT stage are summarized in Table 1. Advanced aT stage was significantly associated with older age, male sex, and ever smokers (p = .004, p = .003, and p < .001, respectively). Tumors with advanced aT stage had significantly more nuclear atypia, micropapillary pattern, AS, vascular invasion, necrosis, neutrophils, nodal metastasis, and *KRAS* mutation (all p < .001, except for *KRAS* mutation p = .014). Significant associations between T stage and clinicopathologic features were similarly noted, with the exception of age (p = .101). To further evaluate the clinicopathologic relevance of a predominant invasive pattern, 85 cases with ≥10% invasive patterns were separated into two groups according to the predominant invasive pattern: 59 pattern 2 predominant tumors (69.4%) and 26 pattern 3 predominant tumors (30.6%). Among clinical and pathologic factors, only micropapillary pattern and AS were significantly prevalent in pattern 3 predominant tumors (both p < .001). The two groups showed no significant difference in DFS and extrathoracic recurrence-free survival, when they were

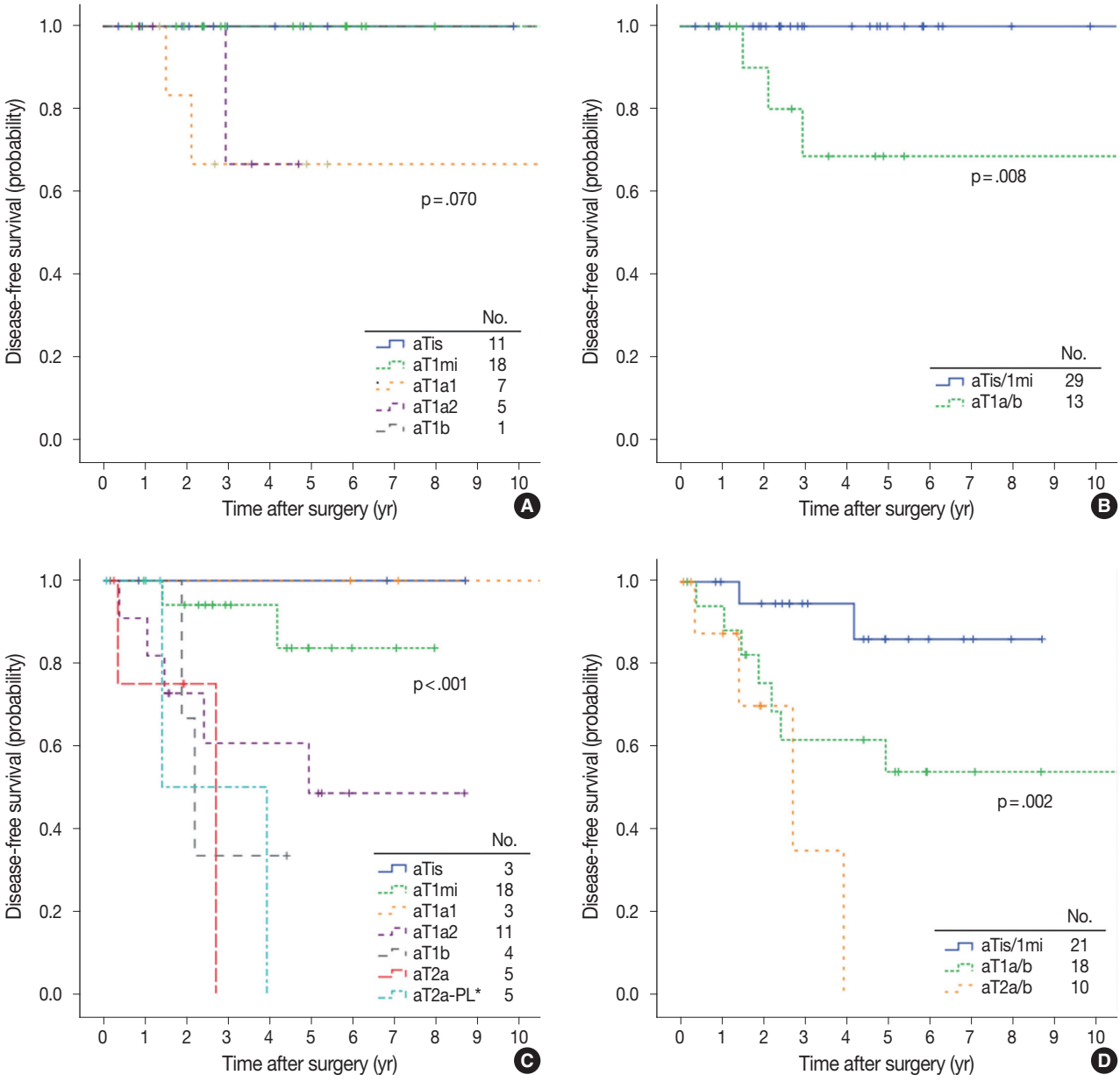

Fig. 4. Disease-free survival in separate T stage subgroups according to the adjusted T stage (A, C, E) and grouped adjusted T stage (B, D, F). (A, B) T1b subgroups (n = 42). (C, D) T2a subgroups (n = 49). *(Continued to the next page)*

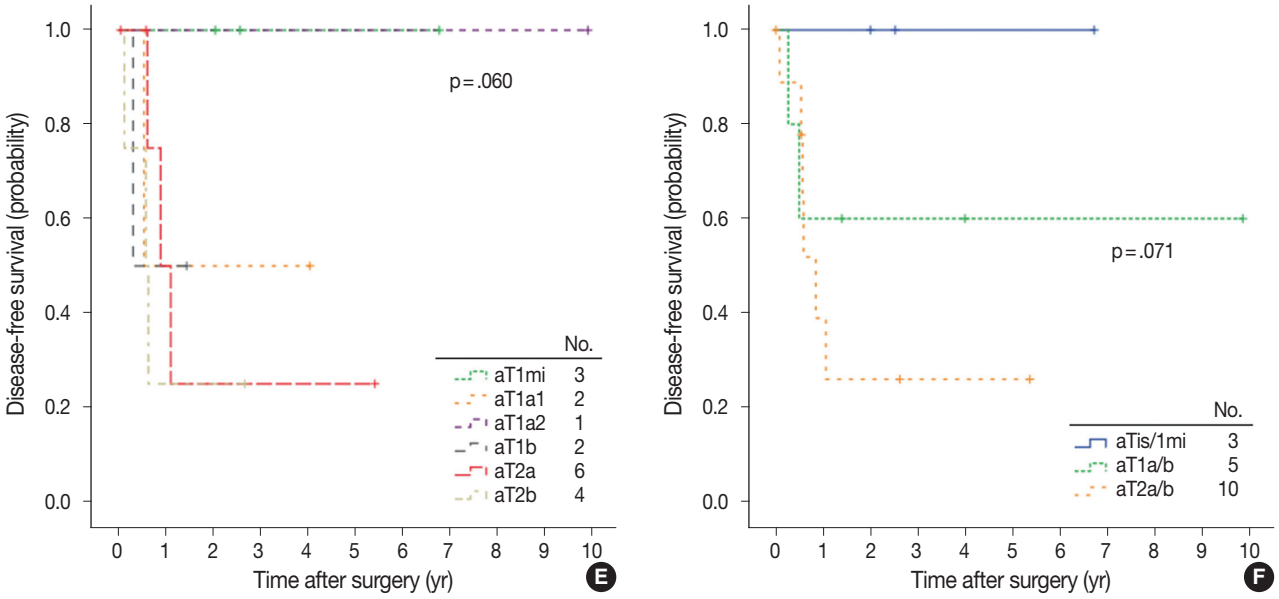

Fig. 4. *(Continued from the previous page)* (E, F) T2b subgroups (n=18). aTis, no invasion; aT1mi, minimal (≤5 mm) invasion; aT1a1, >5 mm, ≤1 cm invasion; aT1a2, >1 cm, ≤2 cm invasion; aT1b, >2 cm, ≤3 cm invasion; aT2a, >3 cm, ≤5 cm invasion with or without visceral pleural invasion (PL1-2); aT2a-PL*, ≤3 cm invasion but with visceral pleural invasion (PL1-2); aT2b, >5 cm, ≤7 cm invasion.

compared in matched aT stage (data not shown).

KRAS and *EGFR* mutation

KRAS mutations were detected in 25 of 59 cases tested (42.4%). Most mutations were found in codon 12, with one case each of codon 13 (G13D) and codon 61 (Q61H) mutation. Among 23 cases of codon 12 mutations, the G12V mutation was most common (11 cases), followed by G12D (seven cases), G12C (four cases), and G12A (one case). *KRAS* mutation was significantly less prevalent in low aT stage (25.8%, 75.0%, and 55.0% in aT0/1mi, aT1a/b, and aT2a/b, respectively; p=.014). *KRAS* mutations showed no significant association with clinical factors including age, sex, and smoking status (all p>.5). Among histologic factors, only neutrophil accumulation was significantly associated with *KRAS* mutations (p=.015). *EGFR* mutation was detected in one of 68 cases tested; the single case was a male smoker with an exon 19 deletion, an invasive pattern greater than 5 mm, and recurrent disease. None of the cases showed concomitant *KRAS* and *EGFR* mutations.

Prognostic impact of invasion size

Thirty-six patients (19.1%) had recurrence or died of disease during follow-up. Extrathoracic recurrence was present in 11 patients (5.9%). None of the 16 patients who underwent sublobar resection experienced recurrence; all had small (≤2 cm) tumors, with 8 mm invasion in one case, ≤5 mm invasion in three cases, and no invasion in 12 cases. The median follow-up for patients without recurrence was 43.5 months (range, 0.5 to 184 months). DFS at 5 years for all 188 patients was 75.6%.

As shown in Table 2 and Fig. 3, DFS was significantly associated with T stage (overall p<.001). Patients with small tumors (≤2 cm, T1a) had 5-year DFS of 100%. Patients with T1b, T2a, T2b, and T3/4 tumors had a 5-year DFS of 89.6%, 62.7%, 51.0%, and 23.4%, respectively. DFS was also significantly associated with aT stage (overall p<.001). Forty-nine cases without invasion (aTis), including nine cases of pure lepidic growth, had no recurrence. In 63 cases with minimal invasion (≤5 mm invasion, aT1mi), 5-year DFS was 95.2%. Of these, tumor size was greater than 3 cm in 23 cases, and two of these cases experienced recurrence. These two cases were grossly 3.5-cm- and 4.5-cm-sized tumors, with 5 mm invasion for both. One case had minute (≤5%) micropapillary pattern foci, and both cases had no other adverse histologic features. Recurrence was not observed in 40 aT1mi cases with ≤3 cm, including five cases with AS, all of which were of lepidic type. Patients with aT1a1, aT1a2, aT1b, aT2a, and aT2b/3/4 stage had 5-year DFS of 75.3%, 54.1%, 41.7%, 20.3%, and 16.8% at 2.7 years, respectively.

aT stage was also a T stage–independent predictor of recurrence when patient survival within the separate T stage subgroups was assessed according to aT stage (Fig. 4). In the T1b subgroup, a significant difference in survival was observed between aTis/1mi group and aT1a/b group (5-year DFS, 100% and 68.6% for

https://doi.org/10.4132/jptm.2016.09.17

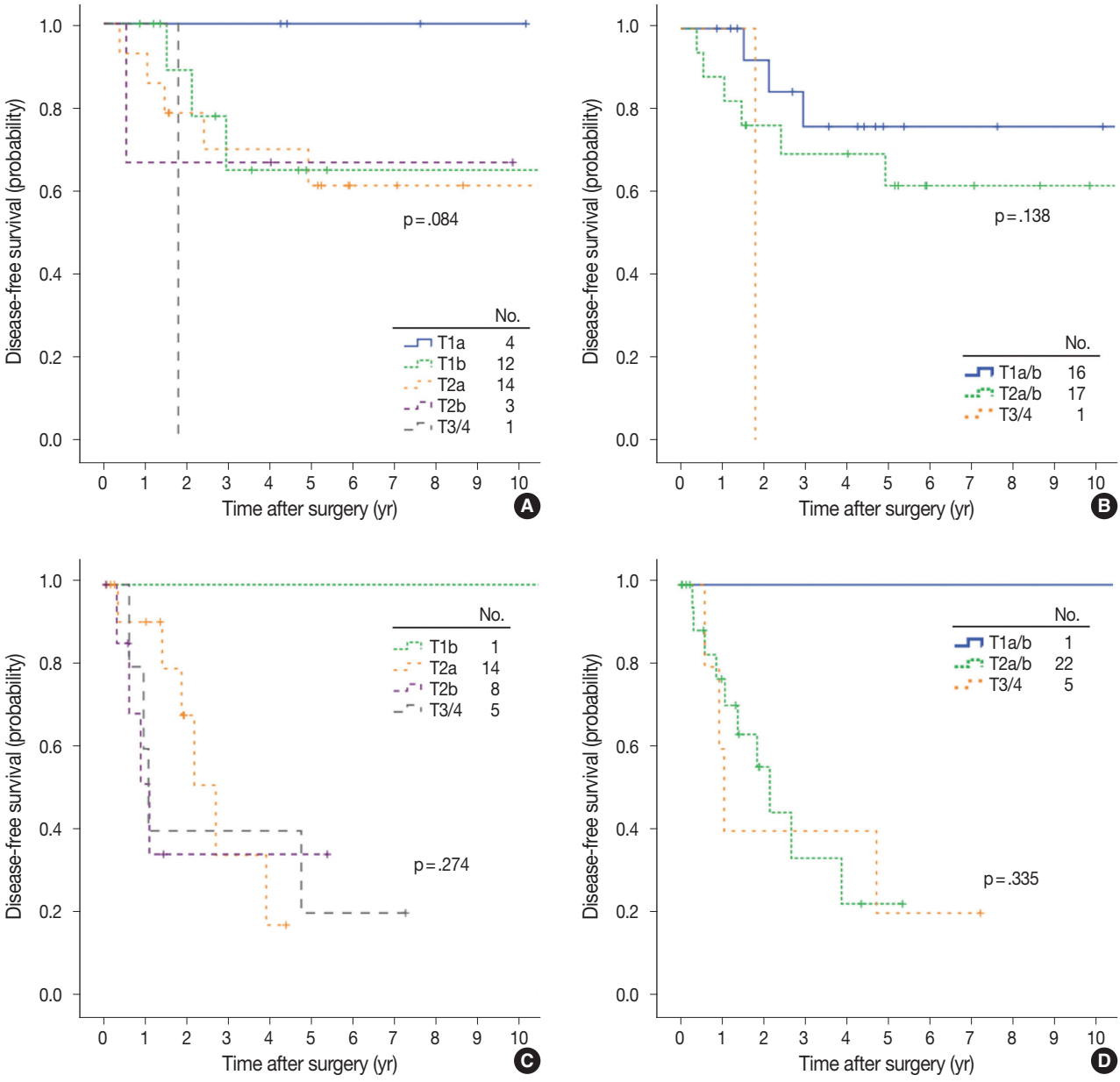

Fig. 5. Disease-free survival in separate adjusted T stage subgroups according to the T stage (A, C) and grouped T stage (B, D). (A, B) aT1a subgroups (n=34). (C, D) aT2a subgroups (n=21). aT1a, >5 mm, ≤2 cm invasion; aT2a, >3 cm, ≤5 cm invasion or visceral pleural invasion (PL1–2).

aTis/1mi [n = 29] and aT1a/b [n = 13], respectively; p = .008). In the T2a subgroup, survival was also significantly stratified by aT stage (5-year DFS, 86.1%, 54.0%, and 0% at 3.9 years for aTis/1mi [n = 21], aT1a/b [n = 18] and aT2a/b [n = 10], respectively; p = .002). In the T2b subgroup, cases with advanced aT stage had a tendency for worse survival (5-year DFS, 100%, 60.0%, and 25.9% for aT0/1mi [n = 3], aT1a/b [n = 5], and aT2a/b [n = 10], respectively; p = 0.071). Conversely, survival within the separate aT stage was not relevant to T stage (Fig. 5).

Univariate analyses of clinicopathologic variables are summarized in Table 2. Smokers had significantly worse DFS (p = .012). Patients with older age and male sex had worse DFS, although this was not statistically significant (p = .097 and p = .159, respectively). *KRAS* mutation showed no significant associations with survival (p = .076). Nuclear atypia, micropapillary pattern, AS, vascular invasion, and intra-alveolar neutrophils were all associated with worse DFS (all p < .001). Pleural invasion and nodal metastasis were also associated with worse DFS (both p < .001).

In multivariate analysis (Table 3), invasion size retained a significant association with DFS (hazard ratio [HR], 5.57; 95%

Table 3. Multivariate analysis for disease-free survival

Factor	HR	95% CI	p-value
Invasion size			.020*
≤5 mm vs >5 mm, ≤3 cm	5.57	1.39–22.39	.015*
≤5 mm vs >3 cm	10.21	1.95–53.59	.006*
Total size			.121
≤3 cm vs >3 cm, ≤7 cm	2.37	0.80–7.05	.121
≤3 cm vs >7 cm	5.36	1.07–26.81	.041*
Micropapillary (<10% vs ≥10%)	2.16	0.84–5.57	.110
Nuclear atypia (mild/moderate vs severe)	1.83	0.74–4.51	.190
Aerogenous spread	0.90	0.36–2.25	.816
Pleural invasion (PL0 vs PL1/2/3)	9.24	3.05–27.96	<.001*
Vascular invasion	2.87	1.01–8.16	.048*
Nodal metastasis (N0 vs N1/2)	1.52	0.37–6.21	.562

HR, hazard ratio; CI, confidence interval.
*p<.05.

confidence interval [CI], 1.39 to 22.39; p=.015 for ≤5 mm vs. >5 mm, ≤3 cm and HR, 10.21; 95% CI, 1.95 to 53.59; p=.006 for ≤5 mm vs. >3 cm). Total size was also associated with survival, but to a lesser degree (HR, 2.37; 95% CI, 0.80 to 7.05; p=.121 for ≤3 cm vs. >3 cm, ≤7 cm and HR, 5.36; 95% CI, 1.07 to 26.81; p=.041 for ≤3 cm vs. >7 cm). Among other factors, pleural invasion (HR, 9.24; p<.001) and vascular invasion (HR, 2.87; p=.048) remained significant predictors of recurrence.

DISCUSSION

In our largest series of pulmonary mucinous adenocarcinomas to date, we have shown that the prognosis of mucinous adenocarcinoma is largely determined by the size of invasive patterns. Although conventional tumor staging by total size was associated with prognosis, tumors within the separate T stage subgroups showed heterogeneous proportions of invasive growth patterns, which were correlated with patient outcome. Our results indicate that the size of invasive patterns may have greater prognostic impact than gross size in mucinous adenocarcinomas.

We also demonstrated that advanced aT stage and T stage tumors were significantly associated with adverse histologic features and clinical features including older age, male sex, and smoking. Notably, low-stage tumors in our cohort had a significantly lower rate of *KRAS* mutation, whereas intermediate- and high-stage tumors showed a mutation rate comparable to that in previous studies.[4,24,25] This unexpectedly low rate of *KRAS* mutation in low-stage, non-invasive mucinous adenocarcinomas was first described by Sato *et al.*[26] However, others with a larger number of cases have shown that *KRAS* mutation status is irrelevant to stage.[4,24] Future studies with data on genetic background in low-stage tumors are needed to support either concept.

In previous studies, mucinous adenocarcinoma accounted for 2%–5% of resected lung adenocarcinomas, which was comparable to 4.6% in our cohort.[7-10,27] The true prognosis of mucinous adenocarcinomas is puzzling, and they are often regarded as aggressive, multicentric, unresectable tumors with dismal prognosis.[28] For resectable cases, however, the most recent study by Shim *et al.*[4] of 83 mucinous adenocarcinomas based on a Korean and American population showed that recurrence-free survival was not inferior to that of non-mucinous tumors. In addition, absence of extrapulmonary recurrence was documented in their study. Ichinokawa *et al.*[27] also reported that 46 adenocarcinomas predominantly composed of goblet cells had 95.7% 5-year DFS and absence of nodal metastasis, although they might have excluded cases showing substantial stromal invasion, which generally have altered cytomorphologic features, since an inclusion criterion of ≥90% goblet cell component was employed in their study. Oka *et al.*[29] reported that, in their series of 13 mucinous adenocarcinomas, eight patients with tumors ≤3 cm had no recurrence. Our data showed results consistent with those from the abovementioned studies in that lymph node metastasis and extrathoracic recurrence rarely occurred in mucinous adenocarcinoma, and small tumors generally showed excellent prognosis. Several studies validating the prognostic impact of the 2011 IASLC/ATS/ERS classification also included cases of mucinous adenocarcinomas. However, due to the rarity of this tumor, only limited numbers were enrolled, and these studies yielded conflicting results.[7-10] We think the limited number of mucinous adenocarcinomas which lack representativeness might have resulted in the varied results observed in these studies. Furthermore, we think it may be misleading to generalize the prognosis of muci-

https://doi.org/10.4132/jptm.2016.09.17

nous adenocarcinomas by comparing them as a whole with other non-mucinous adenocarcinomas showing different architectural patterns, since this could disregard the importance of different stages and invasive growth patterns within mucinous adenocarcinoma, which have significant prognostic impact.

Our study is the first to describe the prevalence, prognostic impact, and the criteria of invasive patterns in mucinous adenocarcinoma. Histologic criteria for invasion in lung adenocarcinomas have evolved for over a decade.[13,14,30] However, no study has yet focused on invasion criteria for mucinous adenocarcinoma. In a review of the literature, the presence of a central scar[27] or back-to-back glands[31] was regarded as a feature of invasion. Interestingly, some pathologists seem to interpret a mucinous lepidic pattern itself as invasion based on the assumption that there will be an invasion in the other area of tumor.[32] According to our data, we believe it is reasonable not to interpret lepidic pattern, or non-distorted acini (pattern 1)—even when they are compactly arranged or embedded in a central scar—as an invasive pattern, since these acini can also represent pre-existing alveolar spaces lined by tumor cells, which are still, by definition, a lepidic pattern. Furthermore, none of the cases exclusively composed of pattern 1 and lepidic pattern showed recurrence, and adjustment for tumor stage by subtracting these components has led to more precise prediction of patient outcomes. Thus, we suggest that pattern 1 is a morphologic spectrum of the lepidic pattern, or at least a pattern that is related to indolent biologic behavior as a lepidic pattern. On the other hand, by using the invasion criteria proposed in this study, as many as 81 of 188 cases in our cohort (43.1%) would be categorized as "adenocarcinoma *in situ*" or "minimally invasive adenocarcinoma" according to the current WHO classification criteria, showing ≤3-cm tumors with ≤5-mm invasion and no other adverse histologic features such as AS.[2] Although this incidence is surprisingly high, none of the cases presented with recurrence, showing that these conceptual diagnostic categories are still valid when our invasion criteria are used.

Our results represent a Korean population from a single institution, and our findings need to be confirmed in further studies with a sufficient number of cases representing other ethnicities. Furthermore, histologic criteria applied in the present study may exhibit interobserver variability, similar to growth pattern analysis for conventional adenocarcinomas.[32,33] Through our histologic review, distinguishing destroyed alveolar spaces from distended alveolar spaces and intra-alveolar proliferation from a lepidic pattern with mild serration was often difficult.

In summary, we showed that the size of invasive patterns determined using the histologic criteria proposed in this study predicts recurrence in pulmonary mucinous adenocarcinomas. Risk stratification relying solely on total size may have pitfalls, since tumors show diverse outcomes that are dependent on the size of the invasive pattern. We expect our data to provide guidance regarding the treatment of this distinct variant of lung adenocarcinoma.

Conflicts of Interest

No potential conflict of interest relevant to this article was reported.

REFERENCES

1. Travis WD, Brambilla E, Noguchi M, *et al.* International Association for the Study of Lung Cancer/American Thoracic Society/European Respiratory Society international multidisciplinary classification of lung adenocarcinoma. J Thorac Oncol 2011; 6: 244-85.
2. Travis WD, Brambilla E, Burke AP, Marx A, Nicholson AG. WHO classification of tumours of the lung, pleura, thymus and heart. 4th ed. Lyon: IARC Press, 2015.
3. Garfield DH, Cadranel J, West HL. Bronchioloalveolar carcinoma: the case for two diseases. Clin Lung Cancer 2008; 9: 24-9.
4. Shim HS, Kenudson M, Zheng Z, *et al.* Unique genetic and survival characteristics of invasive mucinous adenocarcinoma of the Lung. J Thorac Oncol 2015; 10: 1156-62.
5. Fernandez-Cuesta L, Plenker D, Osada H, *et al.* CD74-NRG1 fusions in lung adenocarcinoma. Cancer Discov 2014; 4: 415-22.
6. Nakaoku T, Tsuta K, Ichikawa H, *et al.* Druggable oncogene fusions in invasive mucinous lung adenocarcinoma. Clin Cancer Res 2014; 20: 3087-93.
7. Russell PA, Wainer Z, Wright GM, Daniels M, Conron M, Williams RA. Does lung adenocarcinoma subtype predict patient survival?: a clinicopathologic study based on the new International Association for the Study of Lung Cancer/American Thoracic Society/European Respiratory Society international multidisciplinary lung adenocarcinoma classification. J Thorac Oncol 2011; 6: 1496-504.
8. Yoshizawa A, Motoi N, Riely GJ, *et al.* Impact of proposed IASLC/ATS/ERS classification of lung adenocarcinoma: prognostic subgroups and implications for further revision of staging based on analysis of 514 stage I cases. Mod Pathol 2011; 24: 653-64.
9. Warth A, Muley T, Meister M, *et al.* The novel histologic International Association for the Study of Lung Cancer/American Thoracic Society/European Respiratory Society classification system of lung adenocarcinoma is a stage-independent predictor of survival.

J Clin Oncol 2012; 30: 1438-46.
10. Yoshizawa A, Sumiyoshi S, Sonobe M, *et al.* Validation of the IASLC/ATS/ERS lung adenocarcinoma classification for prognosis and association with *EGFR* and *KRAS* gene mutations: analysis of 440 Japanese patients. J Thorac Oncol 2013; 8: 52-61.
11. Kadota K, Villena-Vargas J, Yoshizawa A, *et al.* Prognostic significance of adenocarcinoma in situ, minimally invasive adenocarcinoma, and nonmucinous lepidic predominant invasive adenocarcinoma of the lung in patients with stage I disease. Am J Surg Pathol 2014; 38: 448-60.
12. Takahashi Y, Ishii G, Aokage K, Hishida T, Yoshida J, Nagai K. Distinctive histopathological features of lepidic growth predominant node-negative adenocarcinomas 3-5 cm in size. Lung Cancer 2013; 79: 118-24.
13. Sakurai H, Maeshima A, Watanabe S, *et al.* Grade of stromal invasion in small adenocarcinoma of the lung: histopathological minimal invasion and prognosis. Am J Surg Pathol 2004; 28: 198-206.
14. Borczuk AC, Qian F, Kazeros A, *et al.* Invasive size is an independent predictor of survival in pulmonary adenocarcinoma. Am J Surg Pathol 2009; 33: 462-9.
15. Nishino M, Klepeis VE, Yeap BY, *et al.* Histologic and cytomorphologic features of *ALK*-rearranged lung adenocarcinomas. Mod Pathol 2012; 25: 1462-72.
16. Yoshida A, Tsuta K, Nakamura H, *et al.* Comprehensive histologic analysis of *ALK*-rearranged lung carcinomas. Am J Surg Pathol 2011; 35: 1226-34.
17. Fukutomi T, Hayashi Y, Emoto K, Kamiya K, Kohno M, Sakamoto M. Low papillary structure in lepidic growth component of lung adenocarcinoma: a unique histologic hallmark of aggressive behavior. Hum Pathol 2013; 44: 1849-58.
18. Compton CC, Byrd DR, Garcia-Aguilar J, Kurtzman SH, Olawaiye A, Washington MK. AJCC cancer staging atlas: a companion to the seventh editions of the AJCC cancer staging manual and handbook. New York: Springer-Verlag, 2012.
19. Warth A, Muley T, Kossakowski CA, *et al.* Prognostic impact of intra-alveolar tumor spread in pulmonary adenocarcinoma. Am J Surg Pathol 2015; 39: 793-801.
20. Kadota K, Nitadori J, Sima CS, *et al.* Tumor spread through air spaces is an important pattern of invasion and impacts the frequency and location of recurrences after limited resection for small stage I lung adenocarcinomas. J Thorac Oncol 2015; 10: 806-14.
21. Bellocq A, Antoine M, Flahault A, *et al.* Neutrophil alveolitis in bronchioloalveolar carcinoma: induction by tumor-derived interleukin-8 and relation to clinical outcome. Am J Pathol 1998; 152: 83-92.
22. Wislez M, Massiani MA, Milleron B, *et al.* Clinical characteristics of pneumonic-type adenocarcinoma of the lung. Chest 2003; 123: 1868-77.
23. Sun JM, Lira M, Pandya K, *et al.* Clinical characteristics associated with *ALK* rearrangements in never-smokers with pulmonary adenocarcinoma. Lung Cancer 2014; 83: 259-64.
24. Ichinokawa H, Ishii G, Nagai K, *et al.* Distinct clinicopathologic characteristics of lung mucinous adenocarcinoma with *KRAS* mutation. Hum Pathol 2013; 44: 2636-42.
25. Kakegawa S, Shimizu K, Sugano M, *et al.* Clinicopathological features of lung adenocarcinoma with *KRAS* mutations. Cancer 2011; 117: 4257-66.
26. Sato S, Motoi N, Hiramatsu M, *et al.* Pulmonary adenocarcinoma in situ: analyses of a large series with reference to smoking, driver mutations, and receptor tyrosine kinase pathway activation. Am J Surg Pathol 2015; 39: 912-21.
27. Ichinokawa H, Ishii G, Nagai K, *et al.* Clinicopathological characteristics of primary lung adenocarcinoma predominantly composed of goblet cells in surgically resected cases. Pathol Int 2011; 61: 423-9.
28. Manning JT Jr, Spjut HJ, Tschen JA. Bronchioloalveolar carcinoma: the significance of two histopathologic types. Cancer 1984; 54: 525-34.
29. Oka S, Hanagiri T, Uramoto H, *et al.* Surgical resection for patients with mucinous bronchioloalveolar carcinoma. Asian J Surg 2010; 33: 89-93.
30. Suzuki K, Yokose T, Yoshida J, *et al.* Prognostic significance of the size of central fibrosis in peripheral adenocarcinoma of the lung. Ann Thorac Surg 2000; 69: 893-7.
31. Borczuk AC. Assessment of invasion in lung adenocarcinoma classification, including adenocarcinoma in situ and minimally invasive adenocarcinoma. Mod Pathol 2012; 25 Suppl 1: S1-10.
32. Thunnissen E, Beasley MB, Borczuk AC, *et al.* Reproducibility of histopathological subtypes and invasion in pulmonary adenocarcinoma: an international interobserver study. Mod Pathol 2012; 25: 1574-83.
33. Warth A, Stenzinger A, von Brünneck AC, *et al.* Interobserver variability in the application of the novel IASLC/ATS/ERS classification for pulmonary adenocarcinomas. Eur Respir J 2012; 40: 1221-7.

 https://doi.org/10.4132/jptm.2016.09.17

Journal of Pathology and Translational Medicine 2017; 51: 69-78
https://doi.org/10.4132/jptm.2016.10.05

■ ORIGINAL ARTICLE ■

Evaluation of Pathologic Complete Response in Breast Cancer Patients Treated with Neoadjuvant Chemotherapy: Experience in a Single Institution over a 10-Year Period

Misun Choi · Yeon Hee Park[1]
Jin Seok Ahn[1] · Young-Hyuck Im[1]
Seok Jin Nam[2] · Soo Youn Cho
Eun Yoon Cho

Department of Pathology and Translational Genomics, [1]Division of Hematology-Oncology, Department of Medicine, [2]Department of Surgery, Samsung Medical Center, Sungkyunkwan University School of Medicine, Seoul, Korea

Received: September 4, 2016
Revised: October 4, 2016
Accepted: October 5, 2016

Corresponding Author
Eun Yoon Cho, MD, PhD
Department of Pathology and Translational Genomics, Samsung Medical Center, Sungkyunkwan University School of Medicine, 81 Irwon-ro, Gangnam-gu, Seoul 06351, Korea
Tel: +82-2-3410-2796
Fax: +82-2-3410-0025
E-mail: eunyoon.cho@samsung.com

Soo Youn Cho, MD, PhD
Department of Pathology and Translational Genomics, Samsung Medical Center, Sungkyunkwan University School of Medicine, 81 Irwon-ro, Gangnam-gu, Seoul 06351, Korea
Tel: +82-2-3410-2817
Fax: +82-2-3410-0025
E-mail: sooyoun.cho@samsung.com

Background: Pathologic complete response (pCR) after neoadjuvant chemotherapy (NAC) has been associated with favorable clinical outcome in breast cancer patients. However, the possibility that the prognostic significance of pCR differs among various definitions has not been established. **Methods:** We retrospectively evaluated the pathologic response after NAC in 353 breast cancer patients and compared the prognoses after applying the following different definitions of pCR: ypT0/is, ypT0, ypT0/is ypN0, and ypT0 ypN0. **Results:** pCR was significantly associated with improved distant disease-free survival (DDFS) regardless of the definition (ypT0/is, $p = .002$; ypT0, $p = .008$; ypT0/is ypN0, $p < .001$; ypT0 ypN0, $p = .003$). Presence of tumor deposits of any size in the lymph nodes (LNs; ypN ≥ 0(i+)) was associated with worse DDFS (ypT0 ypN0 vs ypT0 ypN ≥ 0(i+), $p = .036$ and ypT0/is ypN0 vs ypT0/is ypN ≥ 0(i+), $p = .015$), and presence of isolated tumor cells was associated with decreased overall survival (OS; ypT0/is ypN0 vs ypT0/is ypN0(i+), $p = .013$). Residual ductal carcinoma *in situ* regardless of LN status showed no significant difference in DDFS or OS (DDFS: ypT0 vs ypTis, $p = .373$ and ypT0 ypN0 vs ypTis ypN0, $p = .462$; OS: ypT0 vs ypTis, $p = .441$ and ypT0 ypN0 vs ypTis ypN0, $p = .758$). In subsequent analysis using ypT0/is ypN0, pCR was associated with improved DDFS and OS in triple-negative tumors ($p < .001$ and $p = .003$, respectively). **Conclusions:** Based on our study results, the prognosis and rate of pCR differ according to the definition of pCR and ypT0/is ypN0 might be considered a more preferable definition of pCR.

Key Words: Breast neoplasm; Pathologic complete response; Neoadjuvant chemotherapy

Neoadjuvant chemotherapy (NAC) is used as a standard therapy for inflammatory and inoperable locally advanced breast cancers.[1] NAC may shrink the extent of the tumor and provide prognostic information to test treatment response.[2] Pathologic complete response (pCR) after NAC is associated with improved prognosis in breast cancer and therefore is used as a surrogate of clinical outcome;[3] however, the definitions of pCR have not been standardized, rendering interpretation of NAC data challenging.[3-5]

Differences among definitions of pCR are based on the inclusion of lymph node (LN) status and ductal carcinoma *in situ* (DCIS). The NSABP B-18 trials showed that patients with ypT0/is had a better 5-year disease-free survival than patients with residual invasive disease in the breast,[6,7] and several subsequent trials employed ypT0/is as the primary endpoint.[8-11] However, several studies showed that residual tumors in LNs implied worse prognosis regardless of residual tumors in the breast.[3,12-15] Isolated tumor cells (ITCs) in LNs after NAC are designated as non-pCR by the American Joint Committe on Cancer TNM;[16] however,

pISSN 2383-7837
eISSN 2383-7845

sufficient evidence is lacking to support this recommendation. Including residual DCIS in pCR is another controversial issue regarding the definition of pCR.[3,17] The pooled analysis of 12 neoadjuvant randomized trials by the Collaborative Trials in Neoadjuvant Breast Cancer (CTNeoBC) showed that event-free survival and overall survival (OS) of patients with no tumor cells in the breast (ypT0 ypN0) were comparable to those of patients with residual DCIS (ypT0/is ypN0).[12] Conversly, in the trials by the German Breast Group and Arbeits gemeinschaft Gynäkologische Onkologie-Breast Group (GBG and AGO-B), patients with ypTis ypN0 had a worse event-free survival than patients with ypT0 ypN0.[3] However, the analysis conducted at MD Anderson Cancer Center showed no difference in survival between patients with ypT0 ypTN0 and ypTis ypTN0.[17]

Therefore, the previously proposed definitions of pCR can be divided into two main categories, assessment of pathologic response after NAC in the breast only or in both the breast and LNs. For example, the NSABP-B18 defined pCR as absence of residual invasive tumor cells in the breast (ypT0/is), and CTNeoBC and residual cancer burden proposed by the study conducted at MD Anderson Cancer Center defined pCR as no residual invasive tumor cells not only in the breast but also in the LNs (ypT0/is ypN0). In contrast, the Japanese Breast Cancer Society (JBCS) defined pCR as complete disappearance of tumor cells including DCIS in the breast (ypT0), and the GBG and AGO-B defined it as no residual tumor cells in the breast as well as in the LNs (ypT0 ypN0).[3,6,7,18,19]

Molecular intrinsic subtypes of breast cancer have important prognostic value.[20] Due to the infeasibility of this classification in routine practice, the simplified classification based on immunohistochemical (IHC) results of estrogen receptor (ER), progesterone receptor (PR), and human epidermal growth factor receptor 2 (HER2) can be used to categorize substitutes, classifying ER/PR+HER2– as luminal A, ER/PR+HER2+ as luminal B, ER/PR–HER2+ as HER2-positive and ER/PR–HER2– as triple-negative (TN) tumors.[21] These IHC classifications also have prognostic value similar to those of molecular intrinsic subtypes.[22] Thus, assessment of pCR according to subtype might provide additional prognostic information.

Different definitions of pCR can result in different prognosis. Defining the criteria of pCR that better predict clinical outcome would be important. Therefore, in this study, the prognostic significance of different definitions of pCR were compared and the prognostic significance of LN status, ITCs in the LN, residual DCIS and subtypes were further investigated.

MATERIALS AND METHODS

Study population

We retrospectively retrieved data from 353 individual patients from electronic medical records of Samsung Medical Center in Seoul, Korea, from January 2004 to December 2013. Patients treated with anthracycline and taxane-based NAC and who subsequently underwent surgery with curative intent for primary breast cancer were included. Patients who had histologically confirmed distant metastasis at the time of diagnosis and who were diagnosed with inflammatory carcinoma were excluded. This study was approved by the Institutional Review Board of Samsung Medical Center, and the requirement for informed consent was waived.

Baseline studies including clinical examination, mammography, ultrasound, and magnetic resonance imaging were performed to assess the extent of primary tumor in the breast and LNs. All patients were diagnosed with breast cancer based on core needle biopsies, and LN metastasis was confirmed using core needle biopsy or fine-needle aspiration. All patients were treated with four or six cycles of anthracycline and taxane-based regimen at 3-week intervals, including adriamycin with docetaxel, adriamycin with cyclophosphamide plus docetaxel (AC-T), or AC-T plus trastuzumab. Patients with hormonal receptor–positive tumors received adjuvant endocrine therapy for at least 5 years after surgery. Patients with HER2-overexpressing and/or amplified tumors received neoadjuvant trastuzumab plus chemotherapy followed by adjuvant trastuzumab. Local and regional recurrence was confirmed either histologically or cytologically.

Histologic review

Core biopsies before NAC and surgical specimens obtained after NAC were reviewed. The largest size of tumors, histologic type, histologic grade, lymphovascular invasion (LVI), proportion of DCIS, number of positive LNs, size of the largest metastasis, and treatment response in breast and LN were evaluated. Tumor size and extent in breast and LNs were assessed according to the recommendation proposed by Provenzano *et al.*[23] Histologic type was defined in accordance with the World Health Organization classification,[24] and histologic grade was classified using the modified Scarff-Bloom-Richardson grading system.[25]

To compare the prognostic impact of the pCR components defined previously, all patients were subdivided into the following subgroups according to TNM:[16] (1) no residual invasive tumor cells in the breast, ypT0/is, (2) no residual invasive tumor cells in the breast or LNs, ypT0/is ypN0, (3) no residual invasive tumor

https://doi.org/10.4132/jptm.2016.10.05

cells or DCIS in the breast, ypT0, and (4) no residual invasive tumor cells or DCIS in the breast and LNs, ypT0 ypN0.

ER, PR, and HER2 were assessed on both core biopsies and surgical specimens. ER and PR were considered positive only when greater than or equal to 1% of tumor cells showed nuclear staining. HER2 was positive if tumor cells showed 3+ by IHC or 2+ by IHC with amplification using silver *in situ* hybridization.[26] To assess the prognostic impact of pCR on intrinsic subtypes of breast cancer, all patients were classified into four subtypes according to the IHC results as follows: ER/PR+HER2-

Table 1. Baseline clinicopathologic characteristics and pCR rates according to definition

Variable	No. (%)	ypT0/is		ypT0		ypT0/is ypN0		ypT0 ypN0	
		No. (%)	p-value	No. (%)	p-value	No. (%)	p-value	No. (%)	p-value
All patients	353 (100)	86 (24.4)		50 (14.2)		62 (17.6)		40 (11.3)	
Age (yr)			.192		.284		.152		.308
Median	44.0	45.5		45.5		46.5		45.5	
Range	22–68	22–64		22–64		22–64		22–64	
Menopause			.246		.372		.328		.432
Pre	268 (75.9)	61 (22.8)		35 (13.1)		44 (16.4)		28 (10.4)	
Post	85 (24.1)	25 (29.4)		15 (17.6)		18 (21.2)		12 (14.1)	
Tumor size before NAC (cm)			.001		.001		.036		.058
Median	4.6	3.75		3.45		4.0		3.9	
Range	0.7–11.0	1.1–11.0		1.1–11.0		0.7–10.0		1.1–11.0	
Clinical N stage			.190		.739		.193		.533
cN1	10 (2.8)	5 (50.0)		2 (20.0)		4 (40.0)		2 (20.0)	
cN2	61 (17.3)	16 (26.2)		11 (18.0)		13 (21.3)		9 (14.8)	
cN3	178 (50.4)	38 (21.3)		23 (12.9)		29 (16.3)		20 (11.2)	
cN4	104 (29.5)	27 (26.0)		14 (13.5)		16 (15.4)		9 (8.7)	
Lymph node metastasis after NAC			<.001		<.001		<.001		<.001
No	135 (38.2)	62 (45.9)		40 (29.6)		62 (45.9)		40 (29.6)	
Yes	218 (61.8)	24 (11.0)		10 (4.6)		0		0	
Histologic type			.017		.143		.056		.233
Ductal	323 (91.5)	85 (26.3)		49 (15.2)		61 (18.9)		39 (12.1)	
Lobular	9 (2.5)	1 (11.1)		1 (11.1)		1 (11.1)		1 (11.1)	
Others	21 (5.9)	0		0		0		0	
Histologic grade of pre-NAC tumors			<.001		<.001		<.001		<.001
1	27 (7.6)	1 (3.7)		0		0		0	
2	148 (41.9)	18 (12.2)		8 (5.4)		12 (8.1)		6 (4.1)	
3	178 (50.4)	67 (37.6)		42 (23.6)		50 (28.1)		34 (19.1)	
Lymphovascular invasion			<.001		<.001		<.001		<.001
No	223 (63.2)	83 (37.2)		47 (21.1)		62 (27.8)		40 (17.9)	
Yes	130 (36.8)	3 (2.3)		3 (2.3)		0		0	
ER status			<.001		<.001		<.001		<.001
Negative	167 (47.3)	68 (40.7)		43 (25.7)		48 (28.7)		34 (20.4)	
Positive	186 (52.7)	18 (9.7)		7 (3.8)		14 (7.5)		6 (3.2)	
PR status			<.001		<.001		<.001		<.001
Negative	214 (60.6)	72 (33.6)		44 (20.6)		53 (24.8)		35 (16.4)	
Positive	139 (39.4)	14 (10.1)		6 (4.3)		9 (6.5)		5 (3.6)	
HER2 status			.027		.395		.019		.714
Negative	255 (72.2)	54 (21.2)		39 (15.3)		37 (14.5)		30 (11.8)	
Positive	98 (27.8)	32 (32.7)		11 (11.2)		25 (25.5)		10 (10.2)	
Subgroups			<.001		<.001		<.001		<.001
Luminal A–like	120 (34.0)	6 (5.0)		3 (2.5)		5 (4.2)		2 (1.7)	
Luminal B–like	71 (20.1)	14 (19.7)		5 (7.0)		10 (14.1)		5 (7.0)	
HER2-positive	55 (15.6)	23 (41.8)		8 (14.5)		18 (32.7)		7 (12.7)	
Triple-negative	107 (30.3)	43 (40.2)		34 (31.8)		29 (27.1)		26 (24.3)	

pCR, pathologic complete response; NAC, neoadjuvant chemotherapy; ER, estrogen receptor; PR, progesterone receptor; HER2, human epidermal growth factor receptor 2; Luminal A-like, ER/PR+HER2– tumors with histologic grade 1 or 2; Luminal B-like, ER/PR+HER2– tumors with histologic grade 3 or ER/PR+HER2+ tumors; HER2-positive, ER/PR–HER2+ tumors; Triple-negative, ER/PR/HER2– tumors.

with histologic grade 1 or 2 tumors as luminal A-like; ER/PR+HER2– with histologic grade 3 tumors or ER/PR/HER2+ tumors as luminal B–like; ER/PR–HER2+ tumors as HER2-positive; and ER/PR/HER2– tumors as TN.[3,27]

Statistical analysis

Distant disease-free survival (DDFS) and OS were defined as the time between the date of initial diagnosis to the date of distant recurrence or the date of death from any cause, respectively. The significance of differences in baseline variables was analyzed using two-sided χ^2, Fisher exact or Mann-Whitney U test as appropriate. DDFS and OS were plotted using the Kaplan-Meier product-limit method, and the log-lank p-value was calculated. To assess the prognostic impact of the pCR component, hazard ratios (HRs), 95% confidence intervals and p-value were calculated using Cox proportional hazards model. All tests were two sided, and a p-value less than .05 was considered statistically significant. Statistical analyses were performed using the SPSS statistical software ver. 20.0 (IBM Corp., Armonk, NY, USA).

RESULTS

Patient characteristics

Median age at diagnosis was 44.0 years (range, 22 to 68 years). Median size of tumor was 4.6 cm (range, 0.7 to 11.0 cm) before NAC and 1.5 cm (range, 0.0 to 13.0 cm) after NAC. Most patients (282/353, 79.9%) had cN2 or N3 nodal status before NAC, and median number of positive LNs after NAC

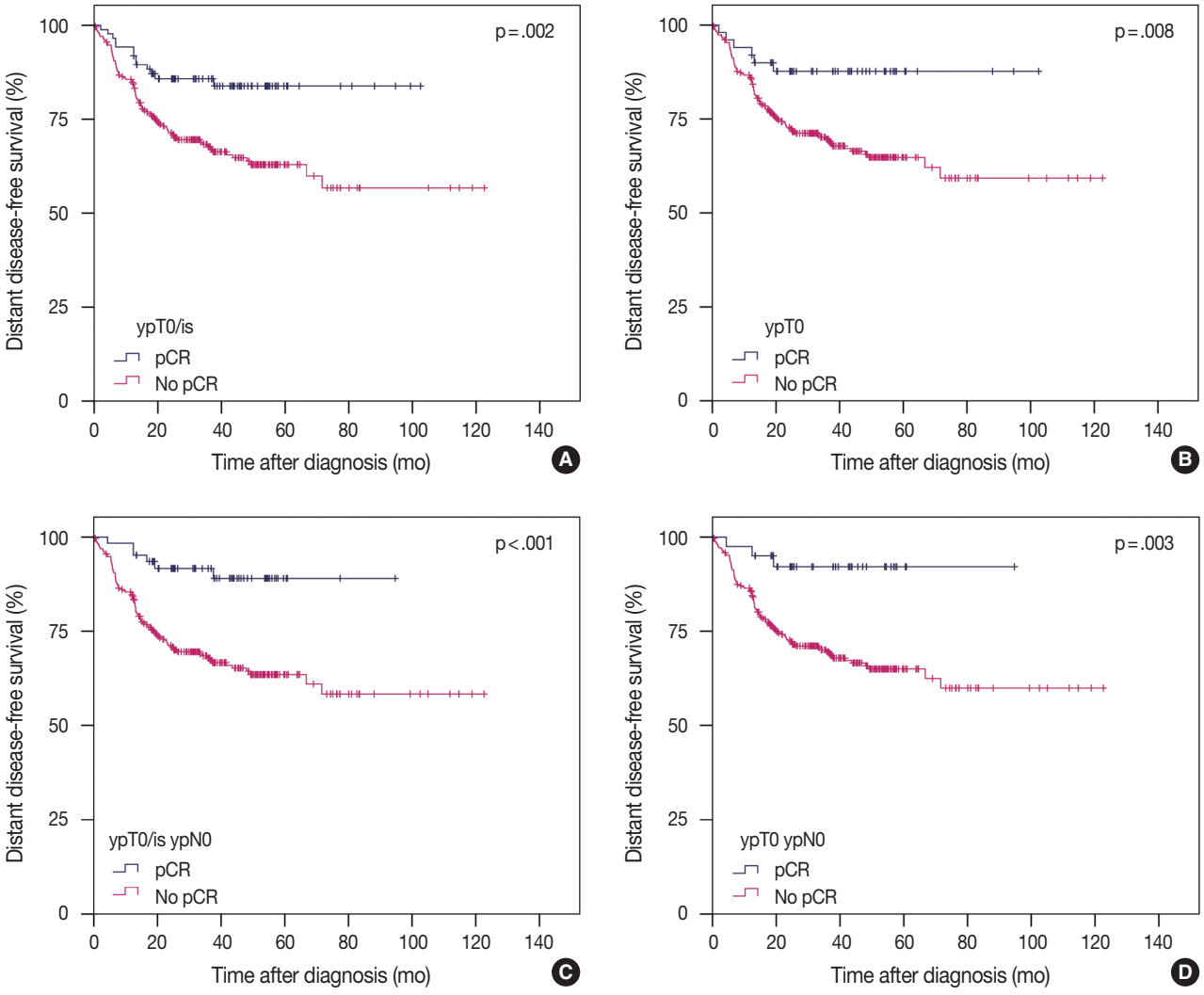

Fig. 1. Survival analysis according to definition of pCR. DDFS and OS according to ypT0/is definition of pCR (A, B), ypT0 (C, D), ypT0/is ypN0 (E, F), and ypT0 ypN0 (G, H). pCR, pathologic complete response; DDFS, distant disease-free survival; OS, overall survival. *(Continued to the next page)*

https://doi.org/10.4132/jptm.2016.10.05

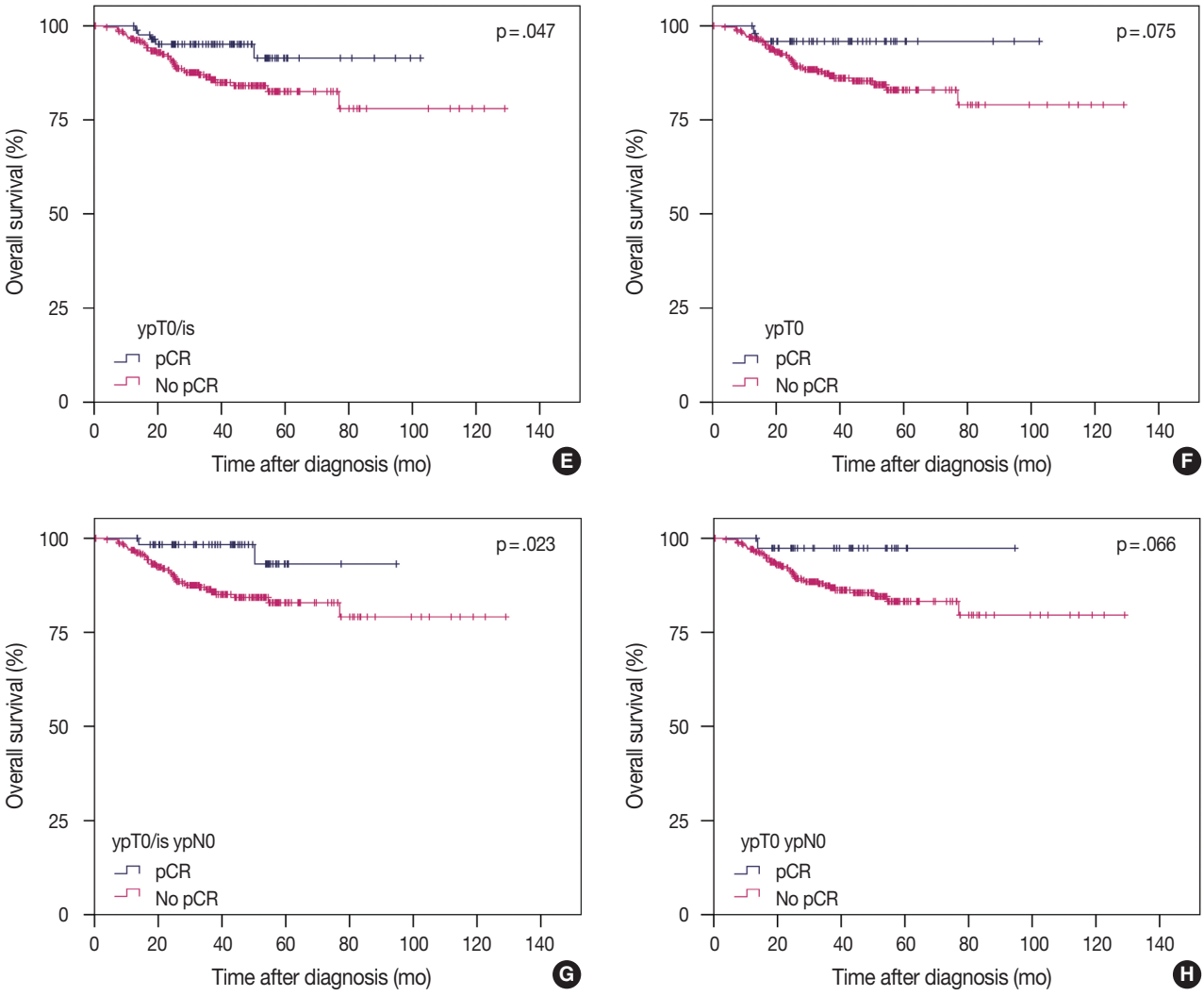

Fig. 1. *(Continued from the previous page)*

was 1 (range, 0 to 39). Baseline clinicopathologic characteristics and corresponding pCR rates according to definition of pCR are summarized in Table 1. In brief, histologic grade, LVI, presence of metastatic LN, and hormonal receptor status showed significant correlation with pCR rate according to definition. Patients with high histologic grade tumors, no LVI, no metastatic LN, and negative hormonal receptor status tended to have higher pCR rates. HER2-positive and TN tumors showed significantly higher pCR rates than luminal A-like and luminal B-like tumors regardless of the pCR definition. The median follow-up time of 353 patients was 36.5 months (range, 0.4 to 129.0 months). During this period, 101 patients (28.6%) had a relapse and 41 (11.6%) died. The 5-year DDFS was 68.0%, and OS was 84.8%.

Correlation between pCR and survival according to definition

According to the four definitions of pCR, 86 (24.4%) patients were diagnosed as ypT0/is, 50 (14.2%) as ypT0, 62 (17.6%) as ypT0/is ypN0, and 40 (11.3%) as ypT0 ypN0. Patients who achieved pCR showed significantly better DDFS than patients who did not (Fig. 1A, C, E, G). Similarly, patients who achieved pCR also tended to have better OS than patients who did not, but this difference was not statistically significant when ypT0 and ypT0 ypN0 were used as the pCR definitions (Fig. 1B, D, F, H). HRs for DDFS and OS increased sequentially as follows: ypT0/is, ypT0, ypT0/is ypN0, and ypT0 ypN0 (Table 2).

Prognostic significance of LN status

In the ypT0 subgroup (n = 50), 10 patients (20.0%) had tumor deposits in the LNs (ypN≥0(i+)) and experienced worse DDFS than patients with no metastatic LNs (5-year DDFS: ypT0 ypN0, 92.1%; ypT0 ypN≥0(i+), 68.6%; p = .036). In the ypT0/is subgroup (n = 86), 24 patients (27.9%) had residual tumor

deposits in the LNs (ypN≥0(i+)) and experienced worse DDFS than patients with no metastatic LNs (5-year DDFS: ypT0/is ypN0, 89.0%; ypT0/is ypN≥0(i+), 70.2%; p = .015). The 5-year OS for patients with ypT0 ypN≥0(i+) and ypT0/is ypN≥0(i+) (88.9% and 86.5%, respectively) appeared worse than for patients with ypT0 ypN0 and ypT0/is ypN0 (97.4% and

Table 2. Prognostic significance of pCR on survival according to definition

Definitions of pCR	Total, n (%)	Distant metastasis, n (%)	DDFS		Died of disease, n (%)	OS	
			HR[a] (95% CI)	p-value[a]		HR[a] (95% CI)	p-value[a]
Breast only							
ypT0/is	86 (24.4)	13 (15.1)	2.472 (1.380–4.426)	.002	5 (5.9)	2.497 (0.980–6.364)	.055
ypT0	50 (14.2)	6 (12.0)	2.900 (1.270–6.618)	.011	2 (4.0)	3.373 (0.814–13.969)	.094
Breast and lymph nodes							
ypT0/is ypN0	62 (17.6)	6 (9.7)	3.954 (1.732–9.026)	.001	2 (3.2)	4.498 (1.086–18.638)	.038
ypT0 ypN0	40 (11.3)	3 (7.5)	4.741 (1.502–14.958)	.008	1 (2.5)	5.277 (0.725–38.398)	.100

pCR, pathologic complete response; DDFS, distant disease-free survival; OS, overall survival; HR, hazard ratio; CI, confidende interval.
[a]HRs and p-values are calculated from the comparison of survival in patients with or without pCR.

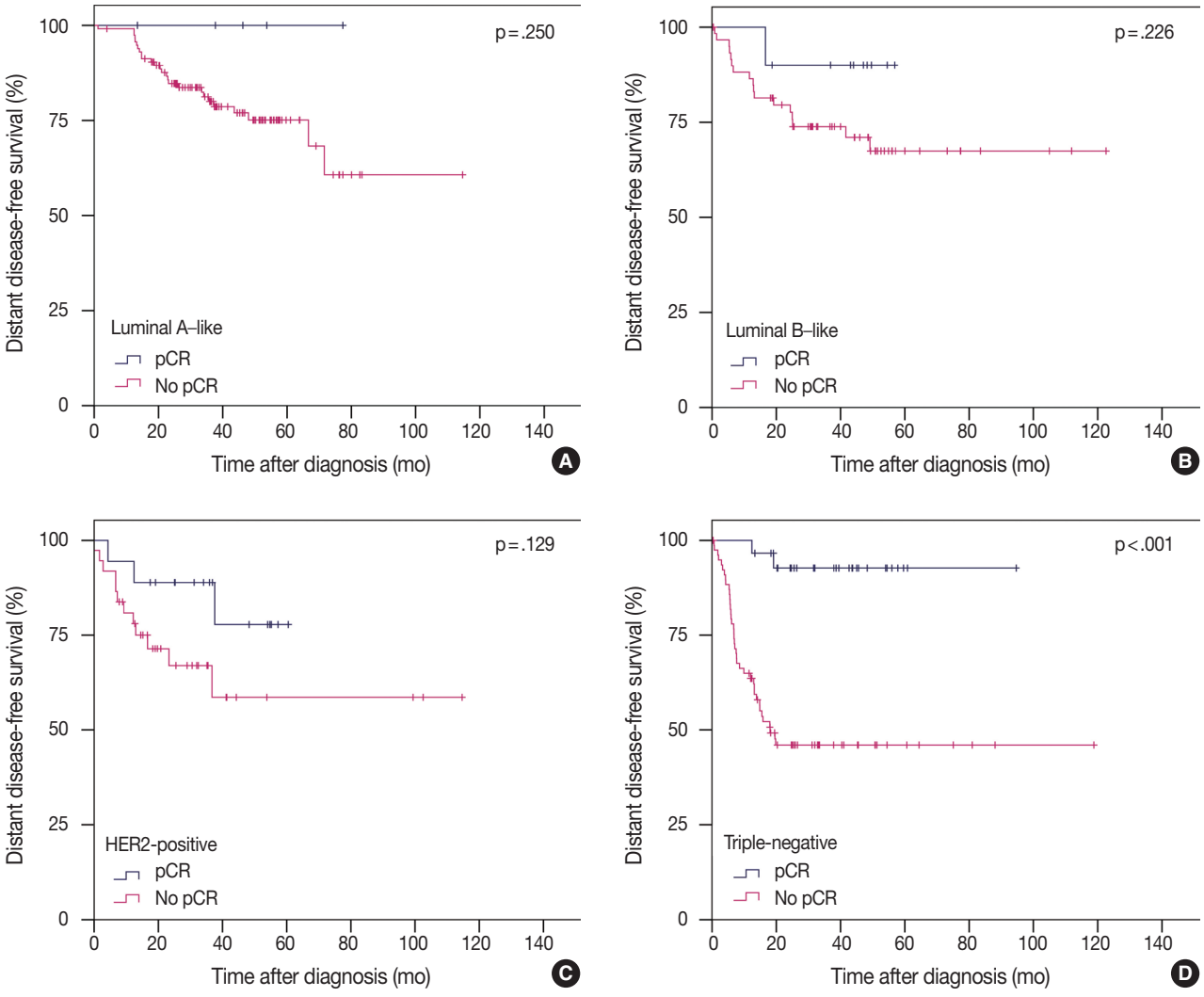

Fig. 2. (A-H) Prognosis between patients with or without pCR according to intrinsic subtype. pCR, pathologic complete response; Luminal A-like, ER/PR+HER2– tumors with histologic grade 1 or 2; Luminal B-like, ER/PR+HER2– tumors with histologic grade 3 or ER/PR+HER2+ tumors; HER2-positive, ER/PR–HER2+ tumors; Triple-negative, ER/PR/HER2– tumors; ER, estrogen receptor; PR, progesterone receptor; HER2, human epidermal growth factor receptor 2. *(Continued to the next page)*

 https://doi.org/10.4132/jptm.2016.10.05

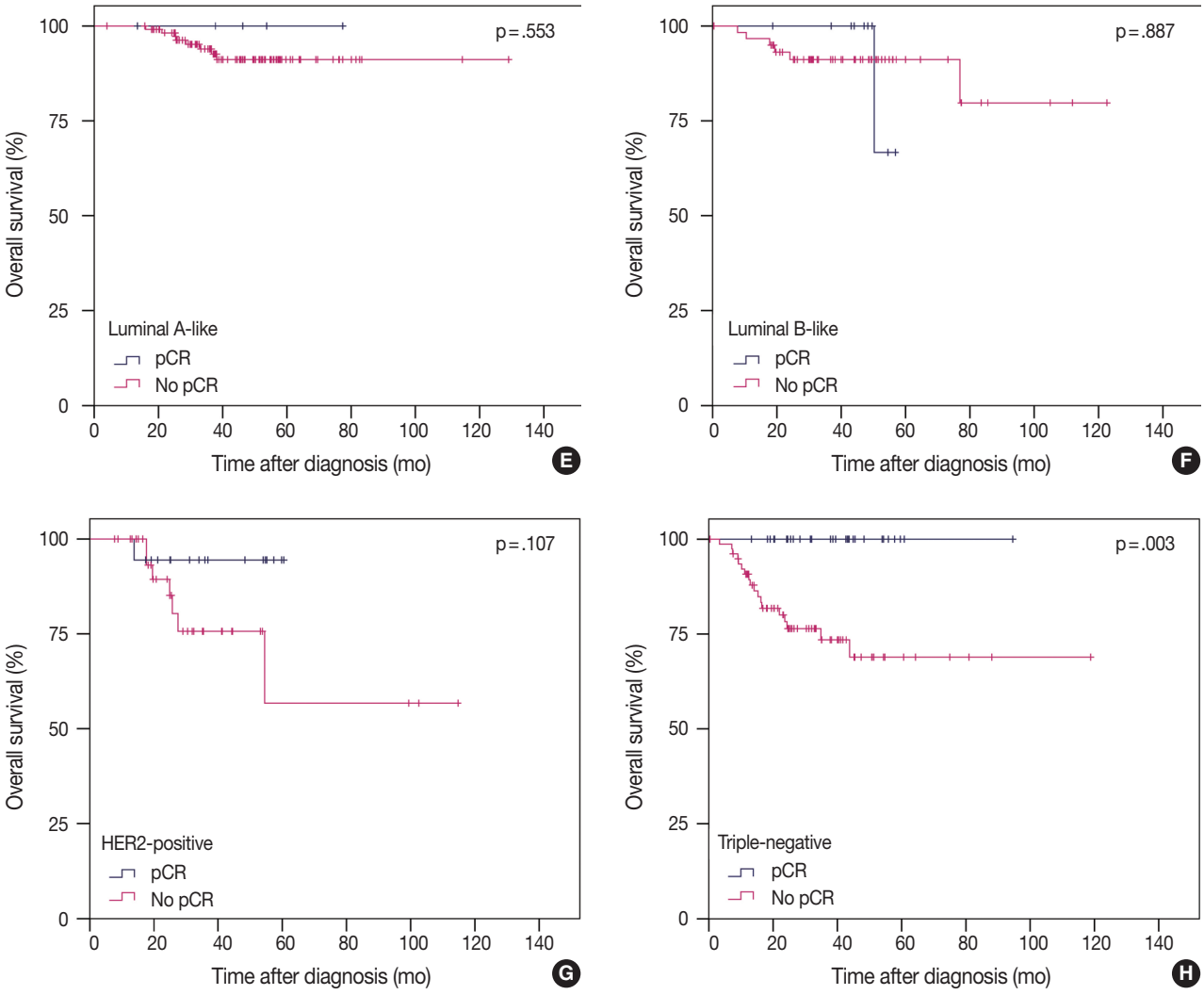

Fig. 2. *(Continued from the previous page)*

93.2%, respectively), but the difference was not statistically significant (p = .236 and p = .095, respectively).

Prognostic significance of ITCs in the LNs

Among patients with ypT0 ypN ≥ 0(i+) (n = 10), 3 had ITCs in the LNs, and none relapsed or died. Among patients with ypT0/is ypN ≥ 0(i+) (n = 24), five had ITCs in the LNs, and showed worse OS compared to patients with ypT0/is ypN0 (5-year OS: ypT0/is ypN0(i+), 75.0% vs ypT0/is ypN0, 93.2%; p = .013). For DDFS, patients with ITCs in LNs tended to experience worse DDFS than patients with no tumor cells in the LNs (5-year DDFS: ypT0/is ypN0(i+), 80.0% vs ypT0/is ypN0, 89.0%; p = .336).

Prognostic significance of residual DCIS

Patients with residual DCIS in the breast tended to experience worse DDFS and OS compared with patients with no residual tumor cells in the breast (5-year DDFS: ypT0, 87.6% and ypTis, 78.3%; 5-year OS: ypT0, 95.8% and ypTis, 85.5%), but the difference was not statistically significant (p = .373 and p = .441, respectively). Considering LN status, patients with ypT0 ypN0 had 5-year DDFS of 92.1% and OS of 97.4%, which appeared better than those of patients with ypTis ypN0 (5-year DDFS, 83.3% and 5-year OS, 87.5%). However, these were not statistically significant (p = .462 and p = .758, respectively).

Among patients who achieved pCR when ypT0/is was used as the definition of pCR, the proportion of patients with residual DCIS was significantly different among IHC subtypes (p = .001); highest with HER2-positive tumors (15/23, 65.2%) followed by luminal B-like (9/14, 64.3%), luminal A-like (3/6, 50%), and lowest with TN tumors (9/43, 20.9%).

Prognostic significance of pCR in IHC subtypes

To analyze the prognosis between patients with or without pCR according to IHC subtype, we defined pCR as ypT0/is ypN0 according to our study results. In TN tumors, pCR was significantly associated with improved survival in terms of both DDFS and OS. However, in luminal A-like, luminal B-like, and HER2-positive tumors, pCR showed no prognostic impact on survival (Fig. 2). In patients without pCR, HER2-positive and TN tumors showed poorer prognosis than in luminal A-like and luminal B-like tumors (Fig. 2).

DISCUSSION

To the best of our knowledge, this study is the first analysis of the prognostic significance of different pCR definitions on long-term outcome in breast cancer patients treated homogeneously with anthracycline and taxane-based NAC regimens as well as neoadjuvant trastzumab plus chemotherapy at a single institute in Korea. We compared the following four definitions of pCR; ypT0/is, ypT0, ypT0/is ypN0, and ypT0 ypN0, and the corresponding pCR rates were 24.4%, 14.2%, 17.6%, and 11.3%, respectively (Table 1). These rates were similar to previous studies. In a study by JBCS (n = 353), pCR rates of ypT0/is, ypT0, ypT0/is ypN0, and ypT0 ypN0 were 20.4%, 9.9%, 18.4%, and 8.2%, respectively.[28] In a meta-analysis by CTNeoBC (n = 13,125), pCR rates of ypT0/is, ypT0/is ypN0, and ypT0 ypN0 were 22%, 18%, and 13%, respectively.[12] In the study by GBG and AGO-B (n = 6,377), pCR rates of ypT0/is, ypT0/is ypN0, and ypT0 ypN0 were 22.8%, 19.8%, and 15.0%, respectively.[3]

In the present study, patients with pCR, regardless of definition, had significantly better DDFS than patients without pCR. Regarding OS, however, patients with pCR when ypT0/is and ypT0/is ypN0 were used as pCR definitions showed significantly better survival than patients without pCR (Fig. 1). Regarding LN status, even if tumor cells were not present in the breast including DCIS, patients with residual tumor cells of any size in the LNs experienced worse DDFS than patients with no metastatic LNs. Presence of ITCs in the LNs after NAC is regarded as non-pCR by the American Joint Committee on Cancer for TNM staging;[16] however, data supporting this recommendation is insufficient. Our study showed that patients with ITCs in the LNs might have poorer OS than patients with no tumor cells in the LNs. However, further studies with larger populations are warranted.

Theoretically, ypT0 ypN0 represents the strictest definition of pCR, meaning complete eradication of all tumor cells in both the breast and LNs. Thus, we compared the prognosis between ypT0 and ypTis as well as between ypT0 ypN0 and ypT0/is ypN0 and found that presence of DCIS did not result in any difference. Thus, based on the results from this study, we considered ypT0/is ypN0 the more preferable definition of pCR. These results were consistent with previous studies by JBCS, CTNeoBC, and MD Anderson.[12,17,28] But not with those of GBG and AGO-B, which suggested ypT0 ypN0 as the best definition of pCR.[3] This discrepancy might be caused by the smaller number of patients and events in ypTis (n = 36) and ypTis ypN0 (n = 22), resulting in a much lower statistical significance to show prognostic differences in this study.

Among the IHC subtypes, HER2-positive and TN tumors achieved high pCR rates. pCR was significantly correlated with DDFS and OS only in TN tumors (Fig. 2). However, in patients without pCR, HER2-positive and TN tumors showed poorer prognosis than in luminal A-like and luminal B-like tumors. These results are in agreement with the previously reported studies by Liedtke *et al.*[29] and Houssami *et al.*[30]

The potential limitations of this study are as follows. First, due to the small number of patients and events, comparison between patients with pCR and without pCR using Cox proportional hazards model was not feasible. Second, because Ki-67 was not available for all patients, subtypes based on only ER, PR, and HER2 status and histologic grade might not be the same as molecular intrinsic subtypes.

In conclusion, the prognosis and rate of pCR varied according to definition of pCR. In our study, pCR defined as ypT0/is ypN0 was considered the most preferable. pCR could be used as a surrogate of favorable clinical outcome in TN tumors but not in luminal A-like, luminal B-like, or HER2-positive tumors.

Conflicts of Interest

No potential conflict of interest relevant to this article was reported.

REFERENCES

1. Kaufmann M, von Minckwitz G, Bear HD, *et al.* Recommendations from an international expert panel on the use of neoadjuvant (primary) systemic treatment of operable breast cancer: new perspectives 2006. Ann Oncol 2007; 18: 1927-34.
2. Kaufmann M, von Minckwitz G, Mamounas EP, *et al.* Recommendations from an international consensus conference on the current status and future of neoadjuvant systemic therapy in primary breast

cancer. Ann Surg Oncol 2012; 19: 1508-16.
3. von Minckwitz G, Untch M, Blohmer JU, *et al.* Definition and impact of pathologic complete response on prognosis after neoadjuvant chemotherapy in various intrinsic breast cancer subtypes. J Clin Oncol 2012; 30: 1796-804.
4. Cortazar P, Geyer CE Jr. Pathological complete response in neoadjuvant treatment of breast cancer. Ann Surg Oncol 2015; 22: 1441-6.
5. Kuroi K, Toi M, Tsuda H, Kurosumi M, Akiyama F. Issues in the assessment of the pathologic effect of primary systemic therapy for breast cancer. Breast Cancer 2006; 13: 38-48.
6. Wolmark N, Wang J, Mamounas E, Bryant J, Fisher B. Preoperative chemotherapy in patients with operable breast cancer: nine-year results from National Surgical Adjuvant Breast and Bowel Project B-18. J Natl Cancer Inst Monogr 2001; (30): 96-102.
7. Fisher B, Bryant J, Wolmark N, *et al.* Effect of preoperative chemotherapy on the outcome of women with operable breast cancer. J Clin Oncol 1998; 16: 2672-85.
8. Robidoux A, Tang G, Rastogi P, *et al.* Lapatinib as a component of neoadjuvant therapy for HER2-positive operable breast cancer (NSABP protocol B-41): an open-label, randomised phase 3 trial. Lancet Oncol 2013; 14: 1183-92.
9. Bear HD, Tang G, Rastogi P, *et al.* Bevacizumab added to neoadjuvant chemotherapy for breast cancer. N Engl J Med 2012; 366: 310-20.
10. Gianni L, Pienkowski T, Im YH, *et al.* Efficacy and safety of neoadjuvant pertuzumab and trastuzumab in women with locally advanced, inflammatory, or early HER2-positive breast cancer (NeoSphere): a randomised multicentre, open-label, phase 2 trial. Lancet Oncol 2012; 13: 25-32.
11. Baselga J, Bradbury I, Eidtmann H, *et al.* Lapatinib with trastuzumab for HER2-positive early breast cancer (NeoALTTO): a randomised, open-label, multicentre, phase 3 trial. Lancet 2012; 379: 633-40.
12. Cortazar P, Zhang L, Untch M, *et al.* Pathological complete response and long-term clinical benefit in breast cancer: the CTNeoBC pooled analysis. Lancet 2014; 384: 164-72.
13. Corben AD, Abi-Raad R, Popa I, *et al.* Pathologic response and long-term follow-up in breast cancer patients treated with neoadjuvant chemotherapy: a comparison between classifications and their practical application. Arch Pathol Lab Med 2013; 137: 1074-82.
14. Rouzier R, Extra JM, Klijanienko J, *et al.* Incidence and prognostic significance of complete axillary downstaging after primary chemotherapy in breast cancer patients with T1 to T3 tumors and cytologically proven axillary metastatic lymph nodes. J Clin Oncol 2002; 20: 1304-10.
15. McCready DR, Hortobagyi GN, Kau SW, Smith TL, Buzdar AU, Balch CM. The prognostic significance of lymph node metastases after preoperative chemotherapy for locally advanced breast cancer. Arch Surg 1989; 124: 21-5.
16. Edge SB, Byrd DR, Compton CC, Fritz AG, Greene FL, Trotti A. American Joint Committee on Cancer (AJCC) cancer staging manual. 7th ed. New York: Springer, 2009.
17. Mazouni C, Peintinger F, Wan-Kau S, *et al.* Residual ductal carcinoma in situ in patients with complete eradication of invasive breast cancer after neoadjuvant chemotherapy does not adversely affect patient outcome. J Clin Oncol 2007; 25: 2650-5.
18. Symmans WF, Peintinger F, Hatzis C, *et al.* Measurement of residual breast cancer burden to predict survival after neoadjuvant chemotherapy. J Clin Oncol 2007; 25: 4414-22.
19. Kurosumi M, Akiyama F, Iwase T, *et al*. Histopathological criteria for assessment of therapeutic response in breast cancer. Breast Cancer 2001; 8: 1-2.
20. Perou CM, Sorlie T, Eisen MB, *et al.* Molecular portraits of human breast tumours. Nature 2000; 406: 747-52.
21. Carey LA, Perou CM, Livasy CA, *et al.* Race, breast cancer subtypes, and survival in the Carolina Breast Cancer Study. JAMA 2006; 295: 2492-502.
22. Onitilo AA, Engel JM, Greenlee RT, Mukesh BN. Breast cancer subtypes based on ER/PR and Her2 expression: comparison of clinicopathologic features and survival. Clin Med Res 2009; 7: 4-13.
23. Provenzano E, Bossuyt V, Viale G, *et al.* Standardization of pathologic evaluation and reporting of postneoadjuvant specimens in clinical trials of breast cancer: recommendations from an international working group. Mod Pathol 2015; 28: 1185-201.
24. Lakhani SR, Ellis IO, Schinitt SJ, Tan PH, van de Vijver MJ. WHO classification of tumours of the breast. 4th ed. Lyon: IARC Press, 2012.
25. Elston CW, Ellis IO. Pathological prognostic factors in breast cancer. I. The value of histological grade in breast cancer: experience from a large study with long-term follow-up. Histopathology 1991; 19: 403-10.
26. Wolff AC, Hammond ME, Hicks DG, *et al.* Recommendations for human epidermal growth factor receptor 2 testing in breast cancer: American Society of Clinical Oncology/College of American Pathologists clinical practice guideline update. J Clin Oncol 2013; 31: 3997-4013.
27. Goldhirsch A, Wood WC, Coates AS, *et al*. Strategies for subtypes: dealing with the diversity of breast cancer: highlights of the St. Gallen International Expert Consensus on the Primary Therapy of Early Breast Cancer 2011. Ann Oncol 2011; 22: 1736-47.
28. Kuroi K, Toi M, Ohno S, *et al.* Comparison of different definitions of pathologic complete response in operable breast cancer: a pooled analysis of three prospective neoadjuvant studies of JBCRG. Breast Cancer 2015; 22: 586-95.
29. Liedtke C, Mazouni C, Hess KR, *et al.* Response to neoadjuvant ther-

apy and long-term survival in patients with triple-negative breast cancer. J Clin Oncol 2008; 26: 1275-81.
30. Houssami N, Macaskill P, von Minckwitz G, Marinovich ML, Mamounas E. Meta-analysis of the association of breast cancer subtype and pathologic complete response to neoadjuvant chemotherapy. Eur J Cancer 2012; 48: 3342-54.

https://doi.org/10.4132/jptm.2016.10.05

Journal of Pathology and Translational Medicine 2017; 51: 79-86
https://doi.org/10.4132/jptm.2016.10.13

■ ORIGINAL ARTICLE ■

Prognosis of Hepatocellular Carcinoma after Liver Transplantation: Comparative Analysis with Partial Hepatectomy

Kyuho Lee · Kyoung-Bun Lee
Nam-Joon Yi[1] · Kyung-Suk Suh[1]
Ja-June Jang

Departments of Pathology and [1]Surgery, Seoul National University College of Medicine, Seoul, Korea

Received: September 19, 2016
Revised: October 4, 2016
Accepted: October 13, 2016

Corresponding Author
Kyoung-Bun Lee, MD
Department of Pathology, Seoul National University Hospital, 101 Daehak-ro, Jongno-gu, Seoul 03080, Korea
Tel: +82-2-2072-2968
Fax: +82-2-743-5530
E-mail: kblee@snuh.org

Background: Liver transplantation (LT) is the treatment of choice for hepatocellular carcinoma (HCC). The aim of this study was to investigate the recurrence rate of HCC after LT and prognostic factors for recurrence by comparing LT with non-transplanted resection. **Methods:** The participants were 338 patients who underwent LT between 1996 and 2012 at Seoul National University Hospital (LT group) and 520 HCC patients who underwent partial hepatectomy between 1995 and 2006 (control group, non-LT group). **Results:** In the LT group, 68 of 338 patients (19.8%) showed relapse, and the recurrence rate was lower than that in the non-LT group (64.9%, 357/520, $p < .001$). Stratification analysis by American Joint Committee on Cancer (AJCC) stage showed that the stage I-II LT group had a lower recurrence rate than the non-LT group. Univariate comparative analysis demonstrated that multiplicity of tumor, tumor size, gross type, Edmondson-Steiner (ES) nuclear grade, extent of tumor, angioinvasion, AJCC stage, Milan criteria, University of California at San Francisco criteria on explant pathology (all $p < .001$), positive expression of cytokeratin 19 ($p = .002$), and preoperative α-fetoprotein (AFP) ($p < .001$) were predictors of tumor recurrence. In multivariate analysis, LT, preoperative AFP, multiplicity of tumor, extent of tumor, size of tumor, and ES nuclear grade were independent prognostic factors. **Conclusions:** LT might have a protective effect against the late recurrence of stage I-II HCC compared to non-LT, and the prognostic factors for recurrence were similar to previously well-known prognostic factors for HCC.

Key Words: Liver transplantation; Hepatocellular carcinoma; Recurrence; Prognosis

Hepatocellular carcinoma (HCC) is the fifth most common malignant tumor in the world.[1] The treatments for HCC vary depending on the stage of the primary tumors and the patient's hepatic function. Resection is the treatment of choice for localized tumors, which are generally early-stage tumors, and liver transplantation (LT) is frequently selected as an alternative, potentially curative treatment for HCC.

After the Milan criteria for deceased donor LT for HCC were introduced in 1996, LT became an alternative treatment choice for early-stage or small HCC to achieve good disease-free survival (DFS).[2] However, as living donor LT has rapidly increased due to the shortage of deceased donors in Eastern countries including Japan and Korea, the development of selection criteria of LT for HCC has become a dominant issue in this field that must include consideration of the balance between the benefit to the recipient and the risk to the liver donor. LT seems to result in a good prognosis for patients with early-stage HCC who are within the Milan criteria. The Milan criteria incorporate the size of the tumor, the number of tumors, and the presence of vascular invasion; patients eligible for LT are those with a single tumor 5 cm or smaller in size or 2–3 tumors each 3 cm or smaller in size, without macroscopic vascular invasion or extrahepatic spread according to preoperative radiologic findings. A low incidence of recurrence is expected among this group of patients.[2] However, there is still a controversy about the cutoff points of tumor size and number of nodules.[3,4] Accordingly, Yao *et al*.[5] re-evaluated the upper limits and effects of tumor number and size in relation to DFS and proposed new criteria. The University of California at San Francisco (UCSF) criteria include the presence of a tumor 6.5 cm or smaller in diameter with a single nodule or no more than three tumor nodules, none exceeding 4.5 cm with a total diameter less than 8 cm, and no vascular invasion according to pathologic evaluation.[5] However, some patients who do not fulfill the Milan or UCSF criteria experienced a prolonged survival time, contrary to expectations.[6,7] Lee *et al*.[8] therefore suggested another set of criteria different from the previous measures and based on pathology. Their criteria are a largest tumor diameter of 5 cm or less, six or fewer tumors, and no gross vascular invasion.

pISSN 2383-7837
eISSN 2383-7845

These criteria are valuable and have a prognostic power similar to that of the Milan and UCSF criteria.[8] In addition to clinical and pathological prognostic factors, immunohistochemical factors are significant; cytokeratin 19 (CK19) is a representative factor.[9]

According to a guideline for the management of hepatocellular carcinoma in Korea, deceased donor LT is the first choice of treatment for HCC within the Milan criteria (single nodule less than 5 cm in diameter or 2–3 nodules less than or equal to 3 cm in diameter) but that has not met the indication for resection. Local ablation or transarterial chemoembolization is recommended during the waiting period for LT. However, LT for HCC beyond the Milan criteria is uncertainly suggested.[10] In addition, in Korea, living donor LT is actively performed as an alternative to deceased donor liver transplantation because of the insufficient number of donors. The survival rate of living donor LT does not differ from that of deceased donor LT, but the disease-free survival rate is worse after living donor LT.[10,11]

This single-center retrospective analysis aimed to investigate the recurrence rate of HCC after transplantation and the patterns of recurrence in LT patients compared to non-LT patients and to determine prognostic factors based on explant pathology.

MATERIALS AND METHODS

Patient selection and clinicopathologic parameters

We divided the study participants into two groups: the LT group and a control group (non-LT group). The LT group included 338 patients who had been pathologically diagnosed with HCC based on LT specimens and who had available medical records and formalin-fixed paraffin blocks of tumor tissue from the archives of the Department of Pathology of Seoul National University Hospital (SNUH) from 1996 to 2012. The non-LT group comprised 520 patients who were pathologically diagnosed with HCC based on partial hepatectomy specimens and who had available medical records and formalin-fixed paraffin blocks of tumor tissue from the archives of the Department of Pathology of SNUH from 1995 to 2006. Patients with combined hepatocellular carcinoma and cholangiocarcinoma or intrahepatic cholangiocarcinoma were excluded. The clinical information collected from existing medical records was age, sex, surgical method, underlying etiology of liver disease, serum α-fetoprotein (AFP), preoperative treatment, and postoperative tumor recurrence. Pathological information was tumor size, number of tumors, site of tumors in the liver, gross tumor type, Edmondson-Steiner (ES) nuclear grade for HCCs, cellular type of tumor cells, histological pattern, vascular invasion, pathological American Joint Committee on Cancer (AJCC) stage, whether the cancer met criteria such as the Milan criteria or UCSF criteria based on pathology, and positivity of CK19 staining, all of which were collected from pathology reports or slide reviews. The AJCC staging followed the liver tumor staging guidelines of the American Joint Committee on Cancer, seventh edition.[12] The clinicopathologic parameters followed "General rules for the study of primary liver cancer of Japan."[13] This study was approved by the Institutional Review Board of SNUH (H-1011-046-339). The demographic details of all patients are summarized in Table 1 according to treatment method.

Immunohistochemistry of CK19

All diagnoses were confirmed by examination of 3-μm hematoxylin and eosin–stained sections of representative formalin-fixed paraffin-embedded blocks. The slides were automatically stained using a Bond-III Automated IHC/ISH stainer and a Bond Polymer Refine Detection Kit (Leica Microsystems GmbH, Wetzlar, Germany). Positive staining with CK19 antibody (mouse monoclonal anti-human cytokeratin 19, clone RCK108, Cat. M0888, 1:200, Dako, Carpinteria, CA, USA) was observed in the cytoplasm and cellular membrane. The criterion for positivity was moderate or strong intensity in ≥5% of tumor cells. CK19 positivity occurred in 243 cases in the LT group and 519 cases in the non-LT group.

Survey of disease progress and classification of recurrence pattern

DFS was defined as the time to local or distant progression. Progression was diagnosed when patients experienced symptoms due to a mass lesion, when serum AFP level increased, or when computed tomography, magnetic resonance imaging, or positron emission tomography reported a new lesion or increasing tumor size. Pathologic confirmation was not necessary. The term intrahepatic progress was used when the tumor recurrence was located only in the liver, and "extrahepatic progress" was used when a metastatic tumor was identified beyond the liver with or without hepatic recurrence. The follow-up period was 36 months (median; range, 0 to 202 months) for the LT group and 73 months (median; range, 0 to 213 months) for the non-LT group.

Statistical analysis

Comparative analyses of discontinuous variables were conducted using the chi-square (χ^2) test, Fisher exact test, or Monte-Carlo resampling methods for small samples. Survival curves were

https://doi.org/10.4132/jptm.2016.10.13

Table 1. Demography of patients in LT and non-LT groups

	LT (n=338)	Non-LT (n=520)	p-value[a]
Sex			.039[b]
Male	266 (79)	438 (84)	
Female	72 (21)	82 (16)	
Age (yr)			.094
≤55	192 (57)	265 (51)	
>55	146 (43)	255 (49)	
Size (cm)			<.001[b]
≤5	298 (88)	312 (60)	
>5	40 (12)	208 (40)	
Multiplicity			<.001[b]
Single	151 (45)	392 (75)	
Multiple	187 (55)	128 (25)	
Gross type			<.001[b]
Expanding nodular, etc.	239 (71)	345 (66)	
Multinodular confluent	73 (22)	174 (33)	
Diffuse/Infiltrative	26 (8)	1 (0)	
Extent			<.001[b]
Confined liver	288 (85)	394 (76)	
Invasion of capsule	45 (13)	87 (17)	
Extension to other organ	5 (1)	39 (8)	
Angioinvasion			<.001[b]
Absent	269 (80)	275 (53)	
Present	69 (20)	245 (47)	
Large vessel invasion			.347
Absent	324 (96)	491 (94)	
Present	14 (4)	29 (6)	
ES nuclear grade			.002[b]
Grade 1–2	251 (74)	334 (64)	
Grade 3–4	87 (26)	186 (36)	
Cell type			<.001[b]
Hepatic	337 (100)	475 (91)	
Non-hepatic	1 (0)	45 (9)	
Histologic pattern			<.001[b]
Trabecular	333 (99)	429 (83)	
Non-trabecular	5 (1)	91 (18)	
Expression of CK19			.348
Negative	223 (66)	479 (92)	
Positive	24 (7)	40 (8)	
Preoperative treatment[c]			<.001[b]
Done	190 (56)	228 (44)	
Not done	107 (32)	285 (55)	
Resection margin			.003[b]
R0	335 (99)	482 (93)	
R1/2	3 (1)	38 (7)	
Underlying CLD[c]			.023[b]
Viral	290 (86)	460 (88)	
Non-viral	48 (14)	53 (10)	
Preoperative AFP (ng/mL)[c]			.016[b]
≤20	191 (57)	250 (48)	
>20	144 (43)	270 (52)	
AJCC stage			<.001[b]
Stage I–II	300 (89)	410 (79)	
Stage III–IV	38 (11)	110 (21)	
Milan criteria			<.001[b]
Within	193 (57)	170 (33)	
Beyond	145 (43)	350 (67)	
UCSF criteria			<.001[b]
Within	253 (75)	331 (64)	
Beyond	85 (25)	189 (36)	
Follow up, median (range, mo)	36 (0–202)	73 (0–213)	<.001[b]

(Continued)

Values are presented as number (%).
LT, liver transplantation; Expanding nodular, etc. including vaguely nodular, expanding nodular with or without perinodal extension; ES nuclear grade, Edmonson Steiner nuclear grade; CK19, cytokeratin 19; CLD, chronic liver disease; AFP, α-fetoprotein; AJCC, American Joint Committee on Cancer; UCSF, University of California at San Francisco.
[a]p-value of chi-square test, or Fisher exact test; [b]p<.05; [c]Some data were not available: 48 preoperative treatment, 7 etiology of CLD, and 3 preoperative AFP data.

calculated using Kaplan-Meier analysis and compared by log-rank testing. Multivariate analysis was performed using a Cox proportional hazards model. Multivariate analysis employing Cox regression analysis was conducted. The results were considered statistically significant when p-values were < 0.05. Most of the tests were performed using IBM SPSS ver. 22 (IBM Corp., Armonk, NY, USA), and the Monte-Carlo resampling method was performed by "coin" package of R statistics.[14-16]

RESULTS

Clinicopathologic characteristics and prognostic parameters of LT and non-LT

As compared in Table 1, many clinicopathologic characteristics of patients in the LT and non-LT groups were different. The LT group had a higher proportion of males, single lesions, expanding nodular gross type, confined lesions in the liver, hepatic histologic type, trabecular pattern, and underlying viral chronic liver disease (CLD) than in the non-LT group (all p < .05). Tumor size was smaller, angioinvasion was less frequent, and ES-nuclear grade and preoperative AFP were lower in the LT group than in the non-LT (all p < .05). Age, CK19-positive expression rate, and large vessel invasion were not different between the two groups. The proportion of patients in a low AJCC stage (I–II stage) and the proportion of those within Milan or UCSF criteria were higher in the LT than in the non-LT group (Table 1). In summary, patients in the LT group had more differentiated tumor histology and a lower stage of HCC than patients in the non-LT group. Hazard ratios of DFS according to the clinicopathologic parameters, which were calculated by univariate Cox proportional hazard model, are plotted in Fig. 1. The prognostic factors associated

with DFS were similar between the LT and non-LT groups. Size, multiplicity of tumor, extent of tumor, angioinvasion, large vessel invasion, ES nuclear grade, positive expression of CK19, resection margin, and preoperative AFP were significant prognostic factors of DFS in both the LT and non-LT groups (all $p < .05$). Gross type was a prognostic factor in the LT group but not in the non-LT group, and this was probably due to the rarity of diffuse/infiltrative type in the non-LT group. Sex, age, tumor cell type, histologic pattern, underlying causes of CLD, and preoperative treatment were not prognostic factors in either the LT or non-LT group. Lower AJCC stage and adherence to the Milan criteria and UCSF criteria were associated with a better DFS (all $p < .05$), but the hazard ratios of higher AJCC stage and non-adherence to the criteria compared to lower AJCC stage and adherence to the criteria were higher in the LT group than in the non-LT group (7.328, 8.727, 5.451 vs 2.312, 1.849, 1.719, respectively, all $p < .05$).

Multivariable analysis of DFS rate of resected HCCs

Significant prognostic factors in univariate analysis in both the LT and non-LT groups were analyzed with transplantation or non-transplantation by multivariable analysis with the Cox proportional hazards model in AJCC stage I–II patients (Table 2). Surgical method was an independent prognostic factor, as were extent of tumor, multiplicity of tumor, angioinvasion, preoperative AFP, size of tumor, and ES nuclear grade. CK19

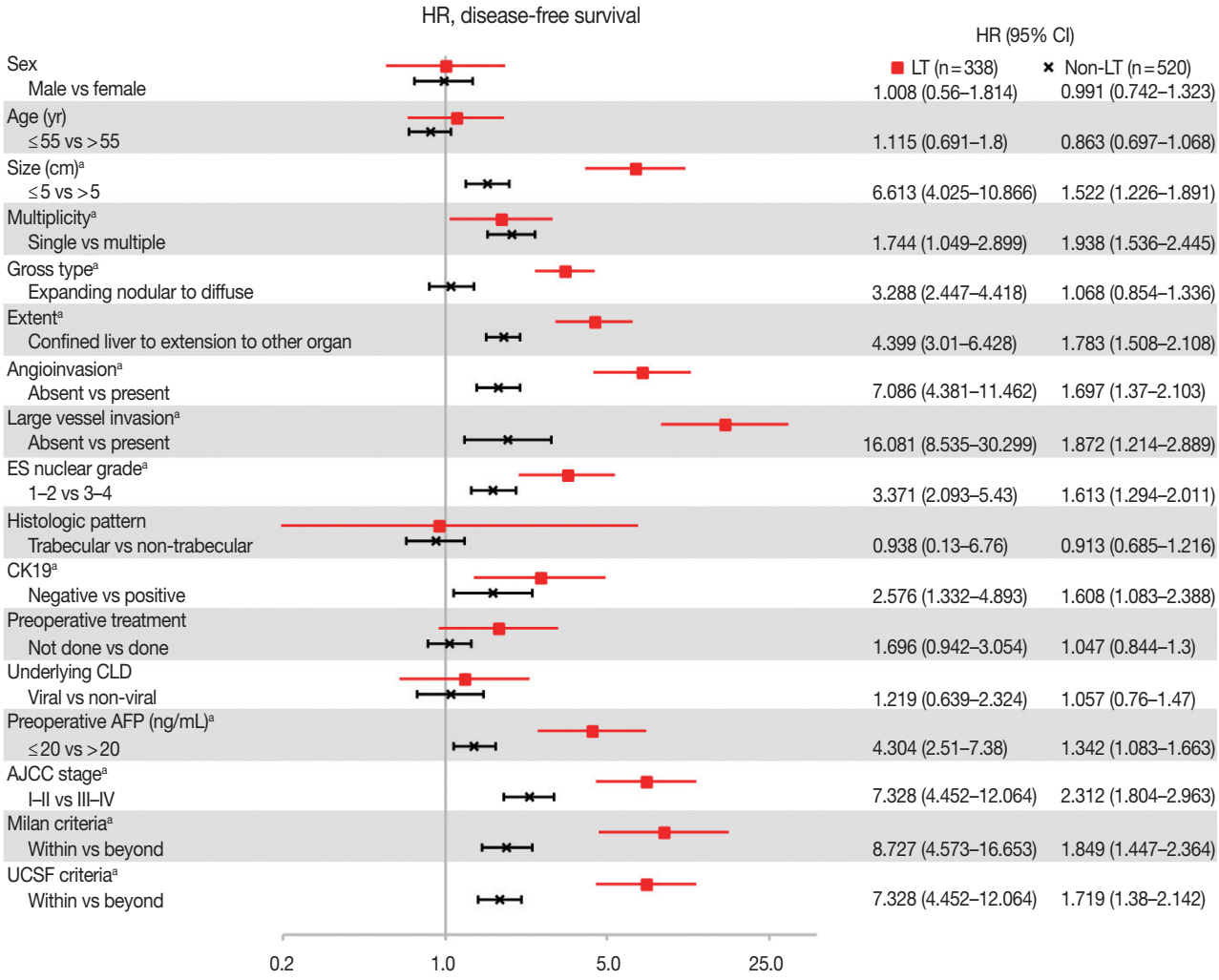

Fig. 1. Comparison of prognostic factors between the liver transplantation (LT) group and the non-LT group by univariate disease-free survival analysis. HRs of LT and non-LT groups calculated by Cox proportional hazard model are plotted in each row. HR (95% CI), hazard ratio (95% confidence interval) by Cox proportional hazard model; LT, liver transplantation; ES nuclear grade, Edmonson Steiner nuclear grade; CLD, chronic liver disease; AFP, α-fetoprotein; AJCC, American Joint Committee on Cancer; UCSF, University of California at San Francisco criteria. [a]Parameters are statistically significant prognostic factors (log-rank $p < .05$).

https://doi.org/10.4132/jptm.2016.10.13

expression and gross type were not independent prognostic factors. The hazard ratio of LT was 0.321 (95% confidence interval, 0.235 to 0.439) compared to non-LT, showing that it might have a protective effect against HCC progress.

Disease-free survival patterns of the LT and non-LT groups

Cumulative DFS is plotted in Fig. 1 with DFS rates in each year according to the AJCC stage (Fig. 2). In the total group, patients who underwent LT had a better DFS than non-LT patients (5-year DFS rates, 79% vs 35%, respectively in LT and non-LT, log-rank p < .001). Further analysis was performed according to AJCC stage, with the entire patient group divided into two groups based on stage I–II and stage III–IV classification. LT in patients with stage I–II HCC resulted in better DFS compared to the non-LT group (5-year DFS rates, 84% vs 40%, respectively; log-rank p < .001). No difference was observed in DFS between the LT and non-LT groups for stage III–IV HCC (5-year DFS rates, 23% vs 15%; log-rank p = .295) (Fig. 2). As shown in Fig. 1A and B, recurrence in the LT group occurred in the early period after surgery, and cumulative DFS was sustained at approximately 80% after 3 years.

Tumor recurrence site and time in the LT and non-LT groups according to stage

The recurrence site and post-operative period of recurrence were compared according to stage and resection method (Table 3). Among patients with tumors classified as stage I–II HCC, 43 patients in the LT group and 250 in the non-LT group experi-

Table 2. Multivariable analysis of disease-free survival rate of stage I–II hepatocellular carcinomas (n=710)

	Beta	SE	p-value	Hazard ratio (95% CI)
Extent of tumor	0.476	0.083	<.001[a]	1.61 (1.367–1.896)
Operation (non-LT vs LT)	–1.135	0.159	<.001[a]	0.321 (0.235–0.439)
Multiplicity (single vs multiple)	0.365	0.115	.001[a]	1.44 (1.15–1.803)
Angioinvasion (absent vs present)	0.33	0.116	.004[a]	1.391 (1.108–1.746)
Preoperative AFP (≤20 ng/mL vs >20 ng/mL)	0.266	0.106	.012[a]	1.305 (1.061–1.606)
Size of tumor (≤5 cm vs >5 cm)	0.256	0.115	.026[a]	1.291 (1.032–1.617)
ES nuclear grade (grade 1–2 vs 3–4)	0.235	0.111	.034[a]	1.265 (1.017–1.573)
CK19 (negative vs positive)	0.3	0.178	.093	1.35 (0.952–1.916)
Gross type	0.165	0.101	.102	1.18 (0.968–1.438)

SE, standard error; CI, confidence interval; LT, liver transplantation; AFP, α-fetoprotein; ES nuclear grade, Edmonson-Steiner nuclear grade; CK19, cytokeratin 19.
[a]p<.05.

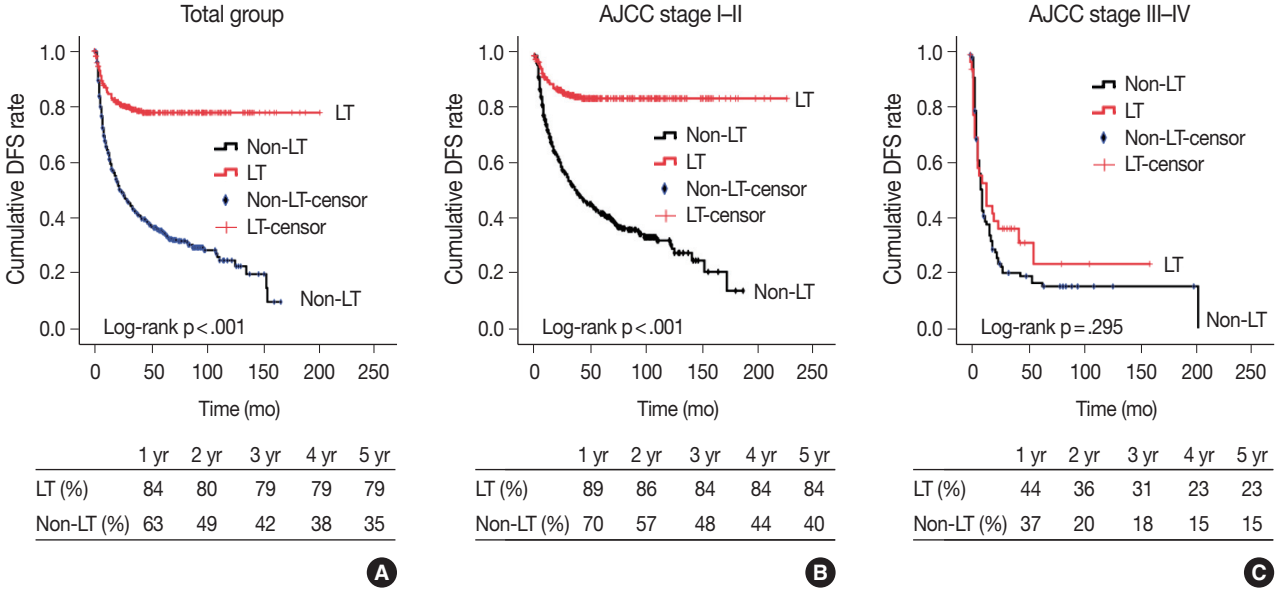

Fig. 2. Kaplan-Meier curves for disease-free survival (DFS) between the liver transplantation (LT) group and the non-LT group. (A) The DFS of patients with any stage disease was significantly longer in the LT group than in the non-LT group (p<.001). (B) Among patients with stage I-II disease, DFS was also longer in the LT group than in the non-LT group (p<.001). (C) There were no significant differences in the DFS of stage III–IV patients between the LT and non-LT groups. AJCC, American Joint Committee on Cancer.

Table 3. Comparison of recurrence pattern between LT and non-LT

	No.	Intrahepatic		Extrahepatic		p-value[a,b]
		≤2 yr	>2 yr	≤2 yr	>2 yr	
AJCC stage I–II						
LT	43	9 (21)		34 (79)		<.001[c]
		9 (100)	0	30 (88)	4 (12)	.376
Non-LT	250	155 (62)		95 (38)		
		29 (57)	66 (43)	79 (83)	16 (17)	<.001[c]
AJCC stage III–IV						
LT	25	9 (36)		16 (64)		.198
		8 (89)	1 (11)	15 (94)	1 (6)	.511
Non-LT	87	44 (51)		43 (49)		
		41 (93)	3 (9)	41 (95)	2 (5)	.600

LT, liver transplantation; AJCC, American Joint Committee on Cancer.
[a]Intrahepatic recur vs extrahepatic recur; [b]≤2 yr vs >2 yr; [c]p<.05.

enced tumor progress. Within the LT group, there were nine cases (21%) with intrahepatic progress and 34 (79%) with extrahepatic progress. In contrast, the non-LT group included 155 cases (62%) of intrahepatic recurrence and 95 cases (38%) of extrahepatic progress. Metastasis to extrahepatic organs was the predominant pattern of recurrence in the LT group among patients with stage I–II HCC, whereas intrahepatic recurrence was predominant in the non-LT group (p < .001). This pattern disappeared in patients with stage III–IV HCC. There were nine cases (36%) of intrahepatic progress and 16 cases (64%) of extrahepatic progress within the LT group, and the non-LT group included 44 cases (51%) of intrahepatic recurrence and 43 cases (49%) of extrahepatic progress, but there was no significant difference between the two groups (p = .198). As previously mentioned, the time to recurrence and recurrence site were different between the LT and non-LT groups. All nine intrahepatic recurrence cases of AJCC stage I–II LT patients recurred within 2 years, but 66 of 155 intrahepatic recurrence cases (43%) of AJCC stage I–II non-LT patients occurred beyond 2 years (p < .001). Most of the extrahepatic metastasis occurred within 2 years in both the LT and non-LT groups for AJCC stage I–II stage patients (30 [88%] vs 79 [83%], respectively, p = .376). This progress pattern also disappeared in stage III–IV patients who showed early progress within 2 years after surgery, regardless of recurrence sites (Table 3).

DISCUSSION

Our study analyzed the recurrence rate of HCC and the recurrence pattern in LT patients compared with non-LT patients, as well as prognostic factors after transplantation. Recurrence after LT usually occurred within 2 years and was more frequently identified in extrahepatic sites; in contrast, recurrence after non-LT frequently occurred beyond 2 years after surgery, and the sites of recurrence were intrahepatic. Furthermore, this difference was clear in stage I-II HCC, but was not observed in stage III–IV HCC.

Many previous studies comparing LT and other treatment choices for HCC reported that patients who underwent LT had a better survival than those who underwent resection.[17] The rationale of LT as a treatment choice for HCC is loco-regional removal of tumor and protective removal of the damaged liver, which plays a major role in the de novo recurrence of HCC. The results of our study support this dual rationale for LT to treat HCC. In our study, intrahepatic recurrence was more frequent in the non-LT group than in the LT group in patients with stage I–II and was sustained for a long period after surgery. Therefore, it is thought that LT is an effective treatment to suppress de novo carcinogenesis, which is the main mechanism of late recurrence of HCC.[18]

In the present study, the high proportion of extrahepatic HCC recurrence after LT was similar to results from other studies.[19] Because of the protective removal of the source of de novo carcinogenesis in LT, tumor recurrence in LT patients can be mainly explained by metastasis or regrowth of remnant tumor cells. Assuming complete resection (R0 resection), potential tumor cells do not exist in the liver after LT. Circulating tumor cells (CTCs) might be considered to explain this phenomenon. According to a recent study, primary tumor cell invasion to the bloodstream and CTCs are responsible for tumor recurrence and metastasis, including that of HCC.[20-22]

Although LT is the treatment of choice for early-stage HCC, it is not a feasible choice because of the shortage of deceased donors. Increasing living donor LT has compensated for the shortage of

 https://doi.org/10.4132/jptm.2016.10.13

organ donations, but maintaining a balance between the benefit to the recipient and the risk to the living donor is another emerging issue in this field. Patient selection criteria tend to expand the range of recipients by up regulation of number or size of tumor. This classical approach used to be based on preoperative radiologic studies. However, the histology and biologic features of the tumor are important prognostic factors for predicting tumor progress.[23] Similar to other studies, the multivariate analysis of prognostic factors in our study also concluded that ES nuclear grade was an independent prognostic factor. However, although CK19 expression was not an independent prognostic factor in our study, it was reported as a prognostic marker of HCC recurrence beyond the Milan criteria in another study.[9]

Another issue concerning the histologic factors of HCC in LT is the gap between preoperative clinical staging and post-operative pathologic staging. The Milan criteria and UCSF criteria consider vascular invasion as an important exclusion criterion. Because the degree of vasculature that can be examined by radiologic study and pathologic study is much different, many cases within the criteria before surgery are changed to beyond the criteria after surgery based on the pathology of the explant. In our study, the Milan and UCSF criteria were applied by explant pathology. Pretransplant tumor staging and explant pathology do not always correlate, and 83 of 145 cases (57%) within the Milan criteria were classified as "beyond Milan" based on the presence of angioinvasion in microscopic findings. There might be discrepancies in the size or number of tumors between the pre-transplant radiological staging and explant pathologic staging.[24,25] Therefore, further studies to reduce the preoperative and postoperative staging are needed.

In conclusion, this study demonstrated that DFS was better in the LT group compared to the non-LT group for patients with stage I–II HCC. Accordingly, there might be a tendency for tumors to occur in the late period after surgery in patients who have not undergone LT. Extrahepatic recurrence is more frequent than intrahepatic recurrence after LT. Once tumor recurrence has occurred, dissemination to additional locations occurs easily. The prognostic factors in patients who have undergone LT are similar to those observed in previous studies; LT, extent of tumor, multiplicity of tumor, angioinvasion, preoperative AFP, size of tumor, and ES nuclear grade were independent prognostic factors.

Conflicts of Interest

No potential conflict of interest relevant to this article was reported.

Acknowledgments

This research was supported by a grant of the Korea Health Technology R&D Project through the Korea Health Industry Development Institute (KHIDI), funded by the Ministry of Health & Welfare, Republic of Korea (grant number: HI14C3298).

REFERENCES

1. Parkin DM, Bray F, Ferlay J, Pisani P. Estimating the world cancer burden: Globocan 2000. Int J Cancer 2001; 94: 153-6.
2. Mazzaferro V, Regalia E, Doci R, *et al*. Liver transplantation for the treatment of small hepatocellular carcinomas in patients with cirrhosis. N Engl J Med 1996; 334: 693-9.
3. Tan KC, Rela M, Ryder SD, *et al*. Experience of orthotopic liver transplantation and hepatic resection for hepatocellular carcinoma of less than 8 cm in patients with cirrhosis. Br J Surg 1995; 82: 253-6.
4. McPeake JR, O'Grady JG, Zaman S, *et al*. Liver transplantation for primary hepatocellular carcinoma: tumor size and number determine outcome. J Hepatol 1993; 18: 226-34.
5. Yao FY, Ferrell L, Bass NM, *et al*. Liver transplantation for hepatocellular carcinoma: expansion of the tumor size limits does not adversely impact survival. Hepatology 2001; 33: 1394-403.
6. Gondolesi GE, Roayaie S, Muñoz L, *et al*. Adult living donor liver transplantation for patients with hepatocellular carcinoma: extending UNOS priority criteria. Ann Surg 2004; 239: 142-9.
7. Todo S, Furukawa H; Japanese Study Group on Organ Transplantation. Living donor liver transplantation for adult patients with hepatocellular carcinoma: experience in Japan. Ann Surg 2004; 240: 451-9.
8. Lee SG, Hwang S, Moon DB, *et al*. Expanded indication criteria of living donor liver transplantation for hepatocellular carcinoma at one large-volume center. Liver Transpl 2008; 14: 935-45.
9. Miltiadous O, Sia D, Hoshida Y, *et al*. Progenitor cell markers predict outcome of patients with hepatocellular carcinoma beyond Milan criteria undergoing liver transplantation. J Hepatol 2015; 63: 1368-77.
10. Korean Liver Cancer Study Group (KLCSG); National Cancer Center, Korea (NCC). 2014 KLCSG-NCC Korea Practice Guideline for the Management of Hepatocellular Carcinoma. Gut Liver 2015; 9: 267-317.
11. Hwang S, Lee SG, Joh JW, Suh KS, Kim DG. Liver transplantation for adult patients with hepatocellular carcinoma in Korea: comparison between cadaveric donor and living donor liver transplanta-

tions. Liver Transpl 2005; 11: 1265-72.
12. Edge SB, Compton CC. The American Joint Committee on Cancer: the 7th edition of the AJCC cancer staging manual and the future of TNM. Ann Surg Oncol 2010; 17: 1471-4.
13. The general rules for the clinical and pathological study of primary liver cancer. Liver Cancer Study Group of Japan. Jpn J Surg 1989; 19: 98-129.
14. R Core Team. R: A language and environment for statistical computing [Internet]. Vienna: R Foundation for Statistical Computing, 2015 [cited 2016 Nov 1]. Available from: https://www.R-project.org/.
15. Hothorn T, Hornik K, van de Wiel MA, Zeileis A. Implementing a class of permutation tests: the coin package. J Stat Softw 2008; 28: 1-23.
16. Hothorn T, Hornik K, van de Wiel MA, Zeileis A. A Lego system for conditional inference. Am Stat 2006; 60: 257-63.
17. Kaido T, Morita S, Tanaka S, *et al*. Long-term outcomes of hepatic resection versus living donor liver transplantation for hepatocellular carcinoma: a propensity score-matching study. Dis Markers 2015; 2015: 425926.
18. Imamura H, Matsuyama Y, Tanaka E, *et al*. Risk factors contributing to early and late phase intrahepatic recurrence of hepatocellular carcinoma after hepatectomy. J Hepatol 2003; 38: 200-7.
19. Scortegagna E, Jr., Karam AR, Sioshansi S, Bozorgzadeh A, Barry C, Hussain S. Hepatocellular carcinoma recurrence pattern following liver transplantation and a suggested surveillance algorithm. Clin Imaging 2016; 40: 1131-4.
20. Attard G, de Bono JS. Utilizing circulating tumor cells: challenges and pitfalls. Curr Opin Genet Dev 2011; 21: 50-8.
21. Zhang Y, Li J, Cao L, Xu W, Yin Z. Circulating tumor cells in hepatocellular carcinoma: detection techniques, clinical implications, and future perspectives. Semin Oncol 2012; 39: 449-60.
22. Zhang Y, Shi ZL, Yang X, Yin ZF. Targeting of circulating hepatocellular carcinoma cells to prevent postoperative recurrence and metastasis. World J Gastroenterol 2014; 20: 142-7.
23. Donat M, Alonso S, Pereira F, *et al*. Impact of histological factors of hepatocellular carcinoma on the outcome of liver transplantation. Transplant Proc 2016; 48: 1968-77.
24. Mejia GA, Gomez MA, Serrano J, *et al*. Correlation between the radiologic and histologic size of hepatocellular carcinoma in patients eligible for liver transplantation. Transplant Proc 2006; 38: 1394-5.
25. El Moghazy W, Kashkoush S, Meeberg G, Kneteman N. Incidence, characteristics, and prognosis of incidentally discovered hepatocellular carcinoma after liver transplantation. J Transplant 2016; 2016: 1916387.

Journal of Pathology and Translational Medicine 2017; 51: 87-91
https://doi.org/10.4132/jptm.2016.06.16

■ CASE STUDY ■

A Rare Case of Recurrent Metastatic Solid Pseudopapillary Neoplasm of the Pancreas

Hye Seung Lee · Han Kyeom Kim
Bong Kyung Shin · Jin Hyuk Choi
Yoo Jin Choi · Ha Yeon Kim

Department of Pathology, Korea University Guro Hospital, Seoul, Korea

Received: March 30, 2016
Revised: May 21, 2016
Accepted: June 16, 2016

Corresponding Author
Bong Kyung Shin, MD, PhD
Department of Pathology, Korea University Guro Hospital, Korea University College of Medicine, 148 Gurodong-ro, Guro-gu, Seoul 08308, Korea
Tel: +82-2-2626-1472
Fax: +82-2-2626-1486
E-mail: tabrega@korea.ac.kr

A 61-year-old woman visited our hospital for bilateral multiple lung nodules and a mass in her thorax. She had a long history of multiple metastatic recurrences of solid pseudopapillary neoplasm (SPN); 24 years previously, the patient had undergone pylorus-preserving pancreaticoduodenectomy for a 9.9×8.6 cm mass in the pancreatic head. The tumor was diagnosed as an SPN. Nine years later, metastatic nodules were found on computed tomography in the patient's liver and peritoneum and were excised. She subsequently underwent an additional eight metastatectomy procedures in diverse organs. For the presented event, the lung nodules were removed. The prevalence of malignant SPN in the general population is 5%–15%. However, multiple metastatic recurrence of malignant SPN is rare; the lung is a particularly rare site of metastasis, found in only three cases in the literature. Here, we describe this exceptional case and provide a literature review.

Key Words: Solid pseudopapillary neoplasm; Lung; Neoplasm metastasis

Solid pseudopapillary neoplasm (SPN) of the pancreas is a rare low-grade malignant neoplasm that accounts for 0.9%–2.7% of all exocrine pancreatic neoplasms. SPN was first reported by Frantz in 1959[1,2] and has previously been called a Frantz tumor, solid-pseudopapillary tumor, solid-cystic tumor, solid and papillary epithelial neoplasm, and papillary-cystic tumor. These tumors predominantly occur in young women, with a female-to-male ratio of 9:1.[1] SPN metastasizes in only 5%–15% of all cases, and common sites include the liver; portal, splenic, or superior mesenteric vein; spleen; omentum; peritoneum; duodenum; or other organs.[1,2] The lung is a very rare metastatic site and has only been reported in three other cases in the literature.[3-5] In this study, we introduce a case of SPN with lung metastasis following 24 years of multiple recurrences.

CASE REPORT

Clinical summary

A 61-year-old woman visited Korea University Guro Hospital (KUGH) for bilateral multiple lung nodules and a mass in the intrathoracic soft tissue. Twenty-four years prior, she had presented to KUGH with epigastric pain; computed tomography (CT) found a 9.9×8.6 cm heterogeneous mass in the pancreatic head. The tumor was removed and histologically diagnosed as SPN. After tumor removal, the patient underwent two choledochojejunostomy procedures but showed no sign of tumor recurrence. Nine years passed before her next visit for this same condition, when some newly developed nodules in her liver and peritoneum were biopsied and confirmed as metastatic SPN. During the next 15 years, the patient suffered eight additional metastatic recurrences in her liver, peritoneum, omentum, spleen, ovary, uterus, colon, mesocolon, and retroperitoneum before finally developing the present multiple lung metastases. A metastatectomy was performed to remove the lung nodules, and the patient is currently alive (Fig. 1). This study was approved by the Institutional Review Board (KUGH 15363-001) of KUGH.

Pathologic findings

The clinical and pathologic features of the primary tumor were reviewed in the patient's electronic medical record. The glass slides and paraffin blocks that had been made from the recurrent tumors were also available for review. Overall, the tumors

pISSN 2383-7837
eISSN 2383-7845

showed a pseudopapillary pattern with relatively monomorphic nuclei and abundant eosinophilic cytoplasm. However, we noted a certain degree of change over time, as summarized in Table 1. In accordance with the histological changes, we subdivided the lesions into early (first to third operations), intermediate (fourth to seventh), and late (eighth to 11th) lesions. In the early metastatic lesions, the tumor showed frequent cystic changes with bland nuclei and indistinct necrobiotic nests without capsular invasion. The Ki-67 labeling index was also very low (< 1%). In the intermediate lesions, however, frequent necrobiotic nests (from the fourth to seventh) and capsular invasions (from the fifth) were noted. The Ki-67 labeling index, which was assessed using an image analysis program, increased to 5% (sixth). In the late lesions, malignant histological features, such as distinct tumor necrosis beyond necrobiotic nests (from the seventh), peritumoral infiltration of the soft tissue or organ (from the seventh), prominent solid architecture (from the eighth), nuclear atypia (from the ninth), and lymphatic emboli (11th), were seen (Fig. 2A–D). The average Ki-67 labeling index increased gradually (0.03%, 2.7%, and 5.6% in early, intermediate, and late metastatic lesions, respectively). Mitosis was usually absent with exceptions of 5/10 high-power field (HPF) (fifth) and 2/10 HPF (seventh) but did not show a significant change. All of the tumors showed identical immunohistochemical results and were diffusely positive for β-catenin, vimentin, neuron-specific enolase, CD10, cyclin D1, progesterone receptor, CD56, and synaptophysin. Inter-

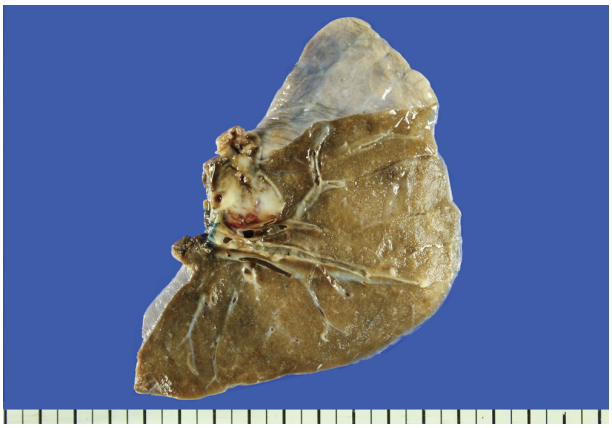

Fig. 1. Gross specimen of the patient's lung metastasis. A solid, well-demarcated and cystic mass with hemorrhage is seen.

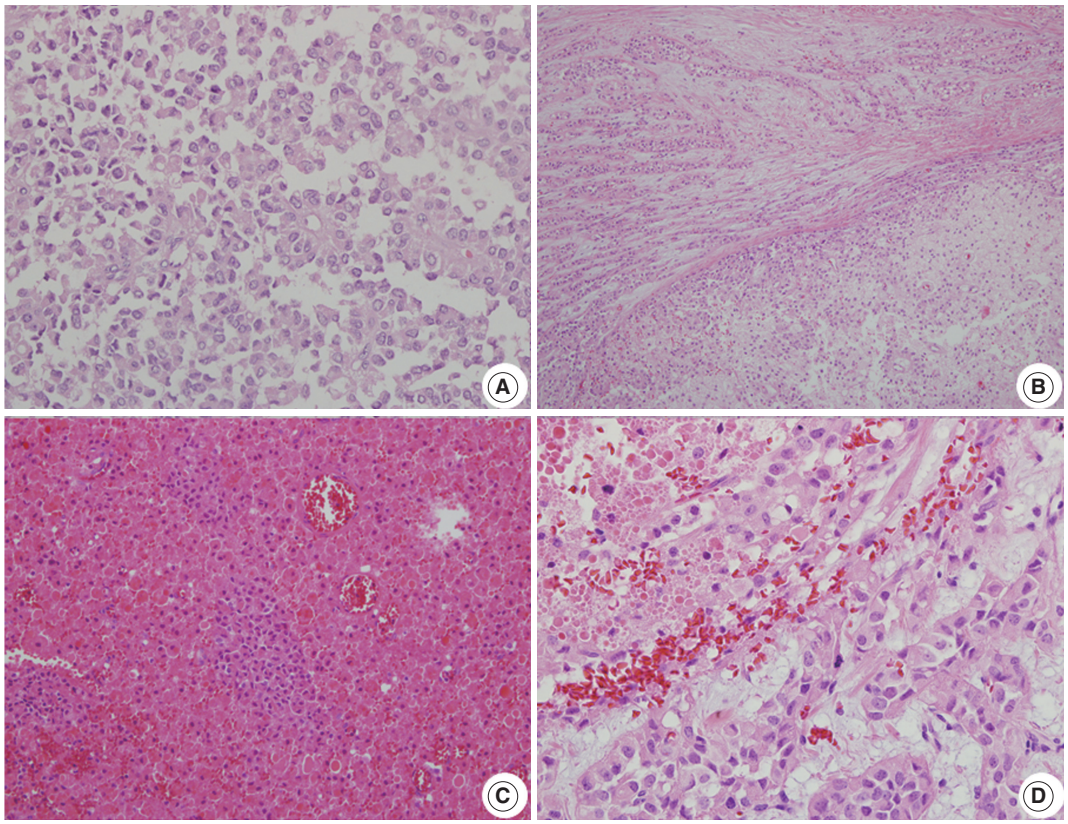

Fig. 2. Microscopic findings. (A) A loosely cohesive pseudopapillary pattern. (B) Capsular invasion with a cord or glandular pattern is visible in the intermediate and late metastatic lesions. (C) Necrobiotic nests are present in the intermediate lesions. (D) Distinct nuclear atypia is seen in the late lesions.

https://doi.org/10.4132/jptm.2016.06.16

Table 1. Clinicopathological data of the patient

Operation No.	Recurrence interval (mo)	Site	Size (largest diameter) (cm)	Necrobiotic nests	Necrosis	Capsular invasion	Ki-67 labeling index (%)	Solid architecture	Nuclear atypia	Mitotic count (/10HPF)
1	0	Pancreas	8	NE	NE	NE	NE	NE	NE	NE
2	107	Liver, peritoneum	5.5 (liver)	N	N	N	<0.1	N	N	<1
3	131	Omentum, peritoneum	4.3 (peritoneum)	N	N	N	<0.1	N	N	<1
4	135	Peritoneum	1.3	Y	N	N	<0.1	N	N	<1
5	180	Peritoneum	3.5	N	N	Y	0.2	N	N	5
6	197	Peritoneum	5	N	N	Y	5	N	N	<1
7	205	Liver, spleen, peritoneum, ovary	10 (ovary)	Y	Y	N	2.9	N	N	2
8	214	Uterus, peritoneum, retroperitoneum, omentum, mesocolon, intrathoracic	3.8 (intrathoracic)	N	Y	N	12.4	Y	N	<1
9	240	Peritoneum, mesocolon, colon	1.5 (colon)	N	Y	Y	6.6	Y	Y	<1
10	272	Spleen, retroperitoneum	3.5 (retroperitoneum)	N	Y	Y	<0.1	Y	Y	<1
11	284	Lung, internal mammary soft tissue	2.8 (lung)	N	N	N	3.4	Y	Y	<1

HPF, high power field; NE, not evaluable; N, absent; Y, present.

Table 2. Cases of solid pseudopapillary neoplasm with lung metastasis

Reference	Sex	Age (yr)	Primary site	Size (cm)	Malignant histologic features	Metastasis	Operation	RI (mo)	Recurrence site	Follow-up (mo)	Survival	Mitoses (/10HPF)	Ki-67 (%)
Takahashi *et al.* (2005)[5]	F	41	Tail	12	Capsule invasion, necrobiotic nests, venous invasion	Liver (multiple)	Distal pancreatectomy, metastatectomy	14	Liver, multiple (14 mo); liver, multiple (27 mo); liver, multiple (38 mo); lung, single (41 mo)	60	Alive	5	10
Hosokawa *et al.* (2014)[3]	F	24	Head	6	Capsule invasion, per pancreatic tissue	PV, SMA, lung	PPPD, PV, resection, pulmonary resection	None	None	34	Alive	-	1.5
Xu *et al.* (2015)[4]	F	42	Body	13	NE	Liver, lung, bone	NE	NE	NE	NE	NE	NE	NE
Our case (2016)	F	37	Head	8.6	Capsule invasion, necrobiotic nests, lymphatic invasion, lymph node invasion	None	PPPD	107	Liver, spleen, abdominal cavity, omentum, mesentery, mesocolon, retroperitoneum, ovary, uterus, lung, thoracic cavity	284	Alive	2	5

RI, recurrence interval; HPF, high power field; F, female; PV, portal vein; SMA, superior mesenteric artery; PPPD, pylorus-preserving pancreaticoduodenectomy; NE, not evaluable.

estingly, they were also positive for chromogranin A, which is very rare in SPN.

DISCUSSION

Generally, the prognosis of SPN is good. Over 95% of patients with a solitary pancreatic lesion are cured by complete excision. Even with local spread, recurrences, or metastases, long periods of disease-free survival have been recorded.[1] The general prevalence of metastatic SPN is 5%–15%.[1,2] Debulking is recommended for these lesions in order to increase the chances of survival.[6] The lung is a very rare metastatic site and was found in only three cases in the literature.[3-5] The first was reported in 2005 by Takahashi *et al*.[5] and showed a lung lesion following three liver metastases. Hosokawa *et al*.[3] reported the second case in 2014, which demonstrated concurrent portal vein and superior mesenteric arterial invasion. The third case was described by Xu *et al*. in 2015,[4] with both liver and bone involvement. Two of the three cases showed a good survival outcome (Table 2). Our case also reveals a long overall survival period despite many recurrences.

After reviewing the eight large studies in the literature, the most commonly quoted malignant SPN characteristics were nuclear atypia (5/8), angioinvasion (5/8), lymph node metastasis (4/8), mitotic count (3/8), advanced age (2/8), size (2/8), capsular invasion (2/8), perineural invasion (2/8), extra-pancreatic invasion (2/8), significant MIB-1 index (2/8), and prominent necrobiotic nests (1/8).[1,3,5-10] Of the four cases with lung metastases (including ours), three showed liver metastasis, three exhibited capsular invasion, and two demonstrated necrobiotic nests (Table 2). Our case initially presented with a bland-looking tumor; however, most of the malignant features including nuclear atypia, lymph node metastasis (upon CT), lymphatic invasion, large tumor size, capsular invasion, and necrobiotic nests developed in later metastases.

Though many studies have claimed that nuclear atypia is a malignant prognostic factor, there is still some debate on this topic. For example, Kim *et al*.[11] recently suggested that some subsets of SPN with nuclear pleomorphism exist with stronger p53 immunoreactivity but do not appear to be more aggressive than conventional SPN. The 2010 World Health Organization classification for tumors of the pancreas also claims that nuclear atypia of pancreas SPN cannot predict malignant tumor behavior.[12] In this study, nuclear atypia accompanied other malignant features. However, due to the patient's relatively good prognosis, the atypia is still a predictor of metastasis but should not be considered a poor prognostic indicator of overall survival. More studies of SPN focusing on nuclear atypia will be needed to further explain this connection.

In conclusion, this case depicts the aggressive progression of tumor cells by repeated peritoneal seeding and lymphatic invasion that still showed an indolent clinical course despite multiple recurrences, including the lung.

Conflicts of Interest

No potential conflict of interest relevant to this article was reported.

REFERENCES

1. Papavramidis T, Papavramidis S. Solid pseudopapillary tumors of the pancreas: review of 718 patients reported in English literature. J Am Coll Surg 2005; 200: 965-72.
2. Yu PF, Hu ZH, Wang XB, *et al*. Solid pseudopapillary tumor of the pancreas: a review of 553 cases in Chinese literature. World J Gastroenterol 2010; 16: 1209-14.
3. Hosokawa I, Shimizu H, Ohtsuka M, *et al*. Preoperative diagnosis and surgical management for solid pseudopapillary neoplasm of the pancreas. J Hepatobiliary Pancreat Sci 2014; 21: 573-8.
4. Xu M, Shi X, Wan T, *et al*. Treatment and prognosis of solid pseudopapillary neoplasms with metastases or recurrence. Zhonghua Wai Ke Za Zhi 2015; 53: 685-9.
5. Takahashi Y, Fukusato T, Aita K, *et al*. Solid pseudopapillary tumor of the pancreas with metastases to the lung and liver. Pathol Int 2005; 55: 792-6.
6. El Nakeeb A, Abdel Wahab M, Elkashef WF, Azer M, Kandil T. Solid pseudopapillary tumour of the pancreas: incidence, prognosis and outcome of surgery (single center experience). Int J Surg 2013; 11: 447-57.
7. Nishihara K, Nagoshi M, Tsuneyoshi M, Yamaguchi K, Hayashi I. Papillary cystic tumors of the pancreas. Assessment of their malignant potential. Cancer 1993; 71: 82-92.
8. Tipton SG, Smyrk TC, Sarr MG, Thompson GB. Malignant potential of solid pseudopapillary neoplasm of the pancreas. Br J Surg 2006; 93: 733-7.
9. Yu P, Cheng X, Du Y, *et al*. Solid pseudopapillary neoplasms of the pancreas: a 19-year multicenter experience in China. J Gastrointest Surg 2015; 19: 1433-40.
10. Ansari D, Elebro J, Tingstedt B, *et al*. Single-institution experience with solid pseudopapillary neoplasm of the pancreas. Scand J Gastroenterol 2011; 46: 1492-7.

 https://doi.org/10.4132/jptm.2016.06.16

11. Kim SA, Kim MS, Kim MS, *et al*. Pleomorphic solid pseudopapillary neoplasm of the pancreas: degenerative change rather than high-grade malignant potential. Hum Pathol 2014; 45: 166-74.
12. Kloppel G, Hruban RH, Klimstra DS, *et al*. Solid-pseudopapillary tumor of pancreas. In: Bosman FT, Carneiro F, Hruban RH, Theise ND, eds. World Health Organization classification of tumours of the digestive system. Lyon: IARC Press, 2010; 327-30.

Journal of Pathology and Translational Medicine 2017; 51: 92-95
https://doi.org/10.4132/jptm.2016.06.21

■ CASE STUDY ■

A Rare Case of Angioleiomyoma Arising in the Subglottic Area to Upper Trachea of a Patient with Underlying Asthma

Yeoun Eun Sung · Chin Kook Rhee[1] Kyo Young Lee

Department of Hospital Pathology, [1]Division of Pulmonary, Allergy and Critical Care Medicine, Department of Internal Medicine, Seoul St. Mary's Hospital, College of Medicine, The Catholic University of Korea, Seoul, Korea

Received: June 2, 2016
Revised: June 15, 2016
Accepted: June 21, 2016

Corresponding Author
Kyo Young Lee, PhD
Department of Hospital Pathology, College of Medicine, The Catholic University of Korea, 222 Banpo-daero, Seocho-gu, Seoul 06591, Korea
Tel: +82-2-2258-1618
Fax: +82-2-2258-1627
E-mail: leekyoyo@catholic.ac.kr

Angioleiomyoma is a rare disease that is histologically characterized by smooth muscle cells arranged around vascular spaces. Although angioleiomyomas occur rarely in the head and neck region, they can cause various symptoms according the site involved. Here, we present a 44-year-old male patient with a 15-year history of asthma, who presented with recent onset of chest discomfort, globus sensation and throat pain. Medication was not effective in relieving his symptoms, and further evaluation revealed a polypoid ovoid mass, almost obstructing the airway at the border of the larynx and upper trachea on chest computed tomography. The mass was completely resected via a rigid bronchoscopy procedure. Histopathologic examination revealed that the excised mass was angioleiomyoma, which was immunohistochemically positive for smooth muscle actin and negative for desmin.

Key Words: Angioleiomyoma; Larynx; Trachea; Bronchoscopy

Angioleiomyoma or vascular leiomyoma is a benign dermal or subcutaneous tumor composed of well-differentiated smooth muscle cells arranged around many vascular channels.[1] It can occur anywhere in the body but is most often seen in the extremities, particularly the lower leg.[2] Angioleiomyoma of the head and neck region is uncommon (~10%), with lips, ears, and nose being the most frequently involved locations.[2,3] Here, we present a case of angioleiomyoma at the border of the subglottic area and upper trachea, with a clinical and pathologic approach.

CASE REPORT

A 44-year-old man presented to the pulmonology department of our hospital for a one week history of chest discomfort, globus sensation, and throat pain. The patient had a history of asthma for 15 years with about 10 events a year but was not taking any medication. He was prescribed a leukotriene receptor antagonist, an inhaled corticosteroid plus long acting beta agonist and a long acting muscarinic antagonist to control bronchial asthma for 3 months. Although his pulmonary function test results showed improvement, the patient persistently complained of globus sensation and throat pain with slight aggravation. Therefore, he was referred to an otolaryngologist for evaluation of his throat and vocal cords.

Laryngoscopy revealed a subglottic mass, which was almost completely occluding the airway. Computed tomography revealed a 2.0×1.5-cm-sized, round exophytic lesion at the border of the subglottic area and upper trachea (Fig. 1A, B). The lesion was well-enhancing and adjacent structures showed no evidence of involvement or destruction. Separately, a 3.0×2.6 cm pituitary mass suggestive of a macroadenoma was also incidentally found.

Excision of the mass was performed by interventional pulmonologists and cardiothoracic surgeons via rigid bronchoscopy. The mass was located 1 cm below the vocal cord, attached to the anterior wall of the trachea by a stalk-like structure (Fig. 1C). It was mobile and resected by snare without any complications (Fig. 1D).

After surgery, the tissue was sent to the pathology department for diagnosis. On gross examination, the tumor was a solid,

pISSN 2383-7837
eISSN 2383-7845

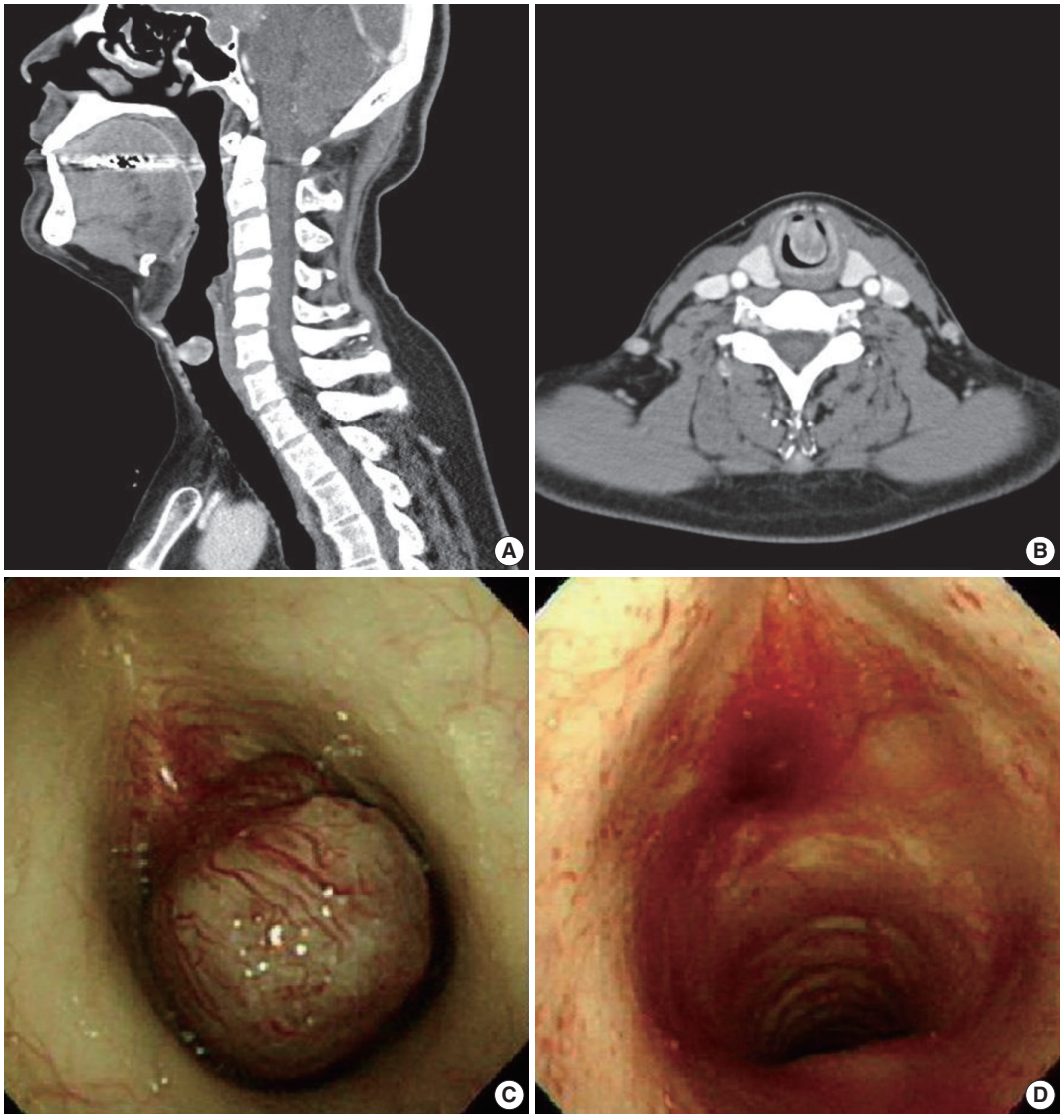

Fig. 1. Neck computed tomography (CT) and bronchoscopic findings. (A, B) Neck CT reveals a 2.0×1.5-cm-sized, round exophytic lesion at the border of the subglottic area and upper trachea. (C) Bronchoscopic finding during the operation, showing an ovoid and polypoid mass located 1 cm below the vocal cord, attached to the anterior wall of the trachea by a stalk-like structure. (D) Bronchoscopic view of the same lesion after the excision; the mass is resected by snare without complications.

ovoid, and polypoid mass with a firm consistency, measuring 1.6×1.4×1.0 cm. It had a grayish and whirling cut surface. Prominent vessels were noticeable on the surface, which resembled feeding vessels as they were thick and more abundant near the resected stalk and spreading branches.

Histologically, the mass consisted of well differentiated smooth muscle cells with intervening vascular channels (Fig. 2A). These channels were mostly venous with variable venous lumens surrounded by muscular coats with dense to relatively loose intervascular smooth muscle cells (Fig. 2B). The muscular coats surrounding the vessels were of variable thickness and some portion of the intervascular stroma was edematous with very sparsely placed smooth muscle bundles. The cells were bland and no mitosis was found (Fig. 2B). A few foci of aggregated adipocytes and mild lymphocytic infiltration were also noted. The surface was covered with ciliated pseudostratified columnar bronchial epithelium (Fig. 2C). Thin walled vessels were abundantly placed in the lamina propria, some of which had an ill-defined muscular coat (Fig. 2C). Immunohistochemically, the tumor cells were positive for smooth muscle actin (Fig. 2D) and negative for desmin.

The patient did not develop any complications after surgery and showed no residual tumor or abnormal lesion in follow-up studies.

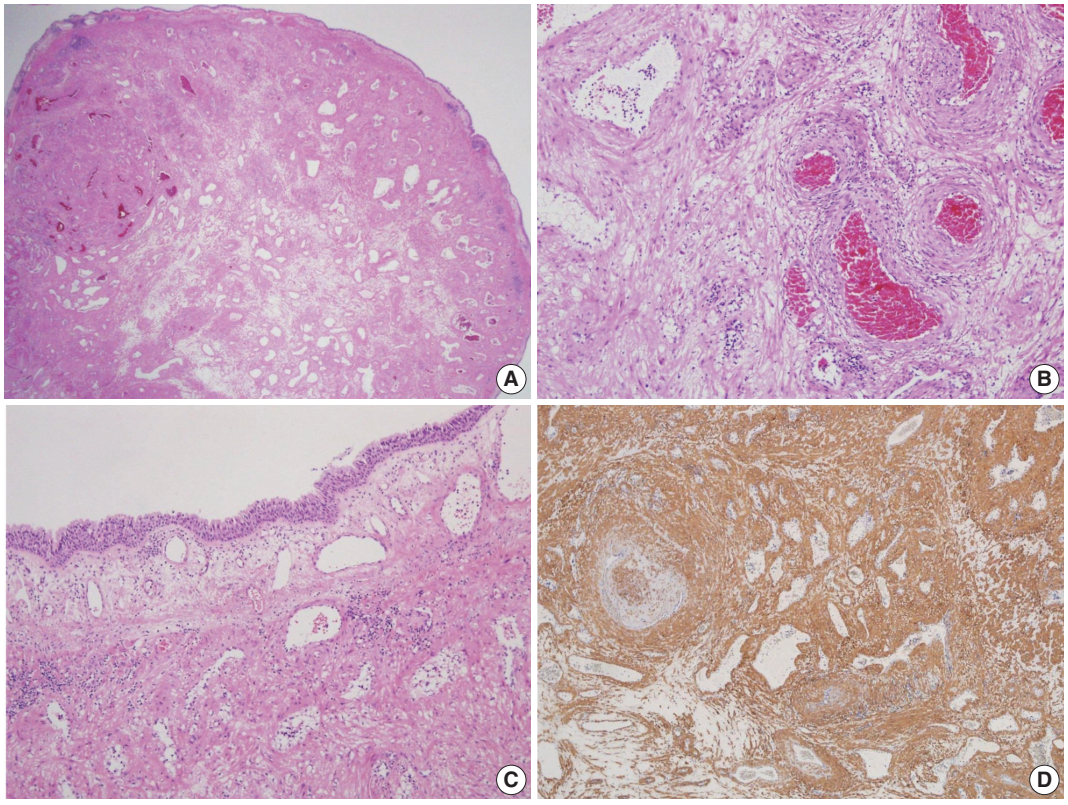

Fig. 2. Histopathologic findings of the mass. (A) Low-power view shows an ovoid and polypoid mass, consisting of well differentiated smooth muscle cells with intervening vascular channels and covered by respiratory epithelium. (B) Variable venous lumens, surrounded by muscular coats with dense to relatively loose intervascular smooth muscle cells are noted. (C) The surface is covered with ciliated pseudostratified columnar bronchial epithelium. Thin walled vessels are abundantly placed in the lamina propria, some of which have an ill-defined muscular coat. (D) Immunohistochemically, the tumor cells are positive for smooth muscle actin.

This case report was approved by the Institutional Review Boards of Catholic Medical Center Office of Human Research Protection Program (KC16ZISE0434).

DISCUSSION

Angioleiomyoma, which is a benign tumor composed of vessels and smooth muscle components, mostly affects the skin of the lower (59%) and upper (15%) extremities.[2] It is rare in the head and neck region, accounting for 13.1% of angioleiomyomas, with mean age of 48 years and male-to-female ratio of 1.3:1.[2,3] Angioleiomyoma in the larynx is even less common, with about 24 total cases estimated in 2008,[4] with several additional cases reported in recent years. In addition, to our knowledge, there is no reported case of angioleiomyoma in the trachea. Our case revealed a lesion located near the cricoid cartilage, making it difficult to decide whether it should be characterized as being within the larynx or the trachea. According to Xu *et al.*,[4] amongst 24 cases of laryngeal angioleiomyoma, the supraglottic region was most common (14/24), followed by the glottis region (7/24) with the subglottic region (3/24) being the least common location.

Angioleiomyoma typically presents as a small, slowly growing firm nodule and generally causes pain, making this the major complaint in more than half of patients.[1] In cases of laryngeal tumors, the main documented symptoms are hoarseness, dyspnea, dysphagia, and a foreign body sensation in the throat. In our case, the patient had complaints of chest discomfort, globus sensation, and throat pain. Globus sensation is presumed to be due to the mass affecting the adjacent pharynx and esophagus when swallowing or any other movement. Also throat pain is easily predictable, as most angioleiomyomas of the skin are known to frequently cause pain in the lesion. Our patient's mass was sufficiently below the vocal cord, and therefore, hoarseness was not noticed. One noteworthy point in our case is that chest discomfort with difficulty in breathing, which was one of the main complaints of the patient, was not discernible from that caused by his underlying asthma. Because of his underlying

 https://doi.org/10.4132/jptm.2016.06.21

asthma, the patient visited the pulmonology department first, and evaluation with management was focused on asthma control for about 3 months.

A standardized treatment for laryngeal vascular leiomyoma does not exist due to its rarity, but complete mass resection is the most frequently chosen treatment. Surgical excision by both endoscope or an external approach are treatment options, with endoscopic surgery being favored due to less tissue damage.[4] In this case, removal of the mass via rigid bronchoscopy, rather than by open thoracotomy, was attempted to minimize risk. The resection was performed without difficulty or any further complications. In a few previously reported cases, patients experienced expectorating fresh blood after the surgery, probably because of the abundant vascularity of the lesion.[4,5] Considering its location, careful management for bleeding control and preoperative investigation of vascularity, for example using angiography, might be necessary.[5]

The major histological variations of angioleiomyomas are solid, venous and cavernous types, with the solid type being the most common (67%).[2] A study of angioleiomyoma in the head and neck also revealed that the solid variant is the most common within this location.[3] Histologically, our case was venous type, showing variable venous lumina surrounded by muscular coats with relatively loose intervascular smooth muscle cells. However, histological classification as such is known to be unnecessary. Also in addition to the main mass, abundant small thin-walled vessels were noted surrounding the mass beneath the mucosa, corresponding with the gross finding of high vascularity even noticeable on the surface.

The immunohistochemical study of our case showed smooth muscle actin (+) and desmin (–) for tumor cells, which corresponds with a previous study regarding immunohistochemical findings in angioleiomyoma.[6] Several studies have consistently revealed variable desmin positivity from 1%[7] to 18%,[8] while actin is positive in every case. A more recent study revealed that the solid variant showed the highest positivity rate for desmin (75.7%) followed by the venous type (51.4%) and cavernous type (18%).[6]

Angioleiomyoma is a benign disease and an extremely rare laryngeal or tracheal lesion. Despite its rarity, this disease entity should be considered when patients complain of possible symptoms, such as hoarseness, difficulty in breathing, chest discomfort or throat pain. Careful investigation might be necessary especially if the patient has underlying respiratory disease, in order to not disregard the symptoms as just being due to aggravation of an underlying disease. Angioleiomyoma is usually easily diagnosed histologically and immunohistochemically. The tumor is mostly resectable without difficulties, but careful monitoring and regular follow up is necessary due to the possibility of postoperative bleeding.

Conflicts of Interest

No potential conflict of interest relevant to this article was reported.

REFERENCES

1. Fletcher CD, Bridge JA, Hogendoorn P, Mertens F. WHO classification of tumours of soft tissue and bone. Lyon: IARC Press, 2013.
2. Hachisuga T, Hashimoto H, Enjoji M. Angioleiomyoma: a clinicopathologic reappraisal of 562 cases. Cancer 1984; 54: 126-30.
3. Wang CP, Chang YL, Sheen TS. Vascular leiomyoma of the head and neck. Laryngoscope 2004; 114: 661-5.
4. Xu Y, Zhou S, Wang S. Vascular leiomyoma of the larynx: a rare entity: three case reports and literature review. ORL J Otorhinolaryngol Relat Spec 2008; 70: 264-7.
5. Hope N, Smith CP, McCluney N. Angioleiomyoma of the larynx: beware the subglottic lesion. BMJ Case Rep 2015; 2015: bcr2015213469.
6. Matsuyama A, Hisaoka M, Hashimoto H. Angioleiomyoma: a clinicopathologic and immunohistochemical reappraisal with special reference to the correlation with myopericytoma. Hum Pathol 2007; 38: 645-51.
7. Lundgren L, Seidal T, Kindblom LG, Angervall L. Intermediate and fine filaments of vascular leiomyomas (angiomyoma), leiomyoma and leiomyosarcomas of large veins. APMIS 1989; 97: 637-45.
8. Hasegawa T, Seki K, Yang P, Hirose T, Hizawa K. Mechanism of pain and cytoskeletal properties in angioleiomyomas: an immunohistochemical study. Pathol Int 1994; 44: 66-72.

Journal of Pathology and Translational Medicine 2017; 51: 96-98
https://doi.org/10.4132/jptm.2016.06.15

■ BRIEF CASE REPORT ■

Adult Intussusception Caused by Inverted Meckel's Diverticulum Containing Mesenteric Heterotopic Pancreas and Smooth Muscle Bundles

Seungkoo Lee · Seong Whi Cho[1]

Departments of Anatomic Pathology and [1]Radiology, Kangwon National University Hospital, Kangwon National University School of Medicine, Chuncheon, Korea

Adult intussusception represents 5% of all intussusceptions.[1,2] Most of these cases are related to organic lesions.[1] Infrequently, an inversion of Meckel's diverticulum (MD) into the lumen of the small bowel can cause intussusception.[3-5] The incidence of intussusception due to an inverted MD accounts for about 4% of all cases of intussusceptions.[1,4] Heterotopic pancreas (HP) is defined as pancreatic tissue located at aberrant sites that lacks anatomic and vascular continuity with the main pancreas.[6-9] The most common location of HP is the proximal gastrointestinal tract.[6,10] The mesenteric location of HP is rare, and only a few cases of HP in the mesentery of the small intestine have been reported in the literature.[8,9] Here, we present a very rare case of adult ileoileal intussusception caused by an inverted MD containing mesenteric HP and smooth muscle bundles.

CASE REPORT

A 55-year-old man presented with intermittent abdominal pain and hematochezia of a 2-month duration. He also reported several episodes of melena-type bowel movements. His medical history was unremarkable except for an appendectomy 10 years prior. Blood tests revealed a hemoglobin level of 8.3 g/dL (NL, 13.3–16.5 g/dL) and a hematocrit level of 23.8% (NL, 38.6–47.3%). All other laboratory findings were unremarkable. An endoscopic study was unable to locate the site of the bleeding. An abdominal and pelvic computed tomography (CT) scan showed a pedunculated intraluminal mass with central heterogeneous fat attenuation (Fig. 1). The patient underwent a mini-laparotomy for segmental resection. Upon gross examination, the specimen consisted of a 15-cm segment of the small bowel with a small dimple in the anti-mesenteric aspect, and there was a pedunculated polypoid mass (5.1×3.0×2.8 cm) with a bulbous-shaped head (Fig. 2A). The stalk of the mass was lined by unremarkable mucosa. The cut section of the mass revealed a nodular lesion within the adipose tissue sandwiched between the continuous lining of the proper muscle layers (Fig. 2B). Microscopic examination revealed that the bulbous tip lesion was covered by the full thickness of the intestinal wall and had deep ulcerations (Fig. 2C). The mucosa of the tip contained nondysplastic epithelial glands. Focal heterotopic antral-type gastric tissue was also present (Figs. 2C, 3A). Interestingly, ectopic pancreatic tissue and smooth muscle bundles were located within the entrapped mesenteric fat (Fig. 2C, D). The mesenteric heterotopic pancreatic tissues were composed of all elements typically found in normal pancreatic tissue (Heinrich type I), such as acini (Fig. 3B), islet cells (Fig. 3B), and ducts (Fig. 3C) and several discontinuous fascicles of smooth muscles (Fig. 3D). Based on the clinical and histopathologic findings, the pedunculated intraluminal mass was diagnosed as inverted MD with a mesenteric HP and displaced smooth muscle bundles. The patient had an uneventful postoperative recovery, with no further episodes of lower gastrointestinal hemorrhage during the follow-up period.

DISCUSSION

Adult intussusception differs from childhood intussusception in its presentation, causes, and management.[1,2,7] The presenting

Corresponding Author
Seungkoo Lee, MD
Department of Anatomic Pathology, Kangwon National University Hospital, Kangwon National University School of Medicine, 1 Gangwondaehak-gil, Chuncheon 24341, Korea
Tel: +82-33-258-9172, Fax: +82-33-258-2475, E-mail: jsklee@kangwon.ac.kr

Received: May 9, 2016 **Revised:** June 8, 2016
Accepted: June 14, 2016

pISSN 2383-7837
eISSN 2383-7845

symptoms of adult intussusception are often nonspecific. In our case, the patient developed only intermittent abdominal pain, melena-type bowel movements, and a few episodes of hematochezia. In adult intussusception, it is important to identify the leading point. Several pathologic conditions have been reported as the leading point in intussusception, such as inflammatory disease, neoplasm, adhesion, MD,[1] and HP.[2] In the present case, the CT scan revealed ileoileal intussusception associated with inverted MD (Fig. 1). Although most MD remains asymptomatic, it can be complicated by intussusception[1,4,5,10] and gastrointestinal bleeding.[10] Ulceration in MD is thought to occur mostly because of acid secretion by the heterotopic gastric mucosa.[10] In the presented case, ulceration and gastrointestinal bleeding were associated with antral-type ectopic gastric tissue in the MD.

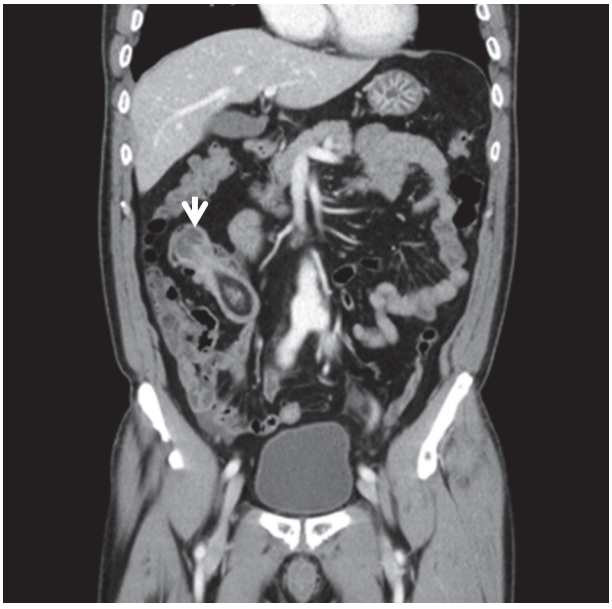

Fig. 1. Abdominal and pelvic computed tomography (CT) scan. The coronal view CT scan reveals an intestinal intussusception with an intraluminal mass (arrow).

MD can invert into the intestinal lumen, but the exact mechanism of this inversion is not clearly understood. One theory is that abnormal peristaltic movement derived from the ulcer or ectopic tissue causes the diverticulum to become inverted.[5] Once inverted, the diverticulum can serve as a site of intestinal obstruction or the leading point for an intussusception. In our case, the patient's inverted MD contained several aberrant displaced smooth muscle bundles (Fig. 2C, D). We propose that these aberrant smooth muscle bundles produced abnormal peristaltic movement.

HP is common in the upper gastrointestinal tract.[6,8,9] Other possible locations include the gallbladder, bile duct, or omentum.[6,9] In descending order of frequency, the involved histologic layers are the submucosa,[1,5,6] muscularis propria,[6] and serosa.[6,7] HP located in the mesentery of the small intestine is very rare.[8,9] In our case, the HP was found within the entrapped mesenteric fat tissue of the ileum. These displaced pancreatic tissues and aberrant smooth muscle bundles were associated with MD, which can act as a leading point for intussusception.

In summary, mesenteric HP and smooth muscle tissue can act clinically as a leading point for inverted MD and ileoileal intussusception.

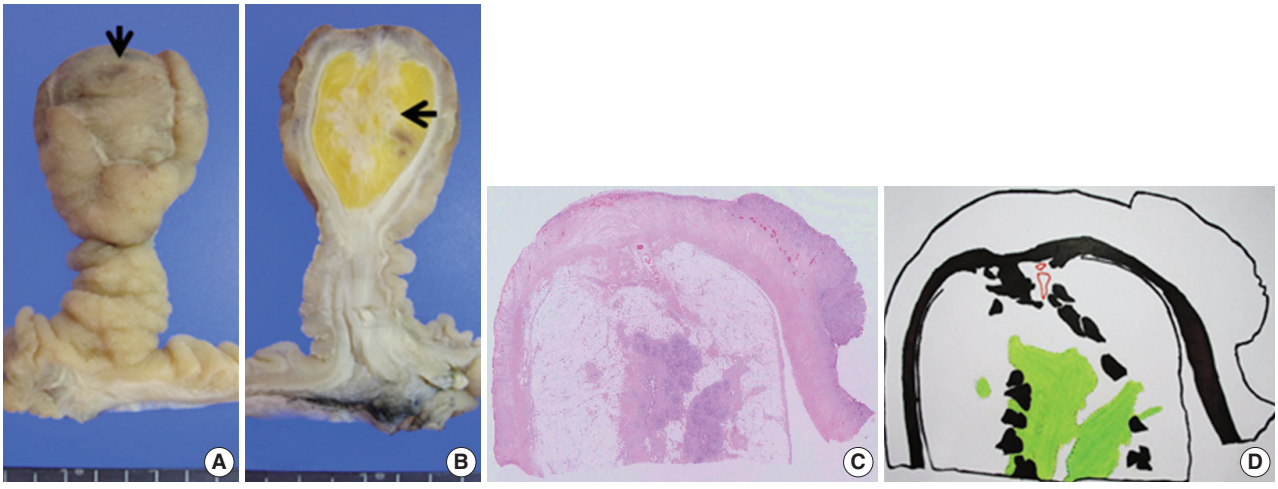

Fig. 2. The gross specimen and a schematic drawing of a hematoxylin and eosin (H&E)-stained slide. The tip of the pedunculated polypoid mass shows a mucosal ulcer (A, arrow) and mesenteric heterotopic pancreatic tissue (B, arrow). The entire image of the H&E slide (C) and its schematic diagram (D) reveal mesenteric heterotopic pancreatic tissue (D, light green area) and smooth muscle tissue (D, black area).

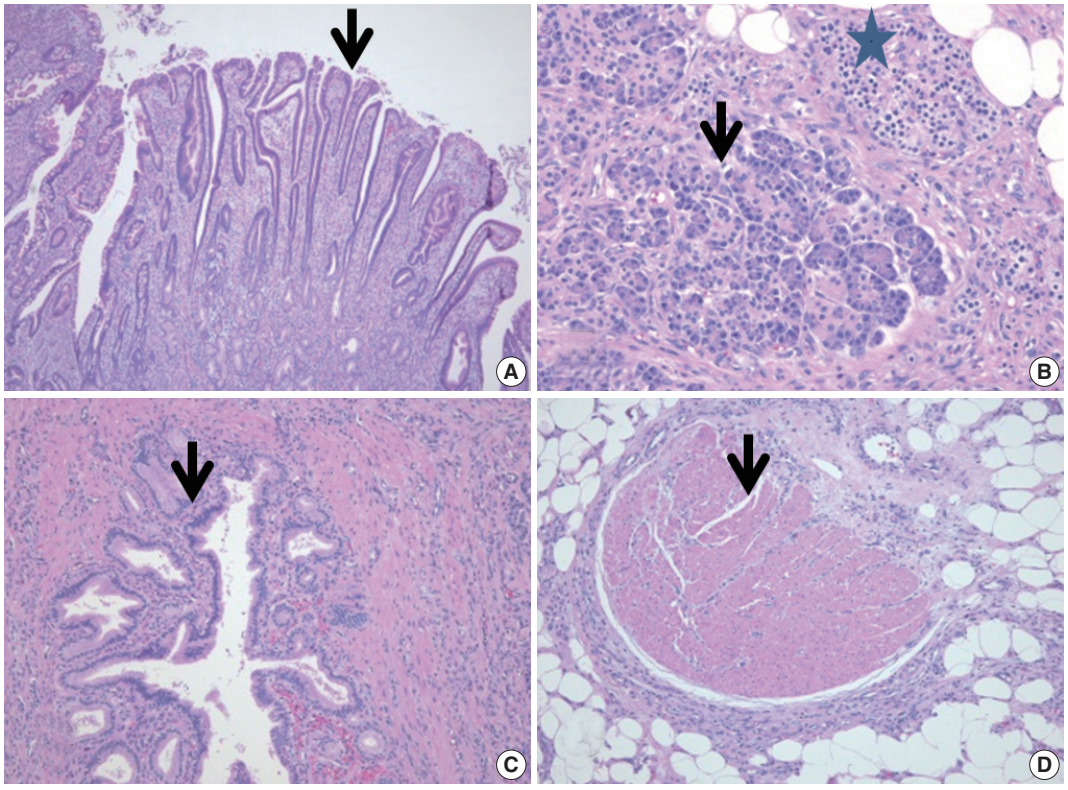

Fig. 3. Histologic features of the ectopic gastric mucosa and heterotopic pancreatic tissues. The inverted Meckel's diverticulum contains ectopic, antral-type gastric tissues (A, arrow) and mesenteric, heterotopic tissues such as acinar (B, arrow), islet (B, star), duct (C, arrow), and smooth muscle bundle (D, arrow).

Conflicts of Interest

No potential conflict of interest relevant to this article was reported.

REFERENCES

1. Ito T, Sato K, Maekawa H, *et al*. Adult intussusception caused by an inverted meckel diverticulum. Case Rep Gastroenterol 2011; 5: 320-4.
2. Chuang MT, Tsai KB, Ma CJ, Hsieh TJ. Ileoileal intussusception due to ileal ectopic pancreas with abundant fat tissue mimicking lipoma. Am J Surg 2010; 200: e25-7.
3. Levy AD, Hobbs CM. From the archives of the AFIP. Meckel diverticulum: radiologic features with pathologic correlation. Radiographics 2004; 24: 565-87.
4. Sioka E, Christodoulidis G, Garoufalis G, Zacharoulis D. Inverted Meckel's diverticulum manifested as adult intussusception: age does not matter. World J Gastrointest Surg 2011; 3: 123-7.
5. Kim SM, Jung MJ, Kim YO. Lipoma within Inverted Meckel's diverticulum: a case report. Korean J Pathol 2013; 47: 86-8.
6. Gupta MK, Karlitz JJ, Raines DL, Florman SS, Lopez FA. Clinical case of the month: heterotopic pancreas. J La State Med Soc 2010; 162: 310-3.
7. Al-Zahem A, Arbuckle S, Cohen R. Combined ileal heterotopic pancreatic and gastric tissues causing ileocolic intussusception in an infant. Pediatr Surg Int 2006; 22: 297-9.
8. Canbaz H, Colak T, Dusmez Apa D, Sezgin O, Aydin S. An unusual cause of acute abdomen: mesenteric heterotopic pancreatitis causing confusion in clinical diagnosis. Turk J Gastroenterol 2009; 20: 142-5.
9. Vyas S, Khandelwal A, Sandhu MS, Verma S, Khandelwal N. Asymptomatic heterotopic pancreas in the mesentery. Trop Gastroenterol 2012; 33: 289-92.
10. Kopacova M, Vykouril L, Vacek Z, *et al*. Inverted Meckel's diverticulum with ectopic pancreatic tissue as a source of severe gastrointestinal bleeding. J Gastrointest Surg 2010; 14: 578-81.

https://doi.org/10.4132/jptm.2016.06.15

Journal of Pathology and Translational Medicine 2017; 51: 99-102
https://doi.org/10.4132/jptm.2016.09.30

■ BRIEF CASE REPORT ■

Human Herpes Virus 8/Epstein-Barr Virus–Copositive, Plasmablastic Microlymphoma Arising in Multicentric Castleman's Disease of an Immunocompetent Patient

Yong-Moon Lee · Jin-Man Kim · Sam-Yong Kim[1]

Departments of Pathology and Medical Science and [1]Internal Medicine, Chungnam National University School of Medicine, Daejeon, Korea

Castleman's disease is a lymphoproliferative disorder characterized by expanded germinal centers with B-cell proliferation and vascular proliferation. When infected with human herpes virus 8 (HHV8), it may develop multicentric Castleman's disease (MCD) from polyclonal isolated HHV8-positive plasmablasts to monoclonal microlymphomas and frank plasmablastic lymphomas.[1] In MCD-associated plasmablastic microlymphomas, a few cases of HHV8/Epstein-Barr virus (EBV) coinfection to human immunodeficiency virus (HIV)–positive patients have been known.[2] Here, we describe a plasmablastic microlymphoma arising in MCD showing HHV8/EBV co-positivity especially in HIV-seronegative patient.

CASE REPORT

A 53-year-old man was referred to Chungnam National University Hospital complaining of abdominal distention with epigastric discomfort. He denied weight loss, fever, malaise, or any systemic symptoms, and had no remarkable previous medical history. His laboratory test results were within normal ranges and anti-HIV antibody was negative. Computed tomographic scans revealed enlargement of multiple intraabdominal lymph nodes (Fig. 1A). Exploratory laparotomy was done and a huge retroperitoneal lymph node was submitted for the pathological diagnosis (Fig. 1B). The histologic examination demonstrated marked lymphoid follicular hyperplasia with vascular hyalinization showing classical features of Castleman's disease (Fig. 2A, B), and the interfollicular area/sinuses showed a dense infiltrate of large lymphoplasmablastic cells (Fig. 2C, D). These atypical cells had the characteristics of large round or oval nuclei with the irregular nuclear contours similar to plasmablasts, which replaced the periphery of the follicles making cohesive sheets of microlymphoma (Fig. 2D). The immunohistochemical studies showed that the large atypical cells were positive for MUM-1/IRF4, epithelial membrane antigen, HHV8, and EBV encoded ribonucleic acids by *in situ* hybridization (Fig. 3), whereas CD45, CD20, CD79a, PAX5, CD10, Bcl-6, CD4, CD5, CD8, CD138, and CD30 were negative and did not express immunoglobulin heavy or light chains. Interestingly, CD3 was expressed aberrantly throughout the atypical cells, which can occasionally be seen in HHV8/EBV copositive lymphomas.[3] Due to these findings, the plasmablastic microlymphoma arising in multicentric Castleman disease was made. The patient received cyclophosphamide, doxorubicin, vincristine and predinisolone mixed chemotherapy, and has shown to be in a stable state without disease progression for 12 months.

DISCUSSION

The MCD, initially separated from the Castleman's disease by its multicentric nature, is now considered as a different disease with different etiology; however, in some cases, the clinical outcome can be much worse. The patients may present fever, sweats, fatigue, lymphadenopathy, and splenomegaly which can be often fatal.[4]

The HHV8 is well known as the pathogenesis of Kaposi's sarcoma, primary effusion lymphoma (PEL), MCD, and plasma-

Corresponding Author
Sam-Yong Kim, MD
Department of Internal Medicine, Chungnam National University School of Medicine, 266 Munhwa-ro, Jung-gu, Daejeon 35015, Korea
Tel: +82-42-280-7153, Fax: +82-42-280-7189, E-mail: frkim@cnu.ac.kr

Received: August 29, 2016 **Revised:** September 29, 2016
Accepted: September 30, 2016

pISSN 2383-7837
eISSN 2383-7845

blastic proliferations. Although not in localized Castleman's disease, HIV-infected cases of MCD are always accompanied with HHV8 infection, and HIV-negative cases show 40%–50% of HHV8 infection.[5] This HHV8-associated MCD, also known as a plasmablastic variant of MCD, is characterized by the presence of plasmablasts scattered in the mantle zones of the follicles and the plasmablasts harbor HHV8 with both latent (latency associated nuclear antigen, LANA+) and lytic (viral homolog of human interleukin 6, vIL6+) profile. When scattered HHV8-infected plasmablasts make confluent clusters, sometimes to form foci or large sheets, the plasmablastic microlymphoma or frank lymphoma should be considered.[6]

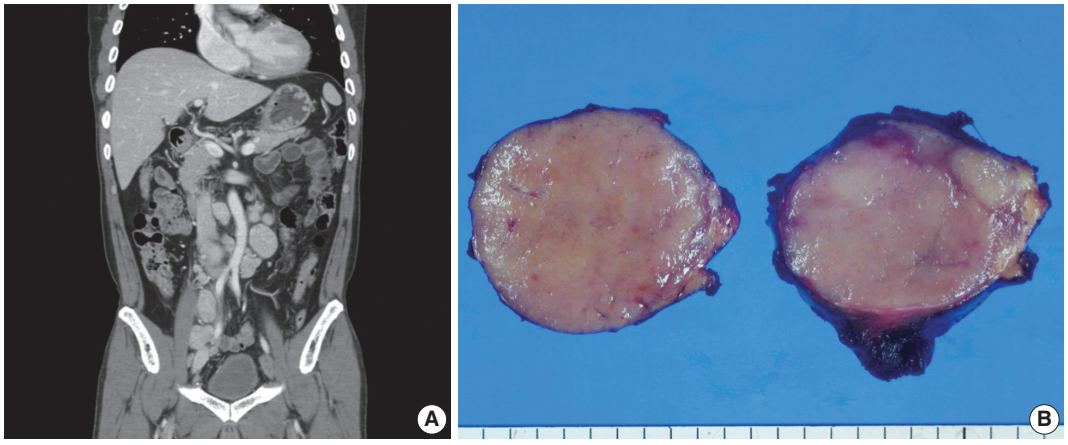

Fig. 1. Imaging and macroscopic findings of the lymph node. (A) Abdominal computed tomography showing multiple enlarged retroperitoneal lymph nodes along the axis. (B) A 5.0-cm round and tan to pinkish contexture demonstrated with vague lobulation on cut section.

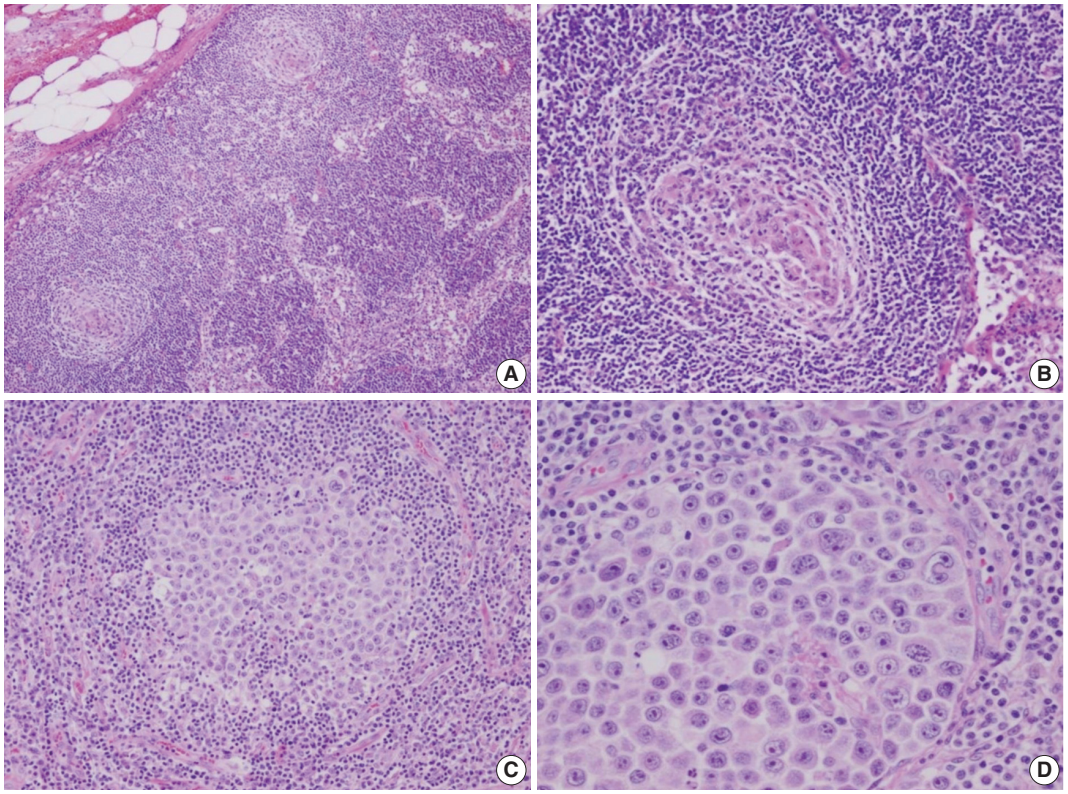

Fig. 2. Microscopic findings of the lymph node. (A) Low-magnification showing multiple, well-formed germinal centers. (B) The hyalinized vascular proliferations surrounding follicles characteristic of Castleman's disease. (C) The confluent aggregates of plasmablasts in the germinal centers indicating the germinotrophism. (D) High-magnification showing the invasion of plasmablasts to the interfollicular spaces with sinusoidal pattern.

https://doi.org/10.4132/jptm.2016.09.30

Certain HHV8 elements have been known to show oncogenic properties, especially vIL6, which is thought to underlie the pathogenesis of HHV8-associated MCD. When expressed constantly in mice, vIL6 can induce symptoms that resemble human MCD. These symptoms can be ameliorated by the blockade of interleukin 6 (IL-6) signaling with anti–IL-6 receptor antibodies.[7] When naïve B cells are infected by EBV, they drive proliferation and expansion of the EBV-infected B-cell pool, analogous to patterns observed in germinal centers via expressing viral latency III or nuclear antigens such as Epstein–Barr nuclear antigen 1 (EBNA) 1, 2, 3A, 3B, 3C, -LP, and latent membrane proteins (LMP1, 2A, and 2B).[8] Interactions among co-infecting viruses may increase cellular transformation and oncogenesis especially in lymphomagenesis which is suggested by the simultaneous detection of co-infecting viruses within the same neoplastic cells harboring HHV8 and EBV infection. In the majority of PEL, the HHV8-positive lymphoma cells are co-infected by EBV, and the analysis of EBV gene expression in PEL shows expression of EBNA1 but not LMP1. Nevertheless, the precise oncogenic mechanism of EBV in PEL remains to be investigated.[9]

In contrast to PEL, HHV8-associated MCD is usually associated with HIV but not with EBV infection and, only a few cases of plasmablastic microlymphoma arising in MCD showing HHV8/EBV co-positivity to HIV-positive patients have been known. Our case demonstrates obvious plasmablastic proliferations in the background of MCD. These infiltrative plasmablasts composed of confluent clusters and sheets, should be interpretated as microlymphoma positive for HHV8, and EBV in HIV-seronegative patients, has not been reported. The germinotropic lymphoproliferative disorder has histologic features similar to those of plasmablastic microlymphoma. In contrast to plasmablastic microlymphoma, it affects localized lymphadenopathy without systemic symptoms and HHV8 infected cells are confined to the germinal centers without MCD background showing a good outcome.[10]

In summary, we describe a case of plasmablastic microlymphoma arising in MCD showing HHV8/EBV co-positivity, and occurring in an immunocompetent patient.

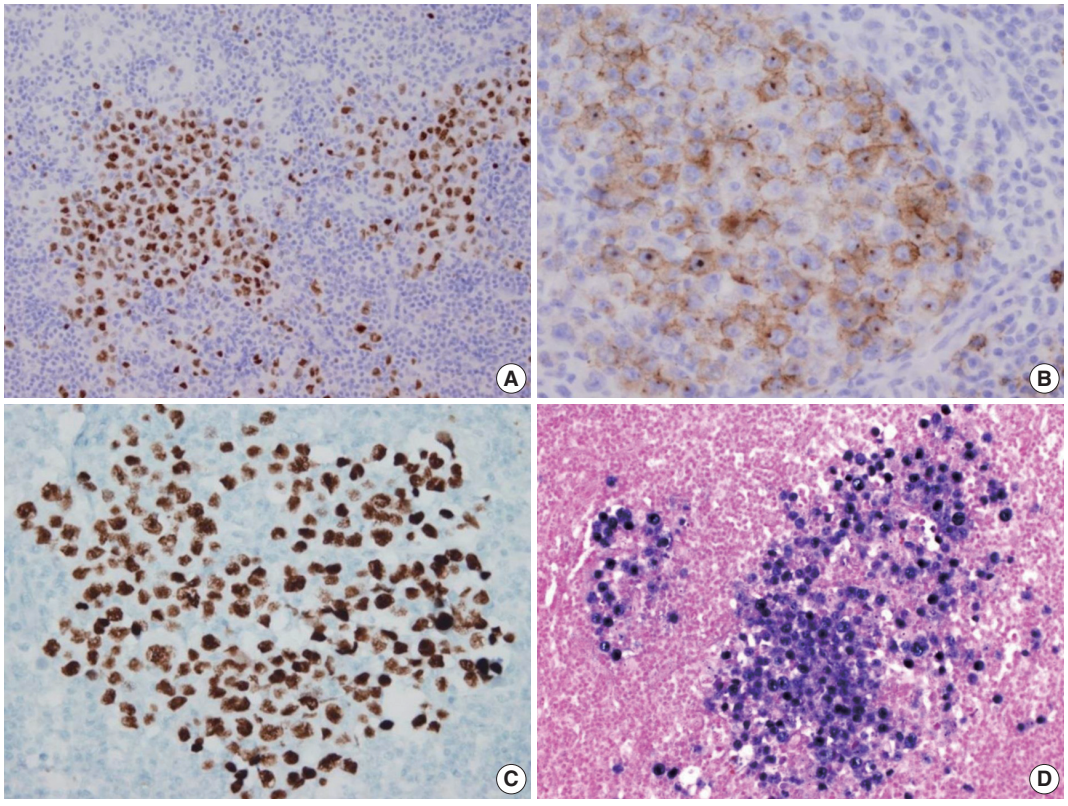

Fig. 3. Immunohistochemical staining results of the lymph node. (A) MUM-1/IRF4-stain highlighting sheets of germinotrophic plasmablasts. (B) Epithelial membrane antigen–stain demonstrating confluent aggregation of plasmablasts with sinusoidal pattern. (C) Human herpes virus 8 encoded latency associated nuclear antigen 1 highlighting the atypical plasmablasts. (D) *In situ* hybridization for Epstein-Barr virus (EBV) encoded ribonucleic acids showing coinfection of EBV in the atypical plasmablasts.

Conflicts of Interest

No potential conflict of interest relevant to this article was reported.

Acknowledgments

This study was funded by research fund of Chungnam National University in 2010.

REFERENCES

1. Du MQ, Liu H, Diss TC, *et al*. Kaposi sarcoma-associated herpesvirus infects monotypic (IgM lambda) but polyclonal naive B cells in Castleman disease and associated lymphoproliferative disorders. Blood 2001; 97: 2130-6.
2. Seliem RM, Griffith RC, Harris NL, *et al*. HHV-8+, EBV+ multicentric plasmablastic microlymphoma in an HIV+ Man: the spectrum of HHV-8+ lymphoproliferative disorders expands. Am J Surg Pathol 2007; 31: 1439-45.
3. Dong HY, Wang W, Uldrick TS, Gangi M. Human herpesvirus 8- and Epstein-Barr virus-associated solitary B cell lymphoma with a T cell immunophenotype. Leuk Lymphoma 2013; 54: 1560-3.
4. Wang HW, Pittaluga S, Jaffe ES. Multicentric Castleman disease: where are we now? Semin Diagn Pathol 2016; 33: 294-306.
5. Chadburn A, Cesarman E, Nador RG, Liu YF, Knowles DM. Kaposi's sarcoma-associated herpesvirus sequences in benign lymphoid proliferations not associated with human immunodeficiency virus. Cancer 1997; 80: 788-97.
6. Dupin N, Diss TL, Kellam P, *et al*. HHV-8 is associated with a plasmablastic variant of Castleman disease that is linked to HHV-8-positive plasmablastic lymphoma. Blood 2000; 95: 1406-12.
7. Katsume A, Saito H, Yamada Y, *et al*. Anti-interleukin 6 (IL-6) receptor antibody suppresses Castleman's disease like symptoms emerged in IL-6 transgenic mice. Cytokine 2002; 20: 304-11.
8. Vockerodt M, Yap LF, Shannon-Lowe C, *et al*. The Epstein-Barr virus and the pathogenesis of lymphoma. J Pathol 2015; 235: 312-22.
9. Fassone L, Bhatia K, Gutierrez M, *et al*. Molecular profile of Epstein-Barr virus infection in HHV-8-positive primary effusion lymphoma. Leukemia 2000; 14: 271-7.
10. Ferry JA, Sohani AR, Longtine JA, Schwartz RA, Harris NL. HHV8-positive, EBV-positive Hodgkin lymphoma-like large B-cell lymphoma and HHV8-positive intravascular large B-cell lymphoma. Mod Pathol 2009; 22: 618-26.

 https://doi.org/10.4132/jptm.2016.09.30


JPTM
Journal of Pathology and
Translational Medicine